

CENTURY GEOPHYSICAL CORPORATION

Tulsa, Oklahoma

TECHNICAL REPORT

SUBJECT: LOG INTERPRETATION MANUAL

DATE: September 23, 1975

SUBMITTED BY: Jim Hallenburg

LOCATION: Tulsa, Oklahoma

APPROVAL: 

REVISION RECORD:

- 3-15-76 - Sec. 3, page 13
T Cyril Noon
Tulsa, Oklahoma
- 7-7-76 - Sec. 6, Add Addendum 1
Larry Rinaldo
Grants, New Mexico

A C K N O W L E D G E M E N T S

Many of the charts contained herein were taken from the Formation Evaluation Data Handbook from Gearhart-Owen Industries, Inc. (Used by permission of Mr. Gearhart). The referenced papers were written by Bruce Rubin of Teton Exploration Drilling Company, Inc., and Merle Crew and E. Berkoff of E.R.D.A., and Hubert Guyod, a consultant.

LOG INTERPRETATION MANUAL

TABLE OF CONTENTS

	<u>Section</u>	<u>Pages</u>
Introduction	1	1
Uses of Gamma Ray Electric Logs	2	1-4
Uranium Roll Front Zonation, Rubin: Reference	2a	1-8
Gamma Ray Anomaly Calculation Methods	2b	1-3
Interpretation of Gamma Ray Logs, Hallenburg: Reference	2c	1-28
Spontaneous Potential Measurements	3	1-17
Interpretation of the Spontaneous Potential Curve	3a	1-9
Interpretation of Single Point Resistance and Resistivity Logs	4	1-9
Interpretation of Density Logs	5	1-10
Neutron Logging Systems	6	1-4
Interpretation of Neutron Logs	6a	1-5
Calibration of Logs	7	1-3
Twopit, A Different Approach to Calibration of Gamma Ray Logging Equipment, Crew and Berkoff: Reference	7a	1-24
Interpretation of Electric and Gamma Ray Logs in Water Wells, Guyod: Reference	8	1-15
Interpretation of Coal Logs	8a	1-6
Multiple Curve Interpretation	8b	1-12
Appendix	9	1-10

LOG INTERPRETATION MANUAL

INTRODUCTION

This manual is a collection of information intended to acquaint an inexperienced operator with a facet of the field he is entering and as a reference for the experienced operator.

The contents of the manual include a brief theory of the operation of each type system and descriptions of the uses and interpretation systems and techniques applicable to Century's equipment.

Naturally, because of its nature the contents will vary with time. As systems are supplanted with newer systems, new descriptions must be added and older ones relegated to the reference file. Interpretation techniques change and improve continually, even for the older tools and systems. Therefore, this is not a static text, but rather, a continually growing, changing, correcting, and improving one.

USES OF GAMMA RAY-ELECTRIC LOGS

The gamma ray-electric logs are used for several purposes in the minerals industry. They are used for wide spaced or large area geologic correlation, medium spaced trend tracing, short spaced profile analysis, ore reserve determination, and pit and mine outlining. The major usages of logs are probably in multiple hole situations.

A. LARGE AREA GEOLOGIC CORRELATION

Use is made of the characteristic signatures of representative formations, beds, and "markers" in large area geologic correlation. Usually a line of logged holes is chosen and the logs are hung on the wall in geographical sequence. Depending upon the end use, the logs may be adjusted to or "hung on" a constant elevation, (or, literally, a sea level reference), or they may be "hung on" a fixed depth or surface reference. Occasionally the logs are "hung on" a particular formation anomaly or "marker."

Specific geological horizons are often identified before hanging the logs. While this is not absolutely necessary at this point it does help with correlations.

Similarities of signature are then identified horizontally whether or not specific geological horizons are identified. Any or all of the available curves are used for this correlation. The most useful are probably the resistance, resistivity or porosity curves. However, the SP curve and gamma ray curve are useful for determining sand-shale sequences. These correlations are traced from one log to the next. Often they are marked with string or crayon lines.

Inconsistencies are looked for after the initial correlations have been completed. It would be unusual, for example, for a big or thick uranium anomaly to occur in a tight shale. Hard stringers, such as a tabular limestone, are not likely to change relative level from one log to the next. Not all of the inconsistencies are false, however. Faulting can result in very sharp changes in relative level and even repeating of or loss of sequence or horizon. Folding can result in a reversal of sequence. A sand can "pinch out" or it can grade into a limestone. So one must be careful about apparent inconsistencies.

After the correlations are made and real inconsistencies or errors are eliminated the formations and other horizons on individual logs are compared with the lithology log and various features are identified. For example, altered and fresh (or unaltered) zones are identified. Grain size changes are often identified. Sand-shale ratios are often logged and correlated. Formation water salinities are sometimes identified. Probable interface trend or mineral locations are sometimes noted.

Taking the distance between logs into consideration geological features such as dips, synclines, and anticlines are quantified.

Cross sections, such as these, give the geologist a very good view of the area in which he is working. If these are combined with a previous knowledge of the area and with surface geophysical information, the picture can be very complete. These cross sectional correlations are commonly reduced photographically and used to illustrate geological reports, progress reports, proposals, submittals, and even stockholders reports.

B. MEDIUM SPACED TREND TRACING OR MAPPING

After obtaining an over-all view of the area in which he is working, the sedimentary exploration geologist is often interested in tracing trends. His profession is finding sedimentary mineral deposits which are small compared to the total area in which he is exploring. These deposits can and do occur in a number of different ways. They can be tabular, massive, or disseminated. They can occur at chemical or physical interfacies or discontinuities. They can occur in stratigraphic traps. The actual mechanism for deposit may or may not still be present.

Starting with the wide area results described in the first section, the geologist searches for the indicators of the type deposit he is looking for. For example, a sedimentary uranium explorationist will search for alteration or redox interfacies. Hopefully these will have radioactive anomalies associated with them, but, at this point, they are not important. A coal or trona geologist will look for traces of minerals and the sand-shale sequences identifying previously swampy areas. Copper, vanadium, and uranium explorationists may look for old channels of braided or meandering streams and for the trash associated with them. Petroleum geologists will look for possible traps.

Upon identifying possible zones, the explorationist then designs a drilling program, often coupled with a surface geophysical program which will trace out the interesting features in detail. This usually involves examining each log as it is made and locating or "spotting" the next hole on the basis of the log, the previous holes, and the geophysical (surface) lines of information. At this stage the explorationist is looking for mineral evidence as well as detailed stratigraphic features.

Use, again, is made of log correlations from hole to hole. Detail of features in the resistivity or porosity logs are usually identified and correlated along short cross sections. Except when stratigraphic discontinuities and traps are sought, not much attention is paid to absolute elevations, since area dip trends are already known. Otherwise the process is much the same as for wide spaced correlation. Trends are then identified and mapped.

C. SHORT SPACED ANALYSIS

The small sizes and linear or sinuous nature of many deposits, such as

uranium roll fronts and other types of geochemical cells, often requires a very short spacing, detailed analysis. These may be as close as five feet apart. Cores are often taken during this phase. Cuttings samples are carefully logged and often assayed chemically.

During the detail phase the logs are usually used individually to "spot" the next hole. However, short profiles or cross sections are later made in the same manner as the two longer ones described earlier. In this case, correlation with depth is usually not important. Horizontal or lateral position is important so hole deviation surveys are often made. Features such as radioactive anomalies, chemical and concentration anomalies, and discontinuities are traced and mapped in detail. All of the available curves are used at this point.

D. ORE RESERVE DETERMINATION

Only the gamma ray curve is used in ore reserve determinations for uranium. In coal determinations the density curve is used. Other types of determinations usually use the lithologic logs and chemical or x-ray assay logs. The hole locations, mineral thicknesses, grades and depths are noted on an area map. A grade cutoff and a grade-thickness cutoff are assigned depending upon the average depth. An area of influence is assigned to each hole. The radius of the area of influence will depend upon the type mineral and the type evaluation desired (i.e. proven ore, inferred ore, probable ore, etc.). For example, uranium proven ore is commonly assigned a radius of 50 feet from the drill hole or half way to the next hole, whichever is less. The tonnage or ore is determined using the area, thickness, and density. The grade is then used to determine the amount of mineral present. The sum of the values from contiguous holes then determines the reserves.

An analysis of the cost of stripping or shafting and drifting, mill siting, transportation, extraction, processing, storage, and financing will then determine if and when the reserves can be mined profitably. All information on stripping amounts, shafting, drifting, and extraction must come from the logs.

A typical ore reserve calculation would be (note that some of the conversions may change, slightly, depending upon the units desired and upon local variations.):

1. Assign areas of influence to each hole. These may be squares 50 feet on a side for proven ore (2500 square feet) and 70.7 feet on a side (5000 square feet) for inferred ore. If another hole is close, then use one half the distance to the next hole. The result will be a series of squares or other polygons. Tabulate areas.
2. Multiply the area by the anomaly thickness to obtain volume of ore. Divide the volume by 27 to obtain it in cubic yards. Tabulate volumes.
3. Multiply the volume by 3375 to obtain pounds and divide by 2000 to obtain tons of ore. Tabulate tons.

4. Multiply the tons of ore by the mineral grade in percent and by 20 to obtain pounds of mineral contained by the ore. Tabulate pounds of ore.
5. The sums of each of these values should be listed for each prospect.
6. Repeat the first three steps for the overburden for pit cost determinations. A strip should be added around the mine area for wall slope and volume. In the absence of better information a wall slope of 45° is usually assumed $\left(\frac{\text{width} \times \text{length} \times \text{depth}}{2}\right)$ for ease of calculation.

E. MINE DESIGN

Pit and underground mine design depends upon a detailed analysis of the location, thickness, and grade of the mineral. This, of course, must be done before any actual mining can be started. The general practice is the same as for reserve calculation except the detail is much greater, costs are evaluated, and estimation is kept to a minimum. Much reliance is placed upon the logs, particularly the thickness and grade indications. In addition, mechanical problems, such as soil competency, the presence of water, bed uniformity, and depths can be obtained from the logs. Commonly, coring is used to a great extent in this phase. However, the sonic log and surface seismic measurements could supplant much of this coring.

Uranium Roll Front Zonation in the Southern Powder River Basin, Wyoming

By Bruce Rubin¹

INTRODUCTION

Techniques in the exploration for uranium in Tertiary Basins of Wyoming have taken a giant step forward over the last decade. No longer is the random drilling, or "hit-or-miss" method utilized by most companies or independents. Instead, the Geochemical Cell, or "roll-front" concept has been used extensively, and its use has been a major factor in recent discoveries, especially in the southern Powder River Basin.

Briefly, the "roll-front" is a "C"-shaped interface between the altered and unaltered portions of a sandstone along which uranium has been deposited. (see fig. 1) The interface probably is caused by oxidizing agents moving down dip through a carbonaceous and pyritic water saturated sandstone (reducing environment). (Rackley, et al. 1968) As the oxidizing agents move through the reducing environment they alter the sandstone and precipitate uranium on the interface ahead of the altered portion of the sandstone.

Alteration consists mainly of sandstone color change, removal of pyrite and carbon, and kaolinization of feldspars. Although interfaces extend yards of feet laterally, the upper and lower faces are only a few tens of feet apart.

Previously, only two general criteria were used to locate "roll-fronts" in sedimentary host rocks. They were, through surface profile drilling:

- 1) to locate altered sandstone,
- 2) to locate unaltered sandstone.

Subsequent splitting of the distances between altered and unaltered sandstone until the so-called high grade "nose" or frontal portion of the "roll-front" was intercepted was a reliable but costly eventuality. (see fig. 2) Geological investigations made during Teton Exploration Drilling Company's recent discovery in the southern Powder River Basin, Wyoming, may have yielded a new technique in the exploration for uranium; a technique based on the altered-unaltered sandstone relationship, but 20-40% more efficient.

Investigation has shown a definite zonation across the "roll-front"; a zoning that, when effectively interpreted and utilized, gives the geologist a better insight into the configuration of the deposit as well as saving time, effort, and money, since fewer holes will be needed for the successful completion of each profile.

Uranium deposits in the Powder River Basin have been found during the past decade through the extensive use of the "roll-front" concept. Until now far too many holes were drilled to successfully complete each profile across the various "roll-fronts" discovered. The recognition of six zones across the "roll-front" has enabled the geologist to effectively utilize his drilling so as to intersect the high grade ORE ZONE with fewer holes per profile. Consequently, time, effort, and money have been saved allowing the geologist more time to do more meaningful geology and imaginative thinking.

¹Geologist, Teton Exploration Drilling Co., Casper, Wyoming.

ACKNOWLEDGEMENTS

Special thanks to Bob Johnson, an early collaborator, whose advice and ideas helped to develop the "zonal" concept. The specific contributions of the many who aided in the collection and interpretation of data upon which this report is based, and the cooperation of the management of Teton Exploration Drilling Company and Duval Corporation, are hereby acknowledged.

STRATIGRAPHY AND ALTERATION ZONING

The ore-bearing formation in Teton's investigation is the Wasatch formation of Eocene Age, overlying the Paleocene Fort Union formation. The Wasatch is continental in nature, consisting of interbedded sand, silt, and shale. Due to deposition in a fluvial environment there are, locally, abrupt changes in rock type such as pinch-outs and scour zones. But, analysis of the area on a gross scale indicates the overall continuity of the sand units to be fairly consistent. (see fig. 3)

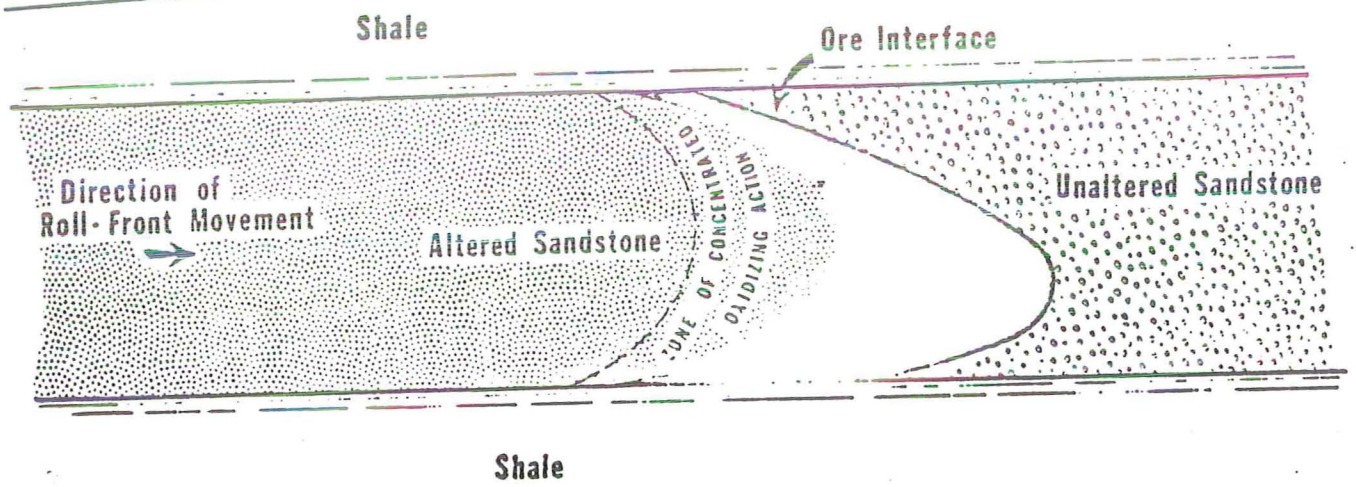
It was this continuity of geology, along with readily discernable alteration products and a large amount of usable data that enabled the writer to recognize the discreet zones across the "roll-fronts." The following describes, in sequence, from unaltered to most altered, the nature of the sandstone and the radiometric characteristics of each zone of the "roll-front." Zones illustrated in Figure 4 have been numbered to facilitate computerization.

Unaltered Host Rock

The unaltered host rock is a light to medium gray, (Geological Society of America Rock Color Chart, 1963), sub-arkosic sandstone. Grain size varies from medium-fine to medium coarse, and sorting commonly is fair. The sand grains are mostly sub-angular; grain size, sorting, and angularity are unaffected by subsequent alteration. Main constituents include clear to medium gray quartz (80%), and light gray to medium red feldspars (15%). Carbon fragments are shiny and firm (<5%); pyrite aggregates are glossy and smooth (<1%). There are no anomalous "kicks" on the gamma log in the unaltered sandstone.

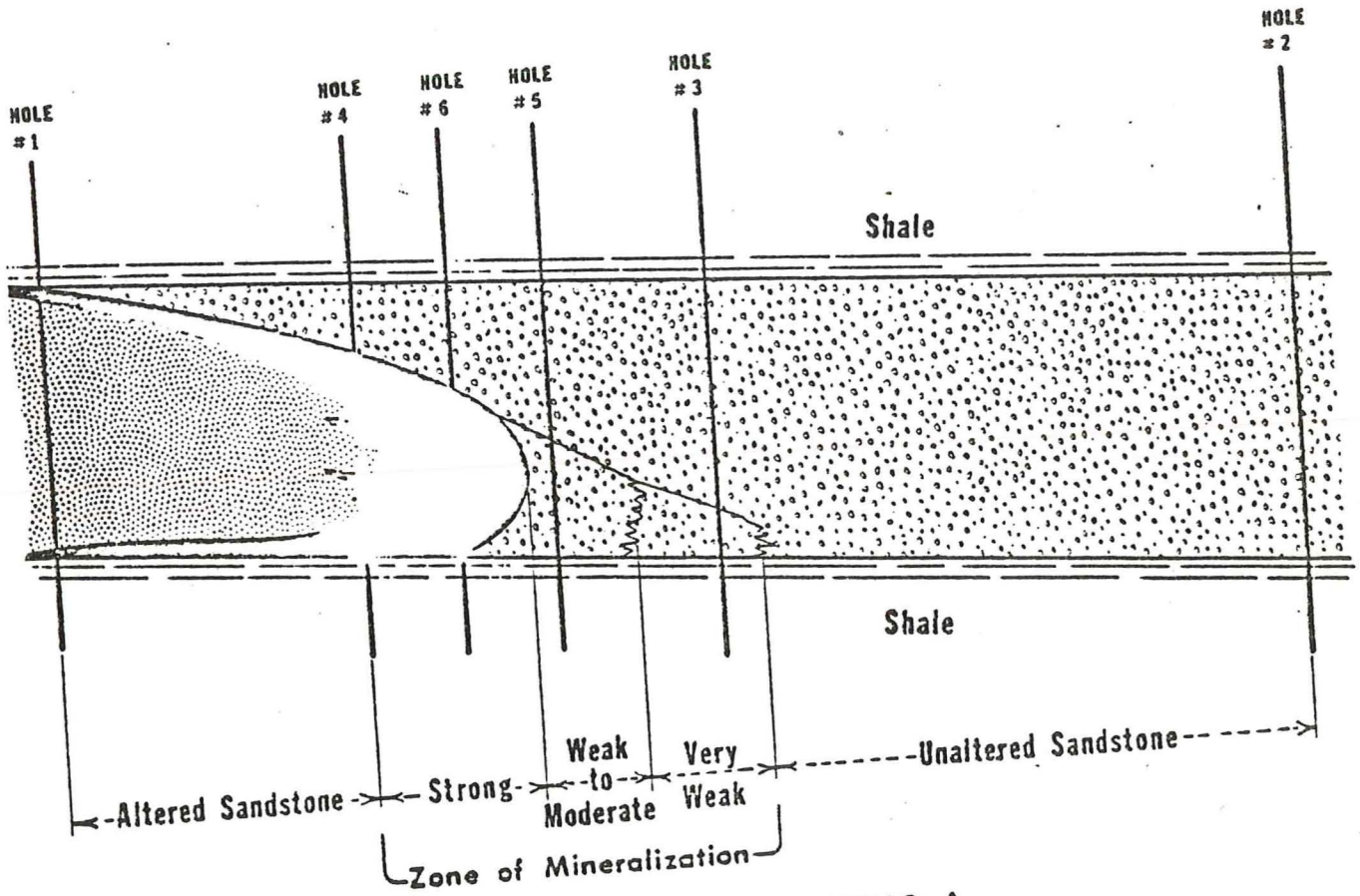
Remote Seepage Zone

The Remote Seepage Zone is very similar to the Unaltered Zone and is recognized only by a weak anomalous "kick" on the gamma log at the base of the sand host. Cores of the Remote Seepage Zone



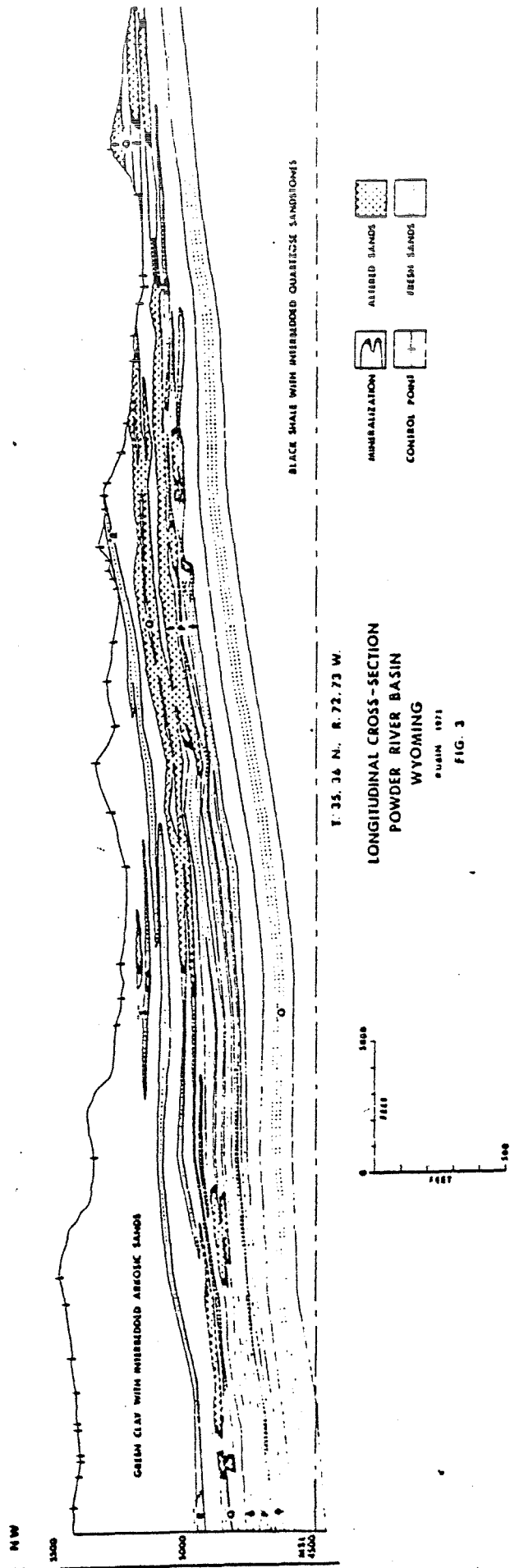
CROSS-SECTION ILLUSTRATING THE "CLASSIC-TYPE" URANIUM "ROLL-FRONT"

FIG. 1



CROSS-SECTION ILLUSTRATING A TYPICAL SOUTH POWDER RIVER BASIN TYPE "ROLL-FRONT" AND HOLES DRILLED USING THE "SPLITTING THE DISTANCE" TECHNIQUE.

FIG. 2



host rock exhibit no visible alteration.

Near Seepage Zone

The first signs of alteration can be detected in the Near Seepage Zone, and are seen as weak, spotty limonite stains on the quartz grains with traces of kaolinite from feldspar. The anomalous "kick" on the gamma log is stronger than that of the Remote Seepage Zone but rarely exceeds an ore grade and thickness of 5' @ .12% U308. Both radiometric anomaly and alteration usually are confined to the lower 1/2 to 1/3 of the sand host.

Ore Zone

Increased mineralization changes the overall color of the host rock to medium gray/medium dark gray in the Ore Zone. Limonite stain increases to about 5%, and the first signs of hematite staining occur. Kaolinite from feldspar increases to about 15%, and initial pyrite breakdown can be seen as slight pitting and tarnishing. The gamma log anomaly is fairly strong and unbroken; grades and thicknesses of the ore are rarely less than 6' @ .15% U308. Both alteration and radiometric anomaly usually are confined to the lower 2/3 to 1/2 of the sand host.

Interface Zone

The Interface Zone includes more intense oxidizing action than any other zone. This oxidizing alteration changes the color of the host rock in the Interface Zone to medium gray/yellowish gray. This is caused by a moderate amount of limonite stain; hematite is scarce, but increasing. Kaolinite from feldspar increases to 25%. Pyrite is more pitted and tarnished, but still readily discernable. Carbon, beginning to show the effects of alteration, is slightly dull and slightly flaky. The gamma log anomaly is broken into a series of at least two, usually three "kicks." The ore grades tend to be greater than .15% U308, while the ore thicknesses tend to be less than 6'. Cores of the Interface Zone host rock show dark gray sand in the position of the "kicks," and yellowish gray sand between the "kicks." Both alteration and radiometric anomaly usually are confined to the lower 2/3 of the sand host.

Near Barren Interior Zone

The alteration of the Near Barren Interior Zone is recognized easily because of its grayish orange/grayish yellow color. Limonite stain is dominant; hematite stain is increasing. Kaolinite from feldspar is greater than 50%; pyrite is pitted and dull and on the verge of being totally destroyed. Carbon is dull and flaky. The gamma log anomaly is usually two strong "kicks"; the upper "kick" is usually about 1/4 the way down from the top of the sand host, and the lower "kick" is at the base of the sand host. Cores of the Near Barren Interior Zone host rock show dark gray sand in the position of the "kicks" and yellowish/orange sand between the "kicks." Grades and thicknesses of the ore commonly are about 6' @ .15% U308.

Remote Barren Interior Zone

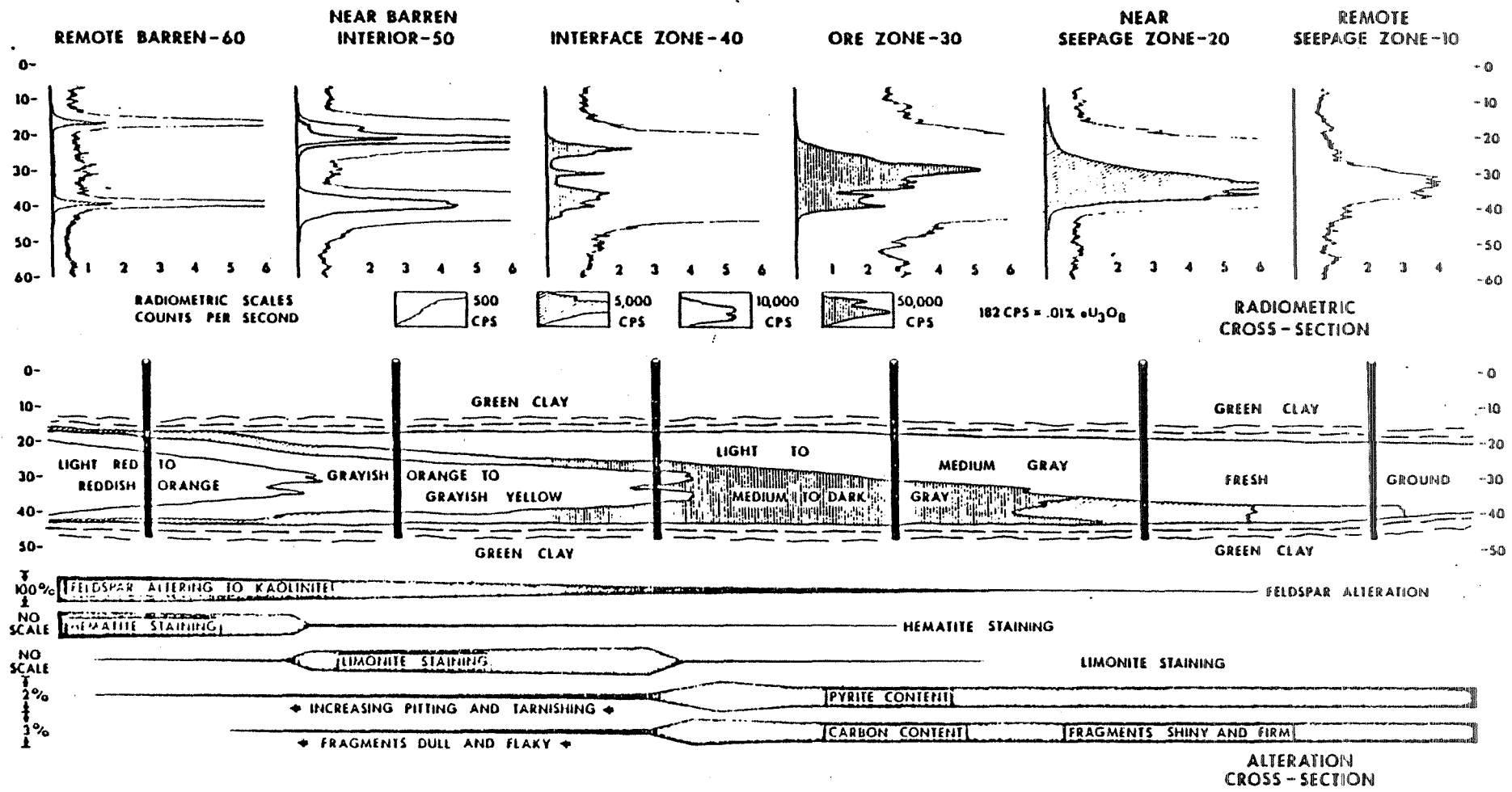
The striking reddish alteration of the Remote Barren Interior Zone is caused by a dominance of hematite stain; limonite stain is weak. Kaolinite from feldspar is greater than 75%, and pyrite and carbon are almost totally destroyed. The gamma log anomaly is usually two "kicks"; one at the top of the sand host, and one at its base. Grades and thicknesses of the ore usually are less than 5' @ .12% U308. Cores of the Remote Barren Interior Zone host rock show medium gray sand in the position of the "kicks," and reddish sand between the "kicks." The horizontal distances between zones is proportional to the sand thickness. For instance, in a 30' sand unit the distance from the Remote Barren Interior Zone to the completely unaltered host rock is about 200'. In a 15' sand unit that distance may be 50 feet or less.

The importance of the recognition of these zones and the effective utilization of subsequent drilling cannot be stressed too strongly. To illustrate this point consider, again, figure 2. Here the "splitting the distance" technique was used to intersect the Ore Zone of the "roll-front." If hole #3 had been recognized as a Remote Seepage Zone, hole #4 and hole #5 would not have been needed. An effective off-set hole to position 6 would have been made instead of drilling positions 4 and 5. (Effective off-sets can be made following the recognition of all zones except the Remote Barren Interior and Unaltered host rock.) Figure 2 shows 33% overdrill for that specific profile. If savings of that magnitude in time, drilling, and probing could be duplicated or even approached using the aforementioned zonal criteria, the cost per pound of uranium found would decrease considerably.

PHYSICAL CONTROL OF "ROLL-FRONT" MOVEMENT

Control of the movement of the "roll-front" by the physical nature of the host sandstone was also revealed by the detailed investigation. The speed and direction of the "roll-front" are definitely affected by the thickness and changes in thickness of the host rock. Note how, in figure 5, the zones of the "roll-front" move around thinner sand zones, and toward thicker sand zones.

Commonly, the shale member between host sand horizons will "lens-out" and the "roll-front" of the upper sand will drop through the shale break and occupy portions of the lower sand host. (see fig. 6) The geometry of the "roll-front" in the lower sand host usually is without definite shape and is surrounded completely by unaltered sandstone.



GENERAL ROCK DESCRIPTION

ARKOSIC SAND - COMPACTED BUT NOT CEMENTED
 MEDIUM TO COARSE GRAIN
 FAIR SORTING
 SUB-ANGULAR TO SUB-ROUNDED SHAPES
 QUARTZ > 80% FELDSPAR < 15%
 CARBON FRAGMENTS < 5% PYRITE \pm 1%
 BLACK AND GREEN ACCESSORY MINERALS < 1%

**"TYPE" GEOCHEMICAL CELL
 POWDER RIVER BASIN
 WYOMING**

RUBIN 1971

FIG. 4

Sec. 2a, p 5 of 8





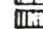
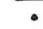


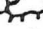

SOUTH POWDER RIVER BASIN

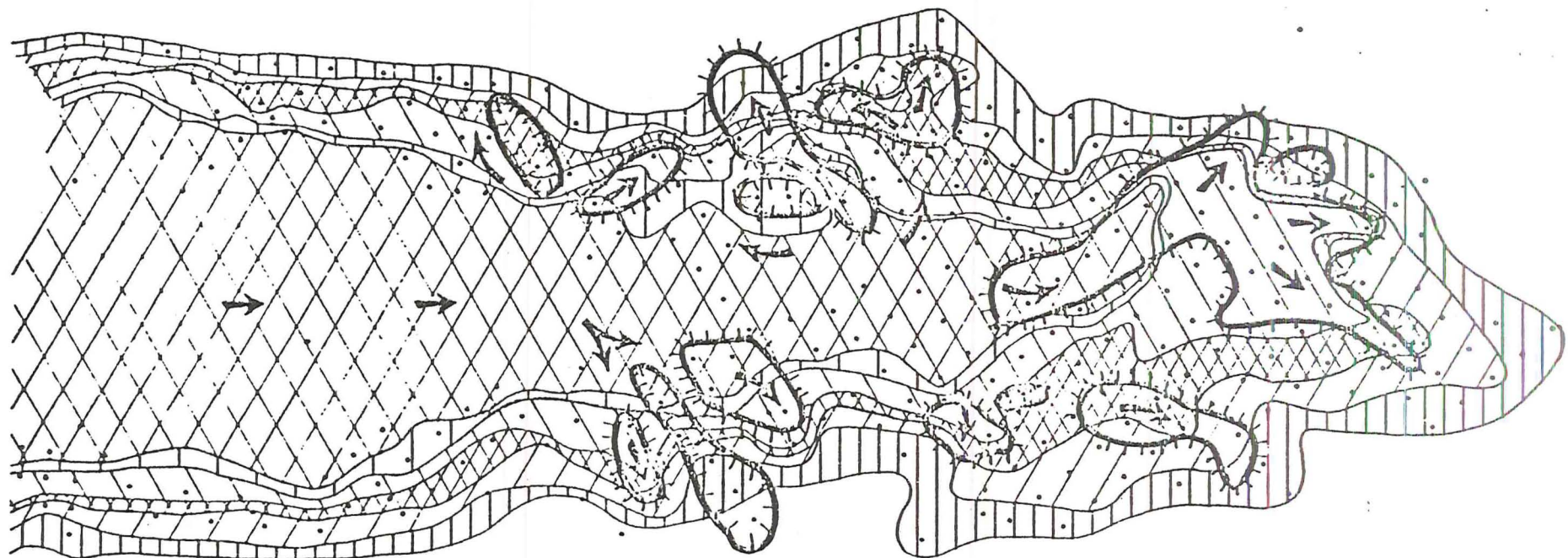
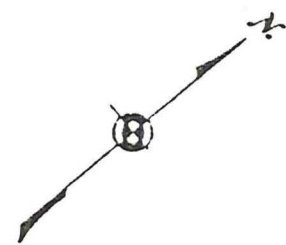
SECTION 14 ORE BODY

T.36 N., R.73 W.

RUBIN 1971

FIG. 5

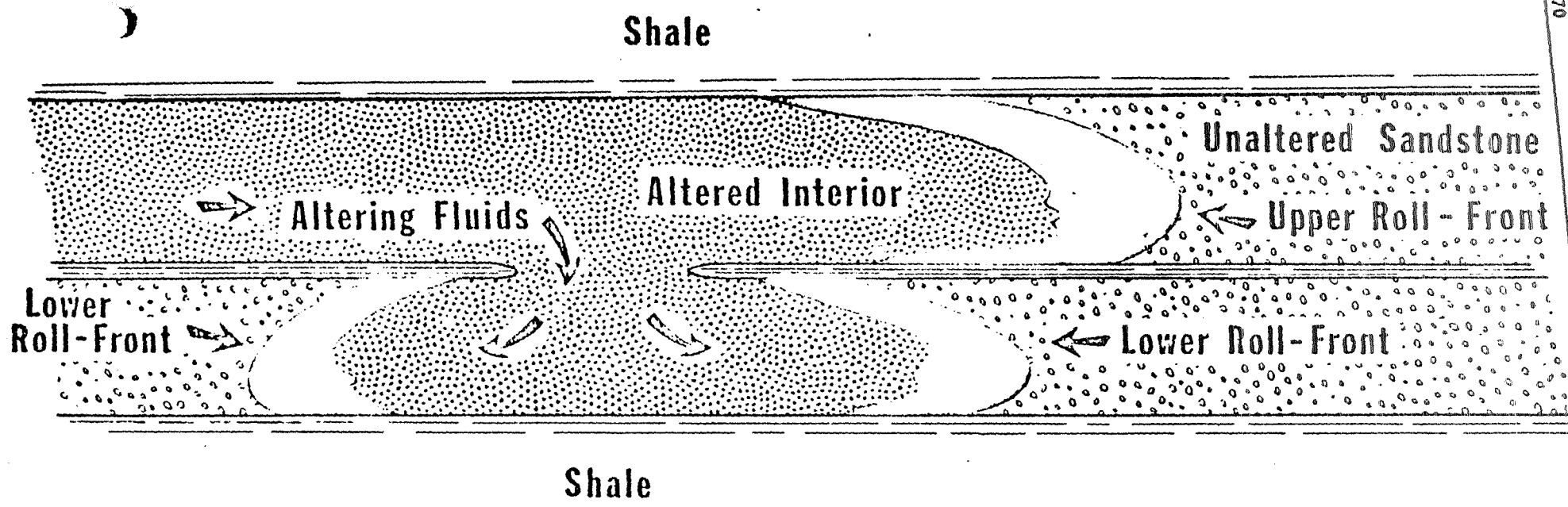
-  REMOTE BARREN INTERIOR ZONE
-  NEAR BARREN INTERIOR ZONE
-  INTERFACE ZONE
-  ORE ZONE
-  NEAR SEEPAGE ZONE
-  REMOTE SEEPAGE ZONE
-  DRILL HOLE LOCATION
-  ZONE OF SAND THINNING
-  ZONE OF SAND THICKENING
-  DIRECTION OF "ROLL-FRONT" MOVEMENT



PLAN VIEW SHOWING MOVEMENT OF "ROLL-FRONT" ZONES WITH RESPECT TO SAND THICKNESS

0 100 200 300

Sec. 2a, p 6 of 8



CROSS SECTION ILLUSTRATING VERTICAL MOVEMENT OF "ROLL-FRONTS"

FIG. 6

Sec. 2a, p 7 of 8

REFERENCES

- Adler, H. H., and Sharp, B. J., Uranium Ore Rolls--Occurrence, Genesis, and Physical and Chemical Characteristics, Guidebook to the Geology of Utah, No. 21, Utah Geological Survey, 1967, pp. 53-77.
- Bailey, R. V., Applied Geology in the Shirley Basin Uranium District, Wyoming, Contributions to Geology, University of Wyoming, Vol. 4, No.1, 1964.
- Johnson, R. L., and Rubin, B. I., Observations on the Relationship of Geologic, Geometric, and Radiometric Characteristics of a Uranium Mineralized Geochemical Cell, 1969. (unpublished company report)
- Melin, R. E., Description and Origin of Uranium Deposits in Shirley Basin, Wyoming, Economic Geology, Vol. 59, 1964, pp. 835-49.
- Rackley, R. I., Shockey, P. N., and Dahill, M. P., Concepts and Methods of Uranium Exploration, Wyoming Geological Association Earth Science Bulletin, September, 1968, pp. 23-24.

URANIUM LOG INTERPRETATION

GAMMA RAY ANOMALY CALCULATION METHODS

There is no "standard" method of calculating the apparent uranium content of a horizon from the gamma ray log. Further, there are few good methods of determining disequilibrium.

The method for manually calculating grade most commonly used by uranium exploration people and mining people is the method proposed by the A.E.C. This method is:

1. Pick bed boundaries at the point where half of the peak counting rate occurs.
 - a. This applies to a simple bed only.
 - b. The bed boundary in a multiple bed situation is taken as half way between the peak and valley.
 - c. The bed thickness is the distance between bed boundaries.
 - d. Bed thickness is often rounded off to the nearest half foot, two tenths foot or one tenth foot depending upon depth and interval used.
2. Start at the top (or bottom) bed boundary the counting rates are read at half foot intervals and tabulated.
 - a. Sometimes the interval used is 0.2 foot.
 - b. Occasionally the interval is 0.1 foot.
 - c. Almost all foreign intervals and some U.S. intervals are 0.1 meter.
 - d. The tabulation is continued to include the next bed boundary or the first value past the next bed boundary.
3. Correct each counting rate for deadtime effects by using this expression to obtain the correct rate, N:

$$N = \frac{n}{1 - \mu n}$$

where n is the recorded or uncorrected counting rate and μ is the deadtime in seconds.

4. Apply the tail factor.
 - a. Multiply the first and last value from a single bed by 1.38.
 - b. In a multiple bed situation do not use the 1.38 factor for interior or shared boundaries.
5. Obtain the area under the curve by adding all tabulated, corrected counting rates.
 - a. Do not use any value more than once.
 - b. Eliminate any valleys more than three feet thick if they are lower than half peak value. These are probably barren

6. Multiply the area by the "water factor" or hole factor. This is obtained empirically. This is the true area.
7. Multiply the true area by the K-factor to obtain the GT product.
 - a. The K-factor will depend upon the calibration of the tool and upon the intervals used.
 - b. The usual U.S. K-factor is for half-foot intervals.
8. Divide the GT product by the thickness to obtain equivalent U_3O_8 grade in percent.
9. If the disequilibrium is known it may be used to correct the value of G at this point.

The deadtime, μ , of the system is obtained by using the expression

$$\mu = \frac{n-mR}{nm(1-R)}$$

where n is the uncorrected counting rate in a known grade low value bed; m is the same for a higher grade bed, and R is the ratio of actual low grade to actual high grade. This is the so-called "two-pit" method and is described in A.E.C. and E.R.D.A. literature.

This method which has just been described is reasonably accurate and is used in most of the manual calculations. Its accuracy improves with the thickness of the bed. At three feet thickness its accuracy is 95.6% of the correct value. At ten feet thickness it is 98.7% of the correct value.

A few people and most computer programs use a "background-to-background" method. This method is identical to the previous or "tail-factor" method, except the T.38 factor (4a) is not applied. Instead, the counting rates are tabulated from three intervals before the first bed boundary until three intervals after the last bed boundary. It is necessary with this method and is part of the A.E.C. Gamlog program to break each multiple bed into a series of apparent, individual beds. This method is described in A.E.C. literature. It has the advantage of increased accuracy. At a three foot thickness it is within 99.4% of the correct value and improves in accuracy as the thickness increases.

A third method is applicable only to uniform anomalies more than three feet thick. Unfortunately, it is applied to many situations incorrectly. In this method the bed thickness is determined as before. The grade, G, is determined with the expression

$$G = 2KN$$

where K is the factor for half-foot intervals and N is the average, peak, corrected counting rate. This method should also have the hole factor applied to its value of G.

These three methods probably represent 80% of the serious interpretations. The first method is, by far, the most popular. The second is used, primarily, in machine calculations (perhaps 10%). The third method is probably used in another 10% of the serious evaluations.

The remaining 20% of calculations is made up of several methods. The 2KN method is often erroneously applied to the average anomaly counting rate instead of the average peak counting rate. Further, it is commonly applied to anomalies less than three feet thick.

A method commonly used for field estimations is an extrapolation of a 1000 cps grade. For example: "1000 counts per second equals .05%" Therefore, 10,000 counts per second equals 0.50%. This makes no allowance for dead-time or other corrections, but is quite satisfactory for field estimations. Unfortunately, it is too often used for reserve calculations. This results in an apparent severe disequilibrium, and worse, in a nonlinear disequilibrium.

Bed thicknesses are often taken from counting rates which are 1/3 peak. However, it is easy to demonstrate, mathematically, that the bed boundary must be at the half value.

In general, contractor methods are one of the first two and are readily accepted.

INTERPRETATION OF GAMMA-RAY LOGS

BY

JAMES K. HALLENBURGABSTRACT

The area under a gamma-ray log curve is a function of the amount of radioactive material within the sensitive volume of the detector. The finite volume of detection results in bed boundary effects and multiple bed effects which can be simplified for analysis.

INTRODUCTION:

The purpose of this discussion is to furnish a working reference for the interpretation of Gamma-Ray logs for uranium exploration. There are discussions and topics included which obviously are not needed for field or even office use. There are many which have been covered previously. However, a thorough knowledge of any system is vital to its' effective use. The principles outlined here are applicable to other fields and to other systems with minor modifications.

The procedures recommended will, undoubtedly be modified from time to time. However, the three important considerations are:

1. Accuracy. The method we use to prepare raw data for the initial filing and compilation must be the most accurate we know to use.
2. Uniformity. If we each use a different interpretation system nothing but confusion will result. Therefore, we must use a uniform system for preparing raw data.
3. Standardization. Since we use our information to compare, trade, bargain, and inform other people and organizations we must use a standard method so we will each know without preamble what we are talking about.

We feel that this paper is a start in this direction as far as our organization is concerned.

INTERPRETATION OF GAMMA RAY LOGS

Downhole gamma ray logs can be run with a number of types of equipment and for a number of purposes. This discussion will be confined to logs made with scintillation equipment in a steel housing. A standard ratemeter and pulse counter will be assumed.

The principles will be applicable to logs made with Geiger-Mueller, proportional, and semiconductor detectors. They will also apply to equipment which scales downhole, corrects or compensates for deadtime, and which measures pulse current.

A discussion of the various systems available will be covered in detail at another time.

It is strongly recommended that the references listed at the end of this be researched; particularly the Atomic Energy Commission papers.

Operation

A scintillation gamma ray detector uses a fluorescent crystal, usually thallium-doped, sodium iodide. This crystal will fluoresce in the visible light range when a gamma photon passes through it. The resulting light pulse is very brief; approximately 400 nanoseconds (4×10^{-7}) in duration. This light pulse is detected with a photo-multiplier (a sensitive, amplifying phototube) and then the number of pulses in a given amount of time is counted. In general, the density of the gamma flux is directly proportional to the amount of gamma emitting material present. That is to say, by counting the number of gamma pulses per second we can determine the amount of radioactive material present, emitting gamma rays. We can detect only gamma rays with our equipment because the housing and drilling mud effectively shield out the beta and alpha particles and there are not enough natural neutrons present to make a good measurement.

Calculations

The area under the gamma ray curve is a function of the amount of radioactive material present within the sensitive volume of the detector. This has been shown in the paper "Quantitative Interpretation of Gamma Ray Logs." Therefore, if we calculate the area under an anomaly we may interpret this in terms of equivalent uranium oxide:

$$A = \int (eU_3O_8) \quad 1)$$

We may calculate the area under any curve by a process of integration.

Integration is merely a process of breaking an area into a number of rectangles whose widths are uniform and as small as possible and whose heights are equal to the average amplitude of the curve. This is shown in Figure #1. As you can see the error of the area determination would increase if the width of the rectangles was increased.

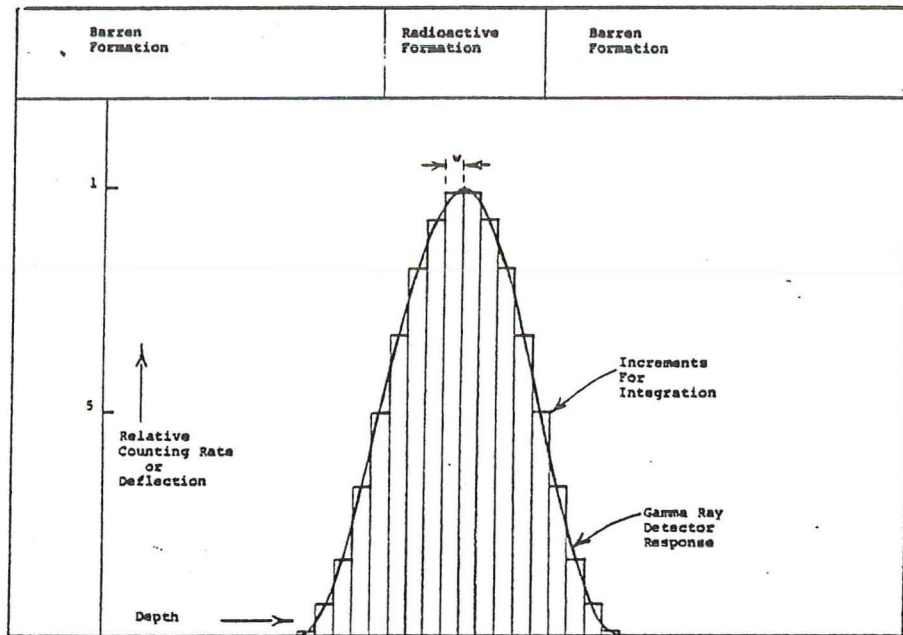


Figure 1

The area under the curve then becomes:

$$A = w h_1 + w h_2 + w h_3 + w h_4 + \dots + w h_b \quad 2)$$

$$A = w \sum_{p=1}^b h_p \quad 3)$$

where b is the number of rectangles, w is the uniform width and h is the height of the rectangle.

The average counting rate for each rectangle, N is an indication of the height, h. Therefore, if the width is constant

$$A = w \sum_{p=1}^b N_p \quad 4)$$

Thus, w times the number of intervals is a function of the thickness of the bed and N a function of the grade, G of the ore in the bed. Therefore,

$$KA = GT$$

5)

where K is a proportionality constant.

We are saying here that we can break an anomaly into a number of uniform width rectangles whose heights are the counting rates and by applying a K factor we can determine the effective average grade of that anomaly.

This can be found in detail in the paper "Quantitative Interpretation of Gamma Ray Logs".

Bed Boundaries, Theory

It is important for us to know the thickness of the bed as well as the grade. Figure 2. A gamma ray detector always "sees" the radioactive bed before entering it and after leaving it.

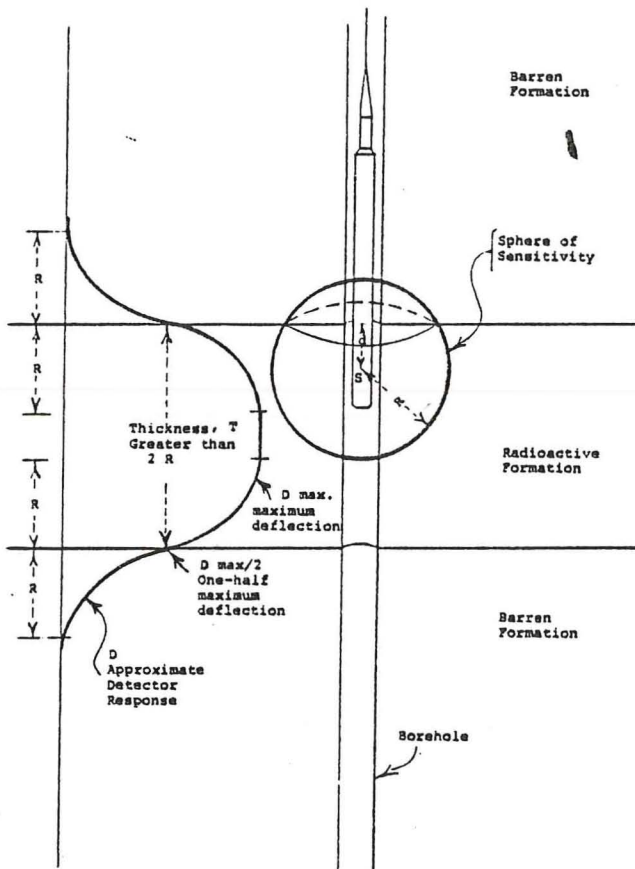


Figure 2

This amount of anticipation is the zone or radius of investigation. It is typically on the order of one foot in an average formation. It will depend upon the type of detector, the size of the detector, the type housing, the hole size, the discrimination level, and the time constants. The response is sinusoidal and is given for a thick bed (T greater than 2 R) by the deflection (neglecting the effect of the borehole):

$$D = 1/3 \pi (2 R^3 + 3dR^2 - d^3)k \quad 6)$$

where d is the distance from the detector to the bed boundary and R is the radius of investigation of the detector. Figure 2.

If we check the slope of the deflection curve by taking the second derivative of D with respect to d and see what happens when d = 0, (in other words, at the bed boundary) we find that the slope passes from positive to negative with the zero, or inflection point at the bed boundary.

The maximum amplitude must occur when the detection volume is all within the bed or at d = R. Then the deflection becomes:

$$D_{\max} = 4/3 \pi R^3 k \quad 7)$$

When the detector is at the bed boundary d = 0 and

$$D_0 = \frac{2}{3} \pi R^3 k \quad 8a)$$

or

$$\frac{D_0}{D_{\max}} = \frac{1}{2} \quad 8b)$$

The minimum is when $d = 2R$ or before the sphere enters the bed. Then $D_{\min.} = 0$.

This is telling us that with a thick, simple bed with a sharp boundary, the inflection point always occurs at the bed boundary and it always occurs at half amplitude.

If the bed is thin (T less than $2R$) then the deflection becomes less than it would be if the bed were of infinite thickness. See Figure 3.

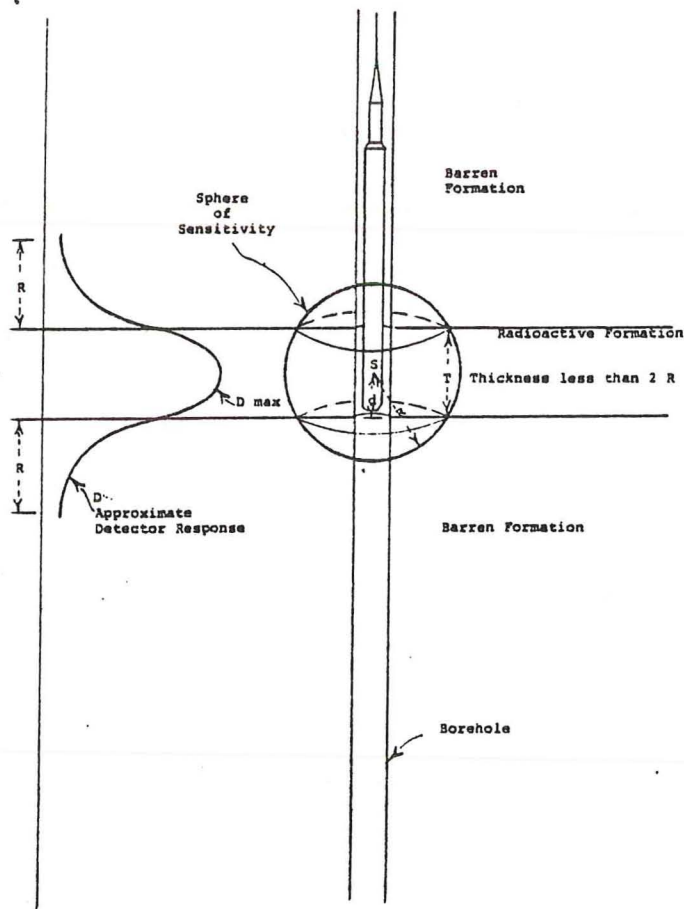


Figure 3

In this case the actual deflection will be:

$$D = C_1 D_1 + C_2 D_2 + C_m D_m \quad 9)$$

where C_1 and C_2 are the volumes of the upper and lower adjacent beds enclosed by the sphere of investigation and C_m is the volume of the beds of interest, enclosed. D_1 , D_2 , and D_m are the infinite

thickness deflections of these beds.

If the detector is centered in a thin bed and the deflections of the adjacent beds are negligible the true deflection or the infinite thickness deflection becomes:

$$D_m = \frac{16 R^3 (D-1) + 1}{T (12R^2 - T^2)} \quad 9A)$$

Counting Rates, Theory

All radioactive events are random occurrences. That is, we are unable to predict exactly when one, individual event will occur.

Further, all electrical (or photo) pulses resulting from the detection of these radioactivity events have a finite length. This is because the area under the pulse is proportional to the power of the pulse. Since all of our instruments need some power to activate them, however sensitive they may be, there can be no such thing as a pulse of zero width (zero deadtime).

Pulses which start out narrow are spread out as they are amplified, clipped and transmitted. The resulting width of a pulse will depend upon the various inherent time constants of the circuits and upon the corrective measures taken. For example, with one major type of equipment the output of the gamma ray tool puts a negative pulse on the downhole power supply line for transmission to the surface. That is, the supply line has a potential of 125 volts which is pulled down, momentarily, to a potential of 120 volts by the pulse. The only place the supply line can obtain the power to recharge to 125 volts is from the surface power supply. The cable has a capacity of .14 microfarads and the power supply has a resistance of about 200 ohms. Therefore, the recharging time constant is:

$$T/C = RC = 200 \times .14 \times 10^{-6} = 28 \text{ microseconds}$$

This means that no matter how short the driving pulse is (it is typically about 2 microseconds), the resulting pulse at the surface will be about 20 microseconds long. That is, unless corrective circuits are incorporated. This is generally done and will not be covered here.

The problem is, that with a finite length and a random nature, there is a statistical probability that one pulse may occur on top of or close to the preceding pulse. The result is that the instrumentation sees these as one pulse. There is a time after the start of a pulse during which another pulse cannot be resolved. This is called the system deadtime and is related to the pulse width. The probability of this occurring is:

$$P = \frac{\Delta N}{N} = \mu n \quad 10)$$

where ΔN is the counting rate error due to coincidence, N is the correct counting rate, μ is the deadtime or pulse width in seconds and n is the recorded counting rate. Similarly, the counting rate error is:

$$\Delta N = \frac{\mu n^2}{1 - \mu n} \quad 11)$$

and the correct counting rate is:

$$N = \frac{n}{1 - \mu n}$$

This is saying that there can be errors in the counting rate recordings caused by the random nature of the signals and finite pulse length. Since we can read the analog recordings to $\pm 1\%$, the correction should be applied any time it is greater than $\pm 1\%$. This point is given for various deadtimes:

System Deadtime	Recorded Counting Rate
μ Microseconds	n % correction point
.5	10,000 cps
1	5,000 cps
2	2,500 cps
5	1,000 cps
10	500 cps
20	250 cps
50	100 cps

Likewise, any time the correction becomes greater than 50% the correction is not reliable. This is not a hard and fast point, but rather, the point at which the reliability of the correction becomes less than the chances of error (reliability becomes less than 1). These points are:

μ Microseconds	n 50% correction
.5	1,000,000 cps
1	500,000 cps
2	250,000 cps
5	100,000 cps
10	50,000 cps
20	25,000 cps
50	10,000 cps

This limit is imposed by the longest deadtime in the system regardless of the correction applied. For example, if a system is corrected so that the readout has zero deadtime, but at some place in the system really has a 5 microsecond deadtime, the limit of reliability is still 100,000 cps. In this case a zero deadtime is only a convenience in reading and calculating logs. It is not a real error correction.

These two relationships illustrate not only the fallacy of a zero deadtime system, but also, the importance of having as short a deadtime as possible. In other words, it is fallacious to label a system as corrected to zero deadtime when really you have a 1 microsecond pulse width corrected to zero deadtime. It is equally erroneous to use a compensating network to obtain a 2 or 3 microsecond pulse width at the surface when the trigger circuit in your ratemeter puts out 30 microsecond pulses.

Interpretation

The explanation on page 3 involved an integration from zero to zero through the anomaly. This is one way of making an integration of this type and is the way the A.E.C. Gamlog program handles the problem. However, for a visual inspection and manual interpretation it is easier to start and end at the bed boundaries. Bed boundaries must be found anyway and we never have a zero indication on our logs because of the radioactivity from adjacent beds. Therefore, we use a different method which will give essentially the same results.

GROSS GAMMA LOG WORK SHEET										
Probe K. Factor _____	Hole Dia. _____	Remarks _____	Hole No. _____							
Air Factor _____	Water Factor _____	Composite Kc _____	Property _____							
Mud Factor _____	Dead Time (t) _____	Interp. by _____	Coord. N. _____							
Casing Factor _____		Section _____	Date _____							
			R. _____							
	n	$N = \frac{n}{1 - nt}$	n	$N = \frac{n}{1 - nt}$	n	$N = \frac{n}{1 - nt}$	n	$N = \frac{n}{1 - nt}$	n	$N = \frac{n}{1 - nt}$
Lower Boundary										
Upper Boundary										
Thickness (T)										
e1	E1									
e2	E2									
	E1 + E2									
(E1 + E2)	(1 38)									
(0.6-1.0)	11 +11									
(1.1-1.5)	12 +12									
(1.6-2.0)	13 +13									
(2.1-2.5)	14 +14									
(2.6-3.0)	15 +15									
(3.1-3.5)	16 +16									
(3.6-4.0)	17 +17									
(4.1-4.5)	18 +18									
(4.6-5.0)	19 +19									
(5.1-5.5)	110 +110									
(5.6-6.0)	111 +111									
(6.1-6.5)	112 +112									
(6.6-7.0)	113 +113									
(7.1-7.5)	114 +114									
(7.6-8.0)	115 +115									
(8.1-8.5)	116 +116									
(8.6-9.0)	117 +117									
(9.1-9.5)	118 +118									
(9.6-10.0)	119 +119									
Total Area (A)										
(A) (Kc) = G1										
G1/T = Obs \downarrow μ U ₂₃₈ (G)										
Thickness (T)										

Figure 4

The first step in any interpretation is to examine the log heading and determine what the conditions were under which the log was recorded. These conditions should be noted and taken into consideration.

There are several numerical values which must be obtained from the log heading and recorded on the top of the Gross Gamma Log Work Sheet, Figure 4.

These are:

1. Probe K factor
2. Water factor
3. Casing factor
4. Deadtime

In addition, these are useful

1. Hole diameter
2. Time constant
3. Hole number
4. Date

For a simple bed the next step is to find the bed boundaries. (Figure 5).

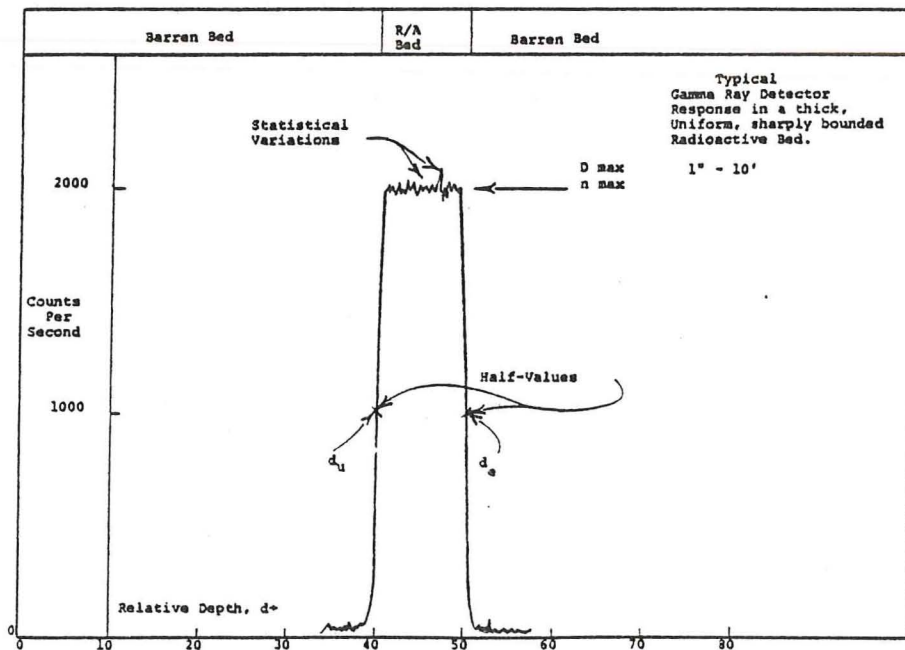


Figure 5

A simple bed is a single, isolated, sharply bounded, homogeneous bed. It is characterized by a simple appearance and a distance of approximately 2 feet from background to maximum deflection. Determine the maximum counting rate, N_{\max} . Divide this value by 2. The two places on the curve where the value $\frac{N_{\max}}{2}$ occurs are the lower and upper bed boundaries if the bed is more than 2-3 feet thick (the diameter of investigation of most scintillation gamma ray probes). If the bed is thinner than 2 feet the error will not be significant. Therefore, always use the half amplitude value to locate a bed boundary.

A bed boundary counting rate and depth is our starting point in determining the amplitudes of the investigation rectangles described on page 3. It makes no difference whether you start on the top or bottom. Just be consistent. The counting rate value of this starting point is labeled e_1 .

Ideally we want the width of the integration rectangles to be as narrow as possible. In a mathematical integration the width is made to approach zero. In the case of a manual integration our resolution is not that good. One-half foot intervals appears to be the best compromise between accuracy and readability. Smaller and larger intervals have been used, but difficulty of reading and reduction of accuracy respectively, become problems. Therefore, our discussion will be limited to half foot intervals.

After determining e_1 the counting rate value of each intermediate half foot through the anomaly must be determined and listed. These values are labeled i_1 , through i_{last} . We are listing the approximate average height of each rectangle which extends $\pm \frac{1}{2}$ foot from the determined point.

Finally, we have listed all of the intermediate values (i_1 to i_{last}) and come to the last point. If the bed is an integral multiple of one-half foot thick (i.e. 1.5, 4.0, 6.5 etc.) the last point, e_2 will coincide with the other bed boundary. If the bed thickness is not an integral half foot the value of e_2 will be the next half foot value after the bed boundary.

Each of these counting rates must be corrected for deadtime error before it can be used. As we saw earlier, the corrected counting rate

$$N = \frac{n}{1 - \mu n} \quad 12)$$

Also, as we saw earlier, the area under the anomaly is a function of the grade, which we are trying to find, and the sum of the counting rates (4). Equation 4 summed the counting rates from zero to zero. We are only summing here from bed boundary to approximate bed boundary. Obviously the detector is affected by the

radioactive material while it is in the barren zone and by the barren zone while it is in the radioactive zone as long as the detector is within one influence radius of the bed boundary. Therefore, the A.E.C. has determined empirically that the value of E_1 , and E_2 (corrected first and last readings) must be multiplied by 1.38 to take into account the "tails". Thus, 1.38 is the "tail factor". We have checked this value and have found that it is very close for beds thicker than 1 foot and thinner than about 10 feet. At a later date a better method will undoubtedly be adopted.

Thus, to find the area, A under the anomaly, the corrected counting rates of the intermediate values (I_1 through I last) must be added, plus $1.38 E_1$ and $1.38 E_2$. Therefore:

$$A = 1.38 (E_1 + E_2) + \sum_{1}^b I_b \quad 13)$$

Corrections

While the idea that the gamma flux density through the detector is proportional to the radioactive material present in the formation through which the borehole passes is essentially correct, there are some other factors which must be considered.

K Factor

Since the anomaly area is a function of the radioactivity, a proportionality constant must be applied to convert from area to equivalent uranium oxide. This proportionality constant is determined empirically by use of the A.E.C. "pits."

The A.E.C. pits are located in Casper, Wyoming; Grants, New Mexico; George West, Texas and Grand Junction, Colorado. The N-3 pit in Grand Junction is the industry standard and the others are secondary standards. These pits are all designed to be infinite in apparent size. That is, they are thicker than 2 feet and have a radius greater than 2 feet. They are filled with uranium ore of a known grade and are sealed in aluminum containers so they are at equilibrium. The reference "A.E.C. Calibration pits" contains the details of these pits.

To use the pits a system (probe, cable, ratemeter, recorder, digital system) is run complete, in two pits, a high grade and a low grade pit. The probe is moved very slowly through the ore or is stopped centered in the ore. The response, in counts per second is noted for that grade of ore. This is repeated for the second pit. Since the grade is known and the response is determined the K factor may be determined.

$$K = \frac{G}{2 N} \quad 14)$$

where N is the corrected counting rate.

Two Pit Method

The method usually used is the so called "Twopit Method" for determining the apparent system deadtime and the average K factor. The details are given in the reference "Twopit, A Different Approach to Calibration of Gamma-Ray Logging Equipment" by Crew and Berkoff. Briefly the method is:

1. Determine the average counting rate in several runs through the ore or for at least 20 seconds. Do this for 2 grades of ore. Record several curves through the ore. Use an expanded depth scale.
2. Determine the approximate system deadtime by using this expression for deadtime in seconds:

$$\mu = \frac{n - Rm}{nm (1 - R)} \quad 15)$$

where n is the recorded counting rate per second in the low pit, m is the rate for the high grade pit and R is the ratio of the grade of the low pit to the high pit (for Casper pits $R = 0.1476$).

3. Use the value found for μ to calculate the K factor for the low pit, using equation 13. Use this K factor and the half-foot values of the high pit to determine the grade of the high pit. If the grade is 2.242% the dead-time is correct. If the grade is high, lower the dead-time slightly. Repeat to agreement.

The K factor lumps several constants. Since the area is in feet-counts per second, the K factor units are % equivalent U_3O_8 per cps. The value is always determined or corrected for an air-filled borehole.

The Area is multiplied by the K factor to determine the uncorrected Grade-Thickness product

$$GT = KA \quad 16)$$

Corrections

Unfortunately, there are a number of modifying influences in the borehole. These must be taken into account and corrected for.

Hole Size

So far we have assumed that the detector is completely surrounded

with formation. This, of course, is only true when using a punch probe in a truck load of ore. Generally there is a borehole through which the probe is passed. Therefore, the uncorrected GT value must be multiplied by an air factor, water factor, or mud factor which will take hole size into account.

Air Factor

If we assume that the probe is centered in the borehole (it usually is not) then the amount of radiation reaching the detector in an air filled, uncased borehole will be a function of the hole diameter. This is because 50% of the radiation reaching the detector originates in the first half inch layer of formation. However, the detector is usually against the wall of the hole, so the effect is somewhat modified. Since the response in this situation is highly complex, the Air Factor is normally determined for a particular probe empirically. Several curves of Air Factor are attached. Normally the Air Factor is small and is usually ignored.

Water Factor

The Water Factor should be used, obviously in place of the Air Factor, when the borehole is water filled. The effect is similar to the Air Factor effect except that the attenuation of the gamma rays by the water between the formation and the detector becomes significant. Therefore, in addition to hole area, path length through the water (and probe diameter must be taken into account). Again, because of the complexity of response, the factors are usually determined empirically. Several curves are included.

Mud Factor

With light, natural muds the value of the Mud Factor is so near that of the Water Factor we generally use the Water Factor. This would not be true if a weighting agent, such as barite is used. However, the quantities of bentonite and other agents used is usually negligible.

These hole size factors must be used to correct the uncorrected GT value because they are quite significant. Notice, for example, that the Water Factor for a commonly used 1-11/16" scintillation probe in a 4-3/4 inch hole is 1.142. The correction is greater than + 14%.

Casing Factor

A Casing Factor must be applied any time a gamma ray log is made through drillpipe or casing. This factor depends upon the thickness and material of the pipe and upon the energy of the radiation. The expression for the Casing Factor is:

$$F_c = e^{at}$$

17)

Sec. 2c, p 14 of 28

Where e is 2.7183, a is the absorption coefficient of the pipe material and t is the pipe thickness in centimeters. For pipe the following table may be used:

Pipe Thickness Inches	Fc Steel Factor	Fc Aluminum Factor
1/16	1.18	1.05
1/8	1.40	1.10
1/4	1.95	1.23
1/2	3.86	1.52
1	14.7	2.29
2	217	5.37

You can see from this that it is absolutely necessary to know the thickness of the steel pipe and, especially the drill collars. This must not be left to the driller to determine. Use a pair of calipers and measure it. Even aluminum or fiberglass pipe can cause a significant correction.

For a large group of calculations these factors may be lumped to give a "Composite K factor" or K_e .

Disequilibrium

We are interested in finding uranium ore. However, all of the uranium isotopes are weak emitters of low energy gamma photons. Therefore, only a small percentage (less than 5%) of the gamma photons which we count indicate the presence of uranium. The rest are daughter products such as lead 214, protactinium 234, and bismuth 214. The chemistry of these elements is such that the uranium is subject to removal by solution in the oxidized state while most of the daughter products are not. Thus, the amount of gamma radiation measured in a borehole is not a measure of the amount of uranium, but only an indicator of the possibility of uranium. Therefore, a gamma ray log is read as equivalent uranium or eU_3O_8 . This is the amount of U_3O_8 which would be present if anomalous formation were in equilibrium. The ratio of the actual uranium (as U_3O_8) to eU_3O_8 is the disequilibrium ratio :

$$D = \frac{U_3O_8}{eU_3O_8} \quad 18)$$

A ratio of 1 represents a condition where the uranium is in equilibrium with its daughter products. A ratio less than one indicates a deficiency of uranium and greater than one indicates an excess of uranium.

Therefore, any value of eU_3O_8 must be corrected for disequilibrium before any meaningful values can be obtained.

The value of D will vary in a predictable manner within a geochemical cell system. The value of eU_3O_8 should be multiplied by D to obtain U_3O_8 .

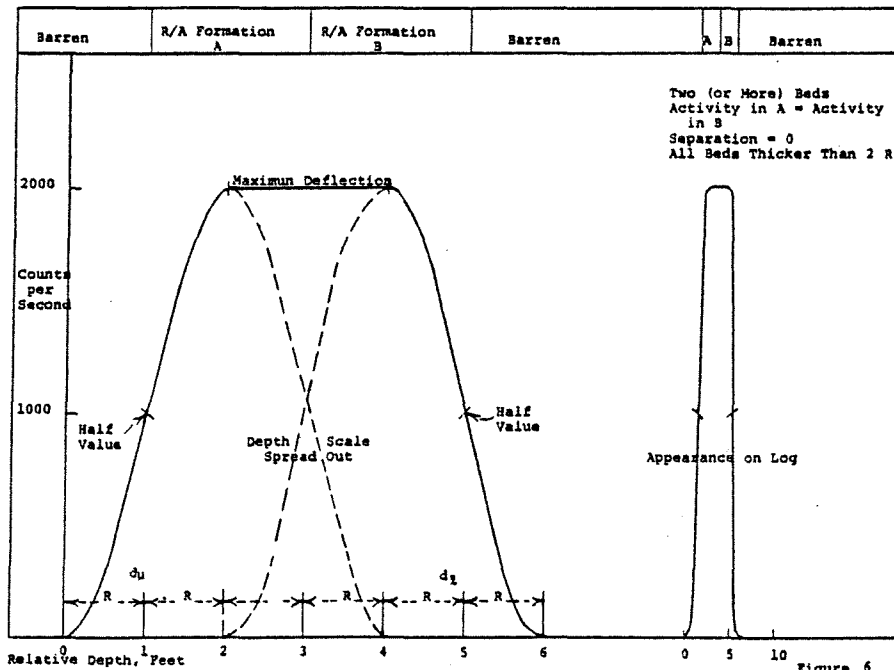
Complex Bedding

So far we have dealt with simple beds. Unfortunately we usually have complex beds to deal with. These take the forms of multiple beds with barren beds or streaks between them, adjacent beds with different grades, and graduated boundaries. There are a number of rules we can follow, but eventually judgement will be required. Judgement must be based upon experience, logic and common sense.

Multiple Beds

We saw earlier that a simple bed with a sharp boundary caused a sinoidal response in the detector. We can use this to determine what the result of 2 beds will be.

If two beds of equal grade and equal disequilibria are adjacent they will appear as one bed. This is calculated in Figure 6. They can be any amount thicker and the result will only be a longer flat top. The distance from zero (or background) to maximum will be 1 sensitive diameter, or about 2 feet.



If the two beds are not of equal grade, but the first is twice the grade of the second, the appearance will be as in Figure 7. Again, increasing the thickness of the bed, over the minimum shown, will only spread out the diagram. There is no real valley between beds but only a change of slope.

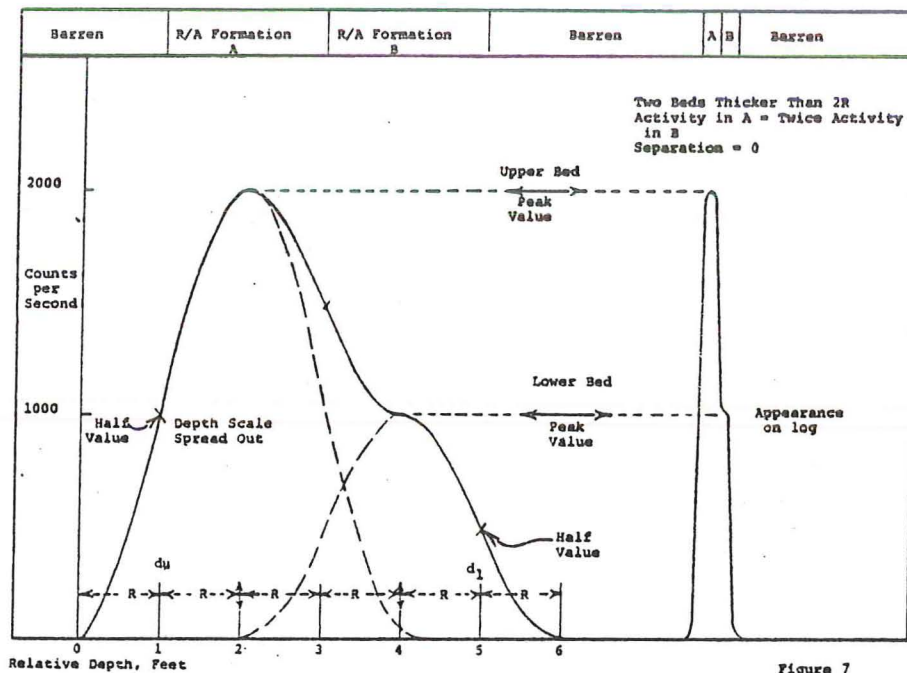


Figure 7

If there is a separation of a barren or low grade bed between two high grade beds, the resulting curves are shown in Figures 8 to 11.

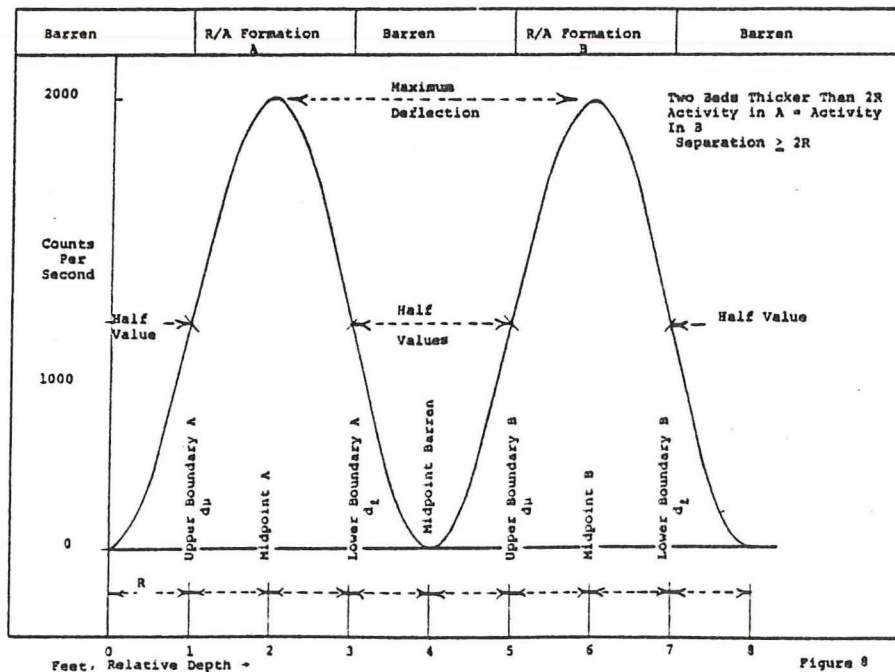


Figure 8

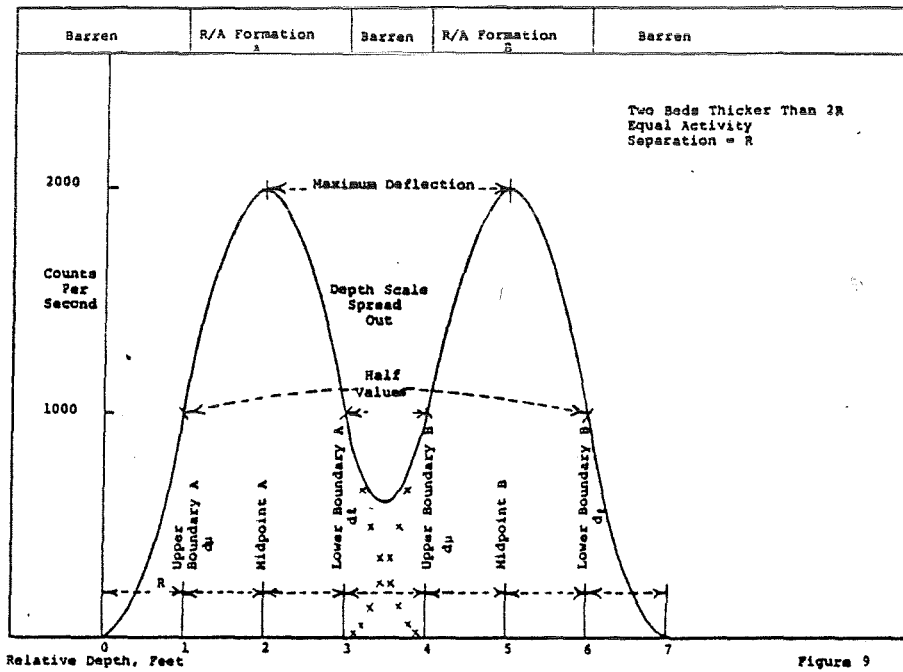


Figure 9

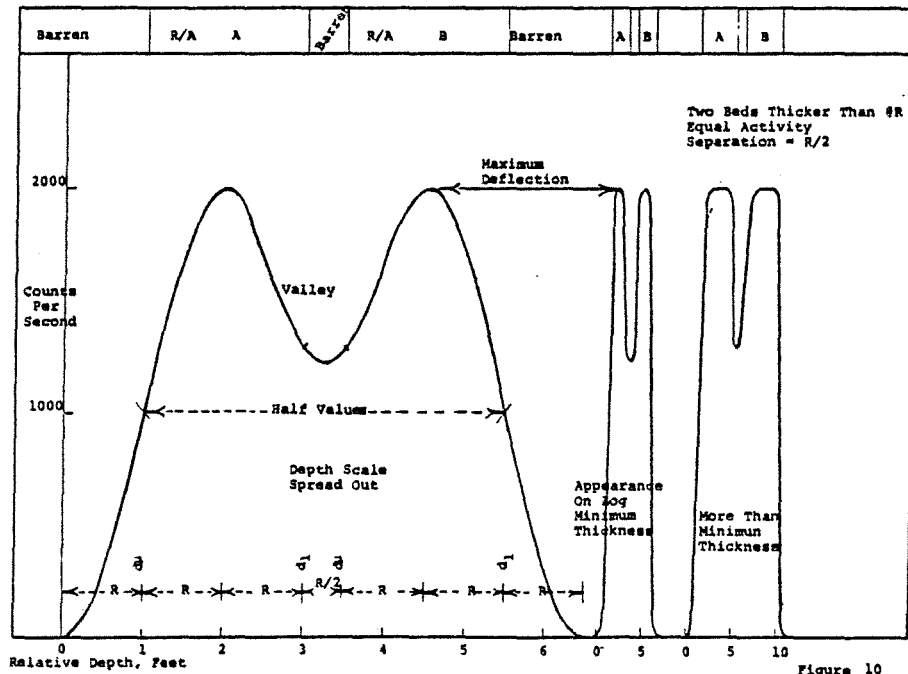


Figure 10

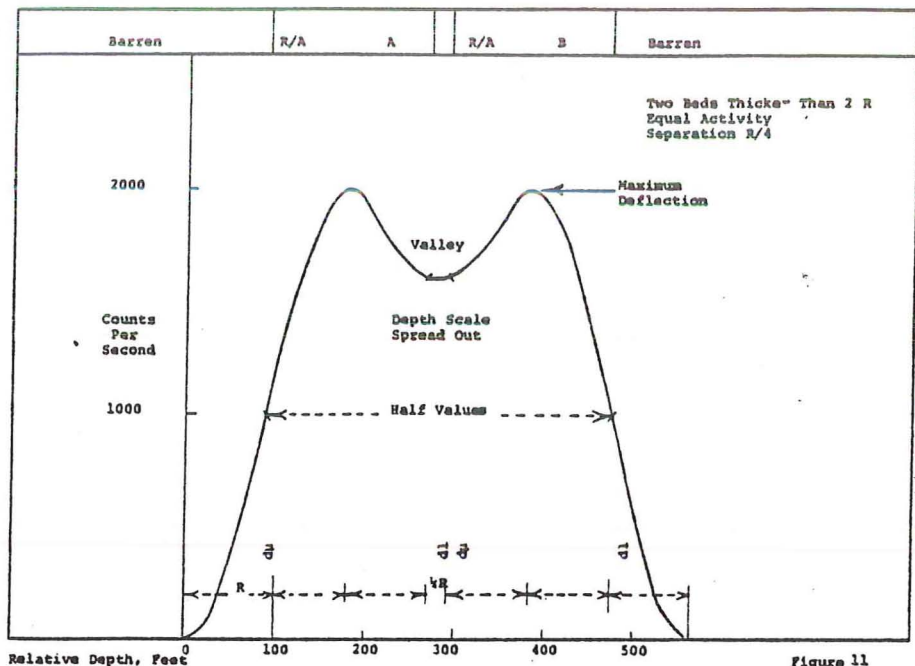


Figure 11

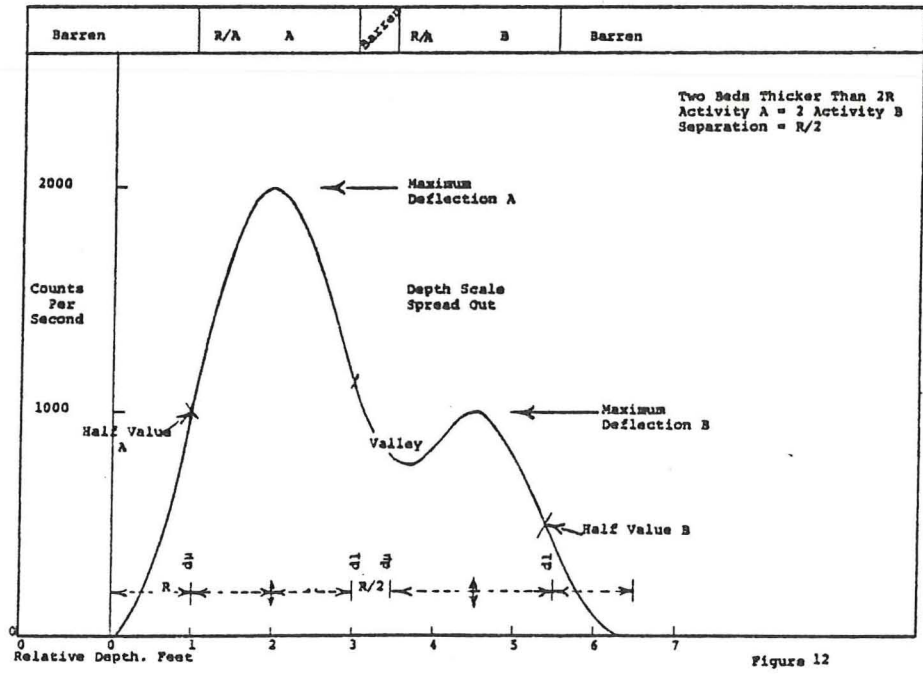


Figure 12

Notice that a barren bed with a thickness of only 1/2 foot will bring the valley between two high grade beds down almost half way. Notice, also, that the peaks of the two high grade beds always occur over the centers of the beds and that the center of the valley always occurs over the center of the barren bed. It is apparent, too, that we have little way of telling (Figure 11) if that center bed is 3 inches of barren bed or 6 inches of low grade.

We may begin to adopt a set of interpretation rules at this point which will eliminate or minimize our errors in determining grade or thickness.

Referring to Figure 6, with a simple bed the bed boundary may be found by determining the maximum deflection, dividing it by 2, and determining the lower and upper depth of these two half-value points. In Figure 6, these occur at a value of 1000 cps since the maximum is 2000 cps. This is the basic situation upon which we base our interpretations.

Start with the lower (or upper) bed boundary, d_1 . Note the depth on the work sheet (Figure 4). Also, note the upper bed boundary depth on the work sheet. The difference between them is the thickness, T in feet. The starting boundary counting rate becomes e_1 . When e_1 is corrected for deadtime error it becomes E_1 . Progress up (or down) the curve noting the counting rate for each half foot interval. These are the values of i_1, i_2, i_3 , etc. When they are corrected for deadtime errors they become I_1, I_2, I_3 , etc. The last point to be noted will be e_2 . It will be at the upper (or lower) bed boundary if the bed is a multiple of a half foot thick. If it is some other thickness it will be the next point past the bed boundary. This value will become E_2 when it is corrected. This procedure, with minor modifications is used on all manual calculations.

If the two beds are adjacent (similar to Figure 6) but of different grades, the result is shown in Figure 7. Note, again, that the upper and lower bed boundaries are at the half values. This time, however, the upper boundary is at half of the upper bed peak value and the lower boundary is at half of the lower bed peak value. Note that the two peaks of the curve occur over the mid-points of the two beds. Also notice that the "valley", in this case, is not over the boundary between the two beds. It is displaced toward the lower bed and the lower side of the high grade bed is distorted. If you wish to find the center boundary, locate the point half way between the upper peak and the lower peak. This will be very close to or on the center boundary.

To determine the average grade, in this case proceed as with a simple bed. Start at either the upper or lower bed boundary and determine the counting rate each half foot.

If you wish to determine the individual grades there are two ways to proceed. The first method is precise but hard to use because it requires experience. The second is a close approximation and is much easier to use. The latter is the recommended method.

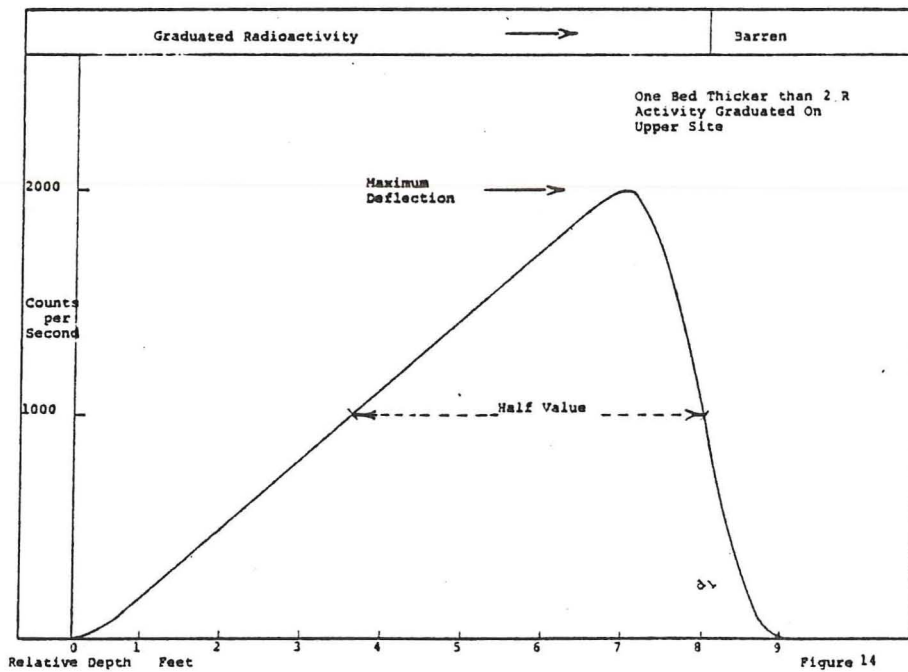
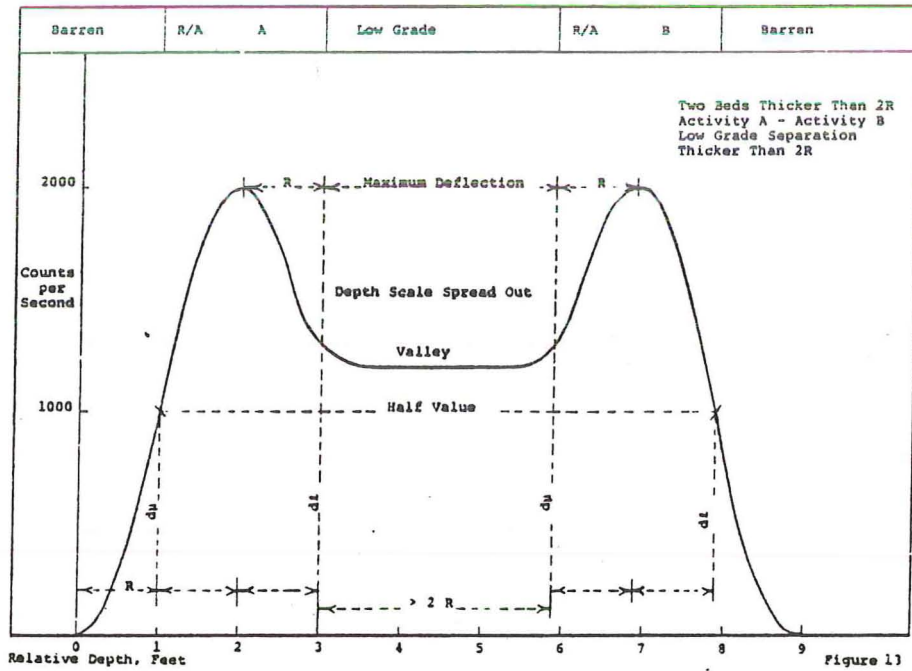
The first method requires that the boundary between the two beds be determined by locating the point half way between the low grade and high grade peaks. Then draw in the probable curve for each bed as if it were simple. The half value for each bed must be at the bed boundary. The result will be as the dashed curves of Figure 7. Then determine the half foot points for each simple curve independently.

The second method only introduces small errors and is much easier to use. In this case determine the center bed boundary as before. Then proceed from e_1 with half foot values to the bed boundary. Do not use an e_2 value for this bed. Otherwise, proceed as if this were a simple bed. Then, start on the second bed at the center bed boundary. This will be i_1 . Do not use a value for e_1 in this case. Proceed to e_1 and treat this as a simple bed. Thus, the lower bed will have $e_1, i_1, i_2, i_3, \dots, i_{\text{last lower}}$. These will correct to $I_1, I_2, I_3, \dots, I_{\text{last lower}}$. The area will be:

$$A^l = 1.38E_1 + \sum_0^{\eta} I_a$$

Similarly the upper bed area will be:

$$A^u = 1.38E_2 + \sum_{\eta+1}^{\alpha} I_a$$



where α is the last lower n value and m is the last upper i value. Do not repeat any values nor use any value twice. The resulting G and T values will be extremely close to the correct values.

If we have a separation of 2 feet or more between beds they will be independent as shown in 8. These high grade beds are drawn as minimum thickness (2 feet thick) beds, but thicker beds would give the same result. When the thickness of the barren bed becomes less than two feet the valley fills in rapidly.

To determine the grades and thicknesses of two beds which have a barren bed between them, treat them as independent beds if the valley between them is lower than the half value. The inside bed boundaries will be at the point half way between the peak and zero. This can be seen in 8 and 9.

If the barren bed is narrower than .7 foot or if it is not barren the valley will be less than half way down from the peak. In this situation we have little or no way of telling how thick the center bed is nor its grade. We can estimate the thickness by measuring one foot from each peak. The distance between the ends of the one foot measure is the probable barren bed thickness. This is shown in 10 and 11. This type should be averaged all the way through. The error incurred by including the barren streak is probably smaller than that due to the uncertainty of the bed boundary or the grade of the streak if it is low, not barren. This idea may be changed in the future if we are able to develop good methods for determining these uncertainties.

The problems in the previous example are aggravated if the two high grade beds are not the same grade. This is shown in 12. Average the whole anomaly if the valley does not come down half way. If the center bed is thick and obviously has grade, as shown in 13, the thickness may be determined by measuring one foot in from each peak. The grade of the center bed will be, if the center bed is more than $2R$ thick:

$$G = 2 KN$$

where N is the average counting rate of the flat part of the valley. The grades and thicknesses of the high grade beds will be found as outlined for Figure 7.

The final case is shown in Figure 14. In this case the lower boundary is no problem. It is at half the peak value. The upper boundary is a problem because it is not sharp. The grade gradually tapers off to zero. In this type bed the boundary should be picked at half value if the area of the discarded tail is negligible. If the discarded portion is significant (high grade and long slope) then place the arbitrary bed boundary at 1 foot in from the departure from background.

References:

1. Quantitative Interpretation of Gamma Ray Logs by Scott, Dodd, Drouillard and Madra. A.E.C. Publication.
2. A.E.C. Calibration Pits - A.E.C. Publication.
3. Handbook of Chemistry and Physics, 51st Edition.
4. Twopit, A. Different Approach to Calibration of Gamma Ray Logging Equipment, by Crew and Berkoff. A.E.C. Publication.
5. Schlumberger Log Interpretation Principles..
6. Application of Borehole Geophysics to Water-Resources Investigations. Keys and MacCary, U.S.G.S. Publication.
7. GOI Log Interpretation Reference Data Handbook. A Gearhart-Owens Industries Publication.
8. Interpretation of Electric and Gamma Ray Logs in Water Wells, by Hubert Guyod.
9. Nuclear Radiation Physics. Lapp and Andrews.

A P P E N D I X

Sample calculations for grades of synthetic curves, using A.E.C. method:

Simple formations of several thicknesses (Figure 11)
(Grade = .100%)

Thickness	2'	2.5'	3.0'	4.0'
A	8160	10160	12160	16160
GT	.204	.254	.304	.404
G	.102	.102	.101	.101
ERROR	+ 2%	+ 2%	+ 1%	+ 1%

Double beds of 2 different grades (Figure 12) (.100% and .050%)

T	4'
A	12071
GT	.302
G	.075
ERROR	0.0%

Two beds of .100% separated by 1/2 foot of barren formation
(Figure 13C)

T	4.5'
A	16160
GT	.404
G	.090
ERROR	-10%
G w/o barren	.101
ERROR	+ 1%

Two beds of .100% separated by 1/4 foot of barren formation
(Figure 13 D):

T	4.25'
A	16343
GT	.408
G	.096
ERROR	- 4%
G w/o barren	.102
ERROR	+ 2%

LP-2 PROBE DATA
June 10, 1970

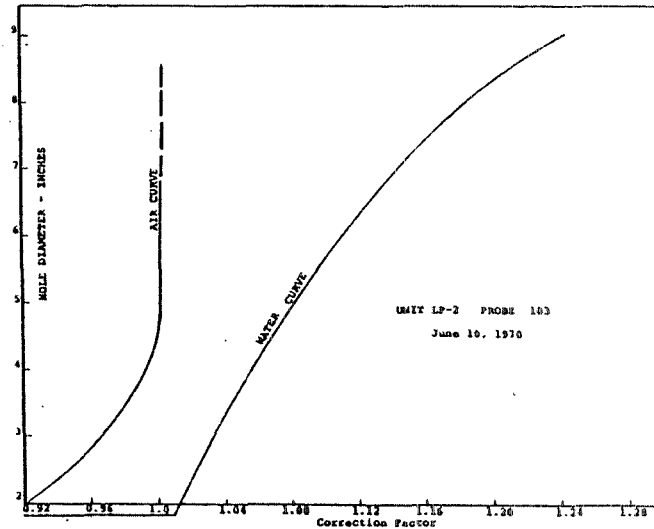
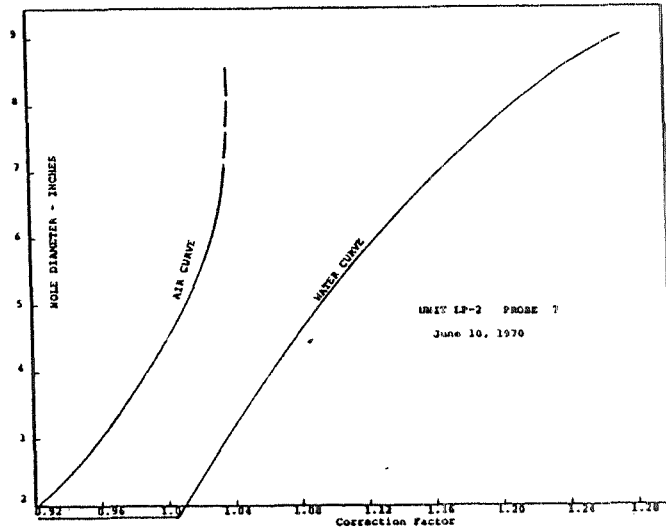
PROBE NO.	DIAMETER	CRYSTAL SIZE	PLATEAU	DEADTIME	K-FACTOR
7	2"	1-1/4" x 1-3/4"	16/1.50	5.0	563 x 10 ⁻⁸
103	1-5/8"	3/4" x 1"	16/1.50	5.0	184 x 10 ⁻⁸
105	1-5/8"	1" x 3"	8/1.75	5.2	470 x 10 ⁻⁸

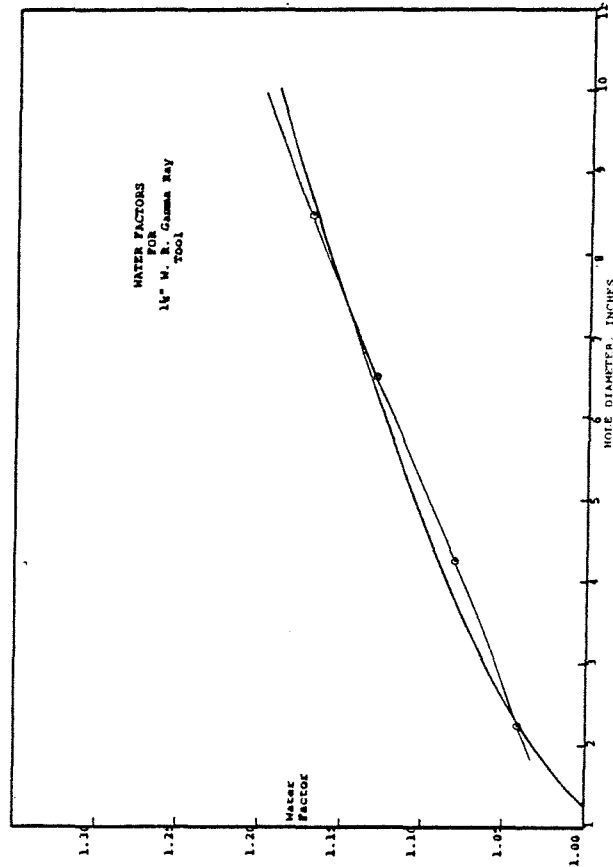
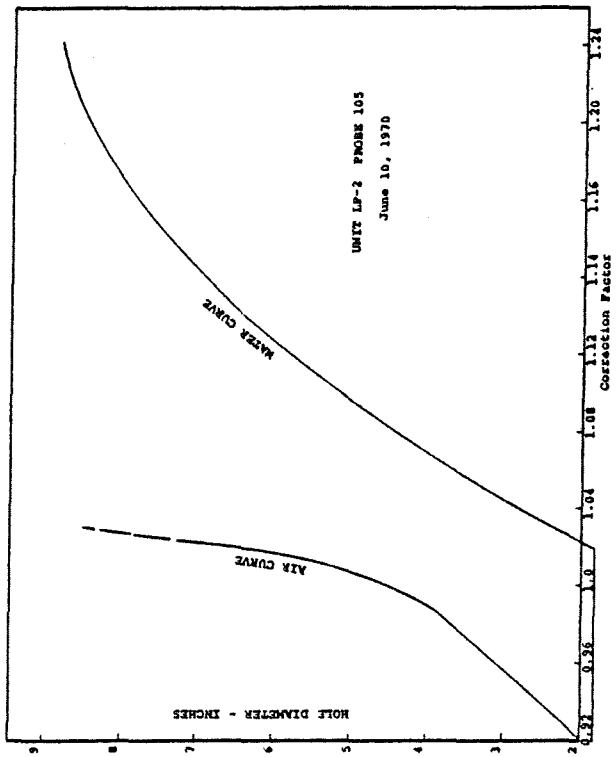
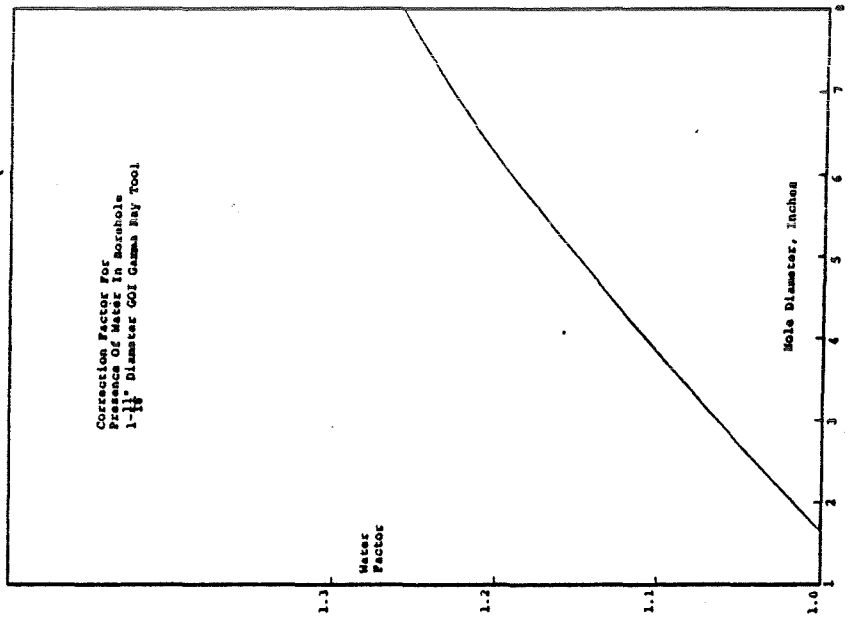
WATER AND AIR CORRECTION FACTORS

PROBE	0 - 2.25"		0 - 4.50"		0 - 6.50"		0 - 8.50"	
	WATER	AIR	WATER	AIR	WATER	AIR	WATER	AIR
PROBE 7	1.0160	0.9317	1.0747	1.0000	1.1458	1.0338	1.2330	1.0197
PROBE 103	1.0181	0.9338	1.0669	1.0000	1.1292	1.0027	1.2066	1.0027
PROBE 105	1.0312	0.9290	1.0742	1.0000	1.1507	1.0203	1.2372	1.0179

CASING CORRECTION FACTORS

WALL THICKNESS	PROBE NO. 7	PROBE NO. 103	PROBE NO. 105
1/2" Steel	2.1240	2.2138	2.1356
3/8" Steel	1.8293	1.9144	1.8618
1/4" Steel	1.5603	1.6020	1.5631
3/16" Steel	1.4167	1.4691	1.4104
1/8" Steel	1.2791	1.3010	1.2819
1/16" Steel	1.1555	1.1692	1.1547
1/8" Aluminum	1.0106	1.0101	1.0183





HIGH GRADE TEST PIT
Casper, Wyoming

August 17, 1967

LUCIUS PITKIN, INC.

Certificate of Assay

Ore Zone

Sample No.	Marked	Dry Basis		% L.O.D.	Bulk Density Dry Basis	
		% U ₃ O ₈	% e U ₃ O ₈		Lbs./Ft ³	
LPI-311	H-1- Casper	2.12	2.09			
LPI-311	H-2- Casper	2.18	2.17	5.94		
LPI-311	H-3- Casper	2.28	2.18	5.99	139	
LPI-311	H-4- Casper	2.09	2.06			
LPI-311	H-5- Casper	2.19	2.09			
LPI-311	H-6- Casper	2.34	2.39			
LPI-311	H-7- Casper	2.11	2.12	6.67		
LPI-311	H-8- Casper	2.22	2.26	6.54	137	
LPI-311	H-9- Casper	2.30	2.34			
LPI-311	H-10-Casper	<u>2.12</u>	<u>2.17</u>	—	—	
	Average	2.19(5)	2.18(7)	6.28(5)	138	
				G-T = 6.57		
LPI 324	- Bottom Barren Zone.			3.68	133	
LPI 325	- Top Barren Zone			3.80	130	

LOW GRADE TEST PIT
Casper, Wyoming

August 17, 1967

LUCIUS PITKIN, INC.

Certificate of Assay

Ore Zone

Sample No.	Marked	Dry Basis		% L.O.D.	Bulk Density Dry Basis	
		% U ₃ O ₈	% e U ₃ O ₈		Lbs./Ft ³	
LPI-311	L-1-Casper	0.284	0.284			
LPI-311	L-2-Casper	0.290	0.299	5.04		
LPI-311	L-3-Casper	0.286	0.278	5.43	140	
LPI-311	L-4-Casper	0.293	0.290			
LPI-311	L-5-Casper	0.305	0.300			
LPI-311	L-6-Casper	0.288	0.286			
LPI-311	L-7-Casper	0.400	0.401	5.30		
LPI-311	L-8-Casper	0.287	0.277	5.13	144	
LPI-311	L-9-Casper	0.284	0.284			
LPI-311	L-10-Casper	<u>0.295</u>	<u>0.292</u>	—	—	
	Average	0.301	0.299	5.22(5)	142	
				G-T = 8.97		
LPI 324	- Bottom Barren Zone			3.68	133	
LPI 324	- Top Barren Zone			3.80	130	

SPONTANEOUS POTENTIAL MEASUREMENTS

The potentials which we measure and record as the Spontaneous Potential curve are made up of three components; the electrochemical, the redox, and the electrofiltration components. There is another which we usually try to eliminate from our logs. These are electrode effects. While there are a number of separate components, they can definitely be interacting even though the connection may not always be entirely clear.

A. ELECTROCHEMICAL COMPONENT

Sand - Shale - Mud Trinity

The classical explanation of the electrochemical component of the S.P. is that the sand, shale, and mud in contact with each other act as electrodes, electrolytes, and conductors by virtue of their different salinities. (See Figure 1,) A voltage drop results in the mud column because of the flow of S.P. current, and since we move our electrode through the mud column, we measure the variable voltage with respect to a surface reference electrode and call it the SP.

How does this current originate? Picture two media, in contact, and containing dilute ionized solutions of different concentrations. (See Figure 2.) Assume, for the moment, that they contain only sodium chloride, NaCl solutions in the form of Na^+ and Cl^- ions. These solutions are nearly neutral and equal in their pH values and about equal in their eH values. Separating the media is a permeable surface perpendicular to the direction of diffusion. In this case the anions (the negative ions) have a higher mobility than the cations (the positive ions). Therefore, as diffusion takes place an unbalance of charges builds up and a potential can be measured across the junction which will be a function of the concentrations and activities of the ions. Since the conductivity of an electrolyte is a function of the ion concentration, the diffusion potential, E_D , across the junction will be approximately:

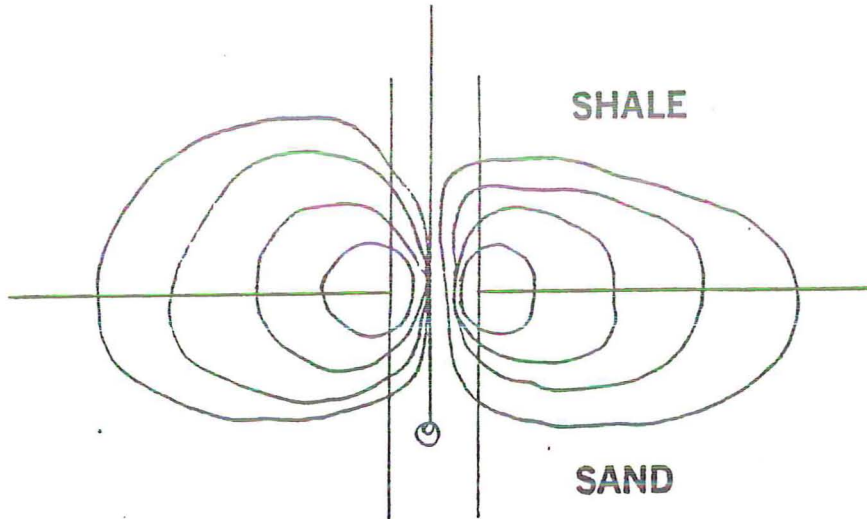
$$E_D = K_D \log \frac{R_d}{R_c} \quad (1)$$

where K_D is the diffusion coefficient. For NaCl this becomes approximately:

$$E_D = - 11.6 \log \frac{R_d}{R_c} \text{ millivolts.} \quad (1a)$$

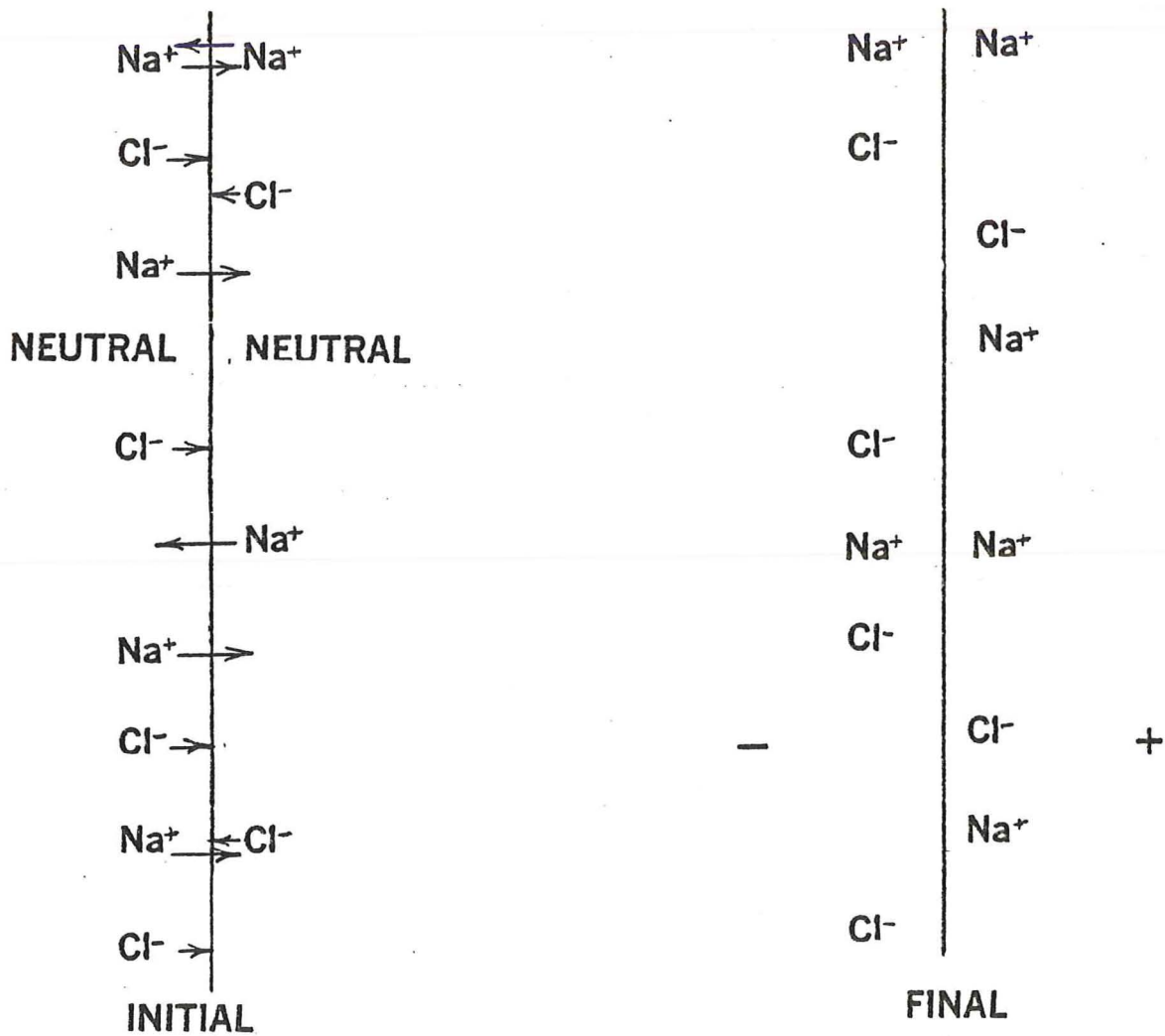
Various salts have different mobilities and will consequently have different K_D 's and different potentials.

We can have an S.P. between any two beds having different salt concentrations. And, the potential will depend upon the relative concentrations of the salts. Also, the potential will depend upon the types or mobilities of the ions.



CLASSIC S.P. DIAGRAM

Figure 1



STYLIZED DIFFUSION PROCESS

Figure 2

This can cause interesting effects in beds where the invasion by hole fluid is rapid. This is the usual case in shallow, freshly drilled exploratory holes. A difference in salinity between the hole fluid and the formation water will usually mean a density difference. If the rate of invasion is more rapid than the diffusion rate within the bed, an uneven invasion distribution will take place. This will often result in a "sawtooth" S.P. curve.

Equation (1a) holds quite closely if we are working in two coarse grained sandstones. But, if there is a little shale in one of the sands, we find that the departure from this theoretical value of -11.6 millivolts is great. The solid minerals in the rock, particularly the colloidal clay fragments, absorb ions from the electrolytes in the pores. There are three processes by which this may take place.

1. Ions which are the same composition as the ions of the solid minerals in rock will form a concentrated layer of ions at the liquid-solid interface as a result of the difference in thermodynamic potential between them. As a result, the composition of the free electrolyte is changed, since the bound ions will have zero mobility (Figure 3).
2. Ions may form insoluble compounds with the ions of the minerals. The result is that the local electric field in the pores is changed so that it may change the rate of diffusion of the free ions (Figure 4).
3. Ions which are unrelated to the ions in the solid mineral may be absorbed because of the tendency to form hydrates. The surface charge on these minerals is commonly negative (Figure 5).

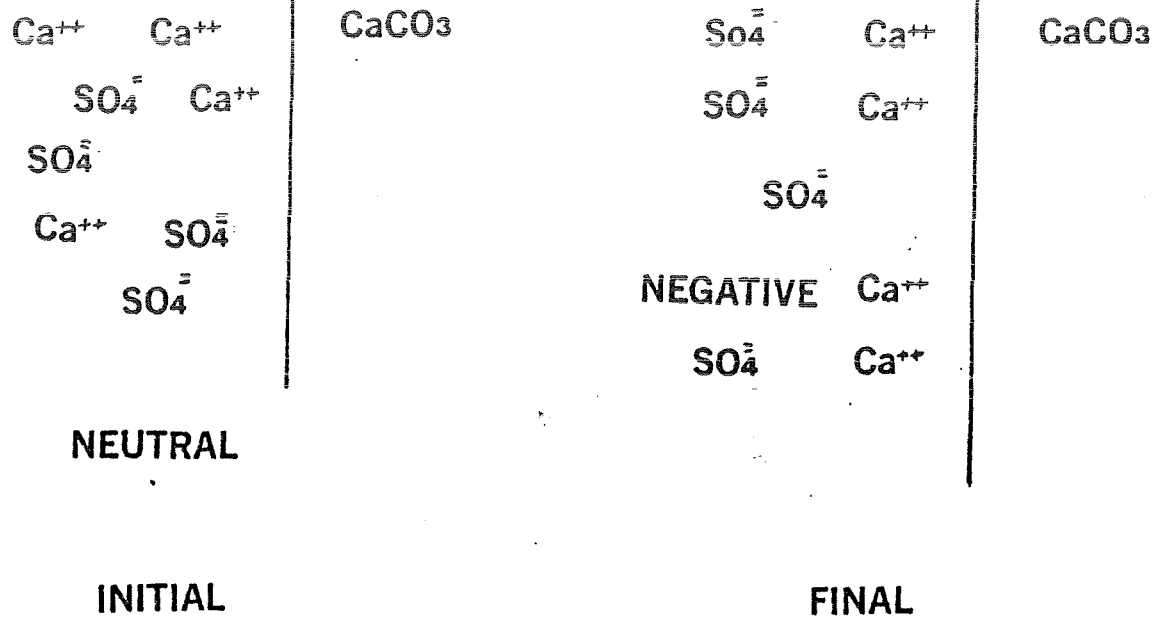
The things which affect this diffusion-absorption potential are:

1. The chemical composition of the rock matrix and the shale or clay;
2. The concentration and composition of the salts in the electrolyte;
3. The surface area exposed to the electrolyte, which include:
 - a. The degree of saturation of the rock with the electrolyte;
 - b. The density of the rock; and
 - c. The grain size of the rock.

These things are defined by the diffusion-absorption activity coefficient, A_{DA} :

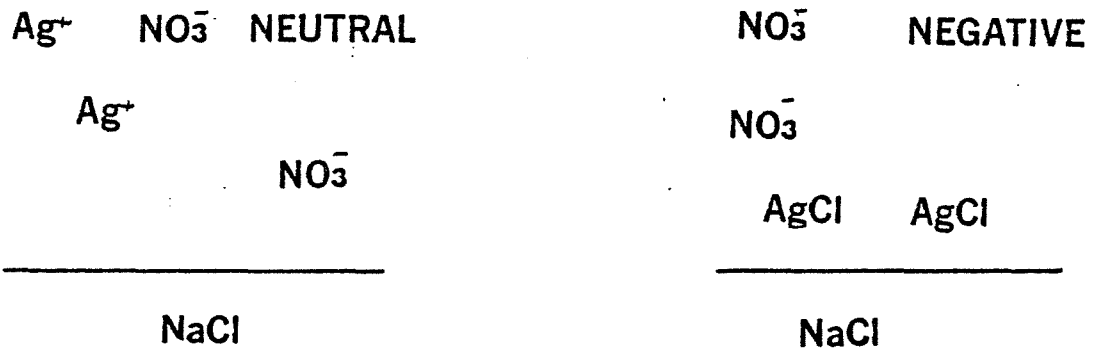
$$A_{DA} = f\left(\frac{S_o}{\phi S_w}, \zeta, \ell\right), \quad (2)$$

where S_o is the specific area, ϕ the porosity, S_w the water saturation, and ℓ the concentration; ζ is the zeta potential.



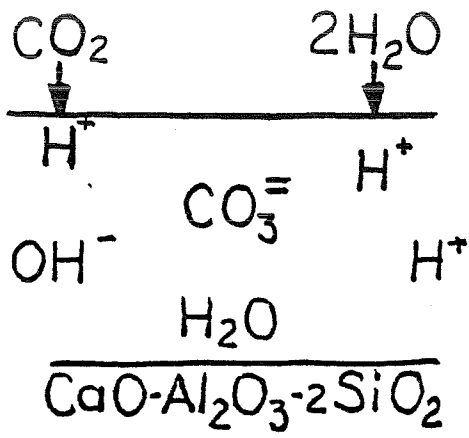
LAYERING OF LIKE IONS

Figure 3



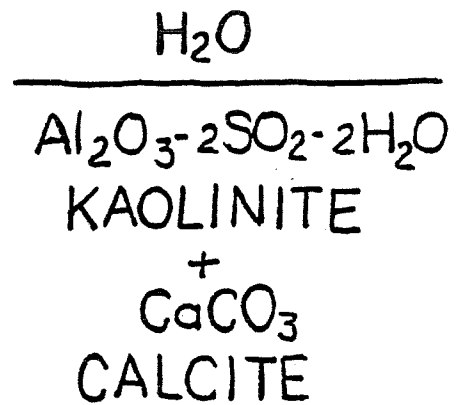
PRECIPITATION OF INSOLUBLE COMPOUNDS

Figure 4



ANORTHITE

INITIAL CONDITION



RESULTANT CONDITION

HYDRATION OF IONS

Figure 5

The total diffusion-absorption component of the S.P. potential, E_{DA} , is:

$$E_{DA} = (K_D + A_{DA}) \log \frac{f_p' c_p'}{f_o c_o} \quad (3)$$

where f_p' and c_p' are the average values for activity and concentration of the electrolyte filling the rock pores. For two formations in contact since the resistivity depends upon the activity and concentration, we may write,

$$E_{2,1} = (K_D + A_{DA,1} - A_{DA,2}) \log \frac{R_2}{R_1} \quad (4)$$

B. REDOX POTENTIALS

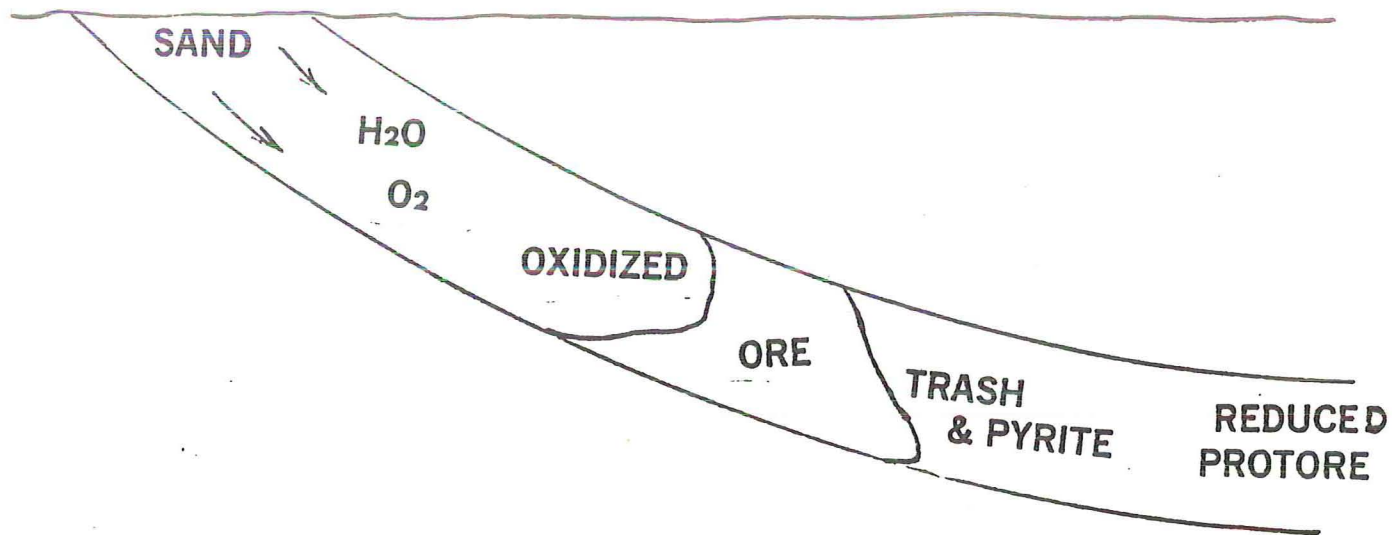
The S.P. which we measure is also influenced by the states of oxidation of adjoining formations. The EMF developed between an oxidizing phase and a phase being oxidized is:

$$E_{ox} = \frac{RT}{ZF} \ln \frac{kc_1}{c_2} \quad (5)$$

where k is the reaction rate and c_1 and c_2 are the quantities of materials present in the more and less oxidized states respectively.

This component is quite important in the shallow beds encountered in minerals logging. The same action of the surface water which carries down oxidizing materials and oxidizes mineralized bodies sets up reduction-oxidation or redox potentials with respect to surrounding beds where oxidation is not taking place. The quantities of organic material, sulfides, and bacteria involved in some roll front depositions will create a reducing environment which will set up a potential with respect to the surrounding beds. The potential will be positive if the bed is in an oxidized state with respect to the neutral beds, and negative if it is in a reduced state. It is extremely difficult to separate pH and eH effects. These potentials may become important in deep wells, also where dissolved oxygen can be carried down in the drilling mud. These potentials, like the diffusion-absorption and activity potentials, are temperature sensitive. The deeper we go the more important all of these factors become. Fortunately, this is balanced by the fact that deeper formations are a more nearly constant environment (See Figure 6).

One of our local problems is explaining the action of the S.P. in coal. Coal may be oxidized by oxygen carried down by drilling mud or surface water and, as a result, a double layer of charge will collect on the surface of the coal with the negative side away from the coal. Oxygen or some other oxidizing agent must be present, however. The presence of sulfide minerals in the coal can intensify the reaction. The carbon content of the coal will influence the potential. On the other hand, the presence of large amounts of clay or shale can reduce this deflection. The same type reaction may be found in metamorphic and graphitic states.



**POSSIBLE REDOX INTERFACE ACTION
ROLL FRONT**

Figure 6

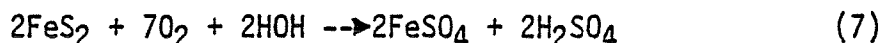
pH

pH is a measure of the hydrogen ion concentration in the solvent. In our case, the solvent is the formation water. By definition:

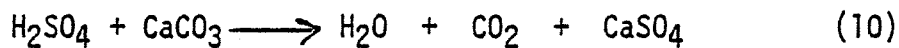
$$\text{pH} = -\log [\text{H}^+] \quad \text{or} \quad (6)$$

$$[\text{H}^+] = 10^{-\text{pH}} \quad (6a)$$

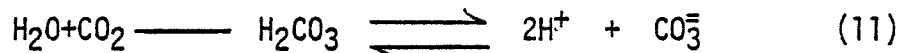
pH reactions are extremely difficult to separate from redox reactions and, in fact, usually are the same reaction. For example, if we have a formation containing pyrites, FeS_2 , washed with surface water containing oxygen, we have a reaction of



and, upon oxidation, also have an increase of hydrogen ions and a lowering of pH. If part of the formation happens to be calcareous, a further change can take place.



In other words, the presence of oxygen in the drilling mud or formation water could conceivably oxidize the pyrites in one formation or one part of a formation, change its pH and further on cause an acid-base reaction with a further change of pH, since



which is weakly ionized.

In one example we found a pH of 5.9 in the altered or oxidized zone along with traces of ferric salts. Below, in the unaltered zone the pH varied from 7.0 in a coal zone to 8.9 in a sand. It is not known if there were ferrous salts in the sand or not, but the color indicated the possibility.

eH - pH Measurements

The potential value of eH - pH logs has been recognized for several years, particularly in the minerals industries. The problem, however, has been one of a representative way to make the measurements. First of all, a simple lead mud fish is often not a suitable reference electrode, because it is too highly influenced by many environmental factors. A metal-metal chloride electrode probably must be used to achieve the required stability. A metal measuring electrode will respond to most factors in a borehole. It will measure a mixture of things which we

call the S.P. Therefore, we must choose our electrodes to measure the parameter or parameters we wish.

Ideally, if we wish to measure pH we should use a glass electrode and refer it to a mercury - mercurous chloride or a silver - silver chloride electrode. The description of electrodes have been described in many texts. These will measure pH as an electrode effect but only if nothing else is present. Silver or platinum is usually used for redox.

If we refer the measure electrode to a surface reference, we would measure the values we want but they would be superimposed upon other things, since a pH electrode will also measure any other potentials present. We can get our measurements by putting the reference electrode downhole and the measure electrode close to it. We aren't particularly interested in the mud column, however, except as a medium for making measurements. The drill hole usually has just been thoroughly flushed with surface water. It has been determined that, with time, diffusion will eventually result in a fluid in the borehole which is representative of the formation fluid next to it. A period of time of from about 4 to 60 days is often required.

This problem can be partially circumvented by inserting the electrodes into the moving mud column and making the pH and redox measurements during drilling. At this point the drilling mud return will contain fresh hole fluids. (See Figure 7.)

C. ELECTROMECHANICAL COMPONENT

When a fluid flows into a formation from the borehole, an EMF is generated across the formation boundary. The direction of flow depends upon the differential pressure between the mud column and the formation.

These electromechanical or electrofiltration EMF's are caused by a preferential absorption of one ion type on the surfaces of the formation matrix. As a result of this absorption, the free water in the pore space becomes enriched with ions of the opposite charge. The difference in potential between the free and the bound water is the contact potential. The capacity to generate these EMF's is called the electrokinetic activity coefficient.

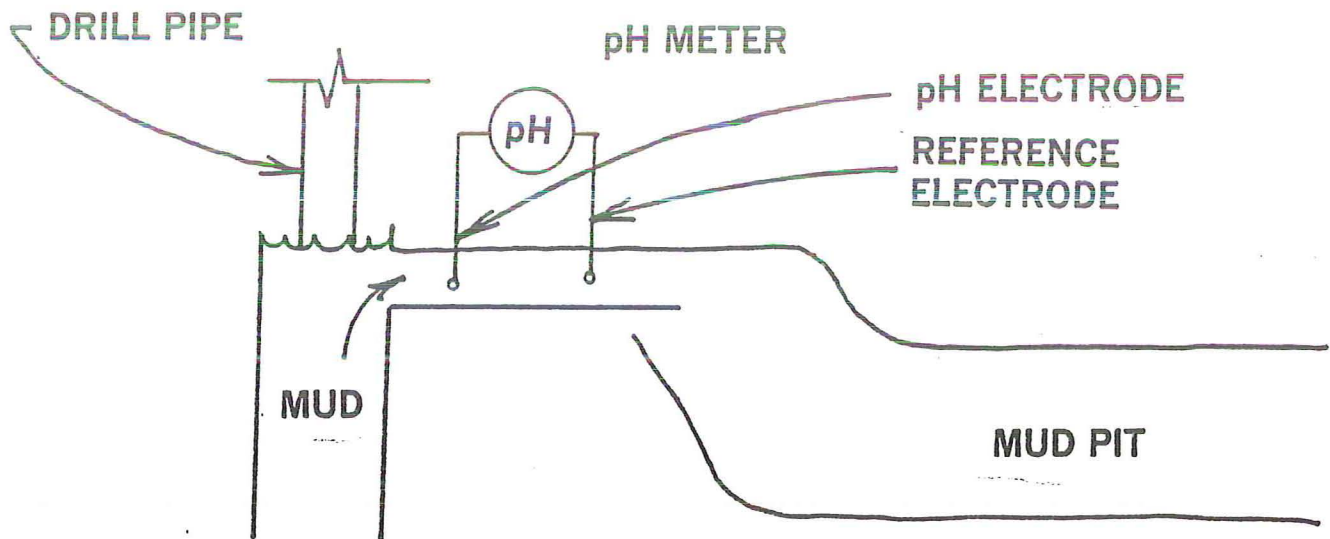
Fluid will flow along a capillary tube (Figure 8) of length "l" and radius "R" with velocity, v:

$$v = \frac{R}{4\mu l} (r_a^2 - r^2) \quad (12)$$

where μ is the liquid viscosity and r_a is the radius of the zero flow along the wall. And, according to Helmholtz's law, the EMF, E_H is:

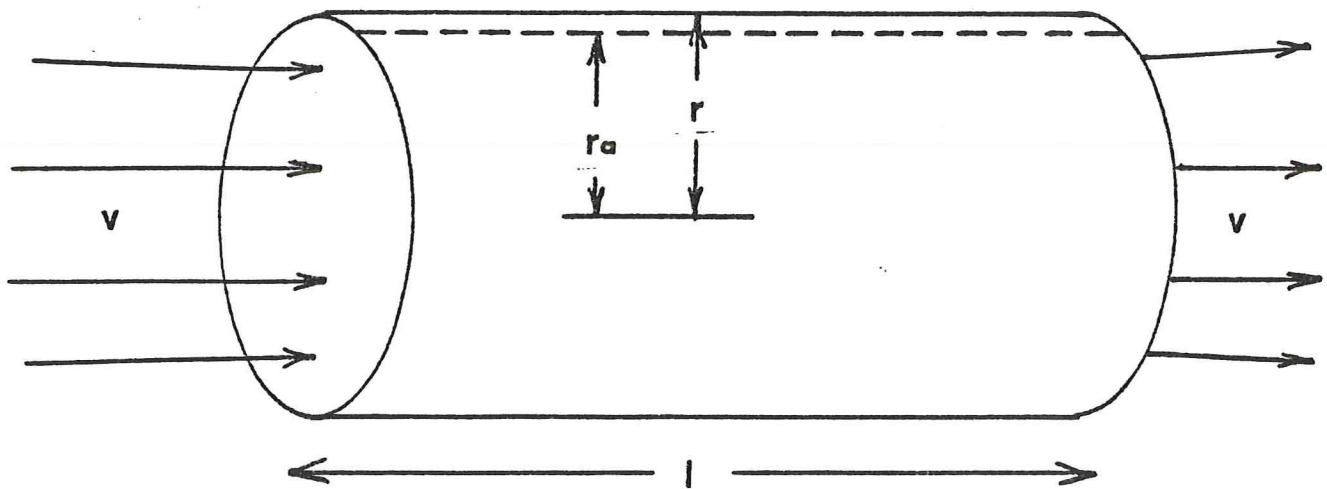
$$E_H = \frac{\epsilon \rho \zeta}{4\pi\mu} P \quad (13)$$

where ϵ is the dielectric constant of the formation fluid, ρ is the



POSSIBLE METHOD OF DETERMINING pH

Figure 7



CAPILLARY FLOW

Figure 8

resistivity of the liquid, ξ is the zeta potential, P is the differential pressure, and μ is the viscosity. ξ , μ , and ρ are always positive while ζ and p can be either polarity. And, since the potential is directly proportional to ρ , it is a function of the chemistry of the formation. A flow of mud filtrate into the formation or a flow of fresh water out of the formation can cause large and rapid S.P. changes at the bed and uphole.

Since this potential is also directly proportional to the differential pressure between the borehole and the formation, any deviation from a linear hydrostatic head in either the formation or the mud column will cause an SP shift. For instance, if the hydrostatic gradient in the mud column is higher than that of the formations, E_H will be near zero at the top of the mud column and positive near the bottom. This may be a reason for the SP drifts in shallow, freshly drilled holes.

Electrode Effects

Electrode effects, including pH and eH, are usually neglected or ignored in a coverage of SP logging. However, they are as important, in several ways, as the formation potentials which we wish to measure.

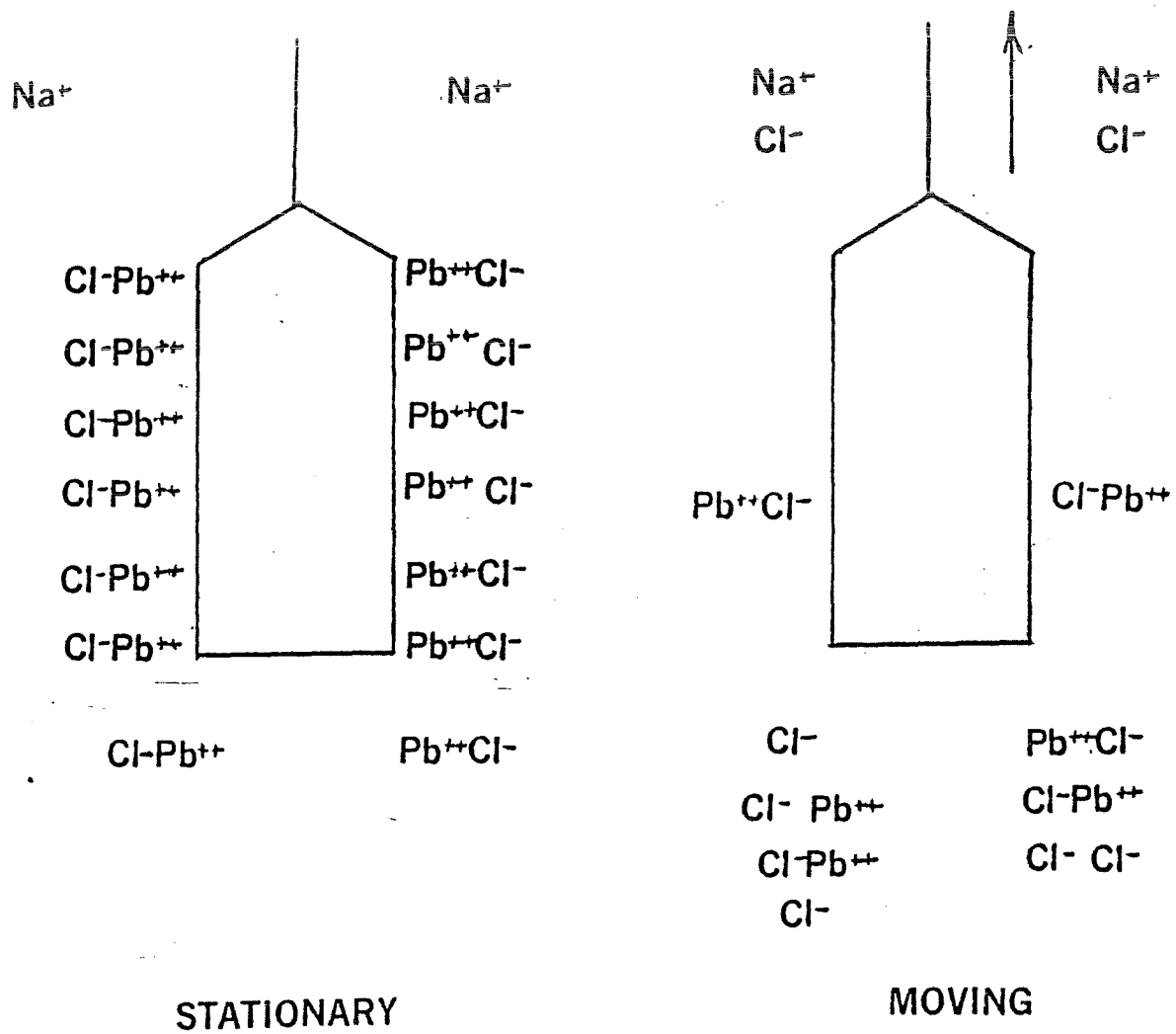
Any time a metal electrode is placed in an electrolyte, a potential develops between the positive metallic ions which go into solution and the charge left behind on the electrode, forming a double layer. The potential drop depends upon the chemistry of the metal and solution and upon the concentration of anions involved.

If the electrode is in contact with an electrolyte containing a salt of the same metal, the entrance of metal ions from the electrode is opposed by the osmotic pressure of the metal ions in solution. Under these conditions the electrode potential is:

$$E_e = E_o - \frac{RT}{ZF} \ln C \quad (14)$$

where E_o is the standard electrode potential of the metal, R is the Universal Gas Constant, T the absolute temperature, Z the valence of the metal, F Faraday's Number, and C is the concentration of metal ions in solution. This type of situation is very stable and the electrode is called a non-polarizing electrode. This is used as a reference for eH and pH measurements.

The electrodes which we commonly use for SP measurements are not of the non-polarizing type. Several effects may arise from this fact. If the electrode is allowed to stand still in the hole in viscous drilling mud, the diffusion of metal ions into the surrounding fluid quickly sets up a situation resembling that of a non-polarizing electrode. (See Figure 9.) The result is a drift to the potential of a non-polarizing electrode whenever the electrode is stopped. As soon as the electrode is moved again, the reaction products are left behind and the potential of the polarized electrode returns. This also accounts for the SP shift upon leaving the bottom. This indicates that, if non-



LEAD ELECTRODE EFFECT

Figure 9

polarizing electrodes cannot be used, the metal electrode should be moved at a constant speed. This potential, due to the movement, is called a triboelectric potential.

The electrode potential depends upon the absolute temperature. This means that there will always be a baseline drift due to the normal temperature gradient in the hole. Further, any entry of gas or formation water into the hole is likely to change the temperature causing further baseline shifts.

Sedimentation potentials may be observed when cuttings in the mud settle out. As the solid particles drop, they absorb anions and become negatively charged. The result is that the bottom of the hole will become more negative and the top more positively charged. While these potentials are usually not large, they are usually found in holes which lack chemical control of viscosity.

Galvanic potentials will be observed if several types of metals are used in the sonde and cable construction and are exposed to the mud. Particularly aggravating potentials may be set up if the logging electrode and the return electrode are dissimilar metals. One observes lead, iron, copper, stainless steel, and solder electrodes in the field. Housings are made of aluminum, brass, steel, stainless steel, and plastic. Suppose we use the standard 8010A tool as an example. And, supposing we do not tape the subs at each end of the tool. The insulated portion of the tool is 47 inches long with a steel top sub and head and a 316 stainless steel bottom sub. Let us suppose further, that we are in 1 ohm meter mud and formation. Then the potential of the top sub would be (Figure 10)

$$E_{Fe} = .441 \text{ volts,}$$

the potential of the stainless bottom sub

$$E_{SS} = -.31 \text{ volts,}$$

and the difference between the two would be

$$E_t = E_{Fe} - E_{SS} = .75 \text{ volts.} \quad (15)$$

Current would flow from the top to the bottom through the mud for 51.25", (1.302m). This constitutes a 2 electrode device with a constant of

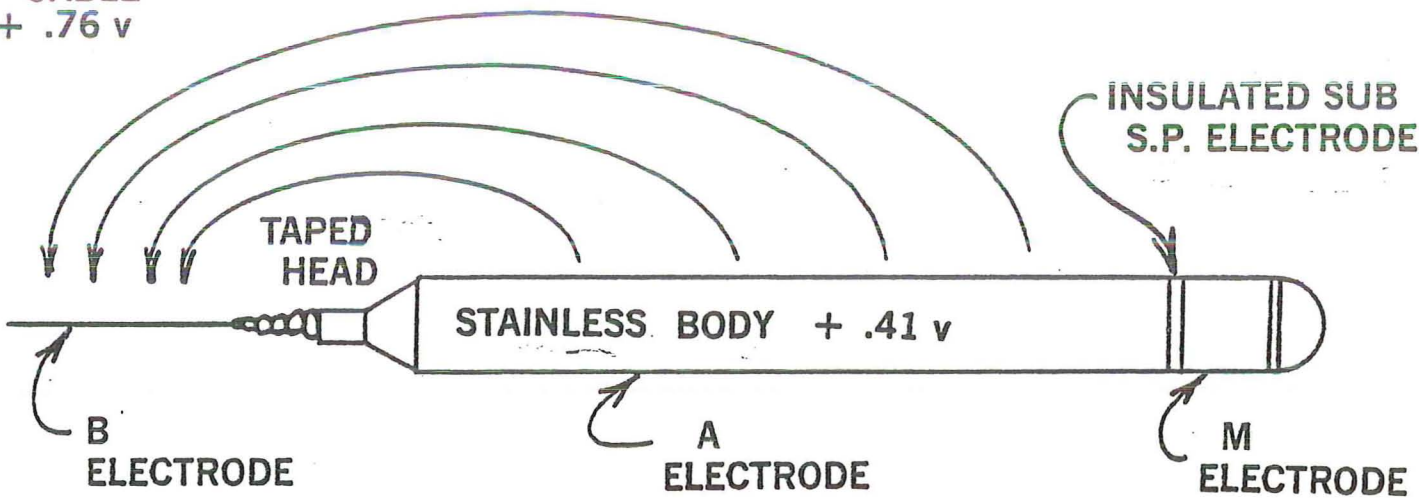
$$K_n = 4\pi L = 1.64\text{m, and} \quad (16)$$

the current would be:

$$I = K_n \frac{E}{R} = 1.24 \text{ amperes.} \quad (17)$$

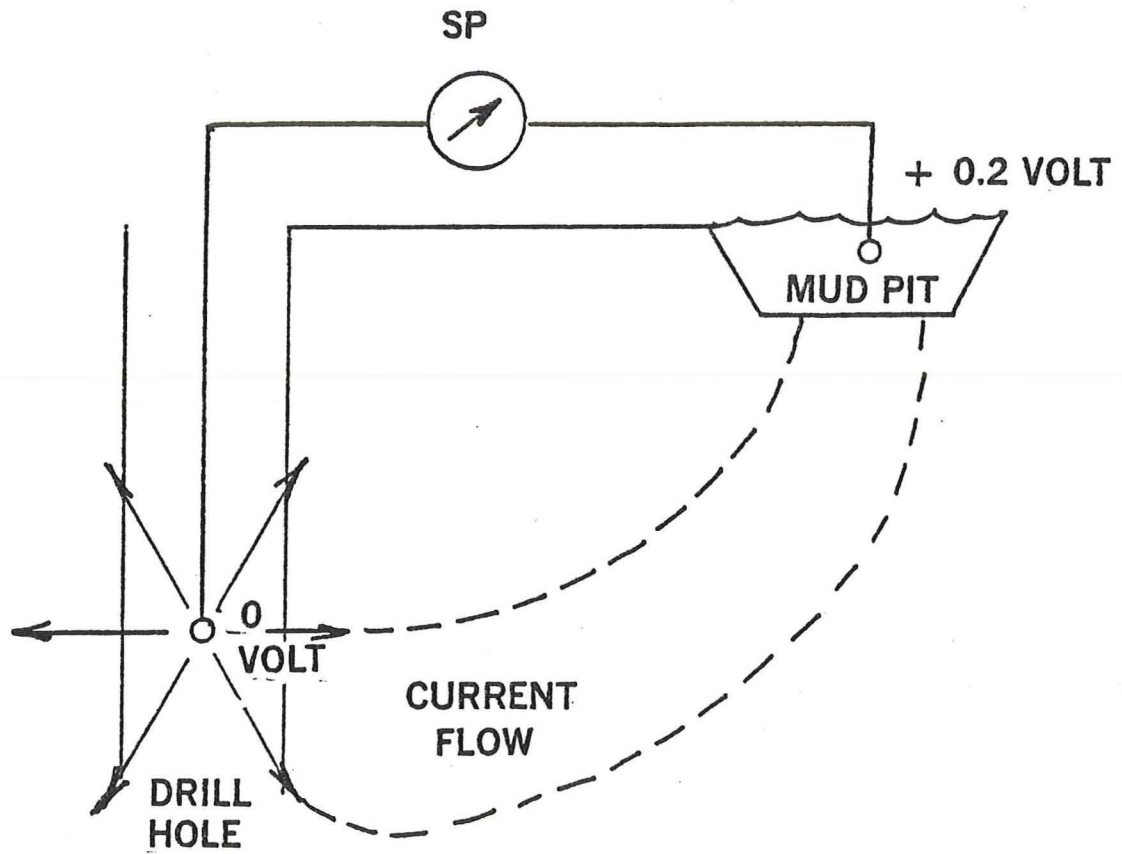
The distance from the SP electrode to the center of the sub is 3" (.076m). This gives a constant

GALVANIZED
CABLE
+ .76 v



EXPOSED TOOL EFFECT

Figure 10



EFFECT OF LOW IMPEDANCE

Figure 11

$$K_L = 4\pi \frac{\overline{AM} \overline{BM}}{\overline{AB}} = 1.01m, \text{ and} \quad (18)$$

$$E = \frac{RI}{K_L} = 1.23 \text{ v}/\Omega \text{ m.} \quad (17a)$$

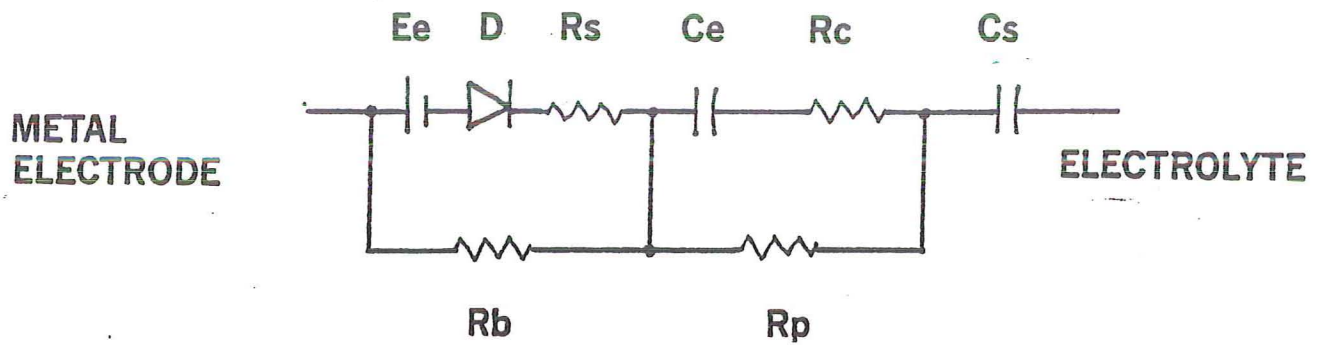
A resistivity or resistance curve can also be obtained by using a measure circuit of too low an impedance (Figure 11). In this case the circuit draws current and a single point resistance curve may result. In other words, the SP would have superimposed upon it a resistivity curve which would be in the direction opposite to, but almost a mirror image of the resistance curve. A "good-looking" SP curve may be worse than useless.

Mechanical damage to the electrode will always result in anomalous excursion of the SP curve. With most tools this is especially noticeable when logging going down. The electrode is not protected by the tool and can easily touch the wall of the hole. This will invariably cause a change of potential by removing some of the double layer and by scraping some of the deposited reaction products.

Finally we come to the question of the best electrode material. We have already determined that the measure and the reference electrode should be of the same metal.

The approximate electrical model of a metal-electrolyte interface is shown in Figure 12. Where E_e is the electromotive or electrochemical potential of the metal, D is the rectification action of the surface salts of the metal, R_s is the contact resistance of the metal surface, R_b is the leakage resistance of the rectification action, C_e is the interface capacitance of the electrode, R_c and R_p are the associated resistance of the interface, and C_s is the surface contamination capacity (oxides, etc.). With this model in mind, let us examine some of the advantages and disadvantages of each metal.

1. The most commonly used is lead. Lead has a low E_e , R_b is zero, R_p is low, C_s is zero. Therefore, it appears the same with the current flowing in either direction. Furthermore, reaction products like lead chloride have a tendency to remain on the surface making an approximation to an impolarizable electrode out of it. It is subject to concentration errors when moving, however.
2. Iron can be successfully used for a different reason. With iron, E_e is low, R_b and R_p are extremely low because when iron rusts, the oxide leaves the surface and the corrosion pits it. This results in a tremendous surface area. Further, it is mechanically strong.
3. Many electrodes are made of stainless steel. The reason stainless steel is stainless is because it forms a protective coating represented by C_s . This effectively insulates the electrode to one extent or another. This is also true of aluminum. Further, stainless steels can exist in an active or a passive state depending upon the pH of the electrolyte. These two states have very different electrode potentials E_e ; active is near +.5 volt while passive



**POSSIBLE EQUIVALENT CIRCUIT
METAL ELECTRODE-ELECTROLYTE
INTERFACE**

Figure 12

is near -1 volt. This can and often does change in the borehole, depending upon the chemical environment.

4. Copper, brass and bronze have been used. The salts of these metals are tough and clinging. They are also excellent rectifiers. R_b is high. Thus, D exists and has very non-linear characteristics.

Telluric Currents

Telluric currents or earth currents are currents flowing within the earth's surface layers. They are normally small but may be unusually large under some conditions. These currents appear to be associated with sunspot activity. They exhibit diurnal variations, and the short period variations are absent at night.

The amplitude of the voltages resulting from telluric currents is typically on the order of 6 to a few tens of millivolts per kilometer. or, in a 1000 foot hole in a low resistivity area, they could amount to 10 millivolts or more.

As you can see, the S.P. curve which we are now recording is a rather complex assemblage. There is a lot of information there. Our problem is chiefly one of trying to extract the useful information. This can be helped by learning more about the curve and by designing our instrumentation to select the useful parameters and reject the others.

INTERPRETATION OF THE SPONTANEOUS POTENTIAL CURVE

While the spontaneous potential or S.P. curve is complex in make up, its interpretation is relatively simple. This is, paradoxically, probably due to its complexity. We have not learned much about it, yet.

The several components of the S.P. signal: the diffusion-absorption component, the redox component, and the electrofiltration component (primarily) can be separated and each used.

A. DIFFUSION-ABSORPTION COMPONENT

The diffusion-absorption or d-a component is found by measuring the distance, in millivolts, of the deflection in a sand from the adjacent shale potential. In Figure 1, this is the distance, d , in each of the four sands illustrated. The deflection, d , is caused by a difference in ion concentration between the fluid in the sand, the drilling mud, and the adjacent shale. It (and the redox component) are the result of the potential drop in the mud column due to the current flow (IR drop) in the column. From the previous section we saw that this potential is E_{DA} :

$$E_{DA} = -11.7 \log \frac{R_{mf}}{R_{we}} \quad (1)$$

Where R_{mf} is the resistivity of the mud filtrate and R_{we} is the effective resistivity of the formation fluid (assuming only NaCl as dissolved solids).

Equation 1 is true at 75°F or 296°K. E_{DA} is directly proportional to the absolute temperature, but we usually can neglect this factor.

The value of E_{DA} can be either positive or negative depending upon the values of R_{mf} and R_{we} . The deflection, d_1 , is negative (or "normal"). The deflection, d_4 , is positive (or "reversed"), because the formation fluid in S_4 is quite fresh; fresher or lower resistivity than the mud filtrate. This is a common occurrence and quite normal. In fact, it is sometimes created artificially by putting NaCl in the drilling mud in order to get a readable S.P. curve.

The value of E_{DA} is used to determine the value of R_w through the use of equation (1). Figure 2 is a plot of equation (1). The determination of R_w involves several simple steps:

1. Determine the deflection, d , for the sand, S . In a simple, clean, homogeneous sand, S_1 , it is the average deflection. See Figure 1. The resistivity curve (or resistance curve) shows, by its simple shape that S_1 is a clean, homogeneous sand. Sand S_2 has shale in the upper part of it. We can tell this because the resistivity increases from top to bottom and the S.P. curve becomes more negative from top to bottom. Sand, S_3 , has either hydrocarbon in the top or

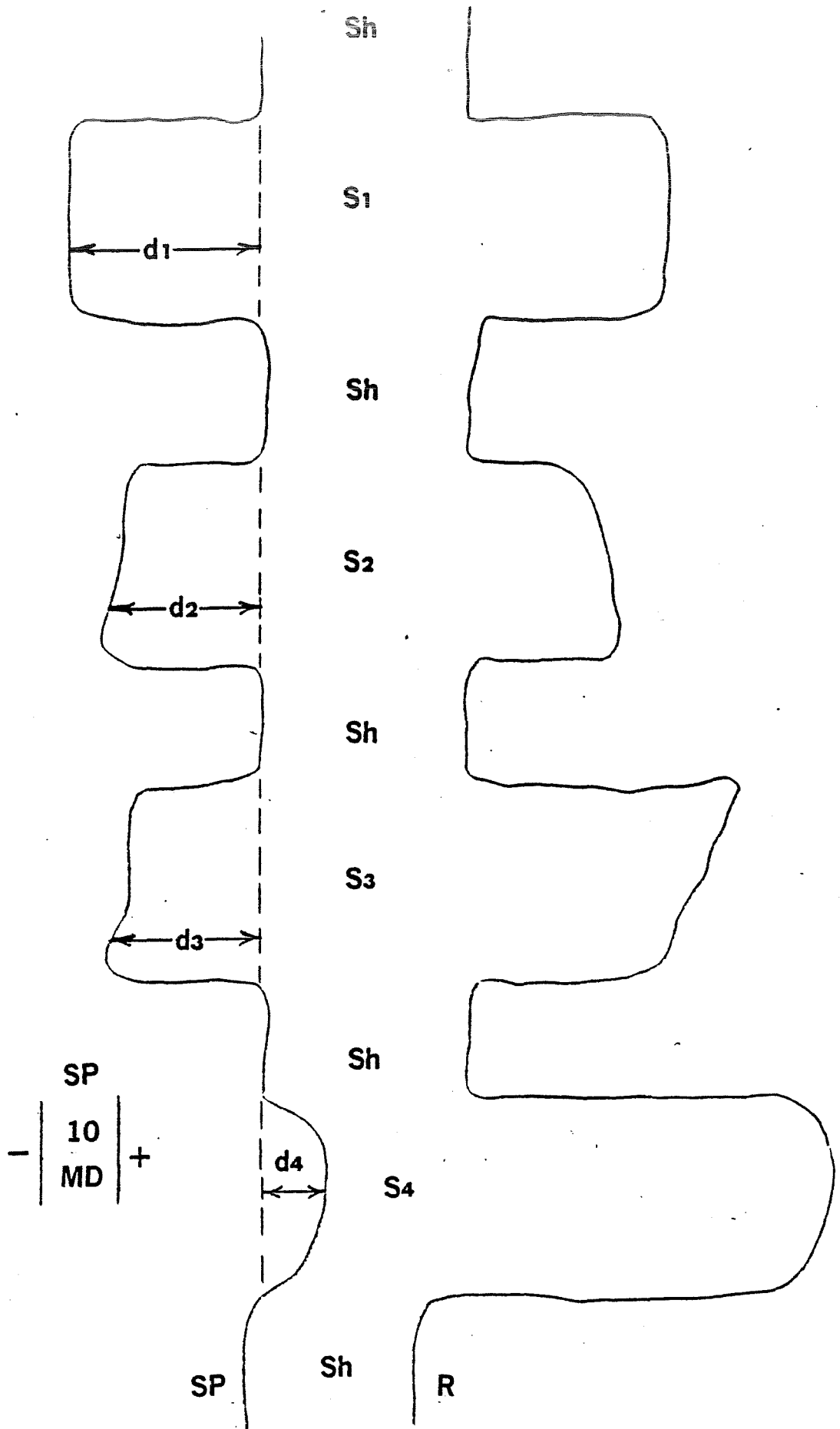


Figure 1

a salinity change from top to bottom. Since there is no evidence on the resistivity curve of shale streaks to isolate a salinity change, the change of deflection is probably due to hydrocarbons. Sand, S₄, is a fresh water sand; very clean.

2. Determine or estimate the value of the formation resistivity, R_t. This is covered in the section on interpretation of resistance logs. The value of the mud resistivity, R_m, should have been recorded at the time of logging. Sometimes the value of R_{mf} has also been noted. If not, the empirical relationship of Figure 3 may be used. Correct the values of R_t and R_{mf} for temperature, if necessary, with the chart in Figure 4.
3. Use the deflection from step 1 to find the value of R_{mf}/R_w from Figure 2. Calculate R_w:

$$R_w = \frac{R_{mf}}{\text{ratio}} \quad (2)$$

This value of R_w assumes that only sodium chloride, NaCl, is dissolved in the formation water.

4. Other salts than NaCl are usually present in formation waters but usually are not particularly important. However, in the areas where we do most of our work, the waters usually have low NaCl contents. Therefore, the effects of the others become important. Figure 5 shows the variations of activities for several salts. If the salt contents are known, the relative activities of each ion can be used to correct the value of R_w. If the content is not known, Figure 6 should be used. This is an empirical chart using average compositions. This value of R_w can be used for further interpretations.

In water well work the value of R_w can immediately tell if the formation will yield potable water or not.

Of course, the amplitude and shape of the E_{DA} deflection can tell much about the quality of the sand. This was pointed out in step 1. Clays and shales will usually reduce the deflection of the E_{DA} component of the S.P. Hydrocarbons will also reduce it. This is the portion of the curve petroleum people usually consider as the S.P.

B. REDOX COMPONENT

The redox component of the S.P. curve has not been used, so far, in field interpretations and very little in rigorous interpretations.

Redox potentials are important because much of the mineralization in sedimentary formations takes place at a reduction-oxidation (or redox) interface. Many of the minerals we seek, or are associated with the minerals we seek, are reducing. These include petroleum, coal, and pyrite (and other sulfides). The roll front zonation described by Rubin

EQUIVALENT FORMATION WATER RESISTIVITY FROM SSP

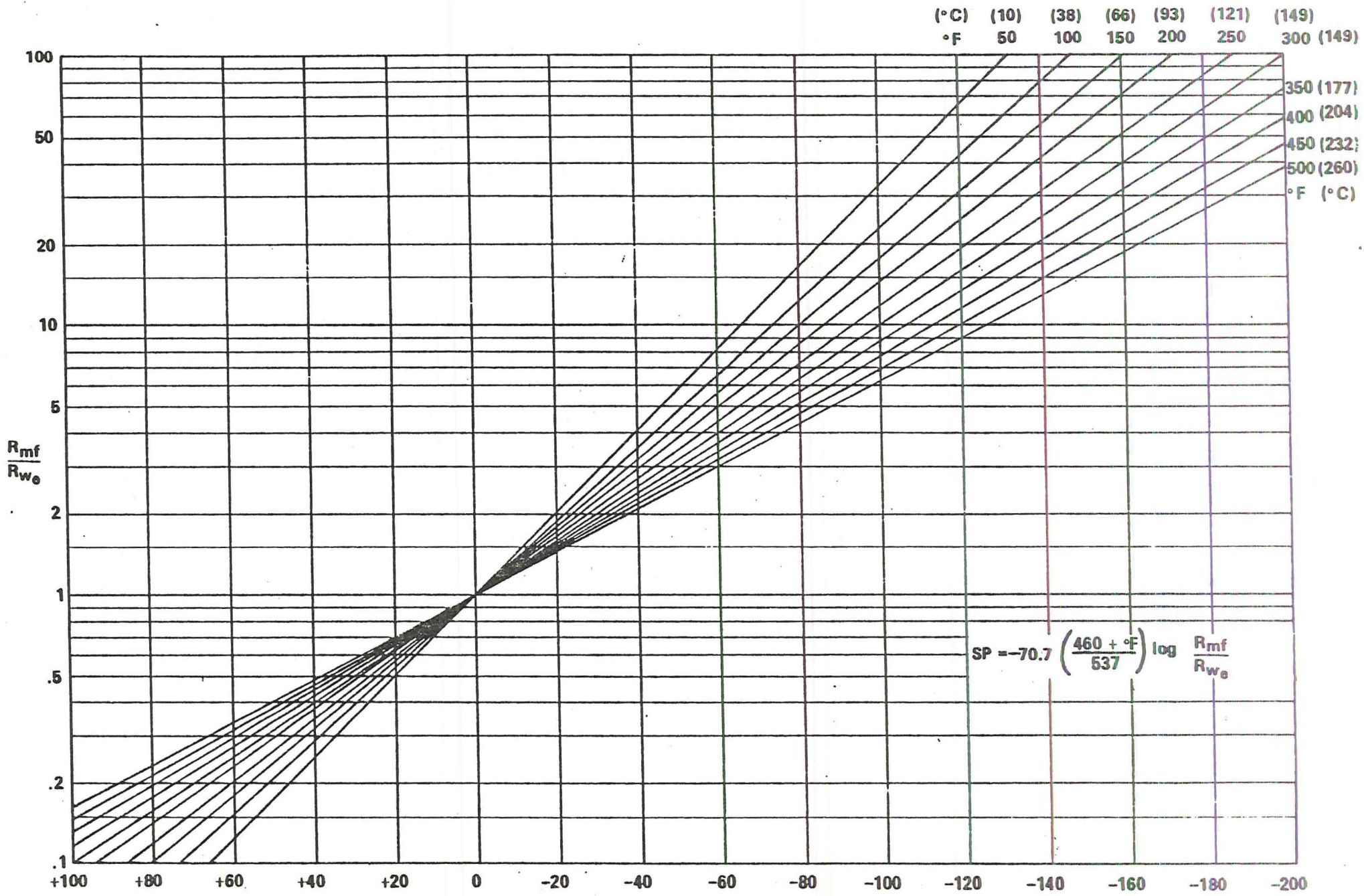


Figure 2

$R_m - R_{mf} - R_{mc}$ RELATIONSHIPS
(EMPIRICAL CHART)

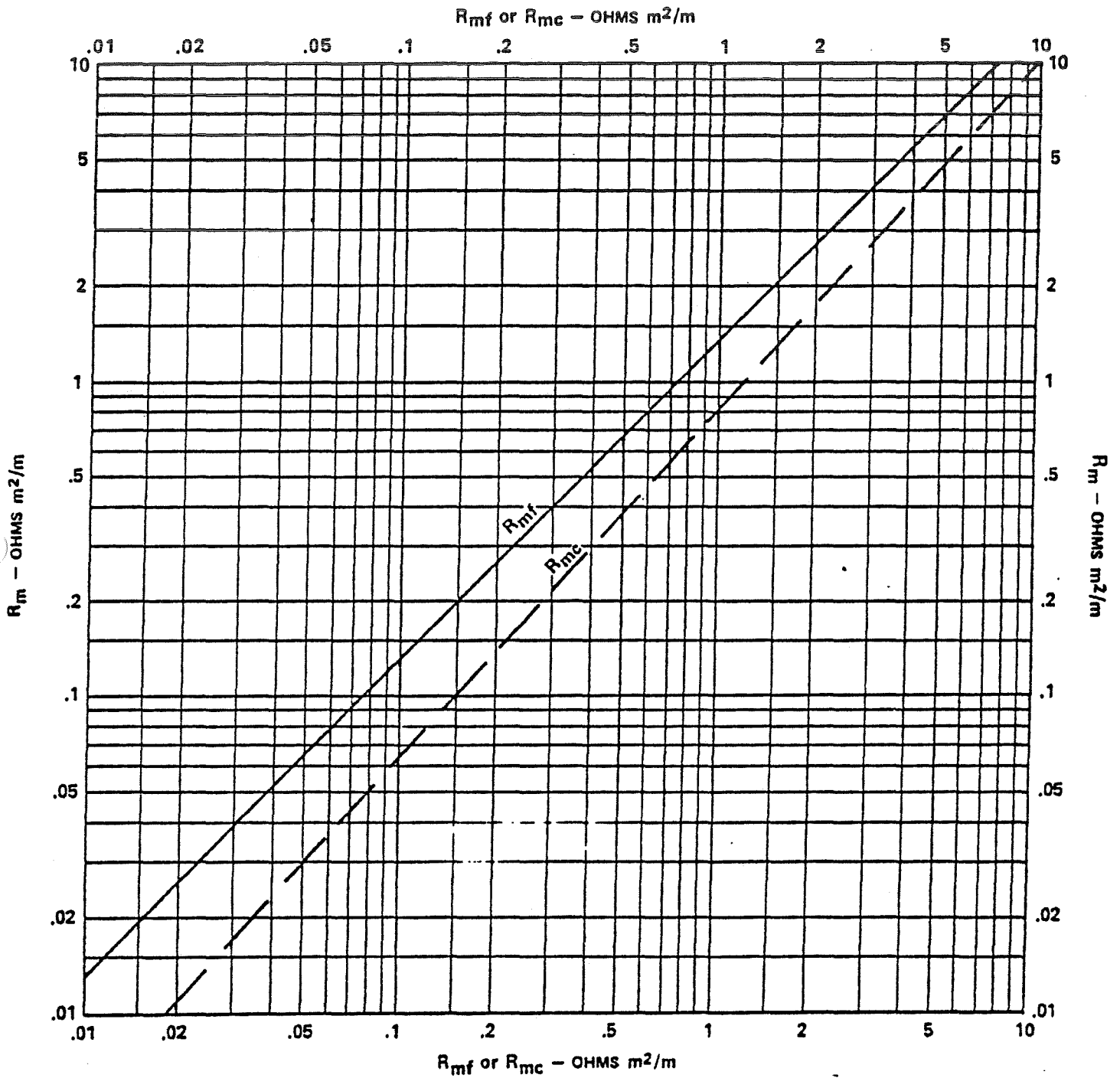


Figure 3

RESISTIVITY VERSUS TEMPERATURE — NaCl SOLUTIONS

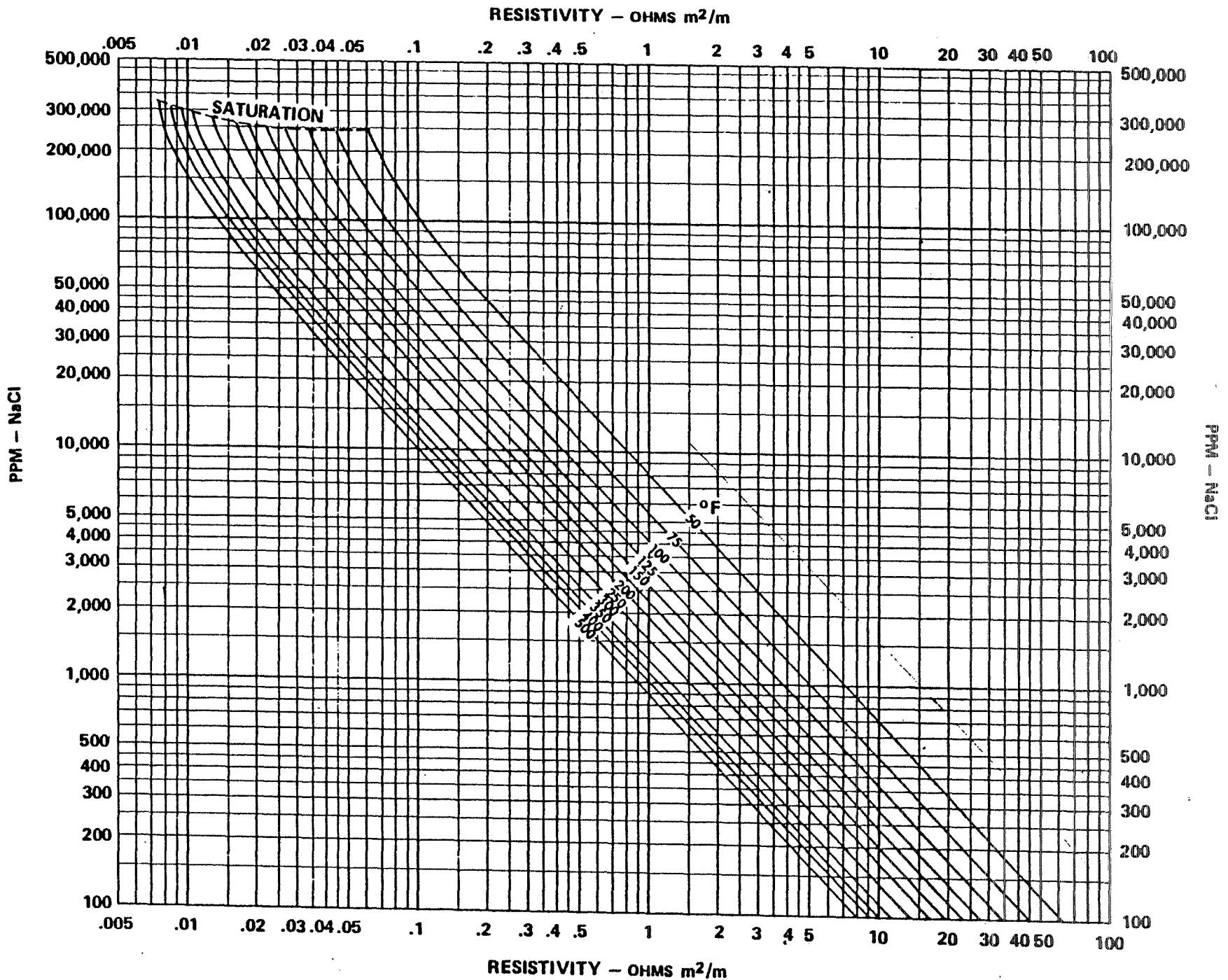


Figure 4

CONDUCTIVITY VERSUS CONCENTRATION FOR VARIOUS SALT SOLUTIONS AT 18°C

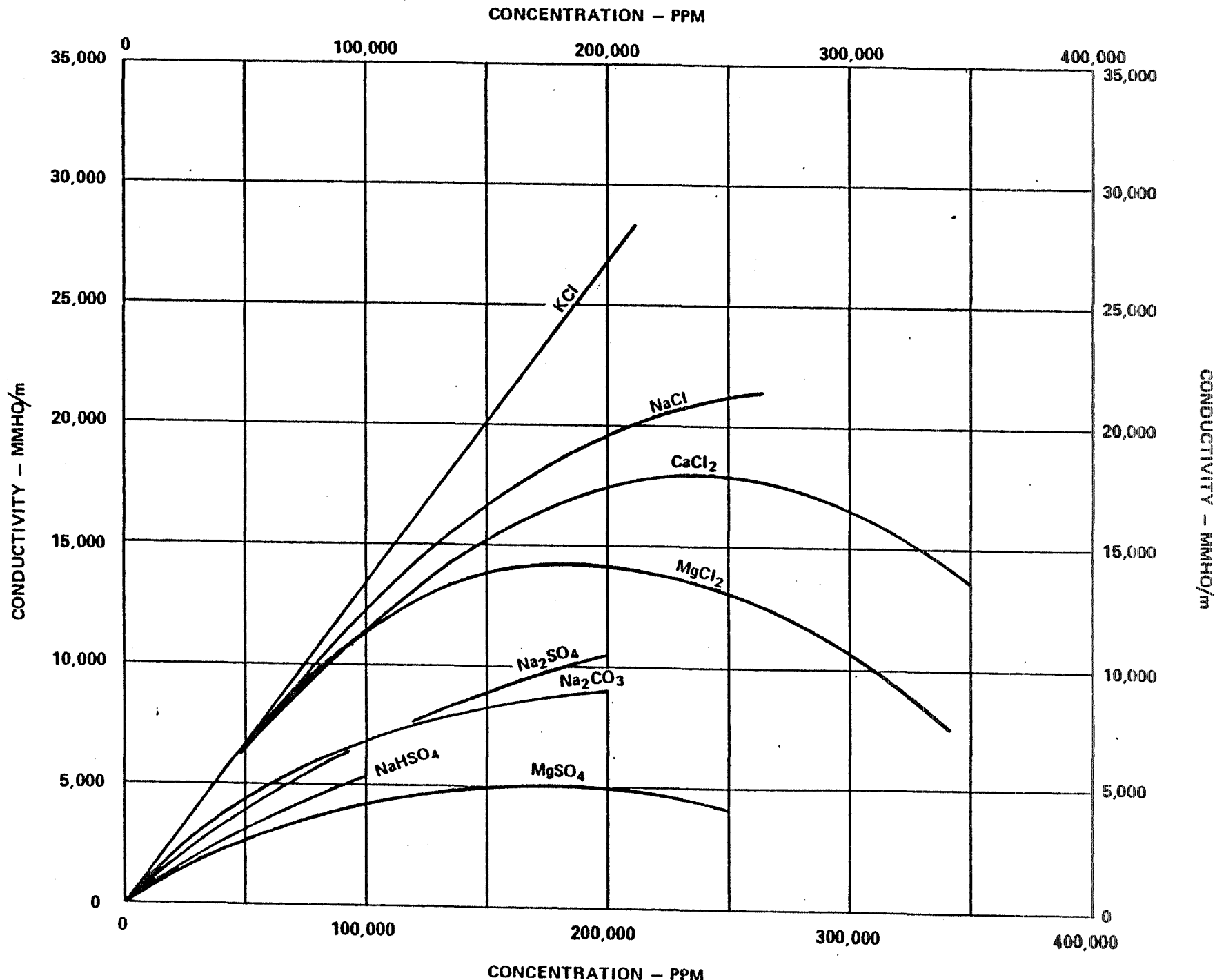


Figure 5

R_w VERSUS R_{w_e} AT VARIOUS TEMPERATURES

R_{w_e} - OHMS m²/m

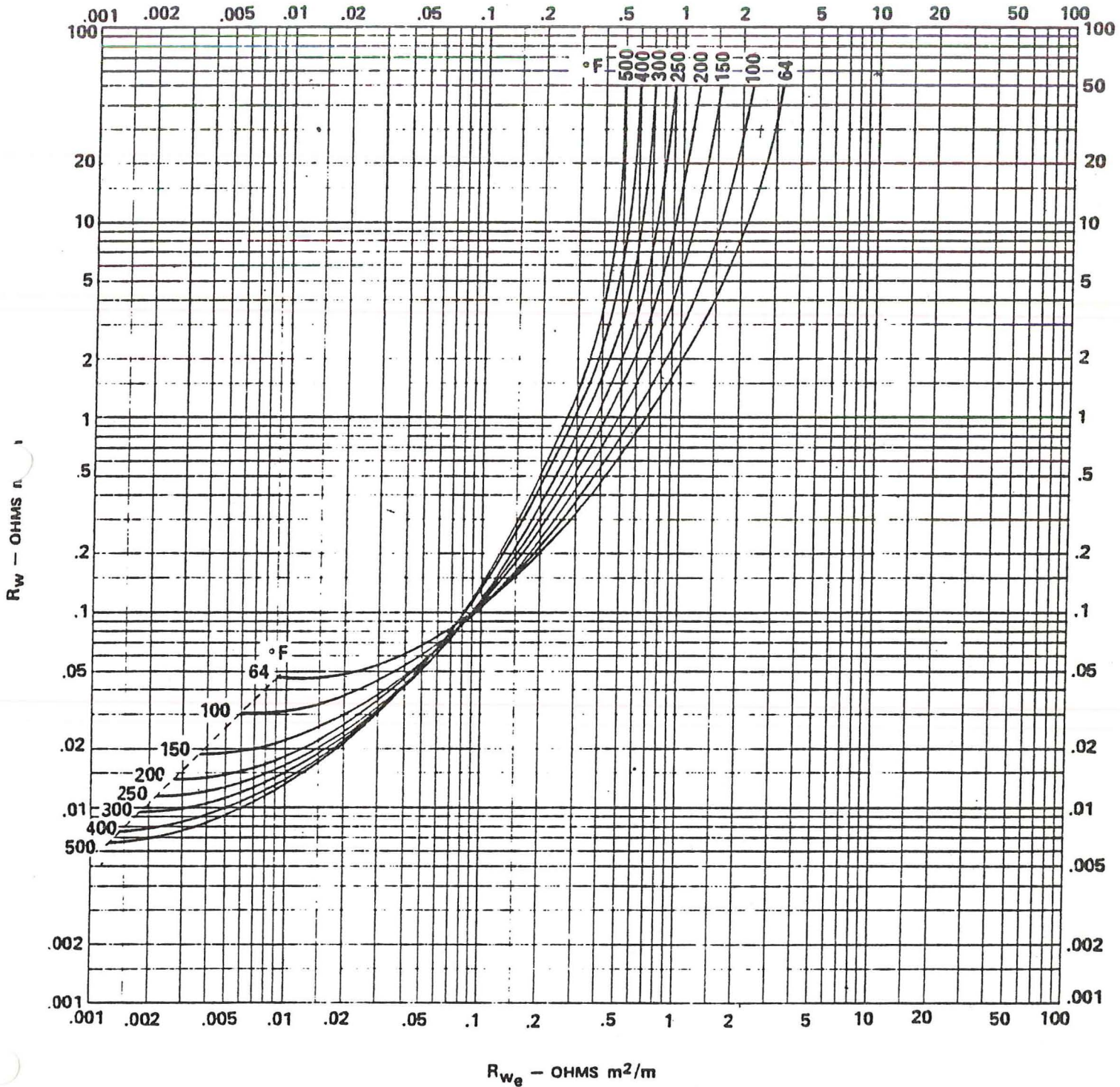


Figure 6

in his paper attached to the Gamma Ray Log Uses section is a redox interface. His descriptions are for uranium, but also are valid for sedimentary iron, copper, vanadium, silver, and other heavy metals.

Each ion change has a redox potential associated with it. If a sulfide ion is oxidized to a sulfate ion, it gives up energy in the form of electrical energy as well as heat. The reverse is also true. These energy changes are detectable as characteristic potentials. Much work is being done on this complex subject. An excellent reference is "Solutions, Minerals, and Disequilibria" by Garrels and Christ.

If the redox potentials are known or derivable, we can tell where we are with respect to a "roll-front," how wide the "roll-front" may be, and where the mineralization may occur.

Most S.P. measurements are made as relative or differential measurements, because the absolute value has not previously been valuable in "oil-field work." Therefore, with old logs we must be content with relative measurements.

One must pick a formation where the redox state is known. This may be the surface, if it is highly oxidized, or it may be a sand such as the Dakota Sand in the New Mexico mineral belt. The Dakota Sand is usually well reduced. If the shale base line is traced, it will have a small drift to the positive or negative direction going from one sand to another and even within a sand. The direction of the drift and position with respect to the reference sand will tell the redox state of the sand. If it is sloping to the positive direction (right) the next sand is more reduced than the last. If the potential is more negative than the potential in the reference sand base line, then the sand is more oxidized than the reference. With practice one can even trace redox trends within sands.

In the future we will measure absolute S.P. potentials. When this is done, we'll be able to map isopotential contours using these for locating trends and probable mineralization.

C. ELECTROFILTRATION COMPONENT

The electrofiltration component of the S.P. curve is usually the result of invasion of a sand by drilling fluids in a freshly drilled hole. They can be detected by repeating an S.P. curve one or more times. If filtration is taking place seriously, the second curve will be displaced from the first with usually little serious change of character.

A lost circulation zone is usually detectable by its large anomalous negative potentials. A sand "making" water will have a positive potential associated with it.

INTERPRETATION OF SINGLE POINT RESISTANCE AND RESISTIVITY LOGS

Electrical resistance is the ratio of the voltage drop or potential gradient produced by a flow of current to that current. In other words; it is the resistance to the flow of electrical current through an electric potential field. In geophysics it is the resistance to the flow of current through the pore spaces in the rock of a formation. Since the pore spaces are typically filled with water solutions, the resistance can be used to determine the amount of pore space in a rock.

Electrical resistance depends upon the geometry of a material and upon its resistivity. Resistance, r is given by:

$$r = R \frac{L}{A} \quad (1)$$

where R is the electrical resistivity of a material, L is its length and A is its cross sectional area. Resistance is defined as:

$$r = \frac{E}{I} \quad (2)$$

where E is the potential across a piece of material and I is the current through it. If E is in volts and I in amperes r will be in ohms. This is Ohms Law.

The reciprocals of resistance and resistivity are conductance and conductivity respectively.

If we pass a known current, I through a sample of material we can measure a voltage drop, E along it. Therefore, we can determine the resistance, r . If we measure the length and cross section of the sample, we can determine the resistivity of that sample.

Resistivity is a basic property of a material as its color and density are. From equation (1) we can say

$$R = r \frac{A}{L} \quad (1A)$$

With most conventional geophysical resistance and resistivity measuring devices, a constant current, I is caused to flow through an electrode into the surrounding formation. The resulting voltage drop, E is measured. From equation (2), r is proportional to E if I is held constant. Similarly, from equation (1A), if A and L are known and constant, a measure of the voltage drop, E can be interpreted in terms of resistivity, R .

The pore space of a clean formation rock is filled with water containing various dissolved salts (assuming no petroleum or gas in the pore space). This formation water will conduct a current of electricity because it, and more especially its dissolved salts, are ionized. If a potential field is placed across it, the positive ions will migrate toward the negative direction or cathode and the negative ions toward the positive direction or anode.

(For this reason negative ions are called anions and positive ones are called cations.) This constitutes a flow of current.

The formation water will usually conduct a current so much more easily than the solid rock around it that virtually all of the current through a formation will flow through the formation water. The relative amount flowing through the solid material will usually be from 0.1% to less than .000001%. Therefore, for our purposes we can assume that all of the current flows through the formation water.

The resistivity of the formation water can easily be measured in the laboratory if we have a sample of it. It can be put into a glass container of known length, l and known cross section, A and a current flowed through it. The voltage drop along the glass can be used to calculate the resistivity of the formation water, R_w . Also, in the section about S.P. we discussed how to determine the value of R_w from the S.P. curve.

In the formation we do not have a glass in which to put the formation to measure its resistivity, R_t . However, we can assume, fairly safely, that the current will follow predictable paths. This is as confining and as good as the glass. We only have to figure out what the size and shape are.

The single point system uses a single downhole electrode to put a constant current through the formation to a return electrode. The potential difference between the two is measured. If the downhole electrode is spherical and in a homogeneous medium and if the return electrode is an infinite distance away, the current will flow radially from the downhole electrode. Similarly, a short cylindrical electrode will have nearly a radial flow of current. In such a situation the resistance of the electrode, r_e will be:

$$r_e = \frac{R_t}{2\pi L} \ln \frac{L}{d} \quad (2)$$

where R_t is the resistivity of the homogeneous medium, L is the length and d the diameter of the electrode.

From equation (2) we could calculate R_t if we know L and d . However, the depth of investigation of a single point device is very shallow. Typically, the response is like Figure 1. Within a radius of 5 inches from the electrode (a 10" diameter sphere) we are already receiving 65% of the signal. When a 4-3/4 inch diameter borehole is put through that 10 inch sphere, there is not much (and an uncertain part) left. If the tool is centered in the borehole, the borehole represents 34% of the volume of the 10 inch diameter sphere and probably 45% of the total response of the device. Fortunately, the tool and electrode usually are against the wall of the hole. In this situation the borehole represents about 25% of the volume of the 10 inch sphere and contributes about 16% of the signal from this sphere. In other words, the borehole contributes a significant, variable, and uncertain part of the total signal and is, thus, difficult to quantify.

If the value of the mud resistivity, R_m has been measured, the value of the formation resistivity, R_a can be found:

$$R_a = \frac{2\pi L r_e}{.85 \ln \frac{L}{D}} - .18 R_m \quad (2A)$$

RADIAL INVESTIGATION CHARACTERISTICS OF VARIOUS RESISTIVITY TOOLS
 (INFINITE HOMOGENEOUS ENVIRONMENT)

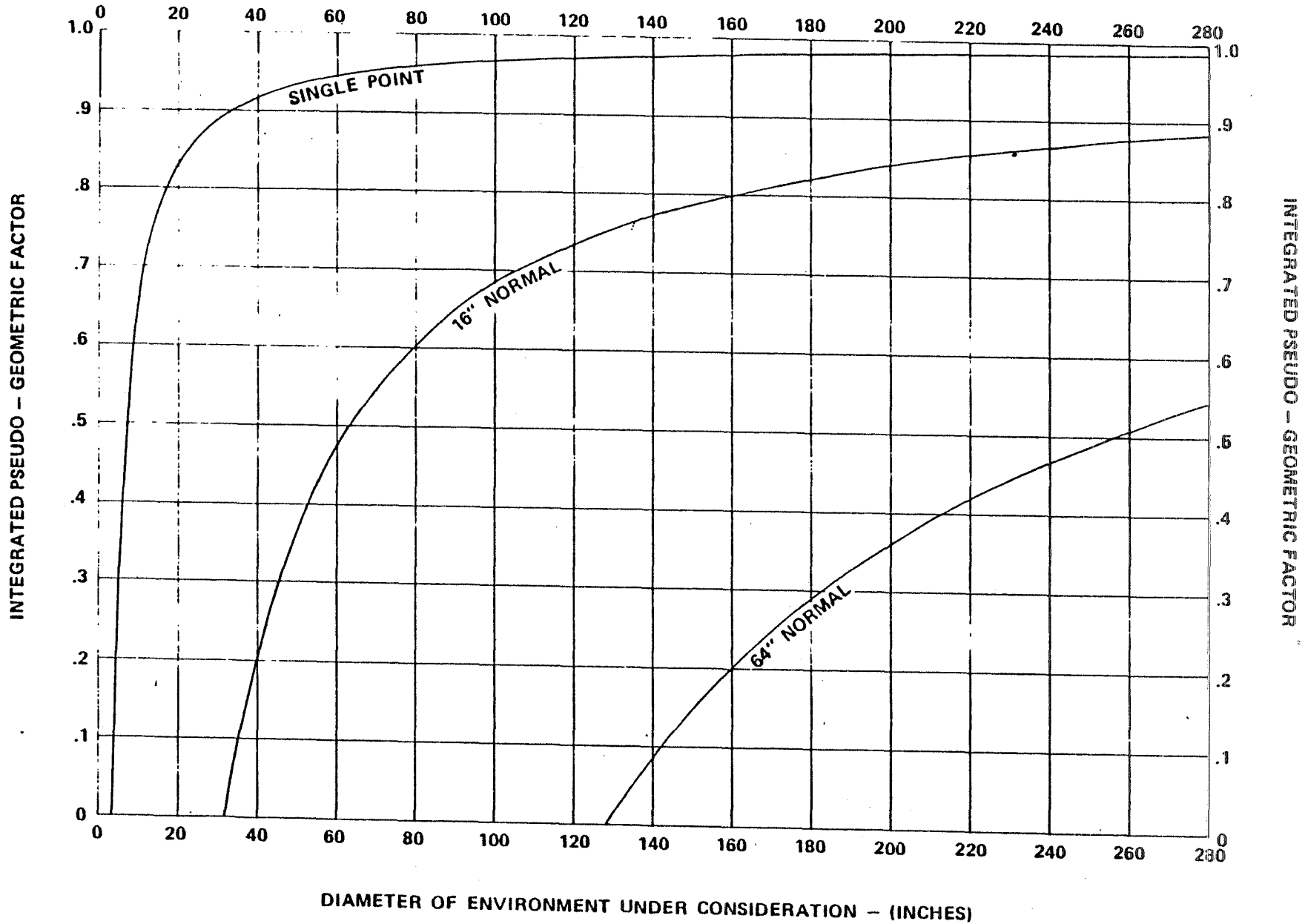


Figure 1

It should be kept in mind that this value of Ra is subject to errors and is only an approximation. This portion of the formation is probably completely invaded with mud filtrate. Therefore, Ra can be considered a measurement of Rxo.

Other resistivity devices are not being used by Century at this time. There are several of them, however. They have various uses and disadvantages. Chart I has a brief description of them. More detailed descriptions can be found in the 1974 edition of Schlumberger Log Interpretation/Principles, Volume I and in Fundamentals of Well Logging by Dr. Sylvain J. Pirson.

Chart I

<u>Device</u>	<u>Feature</u>	<u>Depth of Investigation and Princ. Meas.</u>	<u>Advantages & Disadvantages</u>
Single Point	Stratigraphy	65% in 10" dia. Rxo	Good Resolution, Difficult to quantify
Microlog	Small volume porosity	65% in 2" radius Rxo	No hole effect, high detail, mudcake interferes
Microlaterolog	Focused, Porosity	65% in 12" Rxo	No hole or mudcake effects
16" Normal	Stratigraphy, Porosity	65% in 16" Rxo	Quantified, hole effects, useless in shallow invasion, thin bed effects
64" Normal	Porosity	65% in 64" Rt	Quantified, affected by invasion, bed effects
Laterolog 3	Porosity Focused	65% in 3' Rt/Rxo	Good resolution, heavy, no S.P.
Laterolog 7 and 8	Porosity Focused	65% in 6' Rt	Good resolution, long probes, complex circuitry
Induction Log	Porosity, Focused	65% in 6' Rt	Good resolution, no hole fluid effects, complex

Resistance and resistivity logs are used primarily to calculate formation porosity. They are also used for stratigraphy, lithology determinations, and correlation. The last is probably the most important use in mineral exploration.

Since the formation water fills the pore space in the rock "matrix," we can use this to calculate porosity, ϕ . The ratio of the formation resistivity, R_t to the resistivity of the contained water, R_w is the formation factor, F :

$$F = \frac{R_t}{R_w} \quad (3)$$

R_w can be obtained from the S.P. curve. With our single point measurement we usually "see" the zone of the formation which has been flushed with mud filtrate. The formation factor is also the ratio of the resistivity of the flushed zone, R_{xo} to the resistivity of the mud filtrate, R_{mf} :

$$F = \frac{R_{xo}}{R_{mf}} \quad (3a)$$

R_{mf} can be obtained by direct measurement of a filtrate sample obtained from a Baroid mud press or it can be obtained from empirical charts. These charts can be found in The Formation Evaluation Data Handbook by Gearhart-Owens Industries, Inc. and Schlumberger Log Interpretation Principles, Volume I. The empirical relationship chart is Figure 2.

Regardless of the method used to obtain F , the relationship to porosity is

$$F = \frac{a}{\phi^m} \quad (4)$$

where m is a cementation factor and a is an empirical constant. Generally in sands $a=0.81$ and $m=2$. In compacted formations $a=1$ and $m=2$. General results are obtained with the "Humble formula:"

$$F = \frac{0.62}{\phi^{2.15}} \quad (4a)$$

m can be as high as 3.5 in some oolitic rocks. These relationships are shown in Figure 3 and Figure 4.

These relationships (3 and 4) apply to formations which are clean and 100% water saturated. If part of the pore space is filled with hydrocarbon, gas, or clay these must be modified. Hydrocarbons and gases have high resistivities, so they are difficult to separate electrically from the rock "matrix." Clays are part of the solid, nondisplaceable portion of the rock but are conductive. These things can be determined by measuring the porosity by different methods or under different conditions.

Suppose the resistivity of a formation is measured by two different devices, one of which is deep and focused and the other shallow. The deep portion of the formation will contain undisturbed fluids; formation water and, perhaps, hydrocarbons. In other words, the water saturation, S_w may be less than 100%. The shallow portion of the hole will have virtually all of its original fluid, water and hydrocarbon, replaced by mud filtrate. The apparent porosity or formation factor can be determined in each case. The deep formation factor, F_d is:

$$F_d = \frac{R_t}{R_w} \quad (3b)$$

R_t can be obtained from an induction log or a laterolog. R_w can be de-

**R_m - R_{mf} - R_{mc} RELATIONSHIPS
(EMPIRICAL CHART)**

R_{mf} or R_{mc} - OHMS m²/m

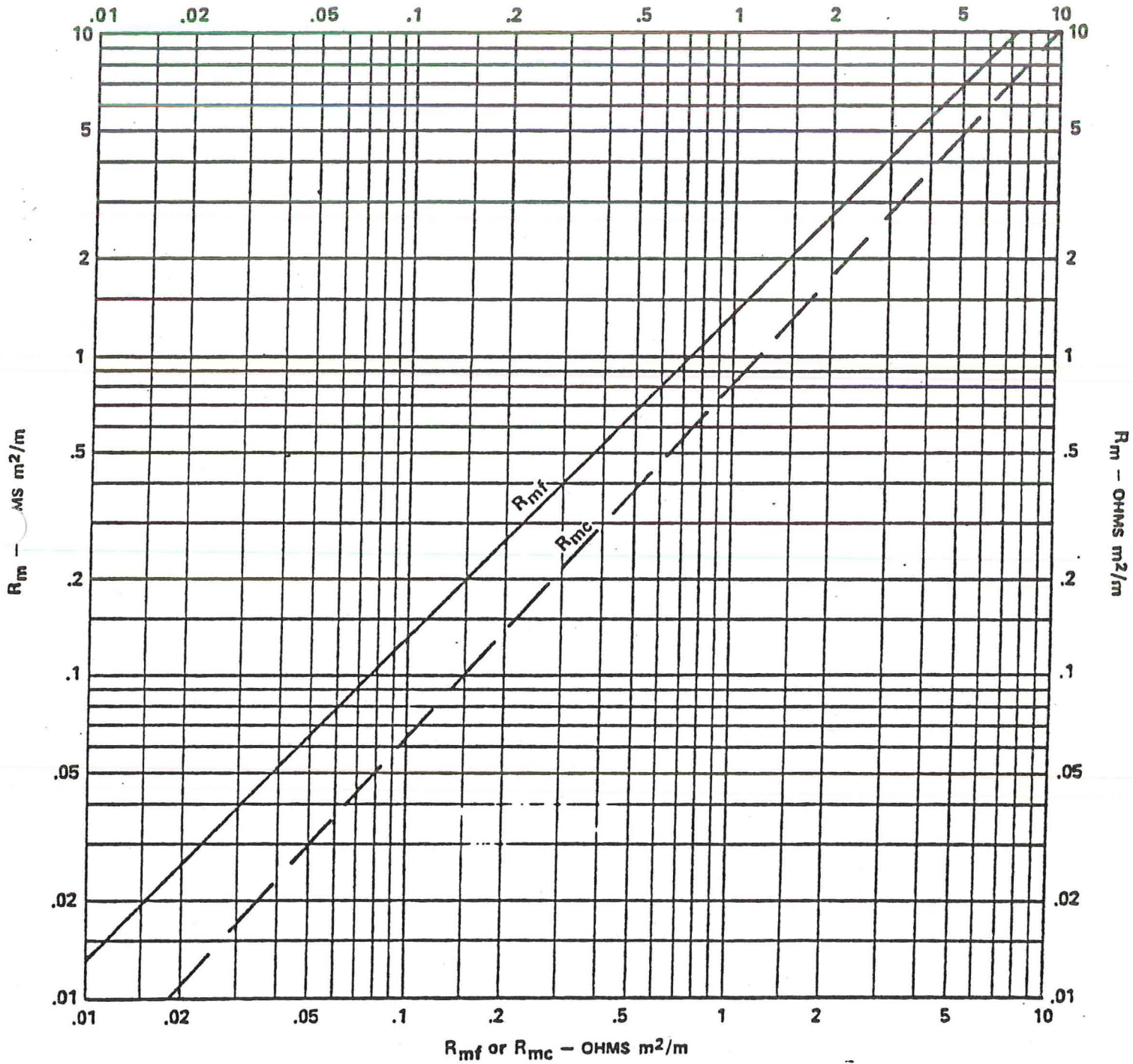


Figure 2

FORMATION FACTOR - POROSITY RELATIONSHIPS

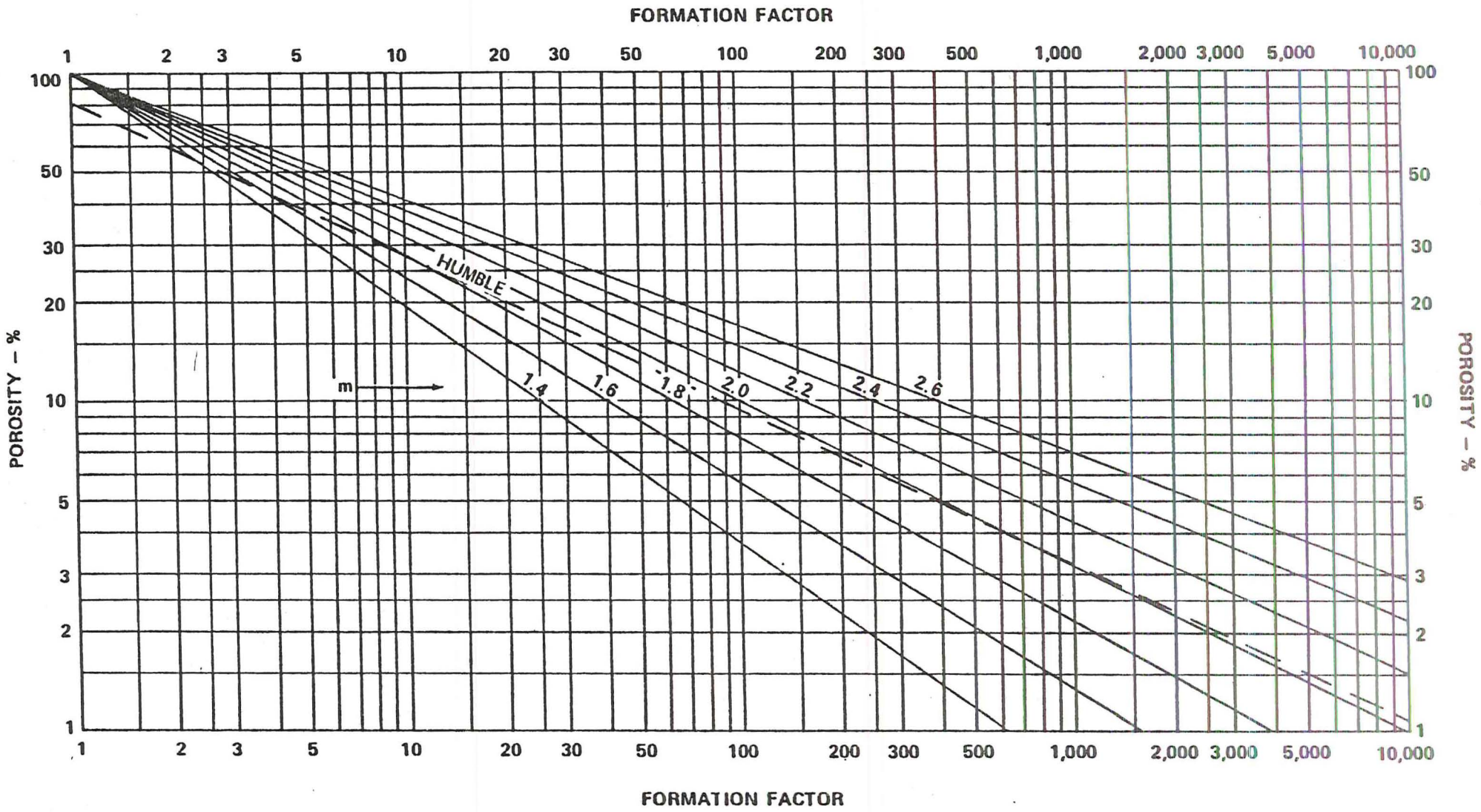


Figure 3

70

Sec. 4, p 7 of 9

WATER FILLED POROSITY-RESISTIVITY RELATIONSHIPS

RESISTIVITY - OHMS M²/M

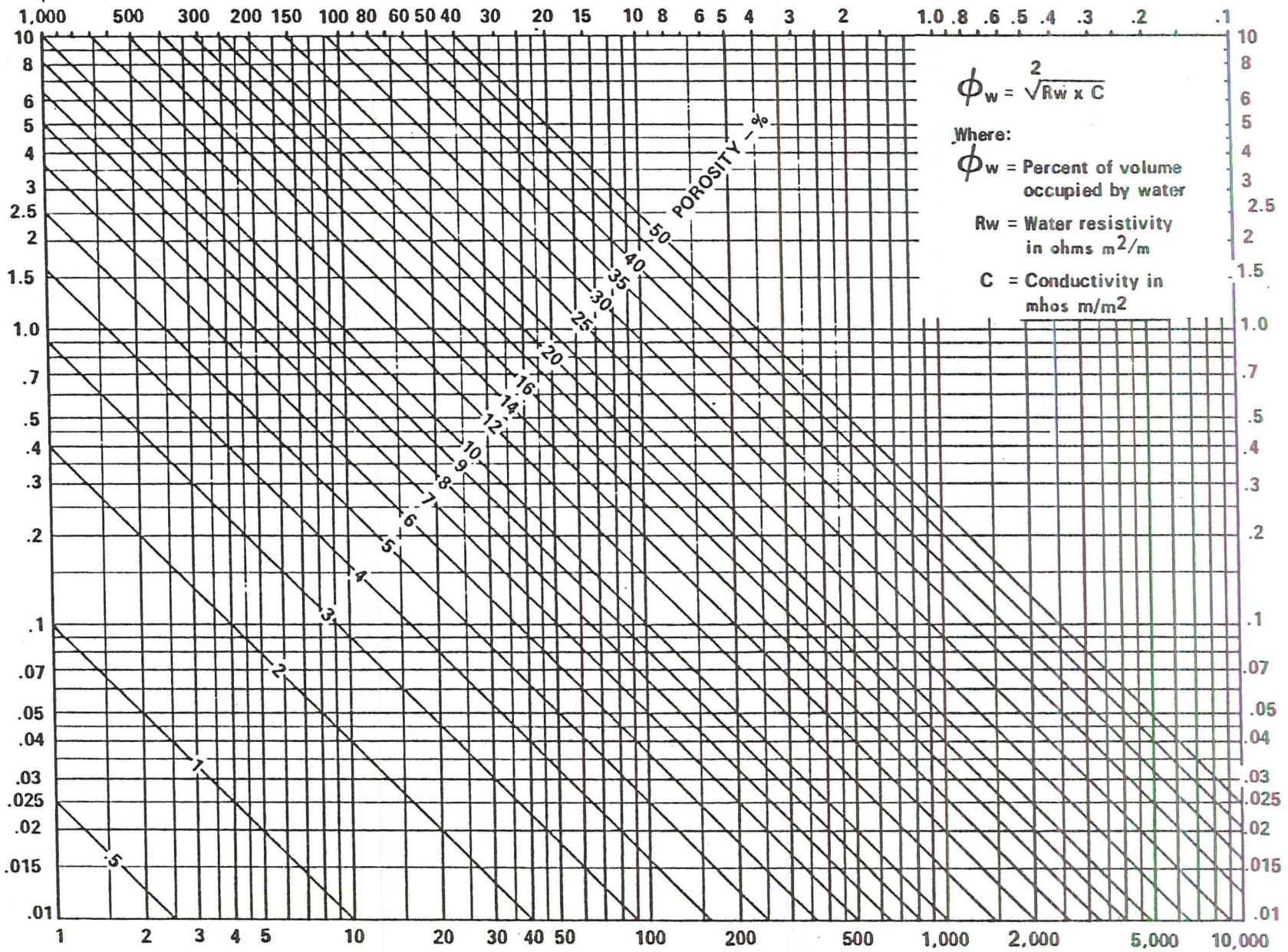


Figure 4
 Sec. 4, p 8 of 9
 R_w OR R_{mf} - OHMS M²/M

R_w OR R_{mf} - OHMS M²/M

Figure 4

terminated from the S.P. The shallow formation factor, F_s is:

$$F_s = \frac{R_{xo}}{R_{mf}} \quad (3c)$$

R_{xo} can be obtained from a 16" Normal or a Microlaterolog. R_{mf} can be obtained from a mud sample. The difference between the two values of F is a measure of water saturation:

$$S_w = \sqrt{\frac{F_s}{F_d}} \quad (5)$$

if the assumption is made that all of the hydrocarbon has been displaced or that that which is left is irreducible.

Much the same process can be used to determine the amount of clay in a sand. In this case the porosity determinations should be made with a resistivity device and a device affected differently, such as a sonic tool. This process will be described later under Cross-Plotting.

INTERPRETATION OF DENSITY LOGS

Density measuring equipment used by Century is usually the scattered gamma ray or gamma-gamma type. This type system emits gamma rays into the formation from an isotopic source and reads the returned, scattered gamma rays. The gamma photons from the source are scattered by collisions with electrons in the formation. Energy from the photon is lost to the electrons upon each collision. Most of the photons scattered in the formation are rescattered and lost. Some are scattered (usually some of those which have been scattered only once) back to the tool detector. Therefore, the more electrons available to scatter gamma photons, the fewer photons get back to the detector. The density of electrons in a material is very nearly proportional to the bulk or mass density of the material. Thus, the counting rate is a function of the mass density of the formation.

As gamma photons are scattered in a material two types of scattering take place. Elastic or Compton scattering involves a transfer of energy from the photons to the electrons upon collision which is very nearly constant per photon and per electron. We can assume, as a first approximation that it is constant. This means that the energy lost by the scattered photons will be directly proportional to the number of electrons (or protons) present per atom or atomic number, Z .

At low energies and/or high atomic weights, photoelectric or inelastic scattering begins to become significant. In this type of scattering a disproportionate amount of energy is transferred to the electron upon collision with a gamma photon. This type of scattering is approximately a function of the sixth power of the atomic number. See Figure 1.

Calcium ($Z=20$) is the heaviest common element in formations. The iridium 192 source has most of its emission at 331 kev. At this energy photoelectric scattering is less than 1% of the Compton scattering. When a cobalt 60 source is used (energy = 1.17 and 1.33 mev.), the photoelectric effect is negligible. Iron ($Z=26$) is beginning to show an appreciable (1%) amount of photoelectric scattering.

We are safe, therefore, in assuming only Compton scattering in normal formations.

The gamma-gamma density tool has a response proportional to the electron density, Z of the formation. The bulk or mass density of a material, however, is a function of the atomic weight, A of the material. Z is the number of electrons around the nucleus of an atom or the number of protons in it. A , however, is the number of protons plus the number of neutrons in the nucleus. The chemical characteristics of an atom are determined by the atomic number. Thus, all calcium has an atomic number of $Z=20$ and identical chemical characteristics. Not all atoms of calcium have the same number of neutrons, however. Thus, they have different weights. These variations are called isotopes. Isotopes are elements with the same number of protons but with different numbers of neutrons. Thus, different isotopes

COMPTON SCATTERING AND PHOTOELECTRIC ABSORPTION:
 ATOMIC ATTENUATION COEFFICIENTS VERSUS ATOMIC NUMBER
 (0.3 MEV GAMMA RAY ENERGY, NARROW BEAM GEOMETRY)
 (FOR TOTAL ATTENUATION COEFFICIENT IN BARNS ADD COMPONENT VALUES)

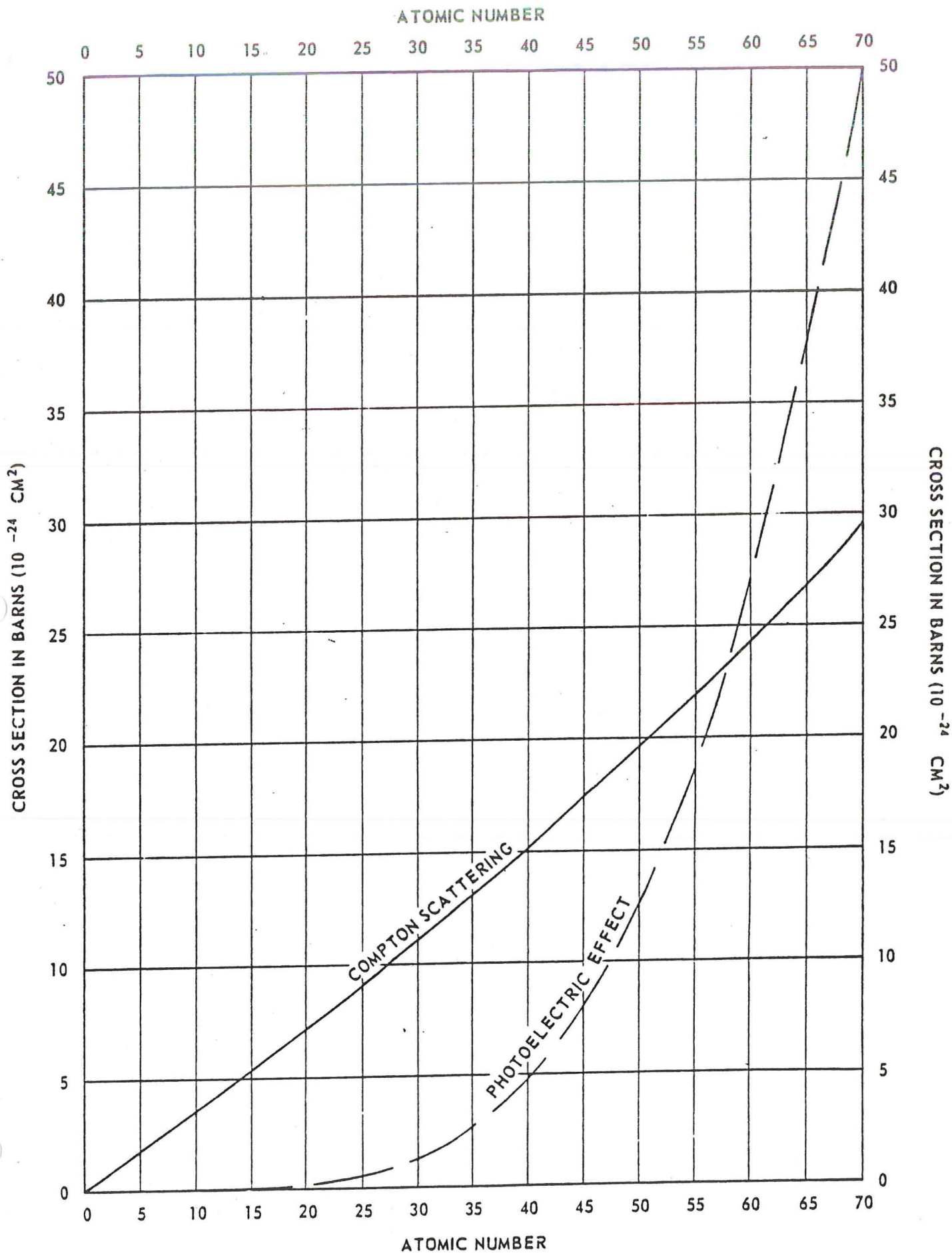


Figure 1

of the same element have different atomic weights, A. Isotopes differ in weight in integral units of atomic mass units. One AMU is approximately the weight of one neutron or one proton. This is true of all elements.

Most naturally occurring elements are a mixture of isotopes. Thus, their natural atomic weights, which are averages, are never integral numbers (oxygen, A=16.000, had its weight assigned on the belief, at the time, that there were no isotopes of oxygen). Approximately Z/A=0.5. But there are significant variations from that ratio. Therefore, a correction for the Z/A departure from 0.5 must be made to convert from electron density to bulk density. For example, silica is silicon dioxide, SiO₂, a major constituent of most rocks. It has a total atomic number of 30 and an atomic weight of 60.06. Thus, the Z/A ratio for silica is .4995. Limestone is calcium carbonate, CaCO₃. Z for limestone is 50, A is 100.09, and Z/A is .4995. Water is H₂O. Z=10, A=18.0159, and Z/A=0.555. Thus, limestone and silica need virtually no correction by themselves. However, both limestone and sand contain water which requires a correction factor.

The Z/A ratio of a material is the sum of the atomic numbers of the constituent atoms divided by the sum of their atomic weights. The Z/A ratio of a porous rock is:

$$Z/A = \frac{\emptyset Z_f + (1-\emptyset) Z_m}{\emptyset A_f + (1-\emptyset) A_m} \quad (1)$$

where \emptyset is the fractional porosity, f is the fluid in the pore space and m is the rock matrix. Therefore, the Z/A ratio of a sandstone with 20% porosity would be

$$Z/A = \frac{(.20 \times 10) + (.80 \times 30)}{(.20 \times 18.0159) + (.80 \times 60.06)} = .5034 \quad (1a)$$

The Z/A ratio is .34% too high, therefore, the density reading in that formation would be reduced by 0.34% to be correct. This, of course, is small and not normally done.

At present Century does not attempt to put a density scale on gamma-gamma logs. Thus, at present the density log is qualitative only. The curve is presented with the counting rate scale increasing to the left so the density will increase to the right. One looks for relatively low densities for indications of coal. A typical lignite will show a counting rate of about 12,500 counts per second with the 8030 probe. Lignite has a typical density of about 1.2 grams per cubic centimeter. Sandstones have typical densities of 1.86 g/c.c. to 2.39 g/c.c. One would expect counting rates of 7500 to 10,000 counts per second with the 8030 probe. Other materials and their densities are shown in Figure 2. A typical 8030 log is shown in Figure 3.

The 8030 probe has a source and a detector which are omnidirectional. That is, they are sensitive in all directions. The borehole has a large effect upon the response of this type tool. This is partly overcome in the 8030 by using a long spacing (14 inches source to detector). Gross features stand out well on this curve, but small details are not seen.

DENSITIES, Z/A RATIOS, AND THERMAL NEUTRON
CAPTURE CROSS SECTIONS PER UNIT VOLUME OF GEOLOGIC MATERIALS

(DENSITY AT ROOM TEMPERATURE AND ONE ATMOSPHERE PRESSURE
UNLESS OTHERWISE STATED)

Material	Z/A Ratio	Matrix Density G/CC	Apparent* Density G/CC	** Σ Material (Capture Units)
Lead Pb	.3953	11.34	8.97	5.61
Uraninite UO ₂	.4000	8.25 (6.5-10.8)	6.60	49.69
Cinnabar HgS	.4143	8.1 (8.0-8.2)	6.71	7,981.16
Iron Fe	.4687	7.87	7.38	214.90
Galena PbS	.4093	7.5 (7.4-7.6)	6.14	12.47
Wulfenite PbMoO ₄	.4187	6.9 (6.7-7.0)	5.78	32.50
Arsenopyrite FeAsS	.4605	6.1 (5.9-6.2)	5.62	165.22
Cobaltite CoAsS	.4517	6.1 (6.0-6.3)	5.51	936.73
Chalcocite Cu ₂ S	.4610	5.65 (5.5-5.8)	5.21	173.56
Hematite Fe ₂ O ₃	.4787	5.26 (4.9-5.3)	5.04	100.47
Magnetite Fe ₃ O ₄	.4774	5.18 (4.97-5.18)	4.95	112.10
Bornite Cu ₅ FeS ₄	.4643	5.15 (4.8-5.4)	4.78	145.63
Pyrite FeS ₂	.4850	5.06 (4.95-5.17)	4.91	89.06
Illmanite FeTiO ₃	.4757	4.75 (4.5-5.0)	4.52	158.23
Zircon ZrSiO ₄	.4691	4.69 (4.2-4.86)	4.40	5.42
Stibnite Sb ₂ S ₃	.4436	4.57 (4.52-4.62)	4.05	17.82
Pyrrhotite Fe ₅ S ₆	.4812	4.55 (4.58-4.64)	4.40	90.52
Barite BaSO ₄	.4454	4.45 (4.30-4.60)	3.96	19.40
Chromite FeCr ₂ O ₄	.4753	4.45 (4.30-4.60)	4.23	102.20
Rutile TiO ₂	.4756	4.20 (4.15-4.25)	3.80	202.75
Chalcopyrite CuFeS ₂	.4751	4.2 (4.1-4.3)	3.99	80.95
Corundum Al ₂ O ₃	.4904	4.02 (3.95-4.10)	3.94	11.04
Carnotite K ₂ O·2UO ₃ ·V ₂ O ₅ ·2H ₂ O	.4350	4+	3.48+	56.21
Rhodocrosite MnCO ₃	.4793	4.0 (3.5-4.0)	3.84	278.93
Sphalerite ZnS	.4720	4.0 (3.9-4.1)	3.78	38.33
Siderite Fe ₂ CO ₃	.4797	3.88 (3.0-3.88)	3.72	68.81
Limonite 2Fe ₂ O ₃ ·3H ₂ O	.4897	3.8 (3.51-4.0)	3.72	74.10
Dunite (4 Samples)	.4978	3.3 (3.24-3.74)	3.29	17.03
Olivine (Mg,Fe) ₂ SiO ₄	.4892	3.3 (3.27-3.37)	3.23	31.74
Magnesite MgCO ₃	.4992	3.1 (3.0-3.2)	3.1	1.48
Norite (11 Samples)	.4970	2.984 (2.720-3.020)	2.97	12.88
Diabase (6 Samples)	.4954	2.98 (2.96-3.05)	2.95	17.12
Gabbro (27 Samples)	.4938	2.976 (2.850-3.120)	2.94	21.47
Anhydrite CaSO ₄	.4995	2.95 (2.89-3.05)	2.95	12.30
Aragonite CaCO ₃	.4995	2.94 (2.85-2.94)	2.94	8.12
Muscovite KA ₁₂ (AlSi ₃)O ₁₀ (OH) ₂	.4966	2.93 (2.76-3.1)	2.91	17.30
Biotite H ₂ K(Mg,Fe) ₃ Al(SiO ₄) ₃	.4900	2.90 (2.65-3.1)	2.84	25.20
Dolomite CaMg(CO ₃) ₂	.4994	2.85 (2.80-2.99)	2.85	4.78
Illite KA ₁₅ Si ₇ O ₂₀ (OH) ₄	.4954	2.84 (2.60-3.0)	2.81	39.90
Diorite (13 Samples)	.4964	2.839 (2.721-2.960)	2.82	14.33
Langbeinite K ₂ Mg ₂ (SO ₄) ₃	.4961	2.83	2.61	78.87
Polyhalite	.5013	2.78	2.79	21.00
2CaSO ₄ ·MgSO ₄ ·K ₂ SO ₄ ·2H ₂ O				
Synite (24 Samples)	.4971	2.757 (2.630-2.899)	2.74	16.43
Granodiorite (11 Samples)	.4963	2.716 (2.668-2.785)	2.696	11.33
Chlorite	.5056	2.71 (2.60-3.22)	2.74	17.56
(Mg,Al,Fe) ₁₂ (Si,Al) ₈ O ₂₀ (OH) ₁₆				
Calcite CaCO ₃	.4996	2.71 (2.71-2.72)	2.71	7.48
Aluminum Al	.4818	2.70	2.60	13.99

*Based on tool calibration using a Z/A ratio of 0.5. **Capture Units in 10²¹ Barns/cm³

Material	Z/A Ratio	Matrix Density G/CC	Apparent* Density G/CC	** Σ Material (Capture Units)
Plagioclase feldspar xNaAlSi ₂ O ₈ ,yCaAl ₂ Si ₂ O ₈	.4925	2.69 (2.62-2.76)	2.65	6.99
Limestone (Av. of 345 Samples)	.5000	2.69 (2.66-2.74)	2.69	8.72
Granite (155 Samples)	.4969	2.667 (2.516-2.809)	2.65	11.62
Quartz SiO ₂	.4993	2.65 (2.65-2.66)	2.65	4.36
Sandstone (Av. of 12 Samples)	.4990	2.655 (2.59-2.84)	2.655	8.66
Kaolinite (OH) 8Al ₄ Si ₄ O ₁₀	.5103	2.63 (2.40-2.68)	2.68	13.06
Albite NaAlSi ₃ O ₈	.4885	2.62 (2.61-2.65)	2.56	6.77
Orthoclase feldspar KA1Si ₃ O ₈	.4958	2.57 (2.55-2.63)	2.55	16.00
Kieserite MgSO ₄ .H ₂ O	.4724	2.57	2.43	12.77
Concrete		2.35 (1.98-2.35)		
Montmorillonite (OH) ₄ Si ₈ Al ₄ O ₂₀ .nH ₂ O (n=1)	.5009	2.35 (2.00-3.00)	2.35	8.10
Gypsum CaSO ₄ .2H ₂ O	.5111	2.32 (2.30-2.35)	2.37	19.40
Glauconite KMg (FeAl) (SiO ₃) ₆ .3H ₂ O	.4998	2.30 (2.20-2.80)	2.30	16.80
Graphite C	.4995	2.22 (2.09-2.23)	2.22	0.38
Serpentine Mg ₃ Si ₂ O ₅ (OH) ₄	.5062	2.20	2.23	8.80
Halite NaCl	.4799	2.16 (2.135-2.165)	2.07	752.36
Nahcolite NaHCO ₃	.4905	2.20	2.16	
Kainite MgSO ₄ .KCl.3H ₂ O	.5140	2.13 (2.1-2.13)	2.19	196.13
Trona Na ₂ CO ₃ HNaCO ₃ .2H ₂ O	.5043	2.125 (2.11-2.15)	2.14	16.21
Sulphur, orthorhombic (below 95.4°C)	.4990	2.07 (2.05-2.09)	2.07	19.06
Potash K ₂ CO ₃ 2H ₂ O	.5049	2.04	2.06	39.70
Sylvite KCl	.4829	1.99 (1.97-1.99)	1.92	570.68
Cement (32 Samples)		1.99		about 13
Sulphur, monoclinic (above 95.5°C at 1 atm; above 150°C at 19,000 psi) S	.4990	1.96	1.96	18.05
Kernite Na ₂ B ₄ O ₇ .4H ₂ O	.5026	1.91	1.92	12,793.69
Carnallite KMgCl ₃ .6H ₂ O	.5095	1.61 (1.60-1.61)	1.64	370.92
Anthracite coal .9350(C) .0281(H) .0097(N) .0272(O)	.5134	1.60 (1.32-1.80)	1.64	1.08
Bituminous coal .8424(C) .0555(H) .0152(N) .0869(O)	.5201	1.35 (1.15-1.7) 1.10 (.5-1.5)	1.40 1.16	1.54
Lignite				
Water (300,000 ppm NaCl)	.5325	1.219	1.298	146.22
(250,000 ppm NaCl)	.5363	1.1825	1.268	122.55
(200,000 ppm NaCl)	.5401	1.146	1.238	100.08
(150,000 ppm NaCl)	.5438	1.109	1.206	78.75
(100,000 ppm NaCl)	.5476	1.073	1.175	58.69
(50,000 ppm NaCl)	.5513	1.0365	1.143	39.02
(30,000 ppm NaCl)	.5528	1.022	1.130	32.56
(Pure Water)	.5551	1.00	1.11	22.08
NaCl solution density at STP ≅ 1 + (.00000073 x ppm)				
Oil n(CH ₂), 10° API, STP	.5703	1.00	1.14	28.02
30° API, STP		.88	1.00	25.89
40° API, STP		.85	.97	24.22
50° API, STP		.78	.85	22.23
(C ₈ H ₁₈), 70° API, STP	.5778	.70	.81	22.12
N-pentane C ₅ H ₁₂ ,STP	.5823	.626	.733	20.80
200°F, 7,000 psi		.603	.702	20.02
N-hexane C ₆ H ₁₄ , STP	.5803	.659	.765	21.38
200°F, 7,000 psi		.628	.739	20.37
N-heptane C ₇ H ₁₆ , STP	.5778	.684	.790	21.80

*Based on tool calibration using a Z/A ratio of 0.5. **Capture Units in 10²¹ Barns/cm³

Figure 2b

Sec. 5, p 5 of 10

Material	Z/A Ratio	Matrix Density G/CC	Apparent * Density G/CC	** Σ Material (Capture Units)
200°F, 7,000 psi		.657	.759	20.84
N-octane C ₈ H ₁₈ , STP	.5778	.703	.812	22.12
200°F, 7,000 psi		.673	.778	21.12
N-nonane C ₉ H ₂₀ , STP	.5768	.718	.828	22.37
200°F, 7,000 psi		.686	.791	21.37
N-decane C ₁₀ H ₂₂ , STP	.5763	.730	.841	22.55
200°F, 7,000 psi		.701	.808	21.65
N-undecane C ₁₁ H ₂₄ , STP	.5759	.740	.852	22.71
200°F, 7,000 psi		.713	.821	21.87
Methane CH ₄ , STP	.5703	.000677	.00076	0.028
200°F, 7,000 psi		.2189	.2497	10.88
Ethane C ₂ H ₆ , STP	.5986	.001269	.00015	0.051
200°F, 7,000 psi		.4104	.4913	16.34
Propane C ₃ H ₈ , STP	.5896	.00186	.0022	0.067
N-butane C ₄ H ₁₀ , STP	.5850	.00246	.0029	0.085
Helium He, STP	.4997	.00017	.00017	0.0000
Carbon dioxide CO ₂ , STP	.4999	.001858	.001857	0.0001
Nitrogen N ₂ , STP	.4998	.001182	.001185	0.004
Oxygen O ₂ , STP	.5000	.001350	.001350	0.00001
Hydrogen sulphide H ₂ S, STP	.5281	.001438	.001519	0.029
Air (dry) (N-78%, O-21%, A-1%)	.4997	.001224	.001223	
Argon A, STP	.4859	.001688	.00144	0.017
Average natural gas, STP	.5735	.0007726	.000886	
200°F, 7,000 psi		.252	.289	
Hydrogen H	.9921	.00009		
Oxygen O	.5000	.001429		
Nitrogen N	.4998	.00125		
Carbon C	.4995	3.52		
Calcium Ca	.4990	1.5		
Sulfur S	.4990	2.07		
Silicon Si	.4985	2.4		
Magnesium Mg	.4975	1.74	1.73	
Potassium K	.4859	.86		
Phosphorous P	.4845	1.83		
Aluminum Al	.4818	2.70	2.60	
Sodium Na	.4804	.97		
Chlorine Cl	.4795	.0032		
Nickel Ni	.4769	8.90		
Iron Fe	.4687	7.86		
Boron B	.4625	2.45		
Chromium Cr	.4614	7.1		
Titanium Ti	.4593	4.5		
Zinc Zn	.4589	7.14		
Manganese Mn	.4568	7.4		
Copper Cu	.4564	8.92		
Vanadium V	.4514	5.96		
Cobalt Co	.4432	8.9		
Arsenic As	.4405	5.7		
Zirconium Zr	.4385	6.4		
Bromine Br	.4380	3.12		
Strontium Sr	.4336	2.6		
Tin Sb	.4312	7.2		
Molybdenum Mo	.4159	10.2		
Barium Ba	.4077	3.5		
Mercury Hg	.3988	13.56		

**Capture Units in 10²¹ Barns/cm³

Material	Z/A Ratio	Matrix Density G/CC
Lead Pb	.3953	11.34
Uranium U	.3865	18.7
Water H ₂ O	.5551	1.0
Carbon dioxide CO ₂	.4999	
Calcium carbonate CaCO ₃	.4996	
Calcium sulfate CaSO ₄	.4995	
Calcium Oxide CaO	.4993	
Silicon oxide SiO ₂	.4993	
Magnesium oxide MgO	.4985	
Aluminum oxide Al ₂ O ₃	.4904	
Phosphorous oxide P ₂ O ₅	.4935	
Boron oxide B ₂ O ₃	.4884	
Potassium oxide K ₂ O	.4883	
Sulfur trioxide SO ₃	.4874	
Sodium oxide Na ₂ O	.4855	
Hematite Fe ₂ O ₃	.4787	
Magnetite Fe ₃ O ₄	.4766	
Iron oxide FeO	.4757	
Titanium oxide TiO ₂	.4756	
Titanium oxide TiO	.4695	
Manganese oxide MnO	.4652	
Zirconium oxide ZrO ₂	.4555	
Strontium oxide SrO	.4439	
Barium oxide BaO	.4173	

*Based on tool calibration using a Z/A ratio of 0.5.

Many of the minerals listed are most often found in nature to be impure.

The values listed are minus photoelectric effects, which may become significant when elements heavier than sodium are present within the volume under investigation. The calculation of Z/A effects in formations rich in heavy atoms is mainly academic because here the Z/A effects become unimportant compared to those of photoelectric absorption. Present-day density log interpretation techniques are not designed for the accurate determination of bulk density in many heavy mineral-rich formations.

Many rich ore deposits contain only 1% to 1-1/2% of the mineral to be extracted. The sought after mineral therefore may not contribute significantly to the bulk density of the ore.

To determine the neutron capture cross section (Σ) of a substance:

- 1) Determine the molecular weight of the substance.
- 2) Divide the molecular weight of the substance by its density.
- 3) Divide Avogadro's Number (6.025×10^{23}) by the above quotient (yields molecules per cm^3).
- 4) Multiply the number of atoms of each element present per cm^3 by the thermal neutron capture cross section (in barns) for the element.
- 5) Sum the capture cross section contributions for each element as determined from Step #4 above to determine the capture cross section (in barns $\times 10^{21}/\text{cm}^3$) for the substance.



Century Geophysical Corporation
Denver, Colo.

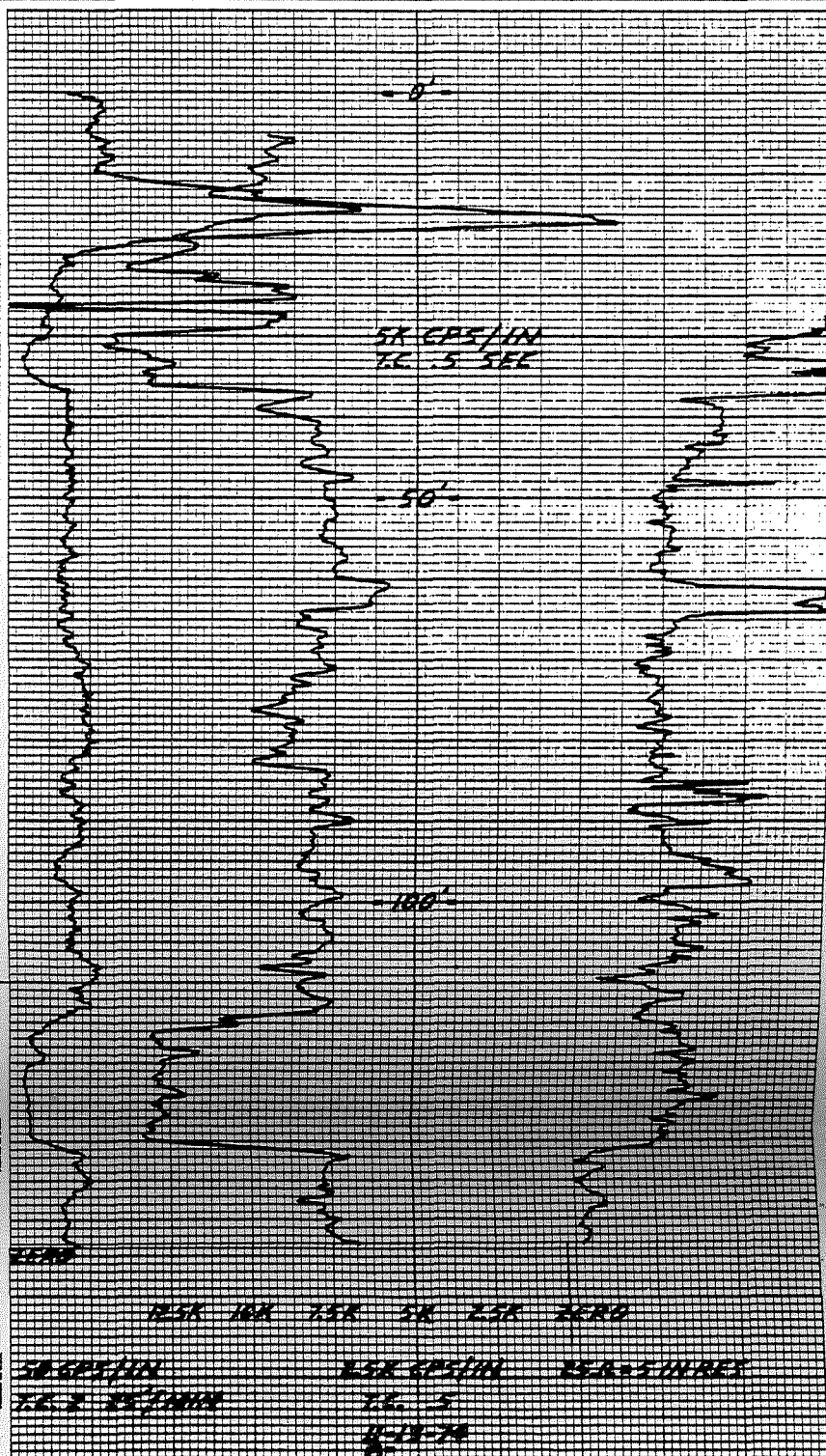
C-3348 12 17 488		DATE	11-13-74	WELL NO.	8-	T.D. FOLLER	300'
COMPANY	CJW	WELL	DELETED	LOG	FL-29	LOG	FL-29
WELL NO.	8-	COUNTY	DELETED	SECURITY	AIR	SECURITY	
WELL	DELETED	STATE	NORTH DAKOTA	OPERATOR	LD ELS	OPERATOR	
COUNTY	DELETED	DATE	11-13-74	UNIT NO.	9208	UNIT NO.	
SECTION	DELETED	LOG MEASURED FROM	66	TOTAL FOOTAGE LOGGED	291'	LOCATION	DELETED
INITIAL RUN	DENSITY			GAMMA RAY			DRIVE
T.D. LOGGED	291'	SCALE	5K	SCALE	3.7	STARTS BY	16:00
GAMMA SCALE	-50	T.C.	.5	LOGGING SPEED	25	LOGGING SPEED	5
TIME CONSTANT	2	FROM		FROM		TOTAL	4.2
CAUSATION & FROM DATA		TO		TO		FOOTSTRIP	
SOURCE NO.	A-323	SOURCE VALUE	4 Mci	TOTAL		SCALE	
FROM NO.	100-11	FROM DIA.	1 3/8			STAMP	
DETECTOR	NaI	TYPE & SIZE	7/8 x 1 1/4				
DEAR TIME		A FACTOR					
WATER FACTOR	1.127	AIR FACTOR	1.00				
REL. SCALE	25		5				

SELF POTENTIAL

DENSITY

NATURAL GAMMA RAY
COUNTS PER SECOND

RESISTANCE
OHMS



TYPICAL LIGNITE FIELD LOG
N. DAKOTA AREA

CENTURY GEOPHYSICAL CORPORATION
TULSA, OKLAHOMA

Figure 3

The 8090 system incorporates some different features. The density portion has a source collimated in one direction. The density detector is also collimated in the same direction. The tool is eccentered so the source and detector will be applied directly to the formation. This virtually eliminates borehole effects. It makes little difference if the hole is air or water filled. The density spacing is shortened (from the 8030) to 5.5 inches from the source to the detector. This allows it to detect much more detail. It, also, can be calibrated to read directly in density units. The principles of interpretation are much the same as for the 8030 system, however, at this time.

If a system is calibrated in density units, it may be used to measure porosity as well as bulk density. The relationship is:

$$d_b = \phi d_f + (1-\phi) d_m \quad (2)$$

where d is the density and b is the total bulk. Figure 4 is a plot of this relationship.

CALCULATION OF POROSITY FROM BULK DENSITY (WATER FILLED HOLES, $\rho_f = 1.0$)

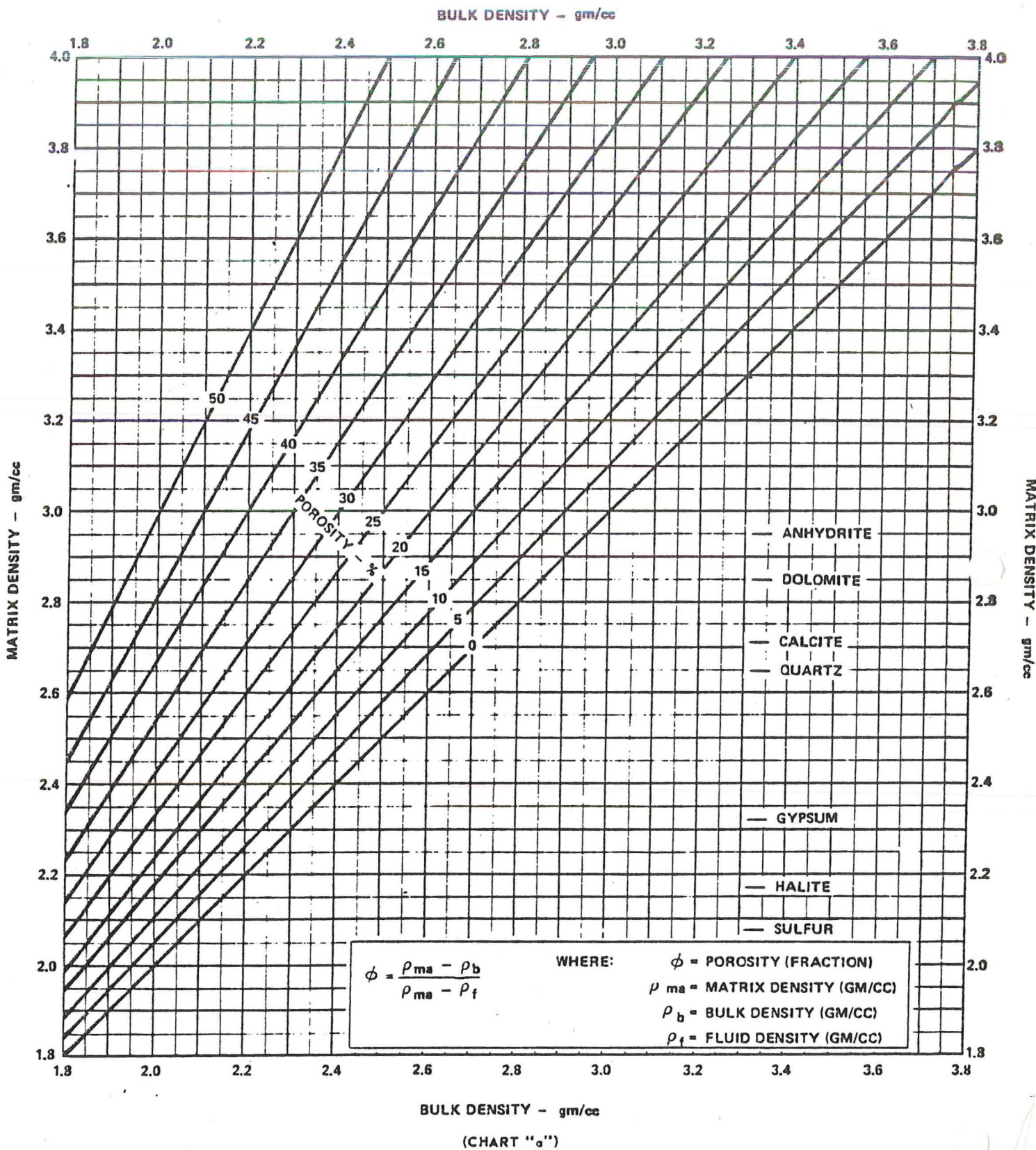


Figure 4

NEUTRON LOGGING SYSTEMS

INTRODUCTION

Neutron logs are used principally for delineation of porous formations and determination of their porosity. They respond primarily to the amount of hydrogen present in the formation. Thus, in clean formations whose pores are filled with water or oil, the neutron log reflects the amount of liquid-filled porosity. Gas zones can often be identified by comparing the neutron log with another log or a core analysis.

PRINCIPLE

Neutrons are electrically neutral particles, each having a mass identical to the mass of a hydrogen atom. High energy (fast) neutrons are continuously emitted from a radioactive source which is mounted on the end of the probe. These emitted neutrons collide with nuclei of the formation materials in what may be thought of as elastic "billiard-ball" type collisions. With each collision a neutron loses some of its energy.

The amount of energy lost per collision depends on the relative mass of the nucleus with which the neutron collides. The greatest energy loss occurs when the neutron strikes a nucleus of practically equal mass, i.e. a hydrogen nucleus. Collisions with heavy nuclei do not slow the neutron down very much. Thus, the slowing-down of neutrons depends largely on the amount of hydrogen in the formation.

Within a few microseconds the neutrons have been slowed down by successive collisions to thermal velocities, corresponding to energies of around 0.025 electron volts. They then diffuse randomly, without losing any more energy, until they are captured by the nuclei of atoms such as chlorine, hydrogen, silicon, etc.

The capturing nucleus becomes intensely excited and emits a high-energy gamma ray of capture. Depending on the type of neutron logging tool, either these captured gamma rays or neutrons themselves are counted by a detector in the probe.

When the hydrogen concentration of the material surrounding the neutron source is large, most of the neutrons are slowed down and captured within a short distance of the source. On the contrary, if the hydrogen concentration is small, the neutrons travel farther from the source before being captured. Accordingly the counting rate at the detector (with the source-detector spacings commonly used) increases for decreased hydrogen concentration, and vice versa.

NEUTRON LOGGING SYSTEMS

Neutron logging systems can be divided into several types. There are the neutron porosity logs, of which there are three types, and the analytic logs, of which there are four types. These logging systems all have features in common. They all contain a source of fast neutrons. Since there are extremely few natural neutrons, they are all of the induced response type. They all depend upon the reaction of the source neutrons with the formation atoms.

Neutrons are atomic nuclear particles with an atomic mass of one and a neutral electrical charge. That is, their net unit charge is zero. They are sometimes pictured as a combination of a proton (mass 1, charge + 1) and an electron (mass 0 and charge - 1). They are, also, simplistically pictured as perfectly elastic balls, like billiard balls.

Neutron sources are usually either a reaction of an isotopic alpha source with beryllium, a spontaneous isotopic source, such as californium 252, or a generator using a reaction between high velocity gas ions and tritium. Each type source has its advantages and disadvantages.

Alpha-Be sources are usually low to medium flux density emitters. They are plentiful, cheap, and have a wide variety of half-lives. The common ones are:

Polonium 210 - Beryllium	2.5×10^6 n/sec/Ci	half-life	138 days
Americium 241 - Beryllium	2.2×10^6 n/sec/Ci	half-life	458 years
Radium 226 - Beryllium	1.5×10^7 n/sec/Ci	half-life	1,620 years
Plutonium 239 - Beryllium	2.2×10^6 n/sec/Ci	half-life	24,400 years
Plutonium 238 - Beryllium	2.5×10^6 n/sec/Ci	half-life	86 years

Some of these sources, such as the PoBe source and the Pu²³⁸Be, have short enough half-lives that corrections sometimes need to be made. RaBe has an appreciable (and potentially dangerous) gamma output. Pu²³⁹Be has a large size and is difficult to handle because of its chemical properties. The AmBe source is the one commonly used at this time because it has a long half-life, it is relatively small, and it has a low gamma output.

Pure neutron sources can be most effectively shielded by a hydrogenous material like water, paraffin, petroleum oil, or polyethylene. Often boron (in the form of boric acid) is added because of its great cross section for neutrons. Larger sources also require an additional shield of cadmium or lead to shield out the x-rays resulting from the absorption of neutrons in the hydrogenous shield. Sources containing radium need a heavy lead shield because of their high gamma output.

A. NEUTRON-POROSITY TOOLS

The alpha-Be sources are used in neutron porosity systems, because they give satisfactory neutron flux outputs for reasonable size sources (2 to 20 x 10⁶ neutrons per second).

The neutron porosity systems all emit neutrons into the formation from the source in the probe. These neutrons diffuse through the formation and collide with the atoms present. The collisions with the atoms nearest the mass of the neutrons, such as hydrogen, result in the greatest exchange of energy. That is, neutrons are slowed down most rapidly by hydrogen atoms. The neutrons leave the source at high energies. They are slowed down to thermal or epithermal energies* (epithermal means just above the energy the particle would have from ambient heat alone. The energy to the normal heat is thermal energy).

At thermal (or even epithermal) energies neutrons can react with various atoms, such as chlorine, hydrogen, boron. The reaction results in one (or more) gamma ray whose energy is characteristic of the atom and the reaction. At any one of these points, epithermal velocity, thermal velocity, or capture gamma emission, the presence or reaction can be detected and interpreted.

The Century neutron-neutron porosity probe (8050) detects neutrons when they have been slowed to a thermal velocity. This is accomplished by a lack of cadmium shielding. Since this slowing has been primarily due to collisions with hydrogen, and most of the formation hydrogen is in pore spaces, the number of thermal neutrons through a detector can be interpreted in terms of porosity. However, because of the severe borehole effects a caliper curve must be used for this quantifying.

The detector used for neutrons is usually a tube operated as a proportional detector filled with high pressure (2 to 10 atmospheres) helium 3. Century uses a 10 atmosphere tube. This system is almost insensitive to gamma rays. It is, however, sensitive to both thermal and epithermal neutrons. Since thermal neutrons result in some borehole effects which may be undesirable, a shield of cadmium is sometimes placed around the tube to shield out the thermal neutrons. Century does not use a cadmium shield in order to use the borehole effects.

Some systems detect the capture gamma rays. These, however, are sensitive to many other common atoms, particularly chlorine. Therefore, this is not used by Century.

B. ANALYTIC NEUTRON SYSTEMS

The analytic neutron systems include the neutron activation systems, the prompt fission neutron systems, the delayed fission neutron systems, and the thermal decay time systems. Century does not use any of these systems, yet. We will have the delayed fission neutron (D.F.N.) system soon. It will be described in detail, then. Briefly, the systems are:

* The terms energy, velocity, frequency, and electronvolts are all approximately interchangeable in nuclear and radiation physics.

1. Neutron activation:

These systems usually detect the capture gamma rays with a gamma ray spectrograph. The spectrograph may be single channel or multi-channel. This system can detect minute amount of materials quantitatively with great accuracy and resolution. It is an excellent laboratory system, but has some problems which have slowed down its use in borehole logging. Either an isotopic source or a generator can be used. High flux densities are required.

One system which has been used commercially with an alpha-Be or Cf252 source makes use of the half-life of a particular reaction to detect the presence, quantitatively, of the desired element. By choosing a particular combination of spacing (source to detector) and logging speed the predominance of capture gamma rays originating within the sensitive volume of the probe can be from the desired element. This has been used successfully to detect chlorine, sulfur, and oxygen both commercially and experimentally.

2. Prompt fission neutron systems:

This system is a specific system for detecting fissionable materials such as uranium. Upon reaching a thermal velocity, the source neutrons react with atoms of uranium 235. The reaction will result in the release of a burst of secondary neutrons due to a splitting or fission of the original atoms. A gated generator source is usually used. High flux densities are required.

3. Delayed fission neutron systems:

This system is similar to prompt fission system, except the neutrons are detected much later and include fission neutrons due to reactions of the secondary neutrons as well. This is the system Century plans to use. It requires medium to high flux densities from the source. Systems have been built using both generators and isotopic sources.

4. The thermal decay time system:

This system is designed specifically for petroleum use. It is almost independent of borehole effects (including casing). It makes use of the fact that after a burst of neutrons has been emitted the neutrons are not all captured immediately, but over a period of time. The primary reaction is with chlorine, so the TDT log is essentially a log of sodium chloride content. The rate of decay is detected by means of the capture gamma rays and interpreted as sodium chloride content. A generator must be used. The flux densities are usually high.

C. NEUTRON SOURCES

The alpha-beryllium sources have already been described to a great extent. Almost any alpha emitter can be used, and there are a lot of them avail-

able. The emitter is physically mixed with powdered beryllium and, for our use, sealed in stainless steel containers. The sizes range from about 0.125 cubic inches to 6 cubic inches.

There are several isotopes, particularly in the transuranic elements which will undergo fission spontaneously with the emission of neutrons. The one commonly used is Californium 252. It has an activity of 4.4×10^9 neutrons per second per curie and a half-life of about 2.6 years. It emits about 2×10^6 neutrons per microgram. Therefore, it is very small and almost a point source. It is being used in more systems as time goes on, since it has only recently become available at a reasonable price (about \$1.00 per microgram).

Neutron generators are accelerator tubes which accelerate Hydrogen 2 (deuterium) ions in an intense electric field to collide and react with Hydrogen 3 (tritium) atoms. The reaction is:



The advantages to a generator are that it can be gated on and off for intense bursts of neutrons, and it can be shut off when not in use. Its disadvantages are the high voltages and currents required (90 to 125 kilovolts and 10 to 100 millamperes) and the short target life (100 hours).

NEUTRON LOG INTERPRETATION

Neutron log interpretation complexity depends, to a great extent, upon the type tool being used and the source to detector spacing. The neutron-thermal neutron porosity tool used by Century is relatively simple and straight forward.

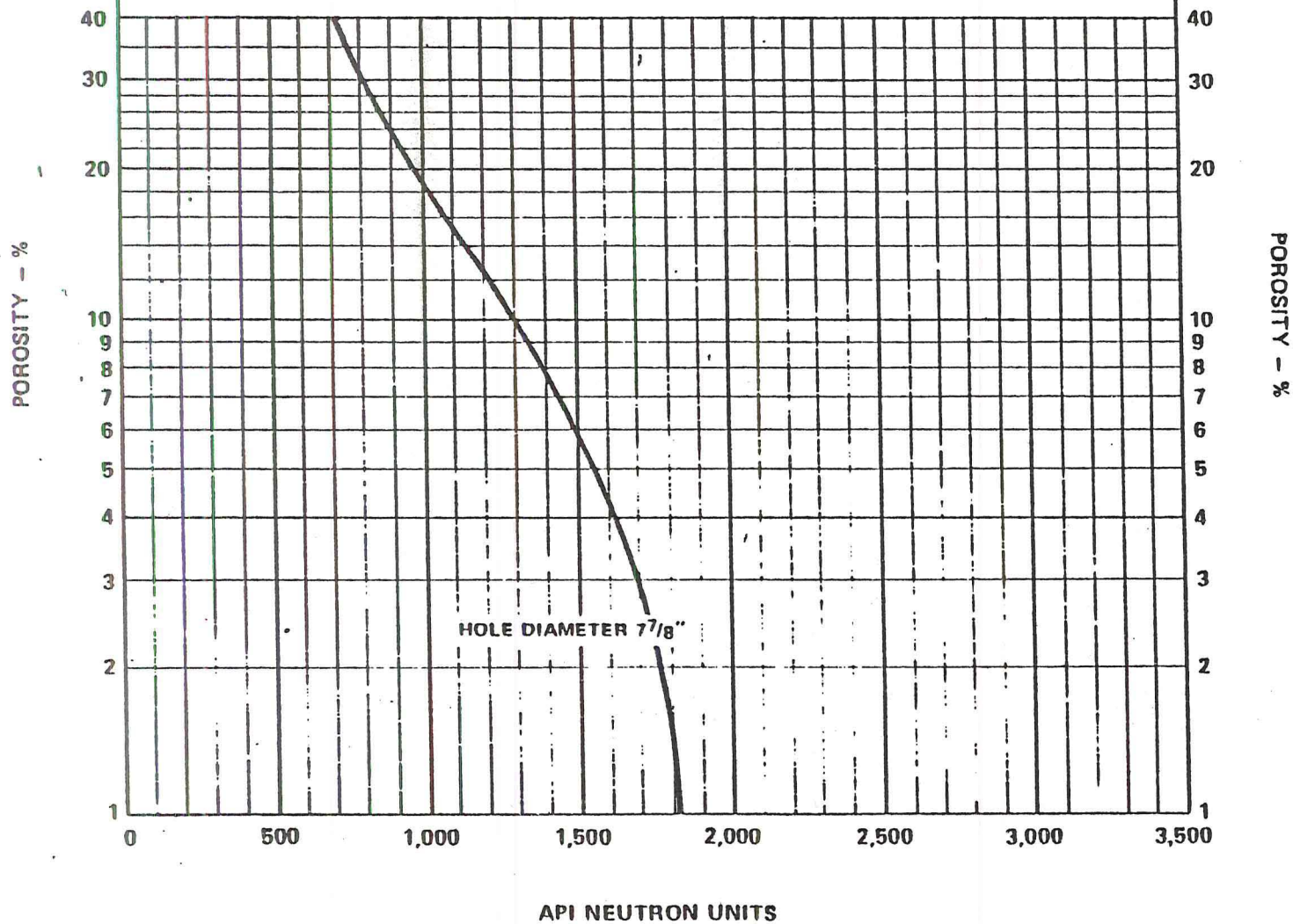
The counting rate of the Century 8050 neutron-neutron porosity tool is inversely a function of the hydrogen content of the formation surrounding the probe. Since virtually all of the hydrogen is contained in the pore space of the formation, the system is generally considered a porosity measurement system. The form of the hydrogen in the pore space is water, oil, or gas.

The counting rate of the neutron system is scaled on Century logs. That is, counting rate increases to the right or hydrogen increases to the left. This makes its appearance somewhat similar to the resistance curve.

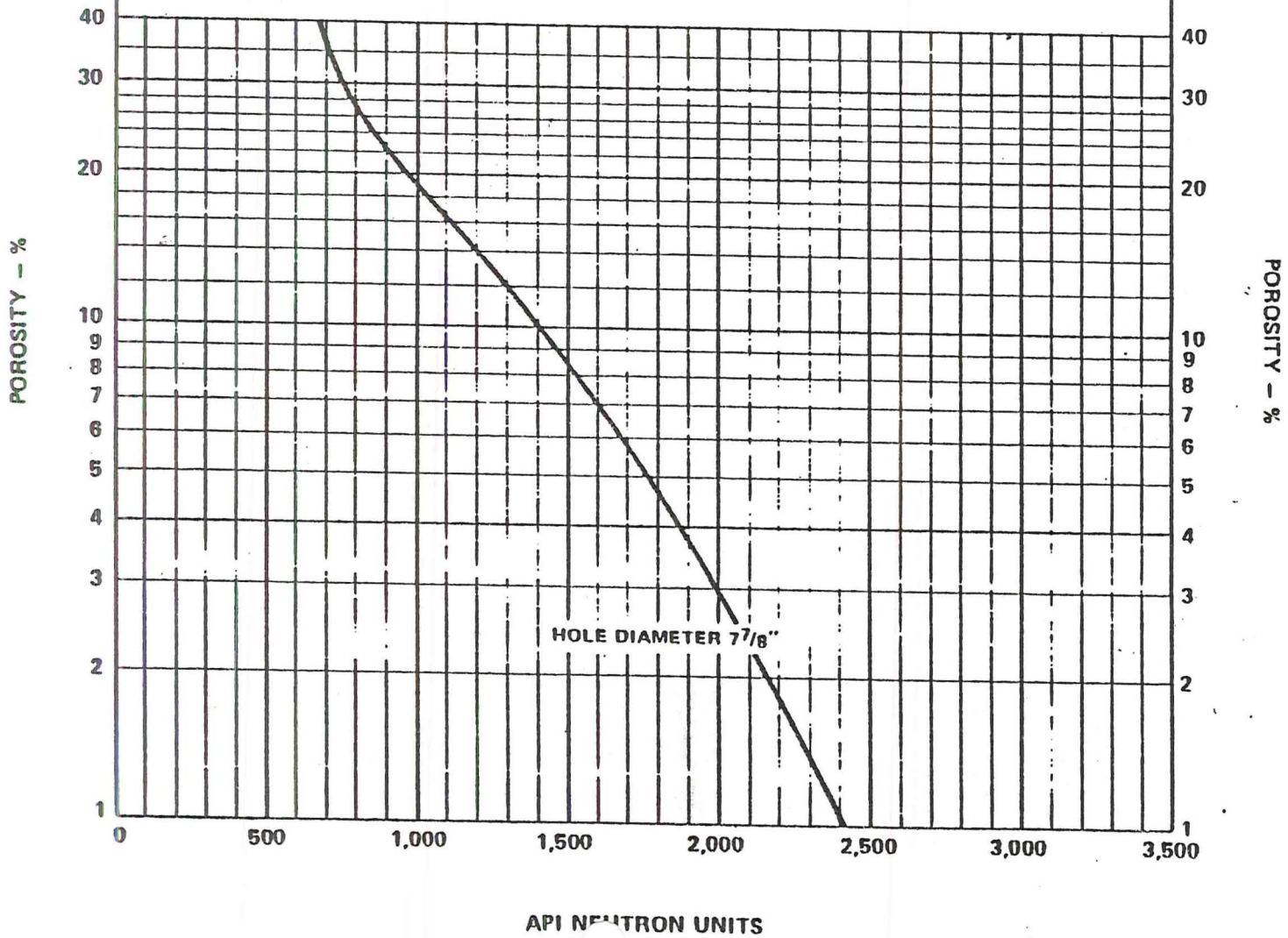
Since the neutron systems are sensitive to hydrogen in any form, the log does not differentiate between sands and clays or shales easily. This is because there is a large amount of bound water in shale and clay. The resistivity or resistance curve and the gamma ray curve are often recorded with the neutron curve for this reason. Thus, a shale would be identified by a gamma ray counting rate of 80 to 100 counts per second (8050 probe), the resistivity would be low, and the neutron counting rate would be low. A fresh water sand would have a gamma ray rate of about 30 to 50 cps, the resistance or resistivity would be moderately high and the neutron rate would be low. A salt water sand would have a low gamma rate (30 - 50 cps), a low neutron rate, and a low resistance. Coal will have a low gamma rate (2 - 10 cps), a medium to low neutron rate, and a high resistivity.

Plans are being made to calibrate the neutron log. This will probably be done in the A.P.I. pit in Houston. There, the middle formation of Indiana limestone has a porosity of about 18% and has a neutron response defined as 100 A.P.I. neutron units. This has resulted in a very desirable standardization of presentations. When this has been done, the scale on the log may be used to determine formation porosity if the borehole size is known. This type presentation, with the matrix correction curves, is shown for another type tool. This is a typical response.

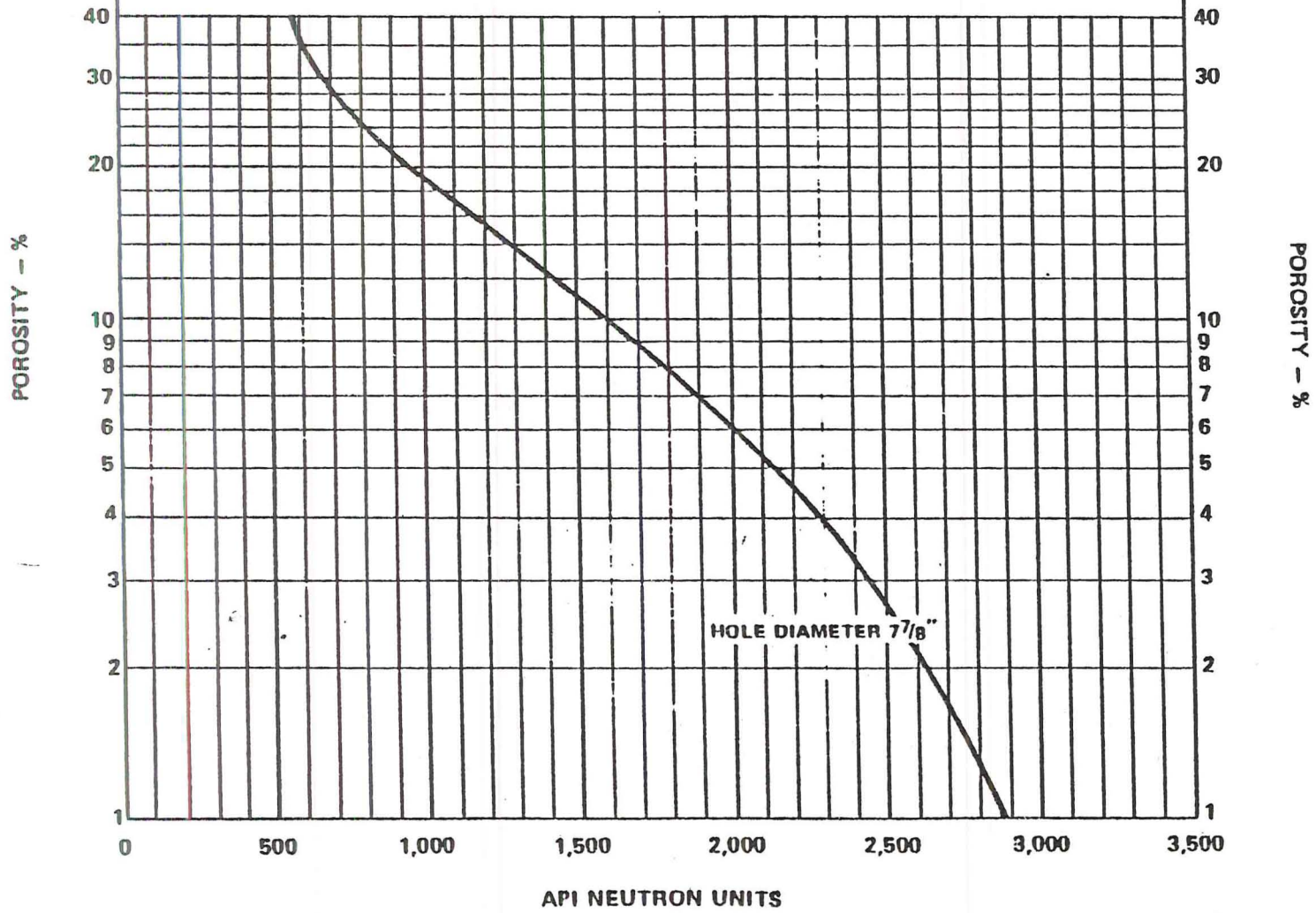
NEUTRON-NEUTRON LOG RESPONSE VERSUS HOLE SIZE AND POROSITY
(Uncased, fresh water filled borehole, limestone formation 1-11/16" diameter
decentralized tool, 13" spacing, americium-beryllium source)



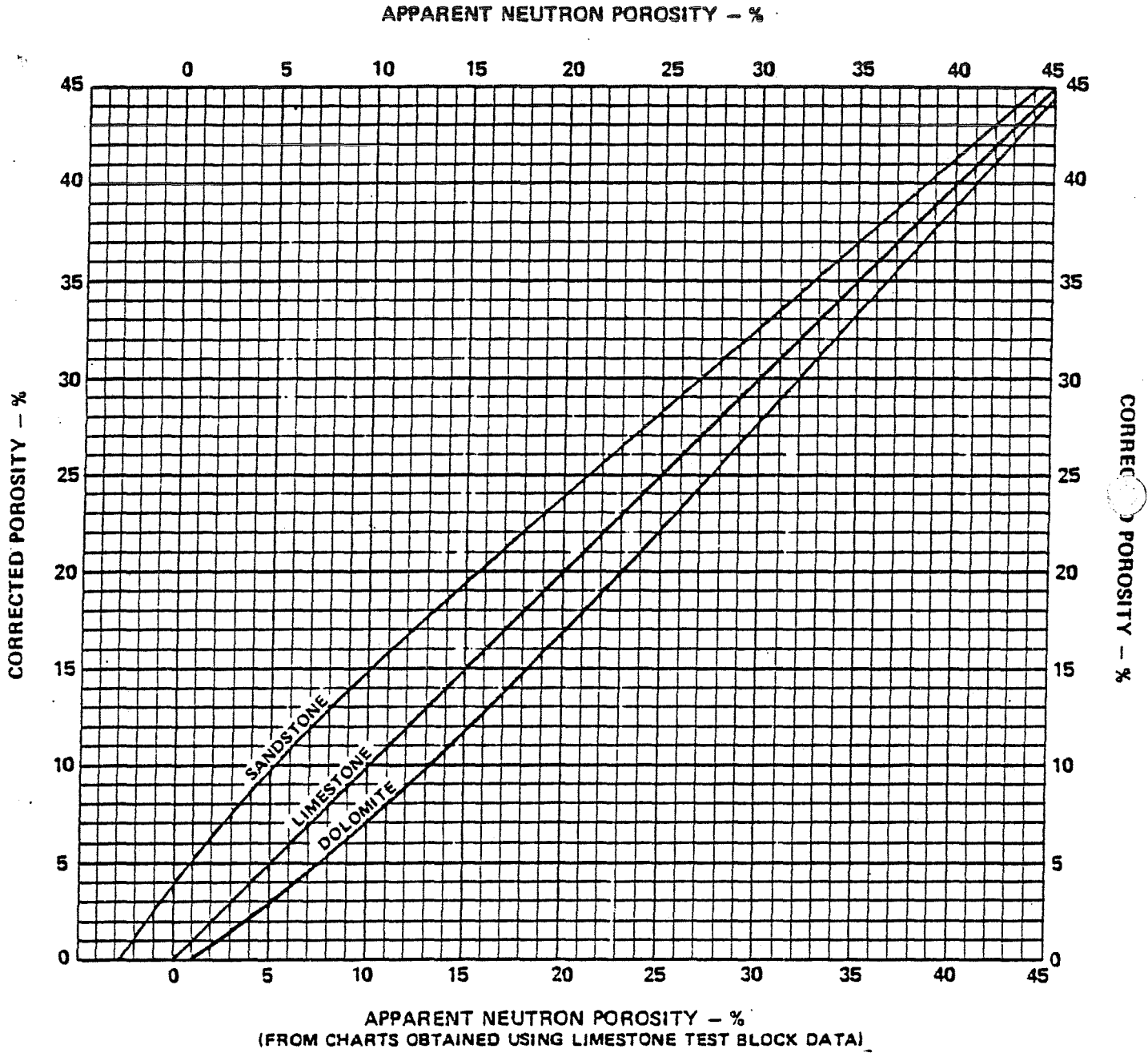
NEUTRON-NEUTRON LOG RESPONSE VERSUS HOLE SIZE AND POROSITY
 (Uncased, fresh water filled borehole, limestone formation, 1-11/16" diameter
 decentralized tool, 15" spacing, americium-beryllium source)



NEUTRON-NEUTRON LOG RESPONSE VERSUS HOLE SIZE AND POROSITY
(Uncased, fresh water filled borehole, limestone formation, 1-11/16" diameter decentralized tool, 17" spacing, americium-beryllium source)



**ESTIMATED NEUTRON CORRECTION
FOR FORMATION CHEMISTRY EFFECTS
(NEUTRON-NEUTRON LOGGING,
WATER FILLED HOLES)**



SOURCES

CHEMICAL

<u>Source</u> <u>γ</u>	<u>Target</u> <u>N</u>	<u>Source</u> <u>α</u>	<u>Target</u> <u>N</u>	
ANTIMONY	} BERYLLIUM	ACTINIUM	} LITHIUM	
RADIUM		— AMERICIUM		
THORIUM		CURIUM		
	} H ₂ O	— PLUTONIUM		BERYLLIUM
		RADIUM		BORON
		THORIUM		FLORINE

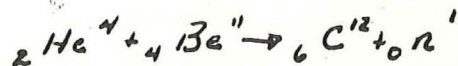
AM-Be

433 YR
3-8 MEV
2.2 x 10⁶ n / Ci SEC
2.5 x mR/hr @ 1m / Ci
EASILY OBTAINED

HALFLIFE
n ENERGY (photo peak)
OUTPUT
γ EXPOSURE

Cf 252

2.65 YR (very short) *frequent checks -*
2 MEV (1.6 MEV)
4.29 x 10⁹ n / Ci SEC
299 mR/hr @ 1m / Ci
EXPENSIVE



GENERATOR

DT or DD tritium or deuterium target.
14 MEV n
10⁸ / SEC neutrons/sec



LINEAR ACCL & REACTOR

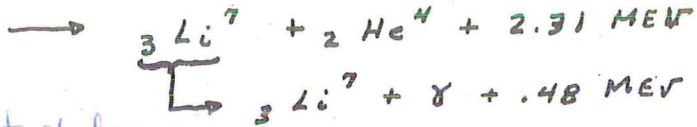
no charge - only mass
 so can't use photomultiplier
 create reaction

DETECTION - thermal detectors

DETECTORS



BF₃
 PROPORTIONAL



also downhole but takes high voltage.



U²³⁵
 PROPORTIONAL

lab use



He³
 PROPORTIONAL

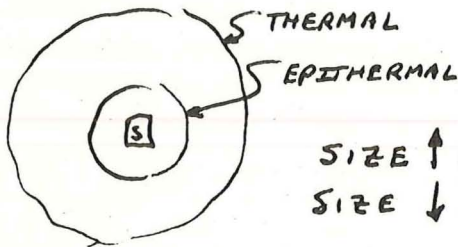
used by Century for downhole



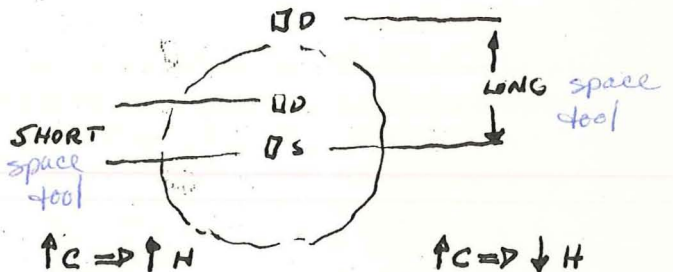
SCINTILLATION

lab use - epithermal n-detection downhole

SPACING



SIZE ↑ WITH ↓ H
 SIZE ↓ WITH ↑ H



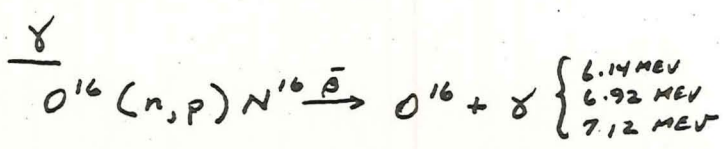
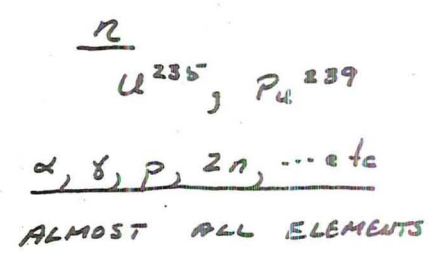
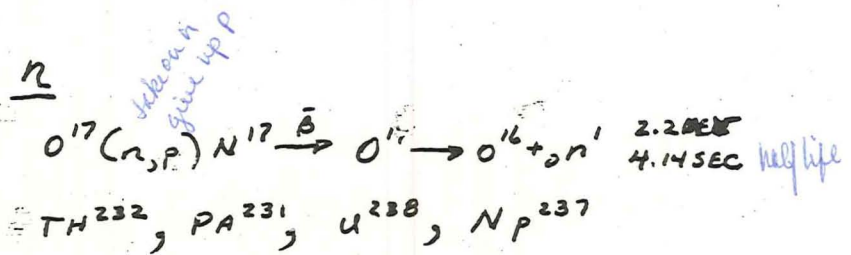
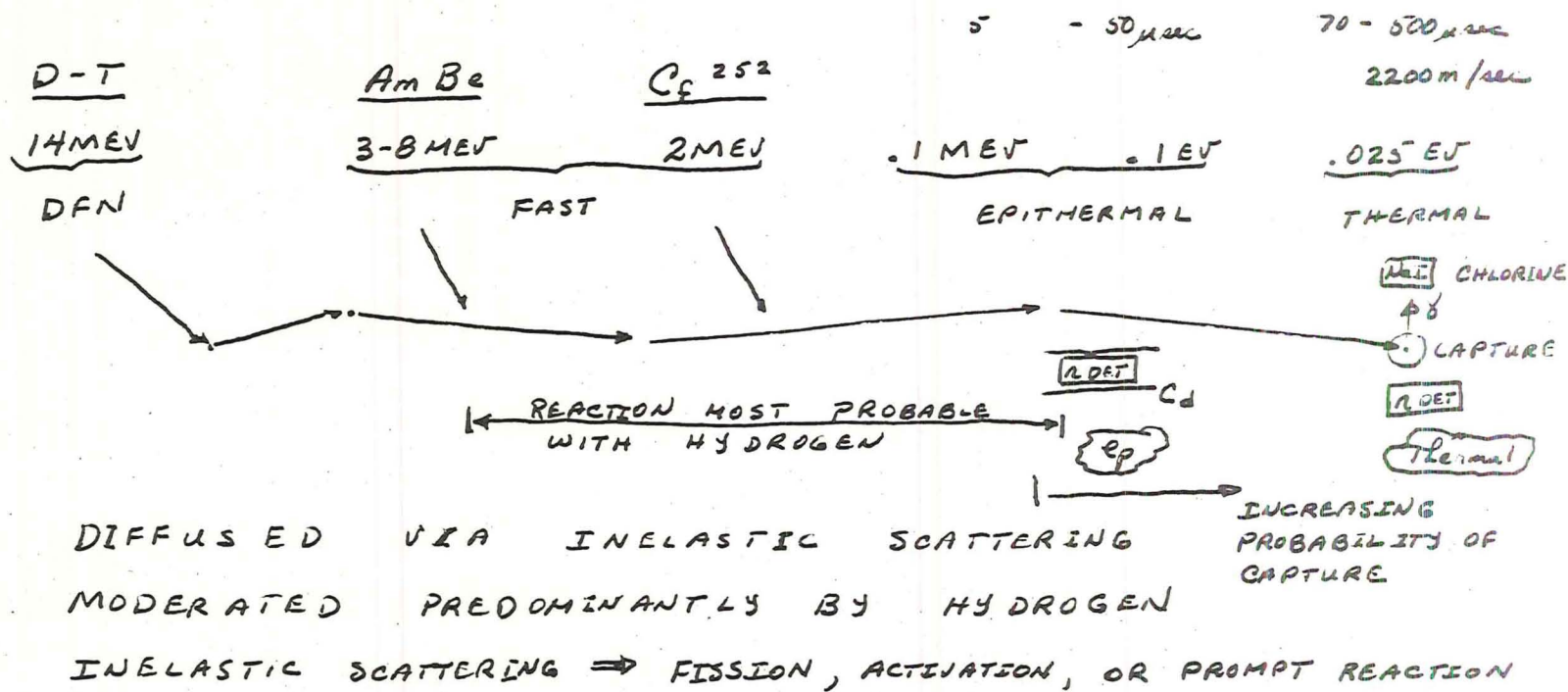
sphere gets larger w/ decreasing H

NO RESPONSE

NO MODERATOR

Gd	49,000	Hg	375
Sm	5820	In	194
Eu	4100	Er	160
Cd	2450	Tm	115
Dy	930	Hf	103
Ir	425		

REACTIONS



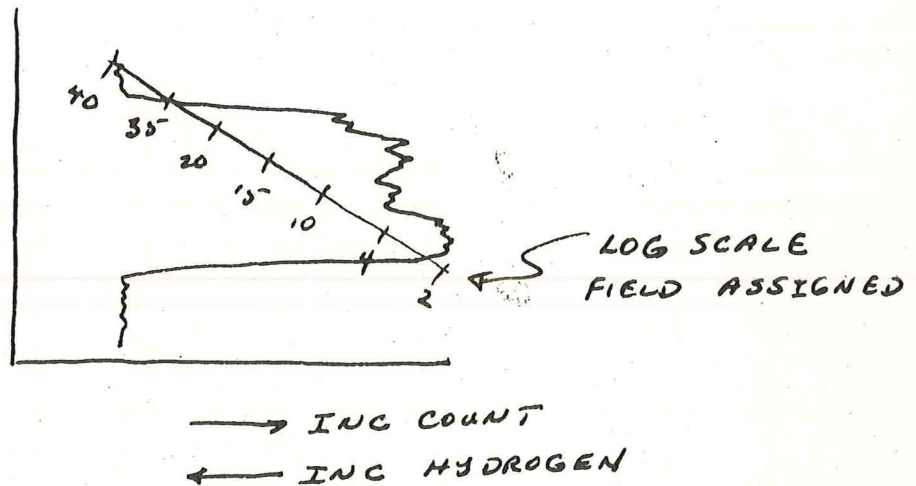
PROBLEMS

MODERATION BY HYDROGEN \therefore POROSITY

- a) COMPETITION FOR O_2 BY OTHER ELEMENTS
- b) BOREHOLE SIZE *use caliper log*
- c) INNER CONNECTED VS NON CONNECTED PORES, *saturated material*
- d) HYDROCARBONS

CALIBRATION

MODELS NOT READILY AVAILABLE



penetration or sphere of influence ~ 40cm

CALIBRATION OF LOGS

The calibration of our logs is extremely important. Whenever a log is used for quantitative purposes as the gamma ray log is in minerals exploration, an incorrect recording is often worse than no curve at all.

The calibration of the Century S.P. and resistance curves is relatively simple. The gamma ray calibration is more involved. The neutron and density calibrations are still being evolved and will not be covered, yet.

A. S.P. CALIBRATION

The primary S.P. calibration for the Century 8010 tool (and related tools) is a millivolt circuit or "box" which can be clamped on externally before logging. This circuit has three clamps, one clamps on the electrode, one on the cable armor, and one on the mud pit electrode.

Refer to the Logging Operator's Manual, Section V, Paragraph 8, A and B.

One merely notes the zero position of the recorder pen with no signal and then sets the switch on the box to the desired signal. This signal may be 25 millivolts for a one inch deflection on a 25 millivolts per inch scale or any other corresponding signal for the desired sensitivity. Similarly, 100 millivolts for a four inch deflection could be chosen. The deflection of the pen will probably be close to correct since the circuits are stable and high impedance. Any small trimming can be done with the amplifier gain control on the S.P. amplifier board. This adjustment should be done by a technician if the operator has not been properly trained. Details are found in TR 43.

A note should be made on the log of the sensitivity in millivolts per inch of deflection, the location of the curve zero, and any shifts made during (or before) logging.

B. RESISTANCE CALIBRATION

Resistance calibration of the 8010 tool (or similar) is done at the same time and with the same equipment as the S.P. In this case, a calibrated resistor is put into the circuit from the downhole electrode to the measurement return.

Refer to the Logging Operator's Manual, Section V, Paragraph 8, A and C.

Again, the sensitivity must be noted on the log. This curve requires ohms full scale (5") deflection, however. Also, the zero must be noted. Any changes should be noted on the log (this is true of any curve).

C. GAMMA RAY CALIBRATION

The calibrated gamma ray curve is the main curve used in thousands of important calculations every year in the uranium and coal industries. It is extremely important for many reasons that this calibration be done correctly and often.

The standard for the gamma ray calibration is a pit filled with uranium ore in equilibrium and carefully assayed. This is the N₃ pit at the E.R.D.A. (formerly A.E.C.) installation at Grand Junction, Colorado. In addition, there are other pits for other calibration problems at Grand Junction. There are, also, secondary pits at Casper, Wyoming, Grants, New Mexico, and George West, Texas. The procedure is essentially the same in each of them.

The equipment to be calibrated should always be a complete system; probe, cable, surface electronics, recorders. It is desirable that this be the system which will be used in the field. However, surface units are interchangeable with the calibration test procedures outlined in paragraph 8-D of TR 23 (pp 5-7) (Section V).

The equipment should be set up at the calibration facility as if one were going to make a standard field log (gamma ray only) including the calibration of the equipment as outlined in paragraph 8-D of TR 23 (Section V). The probe should be lowered to the bottom of one pit (about 11 feet) and withdrawn, logging, with both the analog and digital systems recording. Under no circumstances should this recording be made faster than 5 feet per minute. Preferably it should be much slower. This should be repeated at least once and then duplicated in the other pit. The K-factors should be calculated on the Tulsa computer. However, in the event that this is not possible, the manual procedure is listed.

The manual calculation of the pit runs is covered in the attached paper, "Twopit, a Different Approach to the Calibration of Gamma Ray Logging Equipment," by Crew and Berkoff. Briefly it is:

1. Determine the average peak low pit counting rate, n, and the high pit rate, m.
2. Find the system apparent deadtime, u:

$$\mu = \frac{n-m}{nm} (R) \quad (1)$$

where μ is in seconds and R is the ratio of the grade of the low pit to that of the high pit.

3. Mark the two points on each curve which correspond to one half the peak average amplitude. These two points must be 3.0 feet apart.
4. Start 1.5 feet before one half amplitude point (bed boundary), and note the counting rate each half foot for 13 points. This should end 1.5 feet past the other bed boundary.

5. Correct each counting rate for deadtime effects by using the following expression to determine the correct counting rate, N, from the recorded counting rate, n:

$$N = \frac{n}{1 - \mu n} \quad (2)$$

6. Add all 13 corrected counting rates and divide the sum by the product of the pit grade times the thickness (GT). The result is the K-factor.
7. Compare the two K-factors (low pit and high pit). If the correct grade was used for the high pit, the two should agree within $\pm 5\%$.
8. Compare the low pit K-factor to the standard (1.59×10^{-5}). It should be within $\pm 5\%$.

This calculation is normally done on the Tulsa computer.

For petroleum use the the University of Houston Petroleum Engineering Department, under the sponsorship of the A.P.I., has constructed two pits, one as a gamma ray calibration standard, and the other as a neutron porosity standard.

One Gamma Ray A.P.I. unit is defined as 1/120th of the deflection from background to the center of the A.P.I. formation. The procedure is much the same mechanically as for the E.R.D.A. pits, but no calculation is needed.

NOTE: The factors to convert Century AEC counts to equivalent API standard counts are:

79 Century counts = 100 API counts

1 Century count = 1.26582 API counts

1 API count = .79 Century counts

The above applies to Century's 8010 series probe.

UNITED STATES ATOMIC ENERGY COMMISSION
GRAND JUNCTION OFFICE
MINING DIVISION

TWOPIT, A DIFFERENT APPROACH TO CALIBRATION
OF GAMMA-RAY LOGGING EQUIPMENT

by

M. E. Crew and E. W. Berkoff

April 1969
(Grand Junction, Colorado)

CONTENTS

	Page
Abstract	1
Introduction	1
Two Pit Concept	5
Application	
Effect of Dead Time	8
Evaluation	11
Summary	16
References	17

ILLUSTRATIONS

Figure 1. Loss of area due to dead time	4
2. Dead time correction curves	9
3. Effect of dead time on grade	10
4. TWOPIT output	13
5. Comparison of TWOPIT and conventional factors	14

TABLES

Table 1. Interpretation factors for probe 4	11
2. Interpretation of test pit logs	15

APPENDIX

Appendix A. Description and listing of TWOPIT program	
--	--

TWOPIT, A DIFFERENT APPROACH TO CALIBRATION OF GAMMA-RAY LOGGING EQUIPMENT

ABSTRACT

The standard method of calibrating gamma-ray logging equipment is to first determine dead time, then log test pit N-3 in the Grand Junction AEC compound and determine the K-factor by the equation $K = \frac{GT}{A}$.

This paper suggests a different method, using a computer to solve for apparent dead time and a K-factor. Input to the computer is derived from logs of two test pits with different grades and grade-thickness products, and consists of the value of the GT (grade-thickness product) for each pit and a series of observed counts taken at equal intervals from background to background in each pit. A Fortran computer program for processing this data has been developed for use on IBM 1401 and IBM 1130 computers; but can easily be adapted to any digital computer of similar or greater size.

The method described is not represented to be a calculation of true instrumental dead time, but is a method of arriving at a dead time type correction for several effects combined.

Advantages of the method are (1) determination of dead time type effects based on counting geometry and count rates the same as encountered in field logging, and (2) a calibration based on both a high grade and a low grade pit rather than on a single grade pit.

INTRODUCTION

The construction of the Casper test pits in the summer of 1967 provided the first uniform-high-grade, apparent-infinite-thickness ore zone in a full scale model bore hole. Analysis of both AEC and company logs of these pits, which were obtained using conventional geiger or scintillation probes

resulted in under-interpretation of the high grade pit to varying degrees. Investigations into the reasons for this under estimation led to development of the two-pit concept as a means for correcting for the discrepancy.

To calibrate gamma-ray logging equipment for quantitative evaluation of uranium ore, it is essential to know the dead time of the system. This may be determined electronically or by the two-source method wherein first a background measurement is taken, then a first source is placed close enough to the probe to give a medium counting rate for the system and the count rate in cps taken. Next a second source is placed adjacent to the first and the count rate for both sources combined is determined, then the first source removed the count rate for the second source only is determined.

Dead time can then be calculated by the following equation: $\frac{1}{2}$

$$\text{Dead time} = \frac{\sqrt{C^2 + 3DY} - C}{\frac{3D}{2}}$$

$$\text{where } C = M_3^2 + M_B^2 - M_1^2 - M_2^2$$

$$D = M_3^3 + M_B^3 - M_1^3 - M_2^3$$

$$Y = M_1 + M_2 - M_3 - M_B$$

and M_1 = count rate in cps, first source

M_2 = " " " " , second source

M_3 = " " " " , both sources

M_B = " " " " , background

After dead time has been determined, the next step is to determine the proportionality constant or K-factor which relates the response of the system, commonly expressed in terms of area under the curve, to grade-thickness product. This is done by logging a test pit of known grade-thickness, applying

appropriate correction for dead time, using the equation $N = \frac{n}{1 - nt}$, to each observed count rate, n , to obtain true count rate, N , and using the sum of the true count rates $\sum N$, as a value for the area, A , under the log curve then substituting in the equation

$$AK = GT \quad (2)$$

as developed by Scott, et al, 2/.

Area, as used in equation (2) consists of the observed counts area plus the dead time correction area and is normally obtained by summing the dead time corrected count rates at half foot intervals and is thus in units of half feet times counts per second. The value of K is commonly calculated to relate the area so derived to the GT but can be computed for any interval of integration.

Figure 1, shows the relationship between observed count rate and dead time corrected count rate on a log of the Casper high pit with a grade of 2.242% eU_3O_8 made with a scintillation probe having $3/4 \times 1$ inch crystal and 5 micro seconds dead time. The area between the observed and corrected log curves represents the loss in area, or gamma-rays detected, because of system dead time.

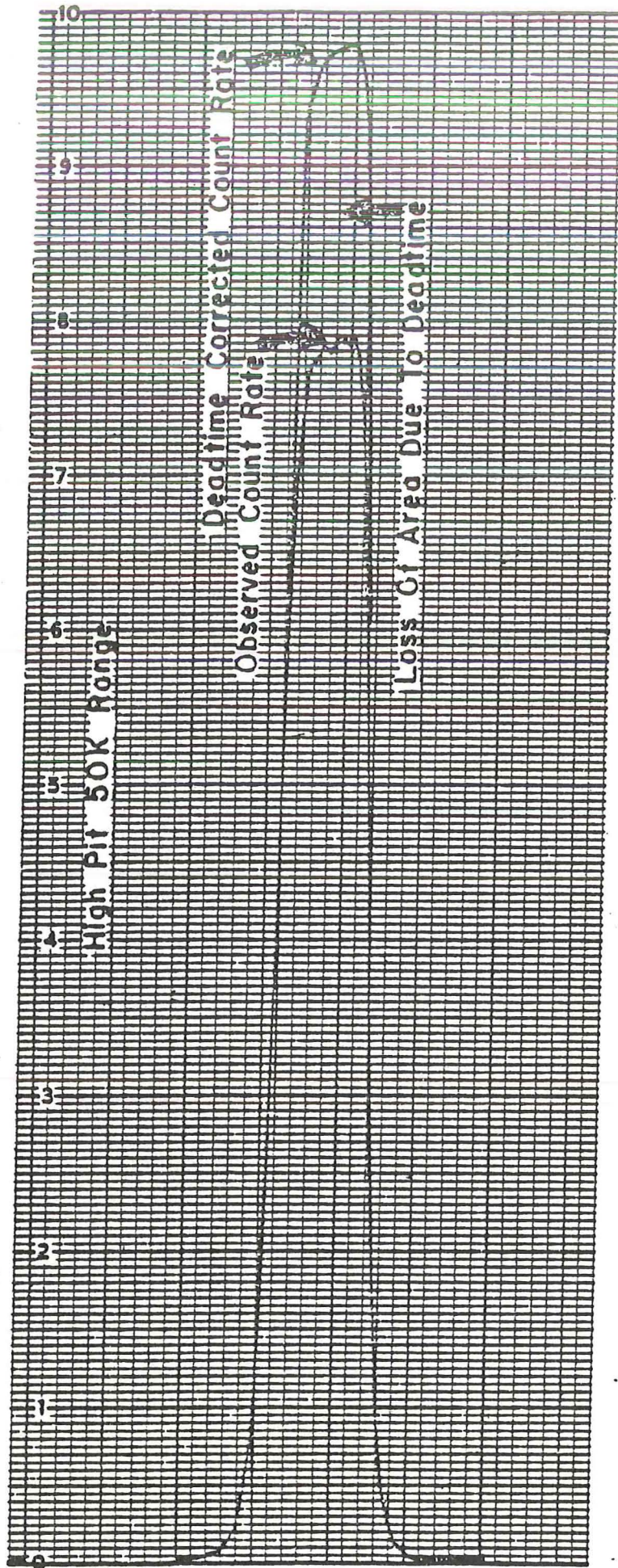


Figure 1. Loss of Area Due to Deadtime

TWO PIT CONCEPT

The method described in this report is not represented to be a calculation of true instrumental dead time, but instead a method of arriving at a dead time type correction for the entire logging system which will result in a closer approximation to equivalent radiometric grade throughout the entire range of count rates encountered in gamma-ray logging of drill holes.

The entire concept to be shown here is based on the previously mentioned equation (2).

$$AK = GT$$

where A = sum of dead time corrected counts

K = proportionality constant of system

G = mean radiometric equivalent grade

T = thickness in feet

Now consider the case of two test pits with different grade-thickness products in which

$$A_1K = (GT)_1$$

represents the low grade pit and

$$A_2K = (GT)_2$$

represents the high grade pit. Since the above relationships are true, it can also be said that

$$\frac{A_1K}{A_2K} = \frac{(GT)_1}{(GT)_2}$$

and since the expression K cancels out that

$$\frac{A_1}{A_2} = \frac{(GT)_1}{(GT)_2} \quad (3)$$

The expression A is defined as the sum of the dead time corrected counts and may be written

$$A = N_1 + N_2 + N_3 \dots N_z \quad (4)$$

and it is known that

$$N = \frac{n}{1-nt} \quad (5)$$

where N = dead time corrected count rate

n = observed count rate

t = dead time in seconds.

Therefore, by substituting, equation (4) can be written as

$$A = \frac{n_1}{1-n_1t} + \frac{n_2}{1-n_2t} + \frac{n_3}{1-n_3t} \dots \frac{n_z}{1-n_zt} \quad (6)$$

and by substituting again, equation (3) can be rewritten as

$$\frac{\frac{n_1}{1-n_1t} + \frac{n_2}{1-n_2t} + \frac{n_3}{1-n_3t} \dots \frac{n_z}{1-n_zt}}{\frac{m_1}{1-m_1t} + \frac{m_2}{1-m_2t} + \frac{m_3}{1-m_3t} \dots \frac{m_z}{1-m_zt}} = \frac{(GT)_1}{(GT)_2} \quad (7)$$

using the term m in the denominator to designate observed counts in the high grade pit whereas the n in the numerator represents observed counts in the low grade pit.

In equation (7) GT_1 and GT_2 are known values and the various values for the n and m terms are observed values, thus leaving t as the only unknown in the equation. A direct algebraic solution is difficult if not impossible because of the indefinite length of the series, but a computer solution by trial and error is relatively simple. First the ratio of the two GT values is determined, then by trial and error, the computer solves for the dead time that will make the ratio on the left side of the equation equal to the ratio of the GT products.

A description and listing of the computer program called TWOPIT which solves the equation is attached as Appendix A.

A close approximation to the dead time evaluation by the above computer method can be made manually or with a desk calculator using ratios of peak observed counts in the respective pits rather than area under the curve, provided that the "ore" zones in the models are of uniform grade and the thickness is equal to or greater than the diameter of the effective sample volume influencing the detector, generally 3 feet or slightly less; or provided that thickness T_1 is equal to thickness T_2 and the ore zones are homogeneous with respect to grade.

It has been shown by Scott, 3/, that under certain conditions

$$G = 2KN \quad (8)$$

Then following the same reasoning as described above with respect to areas under the curve and grade thickness products it can be said that

$$\frac{G_1}{G_2} = \frac{N_1}{N_2}$$

By similar substitutions for N and solution for dead time, t ; this is reduced to

$$t = \frac{n - Rm}{nm(1-R)} \quad (9)$$

where t = apparent dead time, in seconds

n = peak observed count, low pit

m = peak observed count, high pit

$R = \frac{\% \text{ eU}_3\text{O}_8, \text{ low pit}}{\% \text{ eU}_3\text{O}_8, \text{ high pit}}$

Results obtained by this short-cut method are generally within one microsecond of the value obtained by the TWOPIT program.

APPLICATION

Effect of Dead Time

To understand the importance of accurate dead time determination, it is necessary to consider the effect of dead time on the interpretation of gamma-ray logs.

Figure 2 shows dead time correction curves for 5, 10, 20, 30, and 40 microseconds. The previously mentioned equation (5) $N = \frac{n}{1-nt}$ was used in construction of the graphs. As a guide for interpreting this chart, lines have also been drawn to show a 50% and a 100% correction to observed count rates. Because of uncertainties involved in determining a true dead time value, and the large effect resulting from a small change in dead time at high count rates, it would be advisable to choose equipment with detector size and dead time characteristics such that not greater than a 50% correction to observed counts would be required at the highest count rates encountered in ore hole logging. Using this criteria it can be seen that the maximum observed counts should not exceed 65,000 cps for a system with 5 microseconds dead time, 33,000 cps for 10 microseconds, 17,500 cps for 20 microseconds, etc.

Another way of determining the possible error that is introduced by a small error in dead time determination is illustrated in Figure 3. This figure shows the approximate relationship between peak observed count rate and equivalent % U_3O_8 by equation (8), $G=2KN$ modified to $G=2K \frac{n}{1-nt}$.

A value for K of .00002 was used for construction of the graphs. This value is within the range encountered for 3/4 x 1 inch crystals in scintillation logging probes.

At an observed count rate of 30,000 cps it is evident from the graph that if 5 microseconds are used the interpreted grade would be 1.41% eU_3O_8 , whereas if 10 microseconds are used the grade would be 1.71%--a difference of 0.30%, and as dead times were increased the same microseconds difference

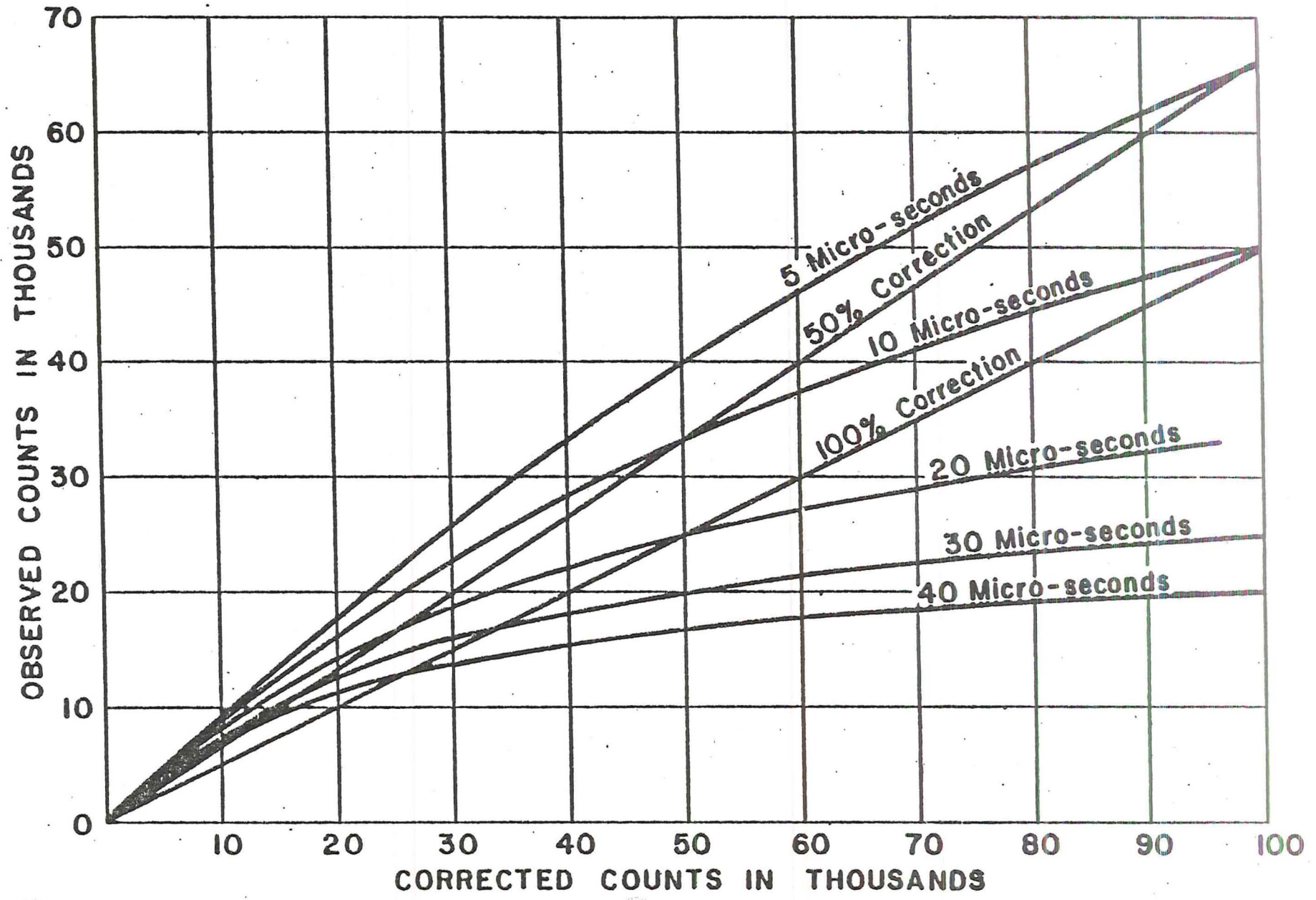


Figure 2. Deadtime Correction Curves

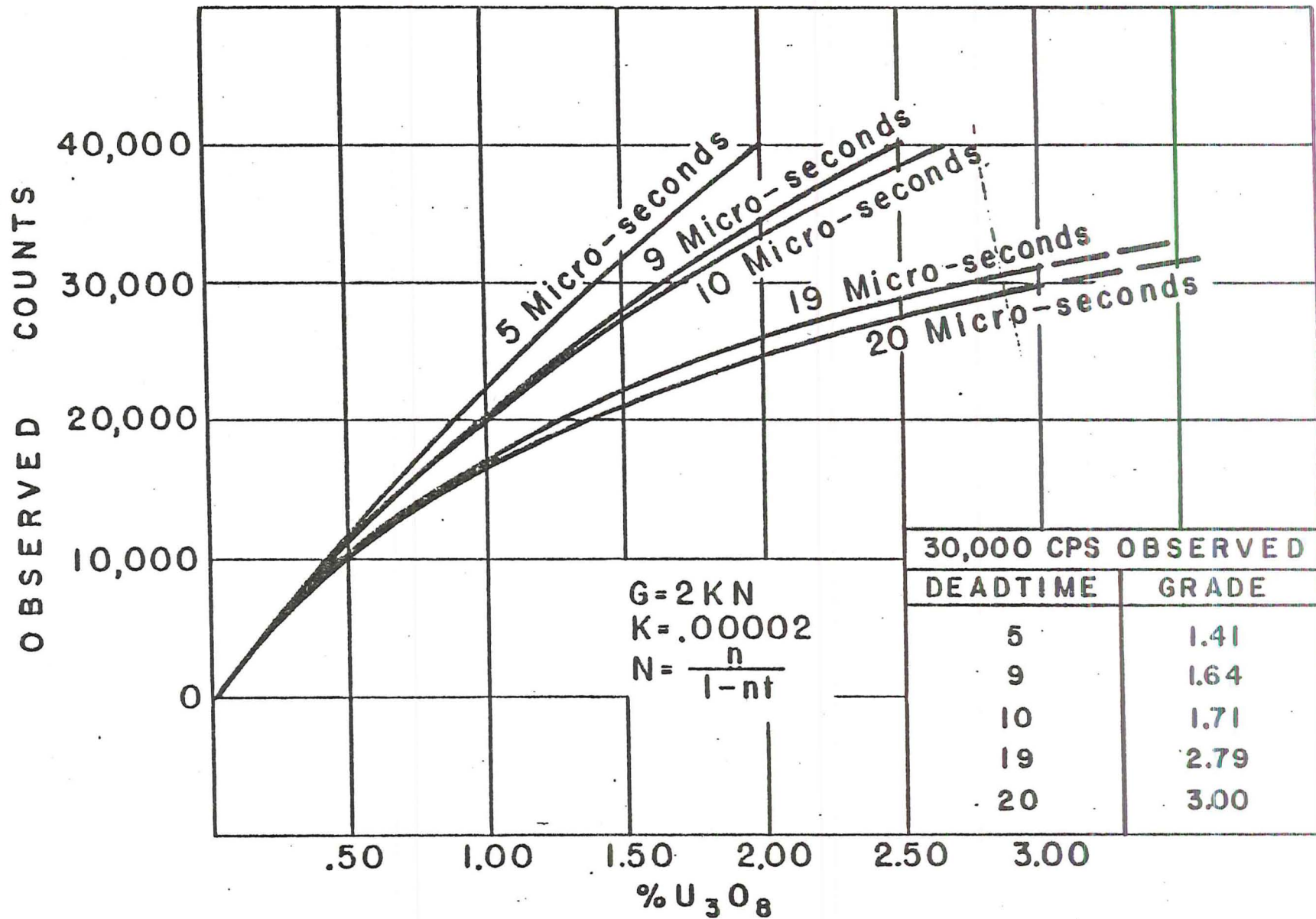


Fig. 3. Effect of Deadtime on Grade

would create a progressively increasing error. To see this effect more clearly, consider a 1 microsecond difference between 9 and 10 microseconds and between 19 and 20 microseconds at a rate count of 30,000 cps. The interpreted grades at 9 and 10 microseconds are 1.64% and 1.71% eU_3O_8 respectively; a difference of .07%, while the interpreted grades at 19 and 20 microseconds are 2.79% and 3.00% eU_3O_8 ; a difference of 0.21% or 3 times as great an effect as 1 microsecond had between 9 and 10 microseconds.

It is obvious that dead time plays a vital role in interpretations and must be determined in a manner which will reduce possible error to a minimum.

Evaluation

To support the premise presented in this paper, the Casper test pits were logged with Unit LP-1, probe 4. This is an AEC owned logging unit developed, constructed, and operated by Lucius Pitkin, Inc., an AEC service contractor. The following table shows the conventional factors and the factors arrived at by the TWOPIT program:

TABLE 1
Interpretation Factors for Probe 4

	<u>Conventional</u>	<u>TWOPIT</u>
Deadtime (microseconds)	4.9	8.66
K Factor	.00001948	.00001925

Figure 4 is a reproduction of the TWOPIT computer program output which generated the TWOPIT factors shown in Table 1.

The data, taken at half foot intervals from the analog record of the test pit logs, were interpreted using both conventional and TWOPIT factors. The total area under the curve was used rather than the customary "tail factor" method. Results are shown in Table 2.

From the results shown, it is obvious that there is little difference at grades in the range of the low grade test pit, but that the error is reduced considerably by use of TWOPIT factors in the grade range of the high grade pit.

The question now is: At what grade does the difference become significant? There is no definite answer to this but a relative comparison of the two methods through a range of grades can be shown by plotting observed counts against percent eU_3O_8 using the previously mentioned approximate relationship, $G=2KN$, and converting observed counts to corrected counts before substituting in the equation. Figure 5 is such a comparison of TWOPIT and conventional factors for probe 4.

It must be remembered that the tables and figures are for specific pieces of equipment and that each logging tool is somewhat different from every other in its response, thus each unit and probe combination must be individually evaluated rather than using a general correction for all combinations.

THE USAEC NEITHER REPRESENTS NOR WARRANTS THE INFORMATION CONTAINED
HEREON TO BE ACCURATE IN ALL RESPECTS AND MAKES NO RECOMMENDATIONS THERETO

PROGRAM TWOPIT RESULTS

DATE OF COMPUTER RUN APRIL 9, 1969
NO RANGE CORRECTION USED FOR THIS DATA

PITS CASPER PITS
COMPANY LUCIUS PITKIN
UNIT LP-1
PROBE 4
XL SIZE = .75X1.00

DATE LOGGED 01/24/69
LOG READINGS TAKEN AT 0.50 FOOT INTERVALS
RATIO - GT(LOW)/GT(HI) = 0.1476360
APPARENT DEADTIME USED = 8.660 MICROSECONDS
WHEN RATIO-AREA(LOW/AREA(HI) = 0.1476771

LOW PIT DATA
GT = 0.99300

OBSERVED COUNTS	CORRECTED COUNTS
100.	100.
300.	301.
1150.	1162.
4900.	5117.
7650.	8193.
8150.	8769.
8020.	8619.
7950.	8538.
6700.	7113.
2800.	2870.
550.	553.
170.	170.
80.	80.

AREA = 51583.
K FACTOR = 0.00001925

HI PIT DATA
GT = 6.72600

OBSERVED COUNTS	CORRECTED COUNTS
200.	200.
700.	704.
2850.	2922.
14500.	16582.
34100.	48390.
39750.	60616.
40000.	61200.
40250.	61787.
38350.	57420.
24500.	31098.
6250.	6608.
1400.	1417.
350.	351.

AREA = 349295.
K FACTOR = 0.00001926

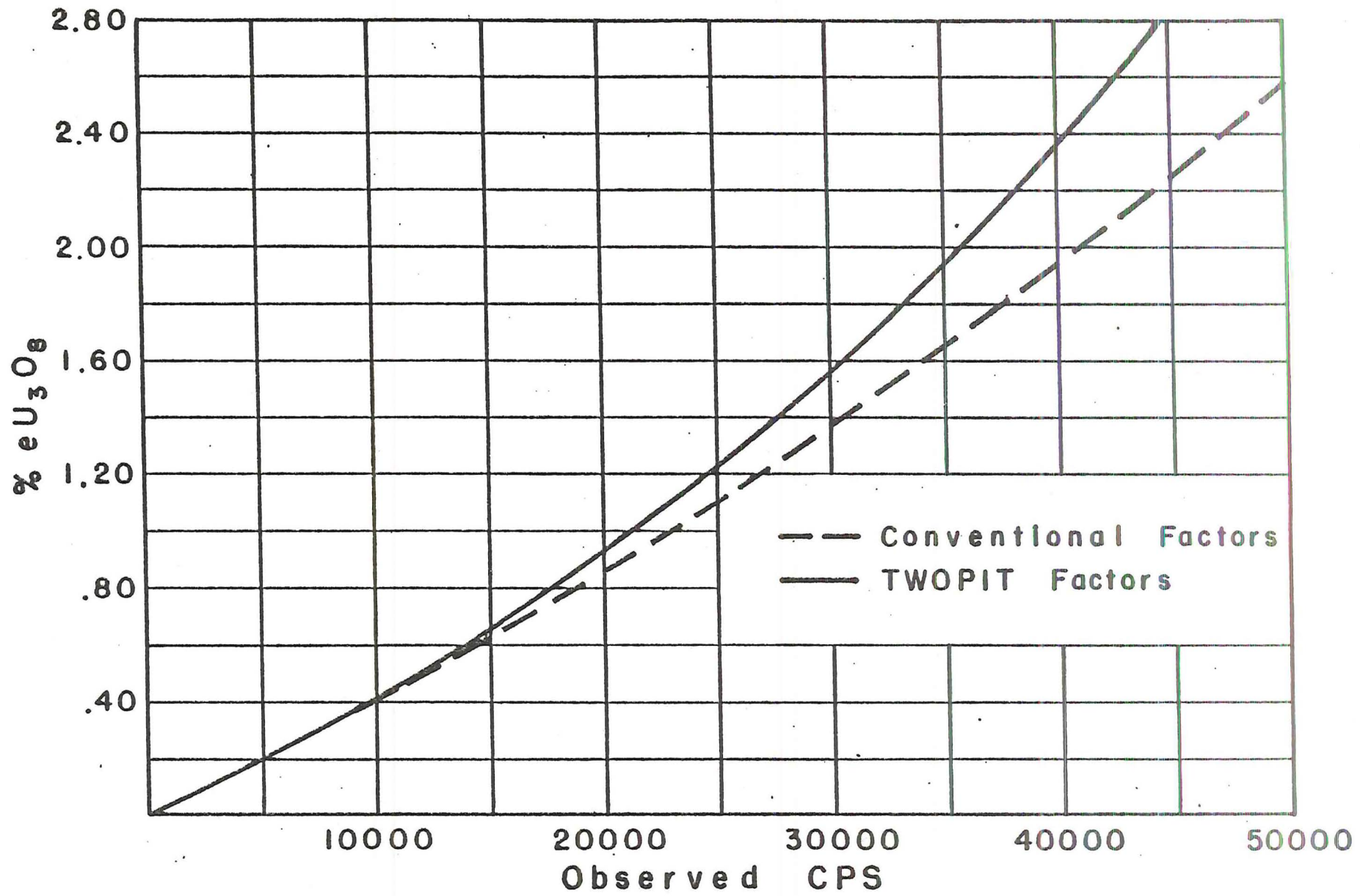


Figure 5. Comparison of TWOPIT and Conventional Factors for Probe 4

TABLE 2
INTERPRETATION OF TEST PIT LOGS, UNIT LP-1, PROBE 4

Observed Count	LOW PIT		Observed Count	HIGH PIT	
	<u>Dead Time Corrected Count</u>			<u>Dead Time Corrected Count</u>	
	<u>Conventional</u>	<u>TWOPIIT</u>		<u>Conventional</u>	<u>TWOPIIT</u>
100	100	100	200	200	200
300	300	301	700	702	704
1,150	1,157	1,162	2,850	2,890	2,922
4,900	5,021	5,117	14,500	15,609	16,582
7,650	7,948	8,193	34,100	40,941	48,390
8,150	8,489	8,769	39,750	49,365	60,616
8,020	8,348	8,619	40,000	49,751	61,200
7,950	8,272	8,538	40,250	50,138	61,787
6,700	6,927	7,113	38,350	47,224	57,420
2,800	2,839	2,870	24,500	27,842	31,098
550	551	553	6,250	6,447	6,608
170	170	170	1,400	1,410	1,417
80	80	80	350	351	351
Total Area =	50,202	51,583		292,870	349,200
Area x K=GT =	.9779	.9930		5.7051	6.7239
Thickness =	3.0	3.0		3.0	3.0
GT/T=% eU ₃ O ₈ =	.326	.331		1.902	2.241
Accepted Value	.331	.331		2.242	2.242
% error	-1.51	0.00		-15.17	-0.04

SUMMARY

The method described in this report is not represented to be a calculation of true instrumental dead time but instead a method of arriving at a dead time type correction for the entire logging system which will result in a closer approximation to equivalent radiometric grade throughout the entire range of count rates encountered in gamma-ray logging of drill holes.

The dead time effect calculated is a combination correction to compensate for true instrumental dead time, non linearity of ratemeter, recorder errors including improper zero adjust, and a photoelectric absorption effect of low energy gamma-rays by high concentrations of uranium (Dodd, personal communication). It is thus a total system evaluation that can be affected by many things other than true dead time.

Certain cautions must be taken before using the method, but in general these cautions are the same for conventional calibration techniques. The equipment used should:

1. Have linear response between all ranges.
2. Have constant electronic dead time, not rate sensitive.
3. Have linear counting capability above the rate encountered in the high grade pit.
4. Operate on the plateau region for the detector and give repeatable results.

If the above equipment conditions are met, the TWOPIT method will give calibration factors which will result in errors of interpretation no greater than the error in the assigned radiometric grades of the test pits.

REFERENCES

- 1/ Bellar, L. S., Farrar, H. IV, 1965, Determination of Paired-Pulse Resolution of Random Counting Systems, Report NAA-SR-MEMO-11132, Atomics International Division, North American Aviation Corp., AEC Contract AT (11-1) GEN. 8.
- 2/ Scott, J. H., Dodd, P. H., Drouillard, R. F., and Mudra, P. J., 1961, Quantitative Interpretation of Gamma Ray Logs: Geophysics, Vol. XXVI, No. 2, p. 182-191.
- 3/ Scott, J. R., 1962, the GAMLOG Computer Program: RME-143, USAEC.

PROGRAM TWOPIT

PROGRAM TWOPT(VERS 3,MOD 1)

	INTEGER FLAG	TWOPT001
	REAL NPITS,KFACL,KFACH	TWOPT002
	COMMON AREAH,AREAL,DT,GTH,GTL,IP,ITMS,JCT,KCT,KFACH,KFACL,NPITS,	TWOPT003
	1 PROBE,PROP,RASH,THK,UNIT,CPNY(3),DATE(3),PITS(3),CONTH(99),	TWOPT004
	2 CONTL(99),CORH(99),CORL(99),LITE1	TWOPT005
	CFACT(GT,AREA,THK)=GT/(AREA*2.*THK)+5.0E-9	TWOPT006
10	DT=0.0	TWOPT007
	LITE1=0	TWOPT008
	JCT=0	TWOPT009
	KCT=0	TWOPT010
	HINC=1.0E-5	TWOPT011
	ALMT=5.0E-5	TWOPT012
	READ(2,500)NPITS,PITS,CPNY,UNIT,PROBE,THK,GTL,GTH,DATE,LITE1,FLAG	TWOPT013
500	FORMAT (12X,A3,2(2A6,A3),2A5,F5.2,2F5.4,2X3A2,2I1)	TWOPT014
	CALL SLITE(LITE1)	TWOPT015
	LITE1=1	TWOPT016
	CALL RDR(CONTL,JCT)	TWOPT017
	CALL RDR(CONTH,KCT)	TWOPT018
	RASH=GTL/GTH	TWOPT019
	RASHL=RASH-ALMT	TWOPT020
	RASHU=RASH+ALMT	TWOPT021
14	DT=DT+HINC	TWOPT022
	IF(DT-2.0E-4)15,15,900	TWOPT023
15	AREAL=0.0	TWOPT024
	AREAH=AREAL	TWOPT025
	CALL CRCTR(JCT,DT,CONTL,AREAL,CORL)	TWOPT026
	CALL CRCTR(KCT,DT,CONTH,AREAH,CORH)	TWOPT027
	PROP=AREAL/AREAH	TWOPT028
	IF(PROP-RASHU)16,18,14	TWOPT029
16	IF(PROP-RASHL)17,18,18	TWOPT030
17	DT=DT-HINC	TWOPT031
	HINC=HINC*0.1	TWOPT032
	IF(HINC-1.0E-11)909,909,14	TWOPT033
18	KFACL=CFACT(GTL,AREAL,THK)	TWOPT034
	KFACH=CFACT(GTH,AREAH,THK)	TWOPT035
	AREAL=AREAL+0.5	TWOPT036
	AREAH=AREAH+0.5	TWOPT037
	RASH=RASH+5.0E-8	TWOPT038
	PROP=PROP+5.0E-8	TWOPT039
	DT=DT+5.0E-10	TWOPT040
	DT=DT*1.0E6	TWOPT041
	IGO=0	TWOPT042
	IP=-1	TWOPT043
	ITMS=KCT	TWOPT044
	IF(JCT-KCT)20,19,185	TWOPT045
185	ITMS=JCT	TWOPT046
	IGO=1	TWOPT047
19	IP=IGO	TWOPT048
20	CALL OWPTPT	TWOPT049
	IF(FLAG)999,10,999	TWOPT050
900	WRITE(3,501)	TWOPT051
501	FORMAT(72H DEADTIME GREATER THAN .0002,ANALYSIS TERMINATED, NEXT	TWOPT052
	1 DATA SET CALLED.////////)	TWOPT053
	CALL SLITET(LITE1,JLT)	TWOPT054
	GOTO(10,905),JLT	TWOPT055
905	READ(2,500)	TWOPT056
	GOTO10	TWOPT057
909	WRITE(3,502)	TWOPT058
502	FORMAT(72H DEADTIME INCREMENTING AT LESS THAN 1.0E-11,ANALYSIS END	TWOPT059
	15,RESULTS BELOW.)	TWOPT060
	HINC=HINC/0.1	TWOPT061
	DT=DT+HINC	TWOPT062
	GOTO18	TWOPT063
999	WRITE(3,503)	TWOPT064
503	FORMAT(//////////45X20H////////END OF JOB////////1H1)	TWOPT065
	CALL EXIT	TWOPT066
	END	TWOPT067

SUBROUTINE RDR

```

C
SUBROUTINE RDR(COUNT,JCT)
      SUBROUTINE RDR
DIMENSION COUNT(99)
JST=-8
DO 2 I=1,11
JST=JST+9
JND=JST+8
500 READ(2,500)(COUNT(J),J=JST,JND)
      FORMAT(15X9P6.0)
DO 2 J=JST,JND
      IF(COUNT(J))3,3,2
      JCT=JCT+1
      RETURN
      END
  
```

```

RDR 001
RDR 002
RDR 003
RDR 004
RDR 005
RDR 006
RDR 007
RDR 008
RDR 009
RDR 010
RDR 011
RDR 012
RDR 013
RDR 014
  
```

SUBROUTINE CRCTR

```

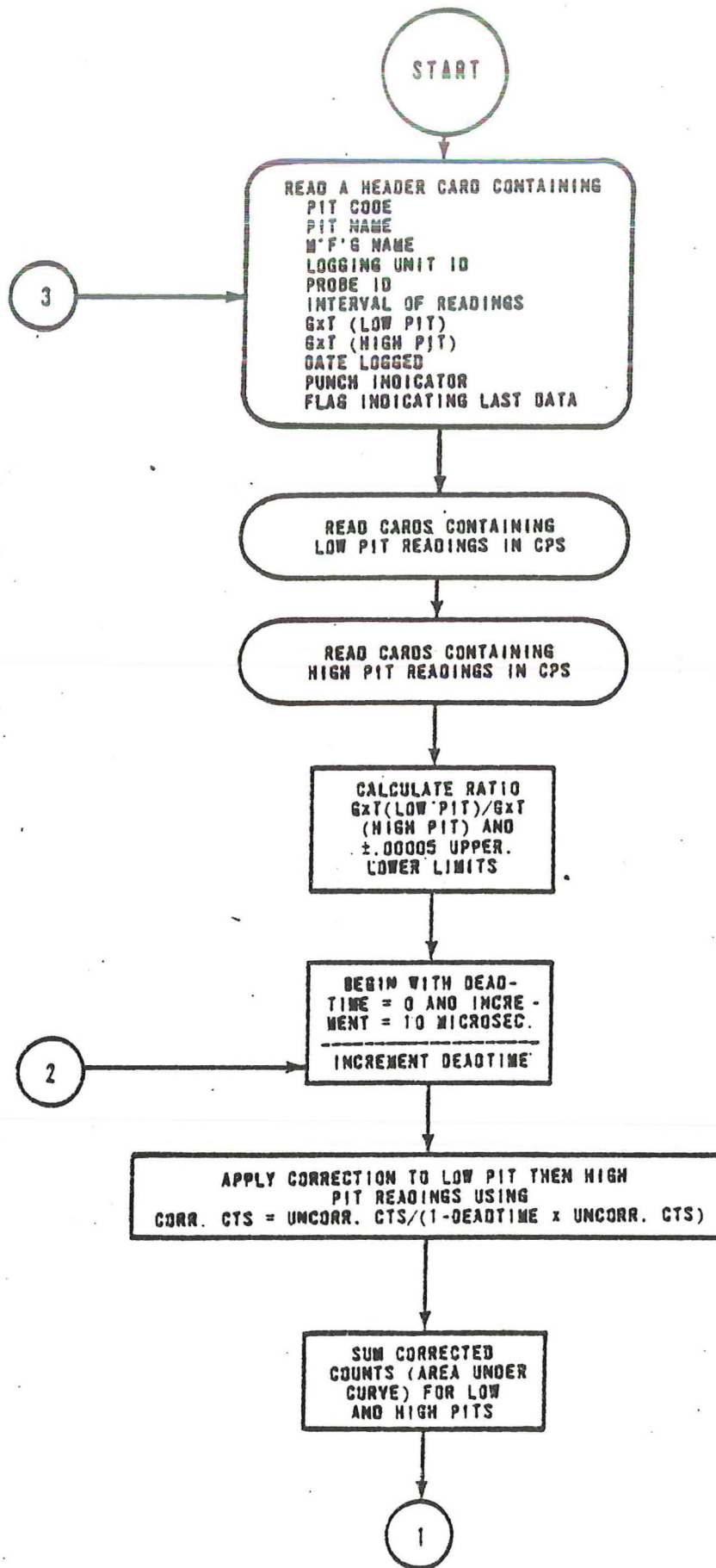
C
      SUBROUTINE CRCTR
SUBROUTINE CRCTR(JCT,DT,COUNT,AREA,CORR)
DIMENSION COUNT(99),CORR(99)
DO 10 I=1,JCT
CORR(I)=COUNT(I)/(1.-DT*COUNT(I))
AREA=AREA+CORR(I)
10 CORR(I)=CORR(I)+0.5
RETURN
END
  
```

```

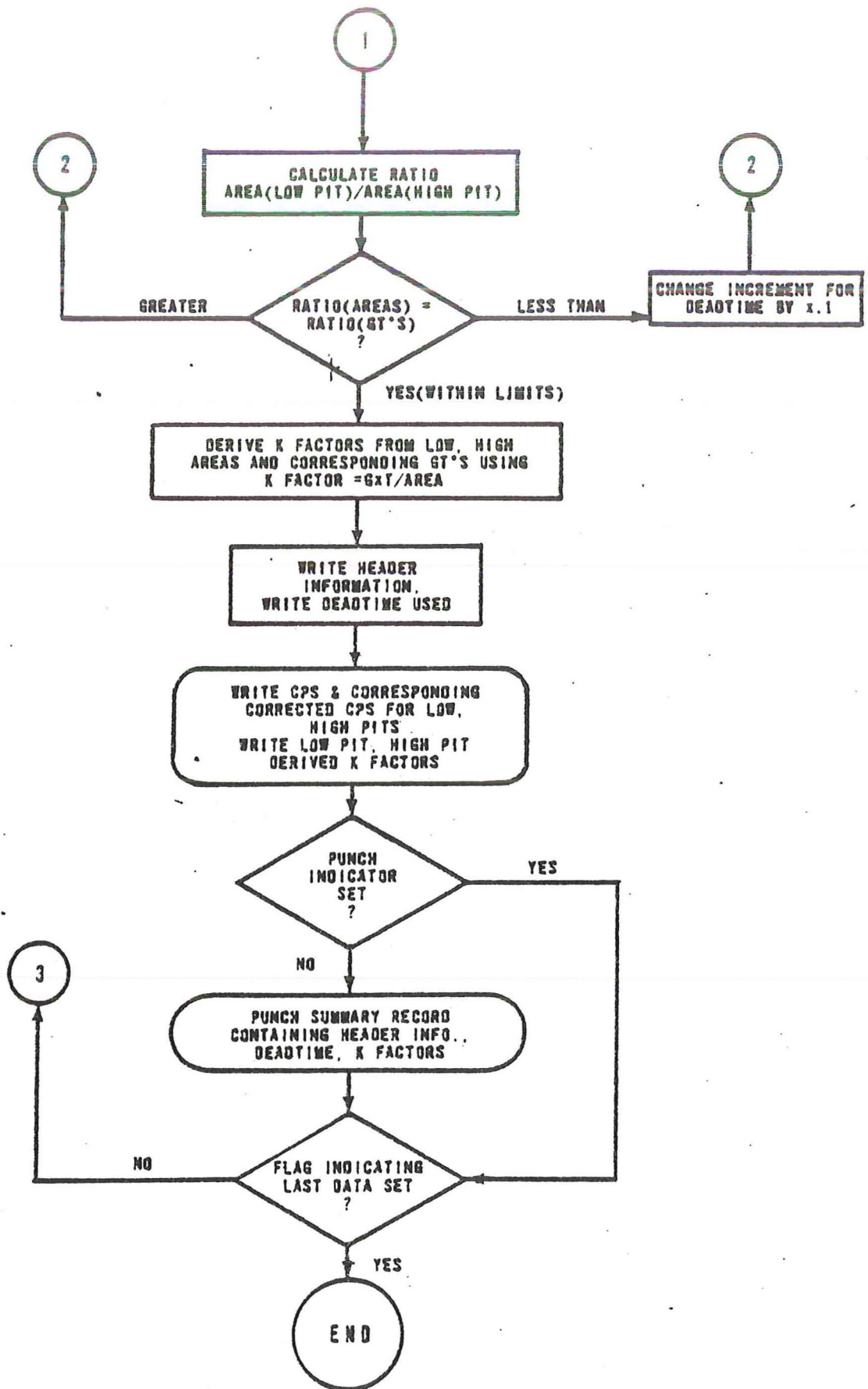
CRCTR001
CRCTR002
CRCTR003
CRCTR004
CRCTR005
CRCTR006
CRCTR007
CRCTR008
CRCTR009
  
```

SUBROUTINE OWTPT

	SUBROUTINE OWTPT	OWTPT00
	SUBROUTINE OWTPT	OWTPT002
	REAL NPITS,KFACL,KFACH	OWTPT003
	COMMON AREAH,AREAL,DT,GTH,GTL,IP,ITMS,JCT,KCT,KFACH,KFACL,NPITS,	OWTPT004
	1PROBE,PROP,RASH,THK,UNIT,CPNY(3),DATE(3),PITS(3),CONTH(99),	OWTPT005
	2CONTL(99),CORH(99),CORL(99),LITE1	OWTPT006
	WRITE(3,500)	OWTPT007
	WRITE(3,501)PITS,DATE	OWTPT008
	WRITE(3,502)CPNY,THK	OWTPT009
	WRITE(3,503)UNIT,RASH	OWTPT010
	WRITE(3,504)PROBE,DT,PROP	OWTPT011
	WRITE(3,505)GTL,GTH	OWTPT012
	WRITE(3,506)	OWTPT013
	DO 14 I=1,ITMS	OWTPT014
	IF(IP)11,10,13	OWTPT015
10	WRITE(3,507)CONTL(I),CORL(I),CONTH(I),CORH(I)	OWTPT016
	GO TO 14	OWTPT017
11	IF(I-JCT)10,10,12	OWTPT018
12	WRITE(3,508)CONTH(I),CORH(I)	OWTPT019
	GO TO 14	OWTPT020
13	IF(I-KCT)10,10,135	OWTPT021
135	WRITE(3,509)CONTL(I),CORL(I)	OWTPT022
14	CONTINUE	OWTPT023
	WRITE(3,510)AREAL,AREAH,KFACL,KFACH	OWTPT024
	CALL SLITET(LITE1,JLT)	OWTPT025
	IF(JLT-1)15,16,15	OWTPT026
15	READ(2,511)	OWTPT027
	WRITE(2,511)DATE,NPITS,UNIT,PROBE,THK,GTL,GTH,DT,KFACL,KFACH	OWTPT028
16	RETURN	OWTPT029
		OWTPT0
	FORMATS	OWTPT0
		OWTPT032
		OWTPT033
500	FORMAT('1',42X'PROGRAM TWO PIT RESULTS'/)	OWTPT034
501	FORMAT(23X'PITS'6X2A6,A3,11X'DATE LOGGED '2(A2,'/'),A2)	OWTPT035
502	FORMAT(23X'COMPANY '2A6,A3,11X'LOGGED AT 'F5.2,' FOOT INTERVAL')	OWTPT036
503	FORMAT(23X'UNIT'6XA5,21X'RATIO - GT(LOW)/GT(HI) = 'F10.7)	OWTPT037
504	FORMAT(23X'PROBE'5XA5,21X'ACCEPTED DEADTIME = 'F8.3,' MICROSEOWTPT038	
	1CONDS'/60X'WHEN RATIO-AREA(LOW)/AREA(HI) = 'F10.7/)	OWTPT039
505	FORMAT(27X'LOW PIT DATA'32X'HI PIT DATA'/2(26X'GT = 'F9.5,4X))	OWTPT040
506	FORMAT(3X2(16X'OBSERVED'10X'CORRECTED')/2X2(18X'COUNTS'13X'COUNTS'	
	1))	OWTPT041
507	FORMAT(2X2(15XF9.0,10XF9.0))	OWTPT042
508	FORMAT(50X2(10XF9.0))	OWTPT043
509	FORMAT(7X2(10XF9.0))	OWTPT044
510	FORMAT('0'1X2(17X'AREA'9X' = 'F10.0)/3X2(16X'K FACTOR =	
	1F11.8))	OWTPT045
511	FORMAT(3A2,A3,2A5,F6.2,2F6.4,3E12.5)	OWTPT046
	END	OWTPT047
		OWTPT048



GENERALIZED FLOW CHART
FOR PROGRAM TWOPIT



GENERALIZED FLOW CHART
FOR PROGRAM TWOPIT

Interpretation of electric and gamma ray logs in water wells * **

by Hubert Guyod

Consultant

* Published by Permission of Gearhart-Owen, Inc., Fort Worth, Texas.

** Much of the material in this paper was presented in a talk by Mr. Guyod at the 1965 Annual Meeting of the American Geophysical Union, Section of Hydrology, in Washington, D. C., on April 20, 1965.

ABSTRACT

A typical inexpensive logging program for water wells consists of a Normal or single-electrode resistivity, the SP and, sometimes, gamma ray measurements. Some of the principles underlying the analysis of these logs are reviewed. The usual logging situations are classified into three groups and simple interpretation procedures are outlined for each. Much useful information is provided by these records, especially when they are supplemented by the bit penetration rate and other data. The logs can solve many common ground-water problems. Those, and the ones that they cannot solve, are reviewed.

INTRODUCTION

Geophysical logging is an accurate and convenient way of obtaining many subsurface data that could be provided otherwise only by coring or testing. Some of the data are read directly from the logs: depth and thickness of beds, for example. Others, such as the water salinity, can be obtained only by analyzing the records.

There are many geophysical logging tools, but the ground-water developer cannot afford the cost of running the comprehensive suite of logs used in the oil industry. In most cases he has to satisfy himself with a rather rudimentary logging program, typically consisting of a shallow penetration resistivity, the SP (spontaneous potential) and, sometimes, gamma ray. Nevertheless much useful information can be extracted from these records, especially when they are supplemented by the driller's log, cuttings, knowledge of the local geology, and some experience.

The methods commonly used for measuring resistivity, SP, and gamma ray have been amply discussed elsewhere. Their descriptions are not included here, but some of the principles underlying the analysis of the results are reviewed when necessary.

CLASSIFICATION OF FORMATIONS

The problems encountered in ground-water work are many, and geophysical logs can solve, or help solve,

only part of them. A log may be a valuable tool in one locality but useless in another, because the water may occur in a different kind of rock. For log interpretation purposes, it has been found convenient to classify formations among one of the following groups.

1. Clean granular aquifers – Comprise gravel, sand, sandstone, and carbonate rocks having only granular-type porosity. Silt must be added to this group provided that its particles are not composed of clay minerals.
2. Clayey granular aquifers – This group includes any granular aquifer that is in part composed of grains formed by clay minerals, or contains clay material within its pore space.
3. Fractured aquifers – Represented by fractured or jointed rocks having little or no granular-type porosity.
4. Complex aquifers, in which the porosity is a type different from those specified above; for example, carbonates that are both granular and fractured, lava and cavernous rocks.
5. Dense formations, i.e., rocks having so little effective porosity that no water could be normally obtained from them. Besides some carbonate rocks, they include anhydrite, gypsum, salt as well as many kinds of igneous and metamorphic rocks.
6. Clay – This group includes all formations, like clay and shale, that consist of very fine, surface-active particles. All have very similar properties as far as electric and gamma ray logs are concerned; they are called clay for the sake of simplicity.

For convenience, especially in gamma ray logging, any formation of types 1 to 5 is called "rock".

Unless specified otherwise it will be assumed that all aquifers are reasonably uniform in texture and fully saturated with water.

RESISTIVITY LOG

Resistivity of Clean Aquifers. – A clean aquifer is made up of a non-conductive rock framework, or skeleton, and water. Its resistivity is determined by

1. the resistivity of the water (i. e., the water salinity),
2. the quantity of water that the rock contains (i. e.,

- rock porosity), and
- the distribution and continuity of the water within the pore space.

It has been found that the resistivity, R_t , of a clean aquifer can therefore be expressed as follows:

$$R_t = F \times R_w \quad (1)$$

where R_w is the water resistivity and F a constant that represents the effect of the pore space (Archie, 1942). This constant, called formation resistivity factor, is given by the following formula:

$$F = A/\phi^m \quad (2)$$

where ϕ is the effective porosity (fraction of total volume), and A and m are non-dimensional numbers that represent the effect of porosity distribution and continuity. A and m vary from rock to rock and their values can be accurately determined only from laboratory measurements.

The resistivity of water, R_w , decreases when the salinity increases. At a given temperature, water resistivity is related to the dissolved solids content, in parts per million (ppm), by the expression

$$R_w = k/\text{ppm} \quad (3)$$

where k is a factor that is nearly constant for a given salt when the salinity is low (less than about 3000 ppm of dissolved solids). For the usual low salinity waters, k averages 6500 at 25 degrees Centigrade. Water resistivity decreases somewhat when temperature increases but this effect is small (2 per cent per degree at 25 degrees Centigrade) and will be neglected here. Figure 1 is a chart representing Formula (3).

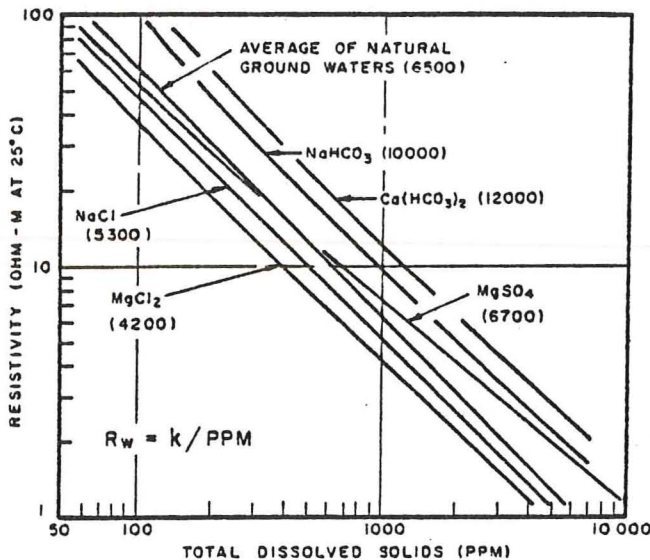


Fig. 1 - Solution resistivity vs. total dissolved solids at 25° C. Figures in parenthesis are k values. (After Agriculture Handbook 60, USDA).

Clean Granular Aquifers. - For clean granular rocks having a porosity greater than about ten per cent A and m have the following average values:

- rocks that are little or not cemented: $A = 0.62$, $m = 2.15$;
- rocks that are more cemented: $A = 1$, $m = 2$.

Figure 2 illustrates the relationship between forma-

tion resistivity factor and porosity, using above sets of values. The first set will be used for the numerical examples given below.

Combining Formulas (1), (2), and (3), and using for the resistivity of clean granular aquifers:

$$R_t = \frac{0.62 k}{\phi^{2.15} \text{ ppm}} \quad (4)$$

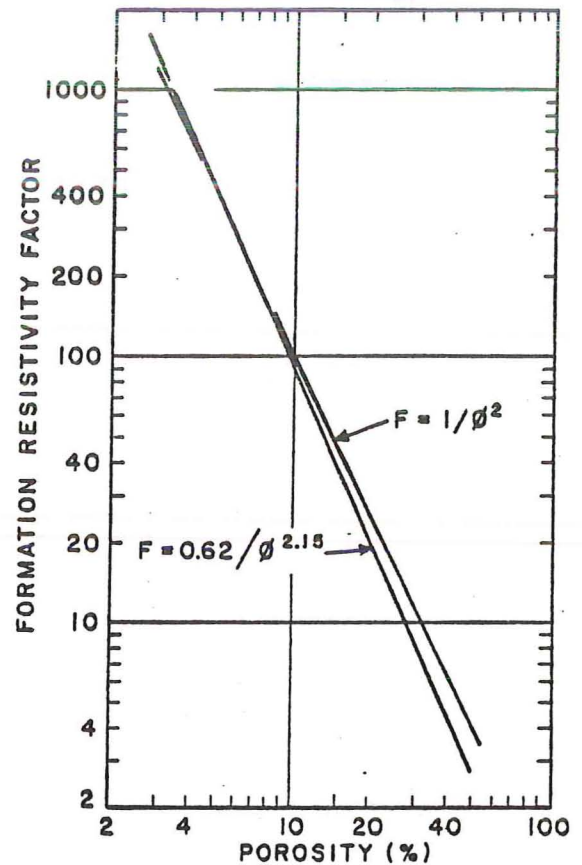


Fig. 2 - Approximate formation resistivity factor vs. porosity for granular aquifers.

Figure 3 is a chart based on this formula, using for k the value 6500. It gives the resistivity of clean granular aquifers as a function of their porosities (expressed in

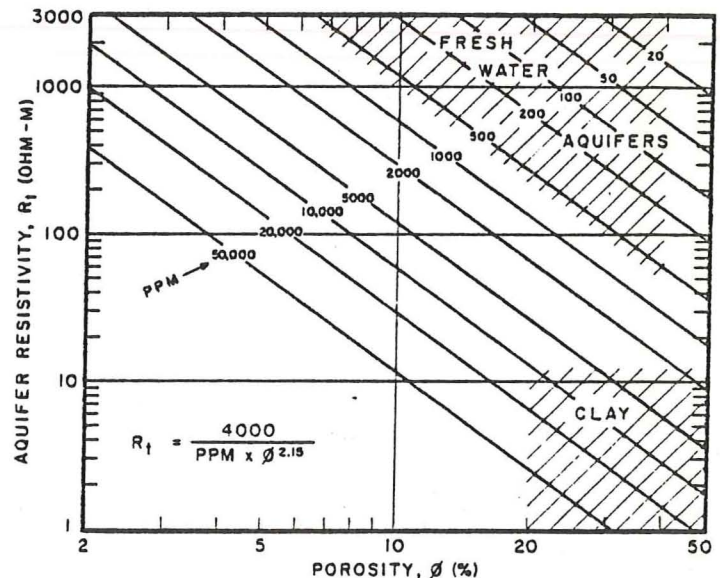


Fig. 3 - Approximate resistivity of granular aquifers vs. porosity for several water salinities.

per cent of total volume) and for a few water salinity values. The chart is only approximate when applied to a particular aquifer since A, m and k have been assigned average values; nevertheless it is accurate in a statistical manner and acceptable when more exact figures are not available, especially when porosity is high.

The geometry and continuity of the pore space in low porosity granular materials is rather irregular and it is not possible to assign to parameters A and m average or approximate values that would be applicable to a given rock. Nevertheless Formula (4) or Figure 3 may be used to obtain semi-quantitative data.

It is seen from Figure 3 that, all other factors being constant.

1. the higher the porosity, the lower the aquifer resistivities,
2. the lower the salinity of the water, the higher the aquifer resistivities.

The upper cross-hatched area of Figure 3 corresponds to clean fresh water aquifers: commonly their resistivities are of the order of 50 to 1000 ohm-m. Brackish and salt water aquifers of good porosity have resistivities which are much less than 50 ohm-m.

Non-granular Aquifers. - The pore space of non-granular aquifers is so variable and irregularly distributed that it would be illusory to seek an expression or establish a chart relating resistivity to porosity. All that can be said with confidence is that resistivity decreases when porosity or water salinity increases, all other factors remaining the same.

Dense Rocks. - Rocks that have no effective porosity have extremely high resistivities, usually of the order of 100,000 ohm-m and more.

Clay. - As far as resistivity is concerned, clay can be considered as a granular material whose pore space has a particular geometry. Hence Formula (2) applies, but the parameters A and m have values which probably are somewhat different from those previously specified. Although no numerical data are available, the resistivity of a clay can be estimated from Formula (4) or Figure 3.

Clays have a high porosity and -- the marine clays at least -- generally contain brackish water, two facts that make their resistivities low: commonly these range from 2 to 10 ohm-m, i.e., they are lower than the resistivities of the fresh water aquifers with which they are associated. This range is shown by the lower cross-hatching in Figure 3.

Clay Granular Aquifers. - Clay disseminated within the pore space reduces the resistivity of fresh water aquifers. Figure 4 gives the resistivity reduction for a granular aquifer as a function of its clay content. The resistivity of the clay is assumed to be one-tenth that of the aquifer water and the double layer effect (Winsauer & McCardell, 1953), if any, is disregarded. The lower curve applies if the clay particles surround the rock skeleton, and the upper one if they do not touch it. If the clay is randomly distributed the geometric average of the two curves probably gives a better account of the resistivity reduction. This average is shown by the dashed line. It will be observed that when the pore

space contains 10 per cent of irregularly interspersed clay, the aquifer resistivity drops to about 60 per cent of the value it would have if clean. The drop would be greater if the resistivity contrast between water and clay were higher than 10, which is often the case for fresh water aquifers.

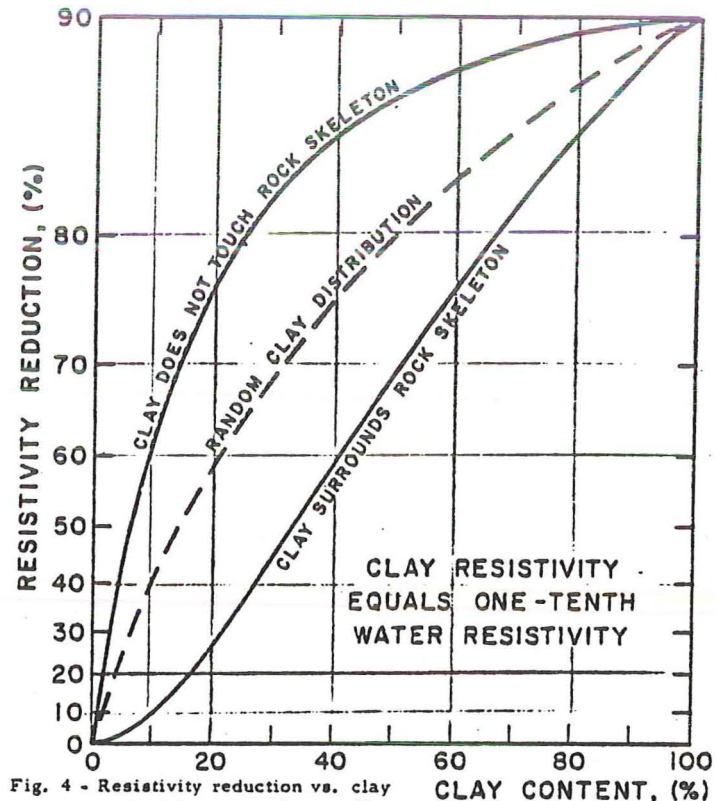


Fig. 4 - Resistivity reduction vs. clay content for a granular aquifer. Clay resistivity is assumed to be one-tenth of water resistivity.

Apparent Resistivity. - Resistivity logging devices measure a weighted average resistivity, called apparent resistivity, of a certain volume of earth material in the vicinity of the logging probe. This zone intercepts a portion of the mud column and, frequently, the adjacent beds also: the larger the contrasts between aquifer resistivity (on the one hand) and mud and adjacent bed resistivities (on the other), the larger the departure between apparent and true values. The departure is small if the aquifers are thick and have high porosities; it is therefore of no great consequence if the log is used qualitatively, as is generally the case for water wells. The departure is large in high resistivity formations, and an aquifer of low porosity may be mistaken for dense rock, or conversely, on the strength of the resistivity curve, if the latter is used alone.

When quantitative data are desired, true resistivities must be determined. The true resistivity of a bed can be obtained provided an appropriate electric log and the related analysis charts are available (Guyod & Pranglin, 1961). In petroleum producing areas service companies run electric logs that are tailored to the needs of the petroleum geologist and to the local conditions; from these logs certain types of quantitative data can be derived. If circumstances do not justify the cost of service company logs, or if logging service is not available, the water well contractor who desires quantitative data must therefore provide his own log. The

only equipment which is adequate, practical, and reasonably priced is one giving two Normal curves, preferably with 16 and 64 inch electrode spacings. Fairly accurate resistivities can be derived from such a log provided all the following conditions are met.

1. The aquifer resistivity is not too large; this requires that the porosity be fairly high and the dissolved solids content of the water be not less than about 100 ppm.
2. The aquifer is at least 15 ft. thick and reasonably uniform in texture; in particular, it should not contain clay or dense layers.
3. The mud invasion is small.
4. The hole diameter is less than 10 inches and the mud resistivity greater than about 1 ohm-m.

There are many areas where the above conditions can be met by aquifers in the depth interval of interest.

Examples of Resistivity Curves. - Figures 5, 6 and 7 are artificial electric and gamma ray logs for three types of formations. Their appearances are approximately those of actual logs for the formations shown, provided the hole diameter is less than 10 inches and the bore-hole fluid resistivity greater than one ohm-m. The resistivity curves are those that would be obtained with a single-electrode or a short Normal probe; they correspond to a weighted average resistivity of the material contained in a sphere having a diameter of approximately three feet. The intervals marked "sand" or "sandstone" could represent granular carbonate rocks since these rocks have nearly the same resistivities, other factors being constant. The beds shown have uniform texture and are 10 to 15 ft. thick; their true resistivities are indicated to the right of the curves. Actual logs have a more irregular shape because the curves reflect the lack of uniformity commonly exhibited by rocks. No scales are shown since apparent resistivities values depend upon many factors such as porosity, water salinity, mud resistivity, etc.

The resistivity curves illustrate the following facts.

1. Fresh water aquifers and dense rocks have much higher resistivities than most other formations.
2. The apparent resistivities of fresh water aquifers with low porosity are of the same order as those of dense rocks. In practice they can be differentiated by reference to the bit penetration rate, the character of the cuttings or, sometimes, the SP curve.
3. Aquifers which contain highly saline water have resistivities close to that of clay. In practice they can be differentiated from clay by using the SP or gamma ray curves.
4. Bed depths and thicknesses can generally be accurately determined from the resistivity curve, but the size of individual fractures in consolidated rock cannot be.

In Figure 5 the apparent resistivity of the bottom salt water sand is shown to be less than that of the adjacent clays; this is frequently the case when there is only little invasion by the mud filtrate. The apparent resistivity is larger when the invasion is important.

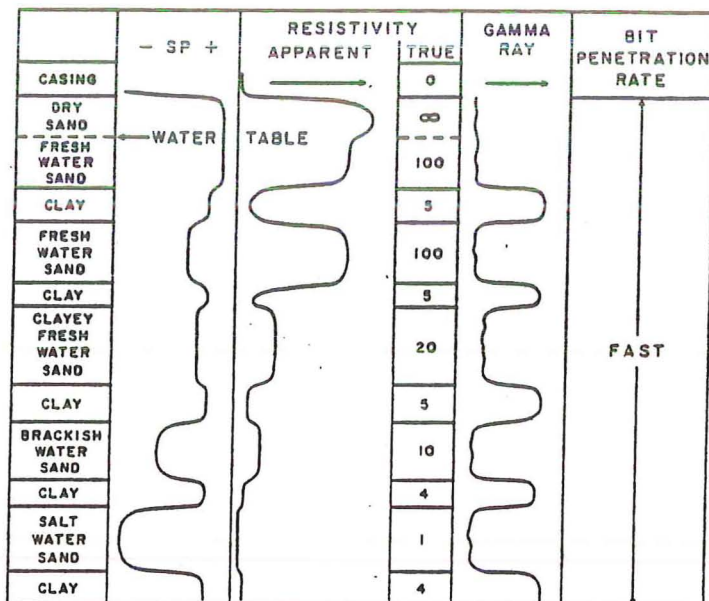


Fig. 5 - Artificial electric and gamma ray log approximating the appearance that an actual log would have in a sequence of clay beds and granular aquifers having good porosities. Aquifers are assumed to be non-radioactive.

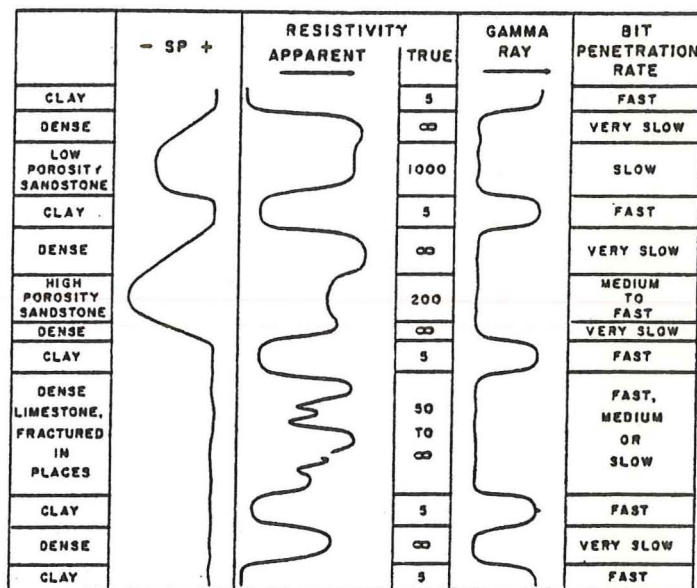


Fig. 6 - Artificial electric and gamma ray log approximating the appearance that an actual log would have in a sequence of clay beds and several types of rock. It is assumed that the water in the aquifers is fresh and that the rocks are not radioactive.

Estimating Water Salinity. - Rearranging Formula (4) gives the following expression for the salinity of the water in a clean granular aquifer:

$$\text{ppm} = \frac{0.62 k}{\phi^{2.15} R_t} \quad (5)$$

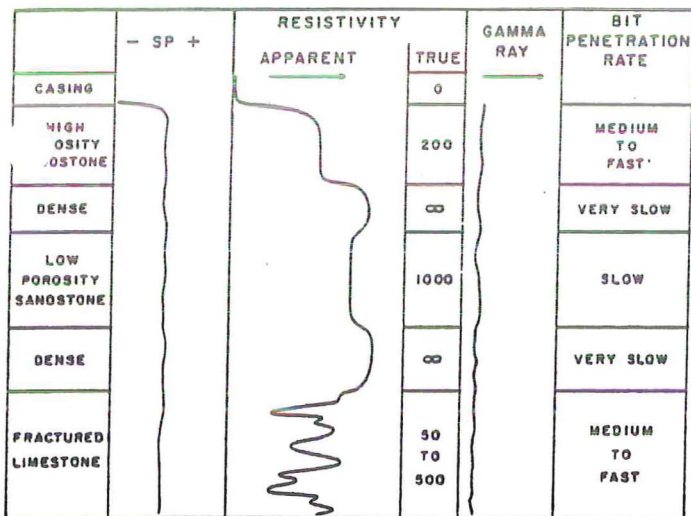


Fig. 7 - Artificial electric and gamma ray log approximating the appearance that an actual log would have in a formation that does not contain clay beds. It is assumed that the water in the aquifers is fresh and that the rocks are not radioactive.

This formula is applicable in practice only if both the resistivity and the porosity of the aquifer are known, requirements that seriously limit its applicability in unknown areas, unless an appropriate suite of logs is available. Further, some knowledge of the type of water likely to be present is required so that the correct k value can be selected; when this is not the case a value of 6500, corresponding to average waters, is generally used and the formula becomes

$$\text{ppm} = \frac{4000}{\phi^{2.15} R_t} \quad (6)$$

Figure 3, based on the numerical values used in this formula, can be employed to obtain or estimate the dissolved solids (slanted lines) in terms of the resistivity and porosity of clean water-bearing formations.

An outstanding example of water quality determination from resistivity and other data is the method developed by Jones and Buford (1951) for obtaining, not only the quantity of dissolved solids, but also approximate water analyses for the important water-bearing formations of Louisiana.

Estimating Aquifer Porosity. - Formula (5) or Figure 3 can also be used to obtain or estimate porosity if the quantity of dissolved solids and the aquifer resistivity are known.

Estimating Permeability. - Quantities ϕ , A and m used in Formula (2) have no dimension. F and, therefore, resistivity are not directly affected by absolute grain size, which means that resistivity cannot be directly used for determining permeability. In particular, it is not possible to distinguish a fine sand from a gravel; the discrimination must be made by reference to the cuttings or other geologic data.

Where aquifer permeability may be directly related to changes in porosity or clay content, the permeability changes are reflected on the aquifer resistivity; this permits semi-quantitative determinations of permeability

from empirical data if true resistivities can be derived from the log.

Water Table. - Since air is non-conductive, the resistivity of a permeable rock is much greater above the water table, where the rock is unsaturated. However some of the borehole fluid generally enters the rock, and measurements made with probes having a small radius of investigation show only a small increase in resistivity; the depth of the water table is difficult to pick, especially if the rock is not of uniform texture.

The best resistivity logging device for determining the depth of the water table is the Guard tool because it has a deep lateral investigation and gives great vertical detail. A combination of two Normal devices, a long one and a short one, can also be used, but the depth determination is somewhat less accurate.

Principal Uses of Resistivity Data. - To a water well driller the most tangible benefits that can be derived from a log are those obtained from a mere inspection of the record. In this respect, the resistivity curve, even that recorded by the least expensive equipment, is the most rewarding. By glancing at it he can determine the depth and thickness of almost every bed, except the thinnest ones. By supplementing it with his own drilling observations or local experience, he can tell what most, if not all, of these beds are; this will permit him to formulate an optimum screen setting program. If he has to venture into the brackish water zone, he finds the decrease in resistivity -- although not unequivocal -- a welcome safeguard; if the bit penetration rate remained essentially the same for all the aquifers logged, he can assume that their porosities are of the same order and therefore interpret a decrease in apparent resistivity as an indication of a salinity increase. Figure 8 (Rose et al., 1944) is a case in point. It represents the lower portions of the electric logs of two water wells which have penetrated a sequence of clays and clean unconsolidated sands having porosities of the same order. Above 1375 ft. the sand apparent resistivities are nearly the same, but below that point they decrease with depth. This decrease can be interpreted as an increase in the water salinity. Incidentally, the bottom sands were plugged below 1375 ft. and the upper ones are producing waters averaging 500 parts per million of dissolved solids.

Conversely, when it is known that the quality of the water remains nearly the same for all the aquifers penetrated, changes in resistivity can generally be interpreted as being caused by changes in porosity, or by a clayey condition. The simultaneous use of the SP or gamma ray curve will generally permit determining which of these two situations exists.

These are the major applications of the resistivity log. A few more are described in the section titled "Applicability of Geophysical Logs to Specific Problems."

In practice, log interpretations are not made with the resistivity curve alone; the SP and all other available data are analyzed simultaneously with resistivity.

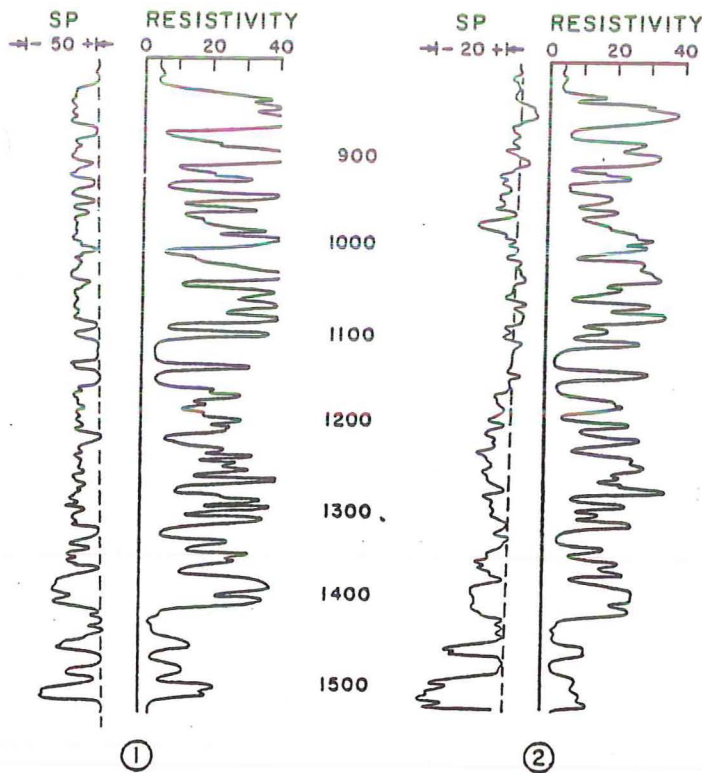


Fig. 8 - Portions of electric logs of two water wells 160 ft apart (Houston area). Mud resistivities are 10 and 1.3 ohm-m in wells 1 and 2, respectively.

Empty Holes. - Good resistivity curves can be obtained in uncased empty holes provided a probe making good contact against the bore wall is employed. Because the borehole effects are greatly minimized, there is usually less departure between true and apparent resistivities. An example of an electric log made in an empty hole is given in Figure 9, left; the log to the right was obtained after the hole was filled with a thin drilling mud.

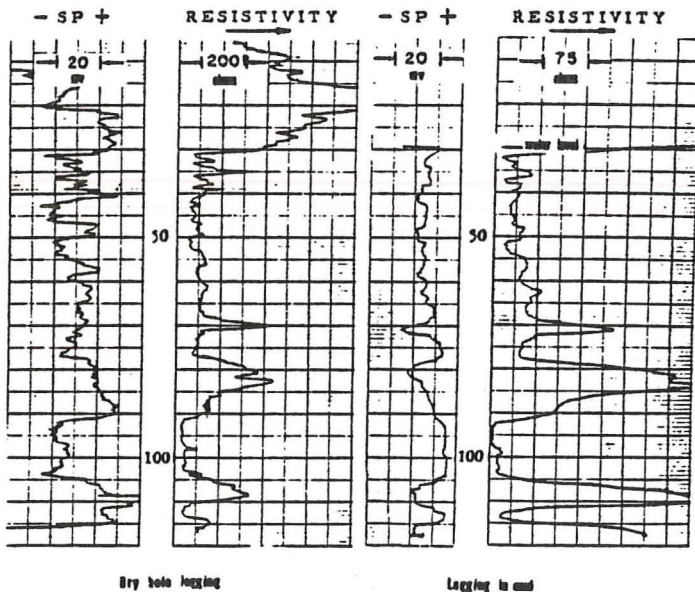


Fig. 9 - Comparison of electric logs made in an empty hole and in the same hole containing mud (Hot Springs, South Dakota).

Cased Holes. - Resistivity measurements made in cased holes are not related to the formation. Steel being an excellent conductor, the resistivity obtained in a steel casing that is not too old is extremely low; its

only usefulness is to permit determining the casing depth. Old steel casings are corroded; the resulting iron oxide is non-conductive and the resistivity changes resistivity changes reflect primarily the degree of corrosion. The data can sometimes be used to obtain some information on the condition of the casing, but the interpretation is difficult and usually problematical. Examples of resistivity curves made in cased holes are given in an article by Bays (1949); the increases in resistivity in little-corroded casings, and the decrease in heavily corroded casings, were interpreted as being due to holes.

Resistivity measurements made in undamaged plastic casings are related to the resistivity of the fluid contained in the pipe. Large holes in casings cause local resistivity decreases.

Resistivity Measuring Tools. - The majority of the resistivity logs recorded in water wells are obtained with a single electrode or a short Normal device; they give good qualitative data and sometimes semi-quantitative information. Long Normals and Laterals are occasionally used, especially when the electric logs are run by commercial logging companies. Other resistivity measuring devices are also available; each of the three mentioned below logs a particular volume of formation.

The Guard electrode measures the resistivity of a thin horizontal disk-shaped zone six to twelve inches high having a diameter of six feet, or more (Owen & Greer, 1951; Guyod, 1964b). The log gives good vertical detail and is valuable in very broken formations; it is the best log for accurately determining the depth of the water table.

The Microlog measures the resistivity of a few cubic inches of the formation situated immediately behind the bore wall (Doll, 1950). It gives still more vertical detail than the Guard log and, in granular rocks, the data can frequently be interpreted in terms of porosity.

The Induction tool (Doll, 1949) makes a measurement which corresponds to a four foot vertical interval; it is little affected by the mud column and the invaded zone. It is an excellent tool for conductive formations, but its efficiency decreases when formation resistivities increase; for this reason the induction log does not permit quantitative determinations in fresh water aquifers, especially in those of low porosity.

These three tools are complicated and expensive they are generally operated only by commercial logging companies.

SPONTANEOUS POTENTIAL LOG

The spontaneous potential curve, usually called SP, is a record of the natural potentials which occur in a borehole (Anonymous, 1958a). When the formation contains clay beds, it is generally observed that these beds have approximately the same potential; on the SP curve this potential defines an almost straight, vertical line, called the clay (or shale) base line, from which the SP deflections in the other beds are measured.

These natural potentials are primarily caused by electrochemical reactions taking place between mud, formation waters and clay. Unless specified otherwise it will be assumed that there are no other sources of potential.

Clean Granular Aquifers Interbedded With Clay Formations. - If the waters in the aquifers are much more saline than the drilling mud, the SP generally is more negative in the aquifers than in the adjacent clays, and if the waters are much less saline than the mud the SP generally is more positive in the aquifers than in the adjacent clays. In these extreme cases the electrochemical potential, $(SP)_c$, expressed in millivolts, is approximately given by the following formula:

$$(SP)_c = -K \times \log_{10} \frac{R_{mf}}{R_w} \quad (7)$$

R_w is the formation water resistivity, R_{mf} the resistivity of the mud filtrate, and K a factor which is generally taken equal to 71 at shallow depths. Conversely, an approximate value of the formation water resistivity can be obtained from the SP curve and the application of above formula.

Because it is possible to closely estimate salinities from water resistivities -- especially if the type of water is known -- the SP seems to be a very significant tool in ground-water investigations. However, it has proved to be a great disappointment in this respect. The main reason is that Formula (7) is an approximation which is permissible only if there is an extremely large difference in salinity between formation water and mud. In water well practice it is generally applicable only when the formation waters are brackish or salty. It breaks down when these waters contain less than about 15,000 ppm of dissolved solids, and another expression has to be considered instead. This expression is based on the activities of the formation water and borehole fluid and it is rather complicated (Wyllie, 1949; Patten & Bennett, 1963). For low salinity solutions whose metal ions are sodium, calcium and magnesium this expression reduces to the following formula (Gondouin et al., 1957):

$$(SP)_c = -K \times \log_{10} \frac{(a_{Na} + \sqrt{a_{Ca} + a_{Mg}})_w}{(a_{Na} + \sqrt{a_{Ca} + a_{Mg}})_{mf}} \quad (8)$$

The numerator of the fraction refers to the formation water, and the denominator to the mud filtrate. The a 's denote the activities due to the ions specified by the subscripts. The portion of the activity due to a particular ion is approximately proportional to the ion concentration, but the coefficient of proportionality may vary greatly with the type of ion, even if the valences are taken into account. This can be seen for example, in the chart of Figure 10 which gives effective activities as a function of salinity for the three ions considered.

As far as the SP value is concerned, a solution containing only 100 ppm of the divalent ions is equivalent to a solution having 1000 ppm of the sodium ion, but their resistivities are in a ratio of 10 to 1. Evidently this bars the application of Formula (7) to salinity deter-

minations. Formula (8) should be used, but this is not possible in practice because all that the field measurements can give is the quantity $(a_{Na} + \sqrt{a_{Ca} + a_{Mg}})_w$ from which salinity cannot be derived unless the activities are known, i. e., unless an analysis of the water is available. The same conclusions are reached regardless of the ion types and concentrations. An empirical chart for estimating water resistivities has been developed by Gondouin et al. (1957), but it is applicable only when the dissolved solids total less than 3000 ppm.

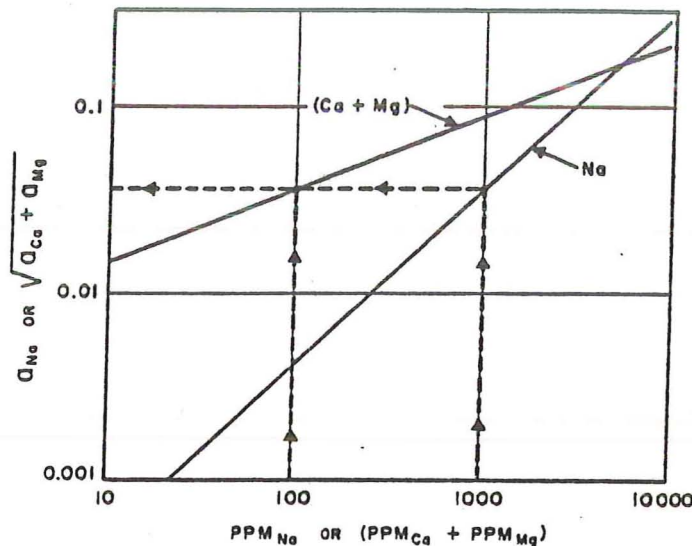


Fig. 10 - Activity due to sodium, calcium and magnesium ions, vs. concentration.

The only possibility of using the SP data for quantitative salinity determinations in fresh water bearing formations would be to establish beforehand empirical data for the waters of an area and use an appropriate chart or formula. This is basically what Jones and Buford (1951) did with resistivity. Unfortunately the difficulties are considerably more numerous with the SP as will be understood from the following comments.

1. The numerical value of the K factor in Formula (7) can be accurately evaluated only when the clay formation bounding the aquifer is a perfect cationic permeable membrane. Actual K values can be determined only from the laboratory measurements.
2. The chemical composition of the borehole fluid must be taken into account.
3. A streaming potential is usually superimposed on the electrochemical potential (Gondouin & Scala, 1958). Although the former is very small at shallow depths, its relative value may not be negligible in deep water wells where the SP amplitude is low, and it is difficult to ascertain this fact.
4. Even if there is no streaming potential, the measured SP is only a portion of the total electrochemical potential, $(SP)_c$, developed in the ground. The reduction, $SP/(SP)_c$, is a function of several factors, in particular the aquifer resis-

tivity and thickness (Guyod, 1964a). A correction can be made (Worthington & Meldau, 1958), but this is difficult in practice. Note that the departure of SP from (SP)₀ is analogous to that between apparent and true resistivities.

The unpredictable behavior of the SP can be demonstrated from the logs of Figure 8 (Rose et al., 1944). The distance between wells 1 and 2 is only 160 ft. and the formation is nearly horizontal. The resistivity curves correlate well, which permits following each main sand from one well to the other. The dashed lines represent the "clay base line", i. e., the line on which the SP falls in the thick clay intervals. The SP amplitude in sands is measured with reference to this base line. It is seen that the SP is negative in all sands of well 1, and that the amplitude is nearly uniform above 1375 ft.. In Well 2 the SP is either negative, positive or nil in the sands of the same interval; if we should use Formula (7) to evaluate salinities we could only conclude that the water resistivities vary rather widely with depth in well 2 and that they are nearly constant in well 1. Considering the short distance between the two wells it is illogical to think, that, for any given sand, the water in well 2 is different from that in well 1. Nevertheless, that is the inevitable conclusion that would be reached for certain sands from the application of Formula (7).

The seemingly anomalous SP curve of well 2 can be explained from the mud resistivity values, 10 and 1.3 ohm-m in wells 1 and 2, respectively, and the qualitative application of Formula (8). The mud of well 2 possibly contained one or several types of ions either absent in the mud of well 1, or present in different relative concentrations.

While the SP curve should not be applied to quantitative determinations of the salinity of fresh waters, except with proper restraint, it is permissible to use it qualitatively according to the following rules of thumb.

1. Aquifers that exhibit a positive SP almost invariably carry waters of low salinity provided the borehole fluid has a resistivity greater than about 5 ohm-m.
2. In the intervals where the SP amplitude in the thick aquifers remains nearly constant with depth, all the formation waters have about the same salinity. This is indicated on the log of well 1 of Figure 8, above a depth of 1375 ft.
3. If the SP of the aquifers penetrated by a borehole becomes more and more negative with depth, the salinity of the aquifers probably increases with depth. If, simultaneously, the aquifer resistivities decrease with depth, the evidence is considerably stronger. This situation is shown in the lower portions of the logs of Figure 8: above a depth of 1375 ft. the water salinities average about 500 parts per million, and below that depth over 1000.
4. Aquifers that exhibit a fairly large negative SP generally carry waters that are much more saline

than where the SP has a low amplitude or positive.

5. Erratic changes in SP polarity, provided that the SP amplitude remains small (less than 25 mv) may or may not correspond to significant changes in water salinity. An example is shown on the log of well 2 of Figure 8 above a depth of 1375 ft. In all the aquifer waters are known to have approximately the same salinity, nevertheless there are several SP polarity reversals.

An artificial SP curve for unconsolidated granular aquifers situated in clay is shown to the left of Figure 5.

Granular Aquifers Interbedded With Clay and Dense Beds. - In this type of formation both the shape and amplitude of the SP are different from those obtained in granular aquifers. The curve is usually distorted and difficult to use alone; even bed boundaries cannot be picked with certainty. A good review of the subject is given by Doll (1948). Figure 6 illustrates this situation for some fresh water aquifers; in practice the curve may be still more confusing when there are reversals in the SP polarity.

Clayey Aquifers. - Clay or similar materials disseminated within the pore space of an aquifer reduces the aquifer SP. Approximate corrections can be made for granular formations (de Witte, 1955; Pirson, 1957), but the procedure is involved and the accuracy uncertain.

Aquifers and Dense Rocks Not Interbedded With Clay Formations. - When there are no clay beds associated with an aquifer, the electrochemical potential discussed above practically vanishes and, if there are no other sources of potential, the SP curve is nearly a straight vertical line, as shown in Figure 7. Many logs exhibit this pattern, but others display some deflections, which signifies that there are other sources of potential. Figure 11 illustrates some of these remarks: the log was obtained in a well drilled by cable tool in a formation consisting of dolomite and sandstone. No clay beds are known to occur in the formation penetrated by this well. The changes in resistivity are due primarily to changes in porosity: the highest resistivities correspond to dense dolomite and the lowest ones to the most porous intervals of the section. The porosity of the dolomite is due primarily to fractures or solution channels (Schreurs, 1964). The SP curve is a straight line, except near 300 and 410 ft. where there are positive deflections of 52 and 15 mv. respectively. Considering their polarity, it is unlikely that these deflections are caused by streaming potentials; they could be due to some clay layers, but too thin to have been noticed by the driller.

Peculiar SP Curves. - Actual SP curves do not always conform to the patterns illustrated in Figures 5, 6 and 7. The most notable exceptions are described and explained below.

1. Drift in the clay base line - Commonly the clay base line is essentially straight and vertical,

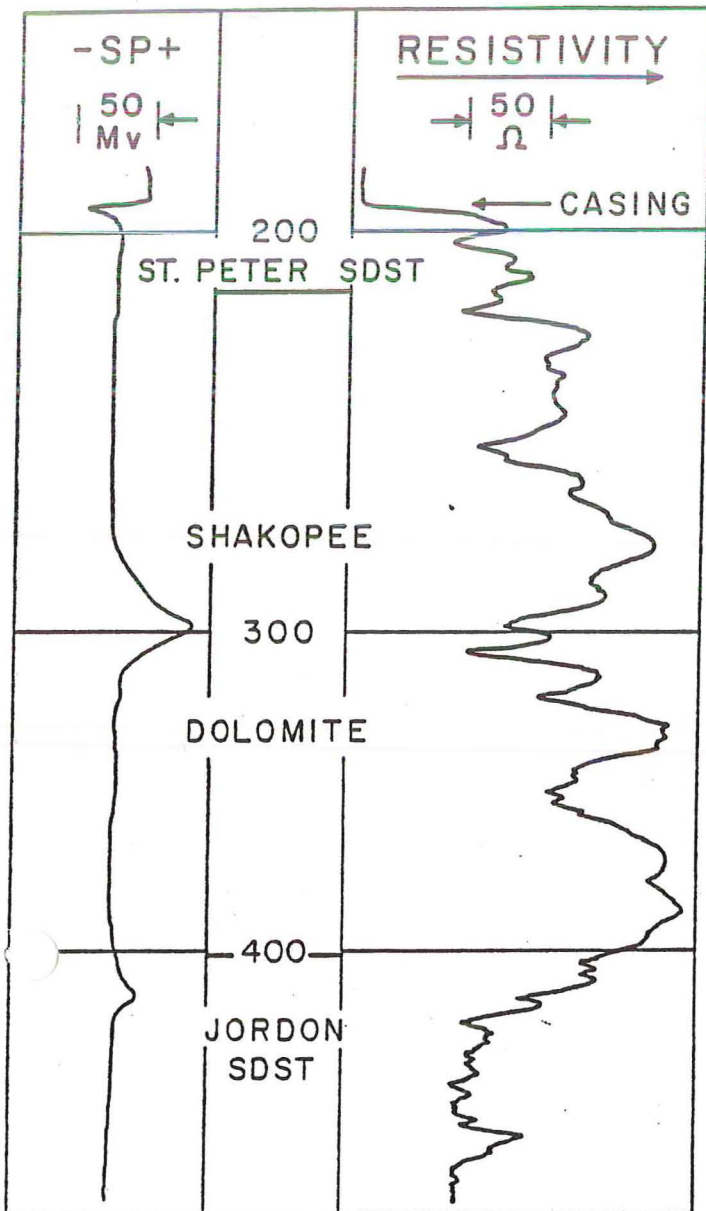


Fig. 11 - Electric log in formation that probably does not contain clay beds (Minneapolis area).

especially below a few hundred feet, as illustrated by the logs of Figure 8. But in certain wells at shallow depths the SP curve gradually wanders, either as a whole or only in the clay intervals, and generally to the left as the depth decreases. No satisfactory explanation has been offered for this phenomenon which appears to be more prevalent in arid areas.

2. Shift in the clay base line - This is frequently observed when there is a rather fast change in the salinity of formation waters. An example is given in Figure 12 (Jones, 1965). A shift can also be caused by a change in the nature of the clay (Doll, 1948).
3. Unstable SP - This is observed in the upper part of holes in which there is an appreciable movement of water, as in artesian wells or above thieving zones: the signal changes constantly

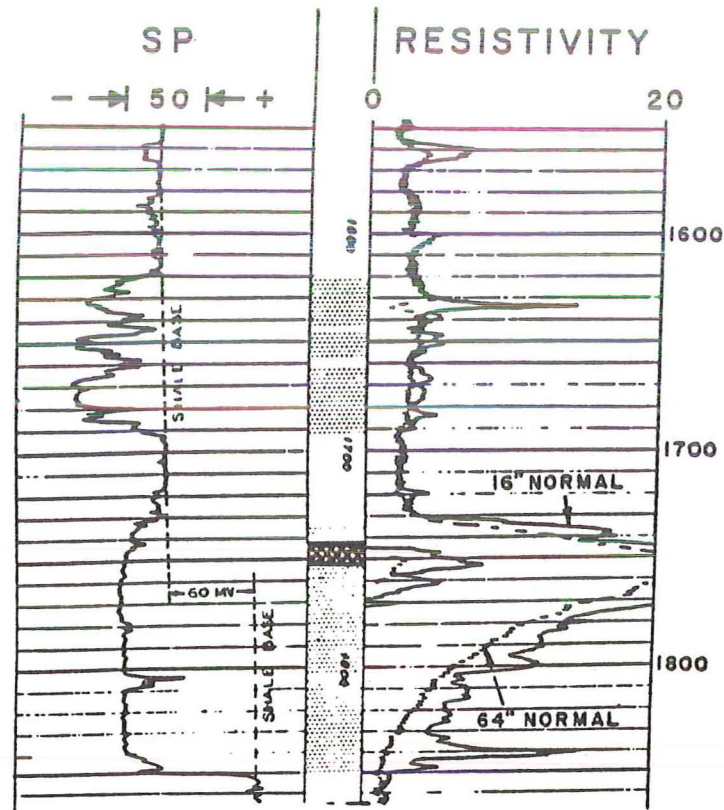


Fig. 12 - Portion of electric log showing shift of SP shale base line through a water sand containing fresh water at top and salt water at bottom (Oakdale, Louisiana).

even if the logging electrode is kept stationary. This condition is due to an unstable electrode potential caused by the water flow. The instability disappears below the zone of water movement.

4. Polarity reversals - Numerous polarity reversals in the aquifers of a given well are sometimes noted even though the waters have salinities of the same order. These reversals are usually due to changes in the type of ions or in the quantities of some of the ions. An example is found in the log to the right of Figure 8 above a depth of 1375 ft.

Estimating Porosity and Permeability. - Although the presence of permeable rocks having intergranular porosity, and situated between clay beds, can generally be inferred from the shape of the SP curve, Formulas (7) and (8) show that neither the curve shape nor the amplitude provides a basis for direct calculations of porosity or permeability.

When the changes in the permeability of a rock are caused by the presence of some clay material within the pore space, they can be quantitatively estimated from the resulting changes in SP amplitude by using empirical data. Obviously the method is applicable only if there are no changes in water composition within the formation of interest.

It has been proposed to estimate permeability from streaming potential measurements made under several well-head pressures in wells where the face of the

object formation is free of mud cake (Gillingham, 1937), for example intake wells in water-flooding operations. The consensus now is that the results simply indicate whether a formation is permeable or impervious.

Effect of Porosity. - Although the electrochemical potential, (SP)_c, is not influenced by porosity, the amplitude of the SP curve is indirectly affected by porosity changes. In fact, a decrease in porosity increases the rock resistivity, and this in turn reduces the SP amplitude as was previously pointed out. In particular, dense beds situated in clay exhibit no measurable SP deflections.

Principal Uses of SP curve in Water Wells. - The SP curve is at its best in formations comprising clay and granular aquifers, especially below a few hundred feet. For interpretation purposes the SP is always analyzed simultaneously with the resistivity curve and all other available data.

Where formation waters are much more saline than the drilling mud, the SP is generally more negative in aquifers than in the adjacent clays; this permits using the curve for formation identification, correlation purposes, and for determining the depth and thickness of certain beds.

Supplemented by a resistivity curve, the SP indicates where the formation water changes from fresh to brackish.

The SP is generally meaningless when there are no clay formations in the sequence of beds penetrated by the well of interest.

Empty Holes. - A repeatable SP curve can be obtained in uncased empty holes provided the measuring electrode is nonmetallic and makes a rolling contact against the bore wall. The SP shape is generally different from that which would be obtained if the hole contained water or mud. An example is given in Figure 9.

Cased Holes. - An SP curve recorded in a steel casing is related primarily to the corrosion at the time the measurements are made. In theory the data can be used to obtain information on the condition of the casing but their interpretation is difficult and usually problematical.

The SP curve in a plastic casing is practically a straight vertical line.

GAMMA RAY LOG

The only borehole geophysical methods giving dependable data on the formations situated behind casing are those based on radiation measurements. They can be used also in open holes, with the added advantage that the measurements are not much affected by the nature of the borehole fluid.

There are two basic radiation logging methods: gamma ray and neutron. Gamma ray logging equipment is fairly simple, not too expensive, and valuable in ground-water investigations. Neutron logging equipment will not be discussed here.

Radioactivity of Clay and Rocks. - The atoms of a few naturally occurring elements spontaneously disintegrate. This disintegration is slow but continuous, and it is accompanied by the production of radiation: alpha rays, beta rays and gamma rays. Alpha rays and beta rays are stopped after traveling less than one inch through matter, but gamma rays can go through two feet of water, more than six inches of common formations, or stopped. All geologic formations contain some radioactive isotopes of the following elements - - generally potassium, thorium, and/or uranium - - in varying amounts; this property makes gamma ray measurements valuable for formation logging.

It is convenient in gamma ray logging to classify sedimentary formations into two groups only: clay, and rock. The latter will be called "rock". Although there is no hard and fast rule regarding the amount of radioactivity that a given formation may have, rocks as a whole are less radioactive than clay, regardless of porosity and fluids contained, but a few rocks have a radioactivity which is sometimes of the same order as that of clay or clayey aquifers.

The gamma ray intensity of clay also varies from area to area. In the Tertiary deposits and more recent formations, such as those found in the Gulf Coast and in California, it is of the order of 5 microroentgens per hour; it is about twice as great for older clays. Some organic marine clays have a much higher intensity than the other clays of the same area; they are relatively thin and not too frequently found in water wells. When present, they make excellent geologic markers on the gamma ray log.

The rocks that have a very low radioactivity when they are free of clay material comprise the quartziferous sands and sandstones, limestone, dolomite, anhydrite, gypsum, salt, most lignites and most coals. Those having a higher radioactivity, although generally less than that of clay, include the arkose and feldspathic sands and sandstones, as well as a few volcanic and igneous rocks.

Potash and rocks containing radioactive ores have activities several times greater than clay.

A short but interesting discussion of the gamma ray activity of common sediments has been given by Patten and Bennett (1963).

Examples of Gamma Ray Curve. - Gamma ray curves are shown to the right of Figures 5, 6 and 7. In these examples only the clay is assumed to be radioactive.

Interpretation of Gamma Ray Curve. - The interpretation of a gamma ray curve in water wells is based on the following observations.

1. In a given area, only the relative intensity measured for the various formations is of significance.
2. Formations exhibiting a low gamma ray intensity are clean sands, gravels, sandstones, limestones, dolomite, anhydrite, sale, lignite or coal. A low

gamma ray reading may indicate a very porous and permeable aquifer or it may indicate an impervious rock. Geological information is needed to remove the ambiguity.

3. If it is known that the rocks in the area of interest have only a very low radioactivity, all the intervals of the log exhibiting a high gamma ray intensity are probably clay. The intervals of intermediate intensity correspond to rocks -- generally aquifers -- containing some clay material; the clay content can be assumed to increase nearly in proportion with the gamma ray intensity.
4. If nothing is known on the radioactivity of the rocks of the area, it is not possible to interpret the intervals of the log that exhibit a high or intermediate gamma ray intensity. Some of the resulting ambiguity can be removed if an electric log or local experience is available.
5. The gamma ray curve should always be correlated with a lithologic log and all other data available.

A few exceptions to above rules of thumb are noted below.

Interpretation Difficulties. -- When water, instead of a properly conditioned mud, is used for drilling, clay and other cuttings settle and may increase the gamma ray amplitude in the bottom five to ten feet of the hole.

Thick drilling mud may have been left behind the casing, or there may be some clay material on the face of certain non-radioactive rocks. The increase in gamma ray intensity at these levels make them appear on the log as sandy clays or clayey sands.

In gravel packed wells the gravel stops an important amount of the gamma rays that would normally reach the detector, thus reducing the gamma ray amplitude.

If the material selected for gravel packing is radioactive, for example if certain volcanic or granitic rocks are used, the gamma ray log deflection show primarily the presence and thickness of this material.

All the potential difficulties listed above illustrate the importance of securing as much information as possible on the well condition and on the formation traversed.

Because radioactive disintegration is statistical in nature (Russell, 1941), special circuits must be used in gamma ray logging to smooth out the signals received. This, in turn, introduces some distortion in the shape and amplitude of the gamma ray curve (Kokesh, 1951). These effects are not important if proper precautions are taken when the measurements are made; they are omitted in the logs of Figures 5, 6 and 7.

Principal Uses of Gamma Ray Curve.

1. The main application of the gamma ray curve is in cased wells for which only insufficient or unreliable data are available. Water wells that do

not produce enough water, or that produce a water that is unfit for its intended use, generally can be rehabilitated after the presence of other aquifers is determined from the gamma ray measurements.

2. The gamma ray curve is also useful for the logging of open holes when an electric log would not be up to standards (brackish or salty borehole fluid, large hole size) or could not be run because of lack of an appropriate probe (empty holes).
3. The depths and thicknesses clay and non-clay beds can be obtained from the gamma ray curve, but the accuracy in measuring the thicknesses of those less than two feet thick is generally poor.
4. The gamma ray data are valuable as a supplement to the electric log, in particular to help identify clay layers and porous zones in dense rocks.
5. The gamma ray data sometimes permit estimating the permeability reduction in a rock due to the presence of clay in the pore space.

MISCELLANEOUS FACTORS AFFECTING THE LOG RESPONSES

Resistivity and gamma ray measurements are averages taken over a certain volume of material about the probe. Changes within this volume are reflected in the shape and amplitude of the curves. The SP curve is affected in a somewhat similar manner. The resulting effects are reviewed below.

Borehole Effects. -- Inasmuch as the logging probe is placed in the mud column, borehole fluid and hole size usually affect the measurements.

An increase in the mud conductivity decreases the apparent resistivities recorded in fresh water aquifers and in dense formations. It also changes the SP, generally making it less negative (or more positive) in all aquifers. The gamma ray curve is not affected.

An increase in hole size decreases the apparent resistivity of fresh water aquifers and of dense formations. It also decreases the changes in the SP amplitude. It has little effect on the gamma ray curve and can be ignored in water well work.

The borehole effects are not important -- especially in soft formations -- when the hole diameter is less than 8 inches and the mud resistivity greater than about one ohm-m.

Bed Boundary Effect. -- A sharp formation change, for example from a clay to a fresh water aquifer, does not result in sharp changes in the curves of a log; the curves are rounded and, for the electric log, the rounding is particularly important when the hole is large or the mud brackish.

Thin Bed Effect. -- The curve amplitudes are reduced when the thickness of the bed of interest decreases, all other factors being constant. This is illustrated in

Figure 13 which represents single-electrode resistivity curves for a number of thin beds. The effect on the SP and gamma ray curves is very similar.

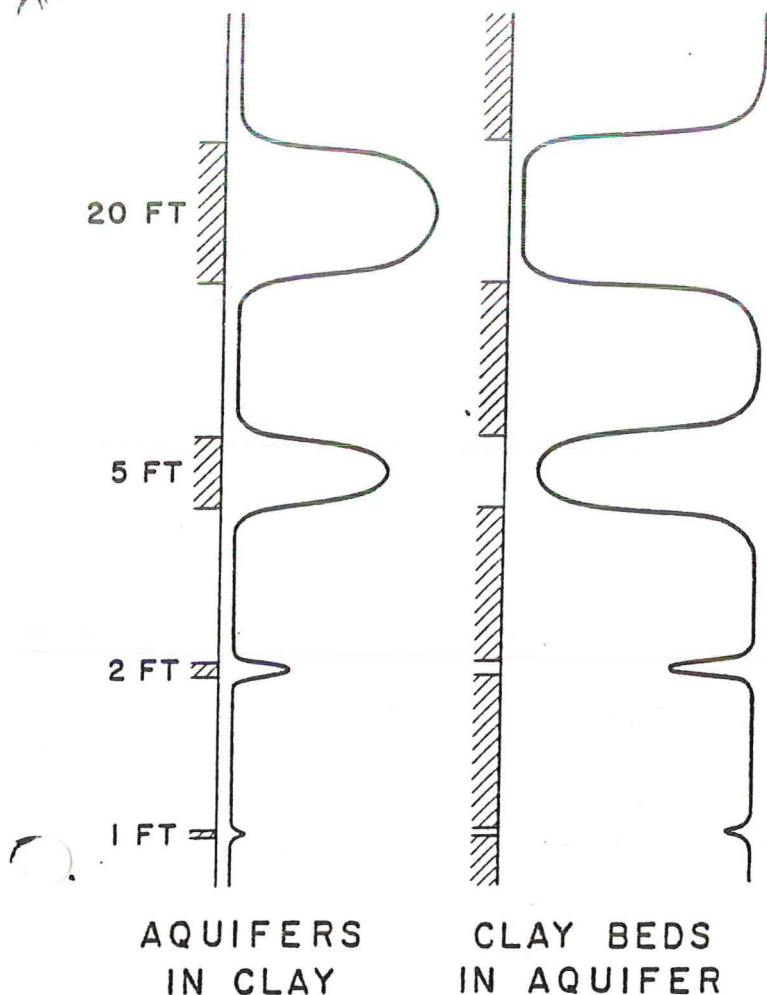


Fig. 13 - Artificial single - electrode resistivity curves for formations containing thin beds. Aquifer waters have low salinities.

APPLICABILITY OF GEOPHYSICAL LOGS TO SPECIFIC PROBLEMS

Electric and gamma ray logs solve or help solve some of the most important problems found in ground-water investigations. A few of these problems are listed below and the degree of applicability of these logs, as well as that of other types of physical or geophysical measurements, is briefly and broadly stated, without qualification. It is assumed that other data that are normally available in ground-water work are at hand and utilized: this is an essential requirement for a successful application and interpretation of the measurements. These data include bit penetration rate, formation cuttings and/or local geology.

No method, or group of methods, can solve a given problem in every case; there is a matter of degree, and there are unusual conditions. The statements made below should therefore be understood as applicable to the most common situations.

Unless specified otherwise, it will be assumed that the measurements are made in uncased holes.

Occurrence of Water. - The presence of aquifers can be inferred from electric log data, sometimes supplemented by the gamma ray curve. The depths and thicknesses of these beds can also be determined from the logs.

In cased holes, the gamma ray log delineates primarily the intervals containing clay. Which of the other intervals contain aquifers has to be determined from other data.

The best logging tool for cased holes is a radiometric log comprising neutron and gamma ray curves (Charrin & Russell, 1952).

Quality of Water. - The resistivity curve, preferably supplemented by the SP, shows where the water salinity appreciably increases.

Quantitative salinity determinations are possible only when aquifer resistivity, aquifer porosity, and type of water likely to be present are known.

No information can be obtained from geophysical logs on the following topics: sulphur water, any particular ions, bacteria, algae.

Quantity of Water, Porosity. - The quantity of water in an aquifer is proportional to net thickness and porosity.

The thickness of a granular aquifer can be accurately determined from the electric log. The log gives also the approximate thickness of thin impervious layers within the aquifer.

The thickness of a granular aquifer and of clay streaks can also be determined from the gamma ray curve when there are no dense rocks; however, the accuracy is not as good as that obtained from the electric log.

The effective thickness of non-granular aquifers cannot be evaluated from logs. The approximate thickness of a fractured interval can be estimated from the resistivity curve, from acoustic attenuation measurements (Walker, 1962), and sometimes from a caliper log (Jones, 1961).

Porosity can be obtained from several types of logs. Electric log, Microlog (Doll, 1950), and Microlaterolog (Doll, 1953) give effective porosity in granular rocks. Neutron (Bush & Mardock, 1951), gamma-gamma (Pickell & Heacock, 1960), and acoustic velocity (Berry, 1959) give total porosity. However, the latter log does not see vugs unless they are several inches in size.

Yield, Permeability. - No data on the possible yield of an aquifer can be directly obtained from geophysical logs described here. However, Flowmeter and Tracer techniques while pumping or injecting can locate sources of water and give approximate amounts.

There are no logging tools giving permeability data directly. In particular it is not possible to distinguish a fine sand from a coarse gravel with an electric log alone. When permeability is related to porosity and almost only to porosity, it can be estimated from an appropriate log supplemented by empirical data. If the

permeability is determined by the clay content in the aquifer, it can be estimated from resistivity, SP, or gamma ray, supplemented by empirical data.

Thin impervious layers that could reduce the vertical permeability of an aquifer can be delineated from electric logs and, if they are clay, from gamma ray.

Bed Identification. - There is no geophysical log that gives the mineralogical composition of a formation, although the presence of some of the elements can be detected by using a rather involved radiation spectral method (Hoyer, 1961). In known areas the nature of most beds can be inferred from the electric log and, sometimes, from the gamma ray log.

Screen Setting Program. - The electric and gamma logs give the depth and thickness of most fresh water granular aquifers; thus they permit placing screens exactly opposite these aquifers, and blank casing sections opposite the undesirable intervals.

Water Table. - If there are no wide porosity changes in the interval of interest, a resistivity measurement having sufficient lateral penetration will generally show the water table. Single-electrode and Normal devices generally do not give dependable information.

Movement of Water. - A fluid velocity meter has been developed by the U. S. Geological Survey for observing the movement of water in cased holes when the water is clean. Quantitative data can also be obtained with this tool for a certain range of velocity. This instrument, as well as other borehole flow measurement devices, is reviewed in a paper by Patten and Bennett (1962).

Probes measuring the conductivity or the temperature of the bore fluid are also used for studying the movement of water (Jones, 1961).

Correlation, Mapping, - Practically all geophysical logs can be used for correlation and subsurface mapping purposes. However the SP is not dependable at shallow depths because of the unpredictable polarity reversals that may occur.

Casing Condition and Casing Depth. - An electric log made in a steel casing exhibits large changes in resistivity and potential which are primarily related to corrosion. Holes can sometimes be detected from the record, but the interpretation of the log is difficult and problematical.

The depth of a steel casing that is not too badly corroded can be determined from the resistivity curve. The SP generally can be used regardless of the casing condition.

Location of Junk Lost in Hole. - The presence and depth of lost casing sections and large size steel junk can be found frequently from the electric log provided that they have not been shoved away from the hole (Addick, 1950; Johnson, 1963).

BRIEF QUALITATIVE INTERPRETATION GUIDE

The following procedure outlines briefly a sequence

of steps that is suggested for locating aquifers and, sometimes, noting large changes in water salinity. It is based on the simultaneous use of an electric log, the bit penetration rate and, if possible, the gamma ray log (WIDCO, 1963). Needless to say, all other available data should also be used in order to confirm or refine the log interpretation.

Procedure in Open Holes.

1. Determine which of the three following situations is anticipated:
 - A. Granular aquifers in clay formation, no dense rocks.
 - B. Any combination of rocks and clay.
 - C. Any combination of rocks, but no clay.

Figures 5, 6 and 7 correspond to these three situations, respectively. Only fresh water aquifers are shown in Figures 6 and 7; brackish and salt water bearing formations would exhibit lower resistivities and, in Figure 6, the aquifer SP's would be more negative than shown.

2. If it is known that formation waters are fresh, the problem reduces to finding permeable rocks. For situation A these rocks are represented by the high resistivity intervals. For situation B the aquifers are found by selecting the medium high resistivity intervals for which the bit penetration is medium to fast. For situation C the aquifers are the intervals of relatively low resistivity; they should correspond to medium to fast penetration rates.

If it is known that there is some brackish water in the interval of interest, or that there is a possibility that such water may be present, the problem of finding the aquifers is handled exactly as in the preceding paragraph, but the qualitative estimation of the water salinity requires a careful study of resistivity and SP. When in doubt, and to remain on the safe side, the following recommendation is made: if, below a certain depth, the resistivity of the aquifers decreases appreciably and the SP simultaneously becomes decidedly more negative, the corresponding zone should be considered as containing water of inferior quality.

3. Once the acceptable aquifers are found, determine their depths and thicknesses from Figure 5 for situation (A), or estimate them from Figures 6 and 7 for situations (B) and (C), respectively.

Note the apparent paradox that, for situation A, the aquifers are represented by the high resistivity intervals while, for situation C, they correspond to the intervals of relatively low resistivity.

Procedure in Cased Wells. - The problem is considerably more difficult because the electric log cannot be used. Generally the only sources of information are the gamma ray log, local experience, and local geology. The gamma ray log is interpreted as follows:

Situation A - All the intervals exhibiting a very low gamma ray intensity are aquifers. The intervals exhibit-

ing some intermediate gamma ray intensity may be clayey, arkose, or feldspar aquifers.

Situation B - The aquifers are among the intervals of lowest gamma ray intensity, but it is not possible from the log alone to determine which intervals are permeable.

Situation C - If the gamma ray is essentially flat with low intensities, it is valueless. If there are changes in amplitude, the higher intensities probably indicate arkose aquifers, feldspar aquifers, or other radioactive rocks; geology is needed to determine which formation intervals may be aquifers.

In no case is it possible to derive any information on the quality of the water from the gamma ray data.

Miscellaneous Remarks Applicable to Open Holes. - The procedure outlined above should permit the handling of most conditions. But every once in a while one will not conform, and the following comments may prove useful.

If the measured resistivity and/or SP of a given aquifer remains essentially the same between two neighboring wells, the aquifer characteristics do not change appreciable between the wells.

A decrease in resistivity in an aquifer, with a decrease in SP amplitude (compared to the clay SP), may indicate an increase in clay content.

A decrease in resistivity in an aquifer, accompanied by an increase in negative SP, may indicate an increase in water salinity.

Occasionally the SP curve for situation A or B will be essentially flat. It can be given more character by adding about one pound of salt per barrel of mud and circulating a few times to homogenize the fluid. The SP measured in the salty mud generally develops positive deflections in the aquifers, and the aquifer resistivities are reduced.

Out of the three geophysical measurements reviewed in this article, resistivity generally is the most dependable if the mud is fresh. If the information given by the three curves is conflicting, more weight should preferably be given resistivity than the others, and more weight should be given the gamma ray than the SP. But if the mud is brackish or salty and the depth of investigation of the resistivity device is small (single-electrode probe, for example), the gamma ray curve may be more reliable than the resistivity.

CONCLUSIONS

Geophysical logs, in particular the electric-gamma ray combination, provide valuable data that lead to the discovery of ground-water supplies and help in their development. These logs cannot be interpreted with confidence without information provided by the driller's log, local geology or local experience. The benefits derived increase with the amount of supplemental data available.

For most investigations small, simple logging units

are satisfactory; they provide considerable qualitative data rapidly and at a reasonable cost. More sophisticated equipment gives logs that frequently permit quantitative or semiquantitative salinity and porosity evaluations, but because the cost in money, time and effort is relatively high, this type of equipment is not often used by the average water well contractor.

ACKNOWLEDGMENT

I wish to express my appreciation to Paul H. Jones, U. S. Geological Survey, who reviewed the manuscript and made many valuable comments.

LITERATURE CITED

- Anonymous, Introduction to Schlumberger well logging. Schlumberger Well Surveying Corp., Doc. No. 8, 1958a.
- Anonymous, Radioactivity well logging, Lane-Wells Co., 1958b.
- Archie, G. E., The electrical resistivity log as an aid in determining some reservoir characteristics. *Jour. Pet. Tech.*, Vol. 5, 1942.
- Bays, C. A., Practical geophysical techniques for the water well driller. *Water Well Jour.*, Vol. 3, No. 3, 1949.
- Berry, J. E., Acoustic velocity in porous media. *Trans. AIME*, Vol. 216, 1959.
- Bush, R. E. and Mardock, E. S., The quantitative application of radioactive logs. *Pet. Trans. AIME*, Vol. 192, 1951.
- Charrin, P. and Russell, J. H., Radiation logging and its application in the oil fields. *Internat. Geol. Cong.*, 1952.
- de Witte, L., A study of electric log interpretation methods in shaly formations. *Pet. Trans. AIME*, Vol. 204, 1955.
- Doll, H. G., The S. P. log: theoretical analysis and principles of interpretation. *Jour. Pet. Tech.*, Vol. 11, 1948.
- Doll, H. G., Introduction to induction logging and application to logging of wells drilled with oil base mud. *Jour. Pet. Tech.*, Vol. 1, No. 6, 1949.
- Doll, H. G., The Microlog - a new electrical logging method for detailed determination of permeable beds. *Trans. AIME*, Vol. 189, 1950.
- Doll, H. G., The Microlaterolog. *Trans. AIME*, Vol. 198, 1953.
- Gillingham, W. J., Electrical logging in the Appalachian fields. *Min. Ind. Exper. Sta. Bull.* 21, State College, Pa., 1937.
- Gondouin, M., Tixier, M. P. and Simard, G. L., An experimental study on the influence of the chemical composition of electrolytes on the SP curve. *Jour. Pet. Tech.*, Vol. 9, No. 2, 1957.
- Gondouin, M. and Scala, C., Streaming potential and the SP log. *Jour. Pet. Tech.*, Vol. 213, 1958.
- Guyod, H., Electrical well logging. *Oil Weekly*, Vol. 114. Nos. 12 and 13; Vol. 15, Nos. 1-3 and 5-7 1944.
- Guyod, H., An investigation of the factors affecting the SP in soft formations. *Trans. Soc. Prof. Well Log Anal.*, 5th Annual Logging Symp., 1964a.

- Guyod, H., Factors affecting the responses of laterolog-type logging systems (LL3 and LL7). *Jour. Pet. Tech.*, Vol. 16, No. 2, 1964b.
- Guyod, H. and Pranglin, J. A., Now - get true resistivities from conventional electric logs. *Oil and Gas Jour.*, Vol. 59, No. 24, 1961.
- Hoyer, W. A., Induced nuclear reaction logging. *Jour. Pet. Tech.*, Vol. 13, No. 8, 1961.
- Johnson, H. M., Logging anomalies associated with metallic fish in drill-holes. *World Oil*, Vol. 157, No. 4, 1963.
- Jones, P. & Buford, T. B., Electric logging applied to ground-water exploration. *Geophysics*, Vol. 16, No. 1, 1951.
- Jones, P. H., Hydrology of water disposal, National reactor testing station, Idaho an interim report. Idaho Oper. Off., USAEC report, prep, in co-op with USGS, 1961.
- Jones, P. H., Personal communication. 1965.
- Kokesh, F. P., Gamma-ray logging. *Oil & Gas Jour.*, Vol. 50, No. 12, 1951.
- Owen, J. E. and Greer, W. J., The Guard electrode logging system. *Jour. Pet. Tech.*, Vol. 192, 1951.
- Patten, E. P. and Bennett, G. D., Methods of flow measurements in well bores. USGS Water-Supply Paper 1544-C, 1962.
- Patten, E. P. and Bennett, G. D., Application of electrical and radioactive well logging to ground-water hydrology. USGS Water-Supply Paper 1544-D, 1963.
- Pickell, J. J. and Heacock, J. G., Density logging, *Geophysics*, Vol. 25, No. 4, 1960.
- son, S. J., Formation evaluation by log interpretation. *World Oil*, Vol. 144, Nos. 4, 5 and 6, 1957.
- Rose, N. A., White, W. N. and Livingston, P., Exploratory water-well drilling in the Houston district, Texas. USGS Water-Supply Paper 889-D, 1944.
- Ruddick, C. H., Location of lost pipe through use of electrical logging. *Drilling*, Vol. 11, 1950.
- Schreurs, R. L., Personal Communication, 1964.
- Walker, T., Fracture zones vary acoustic signal amplitudes. *World Oil*, Vol. 154, No. 6, 1962.
- WIDCO, Water finder guide. Mandrel Industries, Houston Texas., 1963.
- Winsauer, W. O. and McCardell, W. M., Ionic double-layer conductivity in reservoir rock. *Pet. Trans., AIME*, Vol. 198, 1953.
- Worthington, A. E. and Meldau, R. F., Departure curves for the self-potential log. *Jour. Pet. Tech.*, Vol. 213, 1958.
- Wyllie, M. R. J., A quantitative analysis of the electrochemical component of the S. P. curve. *Jour. Pet. Tech.*, Vol. 1, 1949.
- Jour., Vol. 11, Nos. 3 & 5, 1957.
- Johnson, A. I., Geophysical logging of boreholes for hydrologic studies. WRD Bull., USGS, 1963.
- Johnson, A. I., Selected bibliography on Laboratory and field methods in ground-water hydrology. USGS Water-Supply Paper 1799-Z, 1964.
- Jones, P. H. and Skibitzke, H. E., Subsurface geophysical methods in ground-water hydrology. *Advances in Geophysics*, Vol. 3, Academic Press, New York, 1956.
- Rosoff, C., Application des procédés Schlumberger d'étude géophysique des sondages aux problèmes hydrologiques et miniers. *Revue de l'Industrie Minérale*, Vol. 35, No. 610. 1954.
- Russell, W. L., Well logging by radioactivity. *AAPG Bull.* Vol. 25, No. 9, 1941.
- Todd, D. K., Investigating ground water by applied geophysics. *Amer. Soc. Civ. Engr.*, Vol. 81, No. 624, 1955.
- Turcan, A. N., Estimating water quality from electrical logs. USGS Prof. Paper No. 450-C, 1962.

BIBLIOGRAPHY

- Barnes, B. A. and Livingston, P., Value of the electrical log for estimating ground-water supplies and the quality of the ground water. *AGU Trans.*, Vol. 28, No. 6, 1947.
- Bryan, F. L., Application of electric logging to water well problems. *Water Well Jour.*, Vol. 4, No. 1, 1950.
- Guyod, H., Electric detective-Investigation of ground-water supplies with electric well logs. *Water Well*

INTERPRETATION OF COAL LOGS

There are several logs which are useful in coal logging, even as there are in logging for uranium and oil. Century's normal coal log is made with the 8030 probe and consists of a gamma ray curve, a single point resistivity curve, and an omnidirectional density curve.

The 8090 probe is being introduced at this time. It will log a natural gamma ray curve, a single point resistivity curve, a sidewall density curve, and a hole caliper curve.

The neutron-neutron porosity tool, the 8050 makes an excellent auxiliary log for use in coal exploration.

There are several characteristics of coal which may be used to detect it with these "coal" measurements. Coal very often has a very low radioactivity. This is particularly true of western coals. Counting rates of 2 to 3 counts per second are not unusual in bituminous coal with an 8030 probe. Occasionally in Montana one will even see a foot or two with no apparent counting rate. In general, lignites tend to have slightly higher counting rates than bituminous coal.

Coal usually has a very high resistivity. Bituminous and subbituminous coals typically have resistivities of 1000 ohmmeters to 10,000 ohmmeters. Occasionally a highly fractured coal or a very low grade (clayey) one will have lower resistivities. Many lignitic coals have low resistivities because of their clay and water content. In general, however, the electrical resistivity of coals is up in the same range as tight limestones. Table 1 lists a few of the resistivities of coals and some other common materials.

Coal has strikingly low densities. It is always lower, by far, than any of the surrounding formations. Table 2 lists some coal densities and densities of other common formation materials. Notice that coal densities range from 1.16 to 1.64 grams per cubic centimeter. Densities of shales, clays, porous sandstones, and porous limestones are usually all 2.0 grams per cubic centimeter or higher. The density contrast of coals is good.

Coals have low neutron capture cross sections. They are typically on the order of one fourth that of surrounding materials. One must be careful here, however, because coals contain some water. Water has very high cross sections, especially if it is very saline. Capture cross sections are listed in Table 2.

Finally, coal beds typically have a layer of soft, easily erodeable clay above them. This often forms a characteristic cave or washout in the borehole which is detectable with the hole caliper curve. This will also show up on the density curve as a low density zone which may be confused with the coal itself.

The general use of coal logs for exploration and production follows much the same pattern as the use of uranium logs. The initial phase is usually

TABLE 1

<u>FORMATION/MINERAL</u>	<u>RESISTIVITY IN OHMS M²/M</u> <u>(AT STP UNLESS OTHERWISE STATED)</u>
Bituminous Coal	10-10 ⁶
"Sub-bituminous Coal"	10 ² -10 ⁴
Limestone ("Dense")	80 - 6 x 10 ³
Sand	up to 1,000
Siltstone	up to 300
Peat	10 - 300
Shale	up to 15
Anthracite Coal	10 ⁻³ -5 (Most below 1 ohm m ² /m)

TABLE 2

<u>MATERIAL</u>	<u>Z/A</u> <u>RATIO</u>	<u>MATRIX DENSITY</u> <u>G/CC</u>	<u>APPARENT*</u> <u>DENSITY G/CC</u>	<u>** MATERIAL</u> <u>(CAPTURE UNITS)</u>
Limestone (Av. of 345 Samples)	.5000	2.69 (2.66-2.74)	2.69	8.72
Sandstone (Av. of 12 Samples)	.4990	2.655 (2.59-2.84)	2.655	8.66
Montmorillonite (OH) ₄ Si ₈ Al ₄ O ₂₀ ·nH ₂ O (n=1)	.5009	2.35 (2.00-3.00)	2.35	8.10
Anthracite Coal .9350(C) .0281(H) .0097(N) .0272(O)	.5134	1.60 (1.32-1.80)	1.64	1.08
Bituminous Coal .8424(C) .0555(H) .0152(N) .0869(O)	.5201	1.35 (1.15-1.7)	1.40	1.54
Lignite		1.10 (.5-1.5)	1.16	
Water (300,000 ppm NaCl)	.5325	1.219	1.298	146.22
(250,000 ppm NaCl)	.5363	1.1825	1.268	122.55
(200,000 ppm NaCl)	.5401	1.146	1.238	100.08
(150,000 ppm NaCl)	.5438	1.109	1.206	78.75
(100,000 ppm NaCl)	.5476	1.073	1.175	58.69
(50,000 ppm NaCl)	.5513	1.0365	1.143	39.02
(30,000 ppm NaCl)	.5528	1.022	1.130	32.56
(Pure Water)	.5551	1.00	1.11	22.08
NaCl solution density at STP $\cong 1 + (.00000073 \times \text{ppm})$				

* Based on tool calibration using a Z/A ratio of 0.5.

** Capture Units in 10²¹Barns/cm³

a wide spaced drilling of an area. The resulting logs are "hung on elevations" (i.e. they are pinned on the wall so that they are at a constant elevation with respect to sea level) and correlated over lines and areas which may cover miles. The purpose is to determine geological sequences, ages, favorable areas, dip trends, and general favorability of the location.

The second phase is to explore on closer spacings than in the previous phase. In this phase coal deposits are specifically looked for and deposit areas are estimated from log correlations. Sample assays are usually made to determine coal grade.

During this second phase use can be made of estimates from the logs. Of course, bed thickness and areal extent are commonly determined from the logs. One examines the logs for indications of low gamma ray counting rates, high resistivities, and very low densities. Care must be exercised that the bed thickness is not estimated too thick. It is easy to include the washed out clay above the coal in the thickness determination. Examine the caliper and resistivity curves carefully.

The ash content of the coal can be estimated during the second phase by plotting a chart of gamma ray counting rate versus clay content. This is illustrated in Figure 1. Pick a good, solid shale or clay with the resistance curve. Assume this is 100% clay and note the counting rate. Place a point on the chart at these intercepts. Assume the coal has little or no radioactivity. This defines the zero clay (or ash) point as zero counting rate. Therefore, this point is at the origin. Connect the two points with a straight line. Gamma ray counting rates from coal zones can then be used to estimate the ash content.

If the density log has been calibrated, the density reading can be used to determine the quality or heat content of the coal. The higher the density of the coal is (at low ash content) the higher will be the heat content. At this point, the heat content and ash content are only rough estimates. However, they help evaluate a prospect.

If the neutron log is available, it can be used to estimate the moisture content of the coal. Bituminous coal has a hydrogen content typically about 60% that of water and about 200% that of clays and shales. Anthracite coal hydrogen content is about 30% that of water. Table 3 lists some of these contents. Any indication on the neutron log above these values can be taken as contained moisture.

At this point the geologist has a good estimate of the viability of the prospect.

In phase 3 the coal zone is drilled on closer spacings to determine the total amount in reserve. At each hole an area of influence is assigned. This will be a radius of a circle or a diagonal of a square and typically is 50 feet or half the distance to the next hole. The area is multiplied by the thickness to obtain volume. The volume is multiplied by 0.044 to obtain tons of coal.

In phase 3 cores and cuttings samples will be analyzed in the laboratory for

heat content, moisture content, and ash content. The averages of these assay values can be used to correct the charts and determinations made in phase 2. These corrected determinations can then be extended and used in phase 3. Any regional variations should be noted and taken into consideration.

In phase 3 the stripping ratios will be plotted as a contour map. They will have been noted roughly in phase 2. The stripping ratio is the ratio of the thickness of the overburden to the thickness of the bed. Stripping ratios of 10 to 1 or less are usually considered reasonable for western coals.

Phase 4 is the mine planning stage. It involves laying out plans and cross sections of projected mines on the basis of the logs. The amount of overburden to be removed or the depths of the shafts is determined from the logs and evaluated. The locations of offices and facilities, such as loading areas, washers, screeners, etc. are picked on the basis of the maps made from the logs.

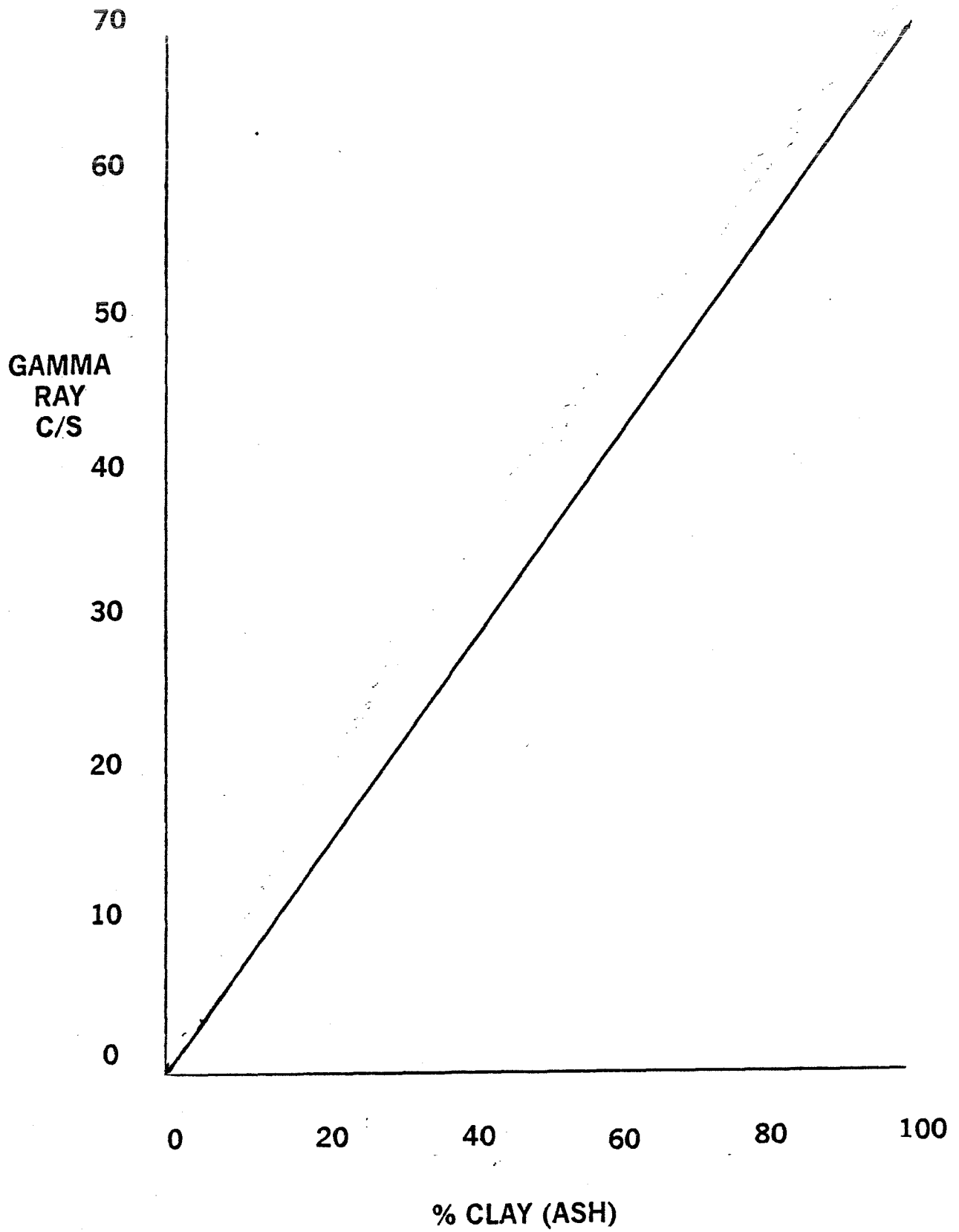


Figure 1

HYDROGEN CONTENT OF SOME GEOLOGIC MATERIALS

Substance	Hydrogen Atoms x 10 ²³ per cc	Hydrogen Index* (See Next Page)
Pure water		
60°F, 14.7 psi	.669	1
200°F, 7,000 psi	.667	1
Salt water, 200,000 ppm NaCl		
60°F, 14.7 psi	.614	.92
200°F, 7,000 psi	.602	.90
Methane CH ₄		
60°F, 14.7 psi	.0010	.0015
141°F, 3,800 psi	.275	.41
200°F, 7,000 psi	.329	.49
Ethane C ₂ H ₆		
60°F, 14.7 psi	.0015	.0023
200°F, 7,000 psi	.493	.74
Average natural gas		
60°F, 14.7 psi	.0011	.0017
200°F, 7,000 psi	.363	.54
N-pentane C ₅ H ₁₂		
68°F, 14.7 psi	.627	.94
200°F, 7,000 psi	.604	.90
N-hexane C ₆ H ₁₄		
68°F, 14.7 psi	.645	.96
200°F, 7,000 psi	.615	.92
N-heptane C ₇ H ₁₆		
68°F, 14.7 psi	.658	.99
200°F, 7,000 psi	.632	.95
N-octane C ₈ H ₁₈		
68°F, 14.7 psi	.667	1.00
200°F, 7,000 psi	.639	.96
N-nonane C ₉ H ₂₀		
68°F, 14.7 psi	.675	1.01
200°F, 7,000 psi	.645	.97
N-decane C ₁₀ H ₂₂		
68°F, 14.7 psi	.680	1.02
200°F, 7,000 psi	.653	.98
N-undecane C ₁₁ H ₂₄		
68°F, 14.7 psi	.684	1.02
200°F, 7,000 psi	.662	.99
Bituminous coal .8424 (C) .0555 (H)	.442	.66
Carnallite	.419	.63
Limonite	.369	.55
Cement	about .334	about .50
Kernite	.337	.50
Gypsum** (See Next Page)	.325	.49
Kainite	.309	.46
Trona	.284	.42
Potash	.282	.42
Anthracite coal	.268	.40
Kaolinite	.250	.37
Chlorite	.213	.32
Kieserite	.210	.31
Serpentine	.192	.29
Nahcolite	.158	.24
Glauconite	.127	.19
Montmorillonite	.115	.17
Polyhalite	.111	.17

MULTIPLE CURVE INTERPRETATIONS

In log interpretation, one curve is seldom used by itself. There is too much danger of misinterpreting an anomaly if it is not indicated by more than one curve. Too, at our present state of the art, one curve seldom contains enough unambiguous information to permit a good interpretation. Some times we have no choice, as with the gamma ray calculation for uranium content. However, it is to be avoided whenever possible.

In most types of logging (subsurface geophysical measurements) we must arrive at the parameters we seek indirectly. The measurements we make seldom measure the desired parameter. We are not really interested in resistivity or the amount of bismuth 214 or the ion concentration. We are interested in the location and amounts of uranium or coal or oil or gas. Since each of these available determinations is made by indirect methods, it is subject to variances which can be quite wide. Therefore, confirmation by several methods is desirable.

We have already described the use of the resistance, S.P., and gamma ray curves for correlation and reserve calculation for uranium. We have covered the use of density, resistivity, and caliper logs for coal and the S.P. and resistivity curves for petroleum. There is another class of techniques which is being applied in petroleum exploration and has much promise in mineral exploration. This is the cross-plotting technique. The principle is to measure the same parameter (or related parameters) by two or more completely different methods. Then, variances in one method will be detectable in another and in themselves, supply useful information.

The original cross-plots were made with the acoustical velocity log and the gamma-gamma density log. These measurements are both indirect porosity measurements. Two points of each measurement are well catalogued. These are the zero porosity point and the 100% porosity point for each type rock material. For example, we can measure in the laboratory (or use previously made measurements) that the matrix travel time in sandstone is 55.1 microseconds per foot. We can similarly determine that the apparent density is 2.655 grams per cubic centimeter (See tables 1 and 2). This, of course, is the point for 0% porosity. In a like manner we can determine the point for 100% porosity (100% water). Water with 100,000 ppm dissolved salt has a velocity of 192.3 microseconds per foot and a density of 1.130 grams per c.c. apparent. A line connecting these two points gives an excellent first approximation curve for interpretation. Of course, careful measurements or calculations for other porosities will give more exact curves. If this process is repeated for all of the rock types we will encounter, we discover that the curves do not fall on top of each other. Such a set is shown in Figure 1. The same technique can be applied to the curves Century commonly runs: the density-neutron cross-plot (Figures 2 and 3) and the porosity-resistivity cross-plot (Figure 4).

After several matrices are plotted on a cross-plot grid, one discovers that the curves of different materials do not coincide with one another. It is

possible then to correct porosity determinations of each type measurement. It is further possible to tell how much dolomitization has progressed in a limestone or how much cementation has taken place in a sandstone, or how much shale is in a sand. If points from logs are extrapolated back to zero porosity, it is possible to make further lithologic determinations. See Figure 5. The possibilities are only limited by ones imagination and the amount of time he can spend.

- CATALOG (STP)

Material	Matrix Travel Time - μ s/ft		Matrix Velocity - ft/sec	
	(Average Value)	(Range)	(Average Value)	(Range)
Dunite	38.2	(34.7-41.1)	26,174	(24,305-28,807)
Gabbro	42.4	(42.4-47.6)	23,586	(20,998-23,586)
Hematite		42.9	-	23,295
Dolomite	44.0	(40.0-45.0)	22,727	(22,222-25,000)
Norite	44.1	(43.5-49.0)	21,683	(20,400-22,967)
Diabase	44.6	(44.0-46.0)	22,435	(21,746-22,730)
Anorthosite		45.4		22,016
Calcite	46.5	(45.5-47.5)	21,505	(21,053-22,000)
Aluminum		48.7		20,539
Anhydrite		50.0		20,000
Albitite	50.2	(49.5-50.6)	19,916	(19,752-20,212)
Granite	50.8	(46.8-53.5)	19,685	(18,691-21,367)
Steel		50.8		19,686
Limestone	52.0	(47.7-53.0)	19,231	(18,750-21,000)
Langbeinite		52.0		19,231
Iron		52.1		19,199
Gypsum	53.0	(52.5-53.0)	19,047	(18,868-19,047)
Serpentine		53.9		18,702
Quartzite	55.0	(52.5-57.5)	18,182	(17,390-19,030)
Quartz	55.1	(54.7-55.5)	18,149	(18,000-18,275)
Sandstone	57.0	(53.8-100.0)	17,544	(10,000-19,500)
Casing* (steel)		57.1		17,500
Basalt		57.5		17,391
Polyhalite		57.5		17,391
Shale		60.0-170.0		5,882-16,667
Aluminum tube*		60.9		16,400
Trona		65.0		15,400
Heulandite		65.1		15,355
Halite		66.7		15,000
Stilbite		68.0		14,699
Sylvite		74.0		13,500
Copper		78.7		12,700
Carnallite		83.3		12,000
Cement (wide variation)	95.0	(83.3-95.1)	10,526	(10,526-12,000)
Anthracite coal	105.0	(90.0-120.0)	9,524	(8,333-11,111)
Concrete (wide variation)	95.2	(83.3-125.0)	10,500	(8,000-12,000)
Bituminous coal	120.0	(100.0-140.0)	8,333	(5,906-10,000)
Sulphur		122.0		8,200
Lignite	160.0	(140.0-180.0)	6,250	(3,281-7,143)
Lead		141.1		7,087
Water, 200,000 ppm NaCl, 15psi		180.5		5,540
150,000 ppm NaCl, 15psi		186.0		5,375
100,000 ppm NaCl, 15psi		192.3		5,200
Pure		207.0		4,380
Glacial Ice		87.1		11,480
Rubber (Neoprene)		190.5		5,248
Kerosene, 15psi		214.5		4,659
Oil		238.0		4,200
Methane, 15psi		626.0		1,600
Air, 15psi		919.0		1,088
Ethane (10°C) .00125 gm/cc		989.6		1,010
Carbon Dioxide .0019776 gm/cc		1176.5		850

To convert meters to feet multiply by 3.2808. To convert feet to meters multiply by 0.3048.
 *Value of extensional ("first arrival") wave in thin rods. Sec. 8b, p 3 of 12

DENSITIES, Z/A RATIOS, AND THERMAL NEUTRON
CAPTURE CROSS SECTIONS PER UNIT VOLUME OF GEOLOGIC MATERIALS

(DENSITY AT ROOM TEMPERATURE AND ONE ATMOSPHERE PRESSURE
UNLESS OTHERWISE STATED)

Material	Z/A Ratio	Matrix Density G/CC	Apparent* Density G/CC	** Σ Material (Capture Units)
Lead Pb	.3953	11.34	8.97	5.61
Uraninite UO ₂	.4000	8.25 (6.5-10.8)	6.60	49.69
Cinnabar HgS	.4143	8.1 (8.0-8.2)	6.71	7,981.16
Iron Fe	.4687	7.87	7.38	214.90
Galena PbS	.4093	7.5 (7.4-7.6)	6.14	12.47
Wulfenite PbMoO ₄	.4187	6.9 (6.7-7.0)	5.78	32.50
Arsenopyrite FeAsS	.4605	6.1 (5.9-6.2)	5.62	165.22
Cobaltite CoAsS	.4517	6.1 (6.0-6.3)	5.51	936.73
Chalcocite Cu ₂ S	.4610	5.65 (5.5-5.8)	5.21	173.56
Hematite Fe ₂ O ₃	.4787	5.26 (4.9-5.3)	5.04	100.47
Magnetite Fe ₃ O ₄	.4774	5.18 (4.97-5.18)	4.95	112.10
Bornite Cu ₅ FeS ₄	.4643	5.15 (4.8-5.4)	4.78	145.63
Pyrite FeS ₂	.4850	5.06 (4.95-5.17)	4.91	89.06
Illmanite FeTiO ₃	.4757	4.75 (4.5-5.0)	4.52	158.23
Zircon ArSiO ₄	.4691	4.69 (4.2-4.86)	4.40	5.42
Stibnite Sb ₂ S ₃	.4436	4.57 (4.52-4.62)	4.05	17.82
Pyrrhotite Fe ₅ S ₆	.4812	4.55 (4.58-4.64)	4.40	90.52
Barite BaSO ₄	.4454	4.45 (4.30-4.60)	3.96	19.40
Chromite FeCr ₂ O ₄	.4753	4.45 (4.30-4.60)	4.23	102.20
Rutile TiO ₂	.4756	4.20 (4.15-4.25)	3.80	202.75
Chalcopyrite CuFeS ₂	.4751	4.2 (4.1-4.3)	3.99	80.95
Corundum Al ₂ O ₃	.4904	4.02 (3.95-4.10)	3.94	11.04
Carnotite K ₂ O.2UO ₃ .V ₂ O ₅ .2H ₂ O.	.4350	4+	3.48+	56.21
Rhodocrosite MnCO ₃	.4793	4.0 (3.5-4.0)	3.84	278.93
Sphalerite ZnS	.4720	4.0 (3.9-4.1)	3.78	38.33
Siderite Fe ₂ CO ₃	.4797	3.88 (3.0-3.88)	3.72	68.81
Limonite 2Fe ₂ O ₃ .3H ₂ O	.4897	3.8 (3.51-4.0)	3.72	74.10
Dunite (4 Samples)	.4978	3.3 (3.24-3.74)	3.29	17.03
Olivine (Mg,Fe) ₂ SiO ₄	.4892	3.3 (3.27-3.37)	3.23	31.74
Magnesite MgCO ₃	.4992	3.1 (3.0-3.2)	3.1	1.48
Norite (11 Samples)	.4970	2.984 (2.720-3.020)	2.97	12.88
Diabase (6 Samples)	.4954	2.98 (2.96-3.05)	2.95	17.12
Gabbro (27 Samples)	.4938	2.976 (2.850-3.120)	2.94	21.47
Anhydrite CaSO ₄	.4995	2.95 (2.89-3.05)	2.95	12.30
Aragonite CaCO ₃	.4995	2.94 (2.85-2.94)	2.94	8.12
Muscovite KA ₁₂ (AlSi ₃)O ₁₀ (OH) ₂	.4966	2.93 (2.76-3.1)	2.91	17.30
Biotite H ₂ K(Mg,Fe) ₃ Al(SiO ₄) ₃	.4900	2.90 (2.65-3.1)	2.84	25.20
Dolomite CaMg(CO ₃) ₂	.4994	2.85 (2.80-2.99)	2.85	4.78
Illite KA ₁₅ Si ₇ O ₂₀ (OH) ₄	.4954	2.84 (2.60-3.0)	2.81	39.90
Diorite (13 Samples)	.4964	2.839 (2.721-2.960)	2.82	14.33
Langbeinite K ₂ Mg ₂ (SO ₄) ₃	.4961	2.83	2.61	78.87
Polyhalite	.5013	2.78	2.79	21.00
2CaSO ₄ .MgSO ₄ .K ₂ SO ₄ .2H ₂ O				
Synite (24 Samples)	.4971	2.757 (2.630-2.899)	2.74	16.43
Granodiorite (11 Samples)	.4963	2.716 (2.668-2.785)	2.696	11.33
Chlorite	.5056	2.71 (2.60-3.22)	2.74	17.56
(Mg,Al,Fe) ₁₂ (Si,Al) ₈ O ₂₀ (OH) ₁₆				
Calcite CaCO ₃	.4996	2.71 (2.71-2.72)	2.71	7.48
Aluminum Al	.4818	2.70	2.60	13.99

*Based on tool calibration using a Z/A ratio of 0.5. **Capture Units in 10²¹ Barns/cm³

TABLE 2a

Material	Z/A Ratio	Matrix Density G/CC	Apparent* Density G/CC	** Σ Material (Capture Units)
Plagioclase feldspar xNaAlSi ₂ O ₈ ,yCaAl ₂ Si ₂ O ₈	.4925	2.69 (2.62-2.76)	2.65	6.99
Limestone (Av. of 345 Samples)	.5000	2.69 (2.66-2.74)	2.69	8.72
Granite (155 Samples)	.4969	2.667 (2.516-2.809)	2.65	11.62
Quartz SiO ₂	.4993	2.65 (2.65-2.66)	2.65	4.36
Sandstone (Av. of 12 Samples)	.4990	2.655 (2.59-2.84)	2.655	8.66
Kaolinite (OH) 8Al ₄ Si ₄ O ₁₀	.5103	2.63 (2.40-2.68)	2.68	13.06
Albite NaAlSi ₃ O ₈	.4885	2.62 (2.61-2.65)	2.56	6.77
Orthoclase feldspar KA1Si ₃ O ₈	.4958	2.57 (2.55-2.63)	2.55	16.00
Kieserite MgSO ₄ .H ₂ O	.4724	2.57	2.43	12.77
Concrete		2.35 (1.98-2.35)		
Montmorillonite	.5009	2.35 (2.00-3.00)	2.35	8.10
(OH) ₄ Si ₈ Al ₁₄ O ₂₀ .nH ₂ O (n=1)				
Gypsum CaSO ₄ .2H ₂ O	.5111	2.32 (2.30-2.35)	2.37	19.40
Glauconite KMg (FeAl) (SiO ₃) ₆ .3H ₂ O	.4998	2.30 (2.20-2.80)	2.30	16.80
Graphite C	.4995	2.22 (2.09-2.23)	2.22	0.38
Serpentine Mg ₃ Si ₂ O ₅ (OH) ₄	.5062	2.20	2.23	8.80
Halite NaCl	.4799	2.16 (2.135-2.165)	2.07	752.36
Nahcolite NaHCO ₃	.4905	2.20	2.16	
Kainite MgSO ₄ .KCl.3H ₂ O	.5140	2.13 (2.1-2.13)	2.19	196.13
Trona Na ₂ CO ₃ HNaCO ₃ .2H ₂ O	.5043	2.125 (2.11-2.15)	2.14	16.21
Sulphur, orthorhombic (below 95.4°C)	.4990	2.07 (2.05-2.09)	2.07	19.06
Potash K ₂ CO ₃ 2H ₂ O	.5049	2.04	2.06	39.70
Sylvite KCl	.4829	1.99 (1.97-1.99)	1.92	570.68
Cement (32 Samples)		1.99		about 13
Sulphur, monoclinic (above 95.5°C at 1 atm; above 150°C at 19,000 psi) S	.4990	1.96	1.96	18.05
Kernite Na ₂ B ₄ O ₇ .4H ₂ O	.5026	1.91	1.92	12,793.69
Carnallite KMgCl ₃ .6H ₂ O	.5095	1.61 (1.60-1.61)	1.64	370.92
Anthracite coal .9350(C) .0281(H) .0097(N) .0272(O)	.5134	1.60 (1.32-1.80)	1.64	1.08
Bituminous coal .8424(C) .0555(H) .0152(N) .0869(O)	.5201	1.35 (1.15-1.7) 1.10 (.5-1.5)	1.40 1.16	1.54
Lignite				
Water (300,000 ppm NaCl)	.5325	1.219	1.298	146.22
(250,000 ppm NaCl)	.5363	1.1825	1.268	122.55
(200,000 ppm NaCl)	.5401	1.146	1.238	100.08
(150,000 ppm NaCl)	.5438	1.109	1.206	78.75
(100,000 ppm NaCl)	.5476	1.073	1.175	58.69
(50,000 ppm NaCl)	.5513	1.0365	1.143	39.02
(30,000 ppm NaCl)	.5528	1.022	1.130	32.56
(Pure Water)	.5551	1.00	1.11	22.08
NaCl solution density at STP ≅ 1 + (.00000073 x ppm)				
Oil n(CH ₂), 10° API, STP	.5703	1.00	1.14	28.02
30° API, STP		.88	1.00	25.89
40° API, STP		.85	.97	24.22
50° API, STP		.78	.85	22.23
(C ₈ H ₁₈), 70° API, STP	.5778	.70	.81	22.12
N-pentane C ₅ H ₁₂ ,STP	.5823	.626	.733	20.80
200° F, 7,000 psi		.603	.702	20.02
N-hexane C ₆ H ₁₄ , STP	.5803	.659	.765	21.38
200° F, 7,000 psi		.628	.739	20.37
N-heptane C ₇ H ₁₆ , STP	.5778	.684	.790	21.80

*Based on tool calibration using a Z/A ratio of 0.5.

**Capture Units in 10²¹ Barns/cm³

Material	Z/A Ratio	Matrix Density G/CC	Apparent * Density G/CC	** Σ Material (Capture Units)
200°F, 7,000 psi		.657	.759	20.84
N-octane C ₈ H ₁₈ , STP	.5778	.703	.812	22.12
200°F, 7,000 psi		.673	.778	21.12
N-nonane C ₉ H ₂₀ , STP	.5768	.718	.828	22.37
200°F, 7,000 psi		.686	.791	21.37
N-decane C ₁₀ H ₂₂ , STP	.5763	.730	.841	22.55
200°F, 7,000 psi		.701	.808	21.65
N-undecane C ₁₁ H ₂₄ , STP	.5759	.740	.852	22.71
200°F, 7,000 psi		.713	.821	21.87
Methane CH ₄ , STP	.5703	.000677	.00076	0.028
200°F, 7,000 psi		.2189	.2497	10.88
Ethane C ₂ H ₆ , STP	.5986	.001269	.00015	0.051
200°F, 7,000 psi		.4104	.4913	16.34
Propane C ₃ H ₈ , STP	.5896	.00186	.0022	0.067
N-butane C ₄ H ₁₀ , STP	.5850	.00246	.0029	0.085
Helium He, STP	.4997	.00017	.00017	0.0000
Carbon dioxide CO ₂ , STP	.4999	.001858	.001857	0.0001
Nitrogen N ₂ , STP	.4998	.001182	.001185	0.004
Oxygen O ₂ , STP	.5000	.001350	.001350	0.00001
Hydrogen sulphide H ₂ S, STP	.5281	.001438	.001519	0.029
Air (dry) (N-78%, O-21%, A-1%)	.4997	.001224	.001223	
Argon A, STP	.4859	.001688	.00144	0.017
Average natural gas, STP	.5735	.0007726	.000886	
200°F, 7,000 psi		.252	.289	
Hydrogen H	.9921	.00009		
Oxygen O	.5000	.001429		
Nitrogen N	.4998	.00125		
Carbon C	.4995	3.52		
Calcium Ca	.4990	1.5		
Sulfur S	.4990	2.07		
Silicon Si	.4985	2.4		
Magnesium Mg	.4975	1.74	1.73	
Potassium K	.4859	.86		
Phosphorous P	.4845	1.83		
Aluminum Al	.4818	2.70	2.60	
Sodium Na	.4804	.97		
Chlorine Cl	.4795	.0032		
Nickel Ni	.4769	8.90		
Iron Fe	.4687	7.86		
Boron B	.4625	2.45		
Chromium Cr	.4614	7.1		
Titanium Ti	.4593	4.5		
Zinc Zn	.4589	7.14		
Manganese Mn	.4568	7.4		
Copper Cu	.4564	8.92		
Vanadium V	.4514	5.96		
Cobalt Co	.4432	8.9		
Arsenic As	.4405	5.7		
Zirconium Zr	.4385	6.4		
Bromine Br	.4380	3.12		
Strontium Sr	.4336	2.6		
Tin Sb	.4312	7.2		
Molybdenum Mo	.4159	10.2		
Barium Ba	.4077	3.5		
Mercury Hg	.3988	13.56		

**Capture Units in 10²¹ Barns/cm³

Material	Z/A Ratio	Matrix Density G/CC
Lead Pb	.3953	11.34
Uranium U	.3865	18.7
Water H ₂ O	.5551	1.0
Carbon dioxide CO ₂	.4999	
Calcium carbonate CaCO ₃	.4996	
Calcium sulfate CaSO ₄	.4995	
Calcium Oxide CaO	.4993	
Silicon oxide SiO ₂	.4993	
Magnesium oxide MgO	.4985	
Aluminum oxide Al ₂ O ₃	.4904	
Phosphorous oxide P ₂ O ₅	.4935	
Boron oxide B ₂ O ₃	.4884	
Potassium oxide K ₂ O	.4883	
Sulfur trioxide SO ₃	.4874	
Sodium oxide Na ₂ O	.4855	
Hematite Fe ₂ O ₃	.4787	
Magnetite Fe ₃ O ₄	.4766	
Iron oxide FeO	.4757	
Titanium oxide TiO ₂	.4756	
Titanium oxide TiO	.4695	
Manganese oxide MnO	.4652	
Zirconium oxide ZrO ₂	.4555	
Strontium oxide SrO	.4439	
Barium oxide BaO	.4173	

*Based on tool calibration using a Z/A ratio of 0.5.

Many of the minerals listed are most often found in nature to be impure.

The values listed are minus photoelectric effects, which may become significant when elements heavier than sodium are present within the volume under investigation. The calculation of Z/A effects in formations rich in heavy atoms is mainly academic because here the Z/A effects become unimportant compared to those of photoelectric absorption. Present-day density log interpretation techniques are not designed for the accurate determination of bulk density in many heavy mineral-rich formations.

Many rich ore deposits contain only 1% to 1-1/2% of the mineral to be extracted. The sought after mineral therefore may not contribute significantly to the bulk density of the ore.

To determine the neutron capture cross section (Σ) of a substance:

- 1) Determine the molecular weight of the substance.
- 2) Divide the molecular weight of the substance by its density.
- 3) Divide Avogadro's Number (6.025×10^{23}) by the above quotient (yields molecules per cm^3).
- 4) Multiply the number of atoms of each element present per cm^3 by the thermal neutron capture cross section (in barns) for the element.
- 5) Sum the capture cross section contributions for each element as determined from Step #4 above to determine the capture cross section (in barns $\times 10^{21}/\text{cm}^3$) for the substance.

SONIC - DENSITY CROSS PLOT (COMMON)

$\rho f_a = 1.24 \text{ gm/cc}, V_f = 5300' / \text{sec}$

(Density Log Calibration to $Z/A=0.5$)

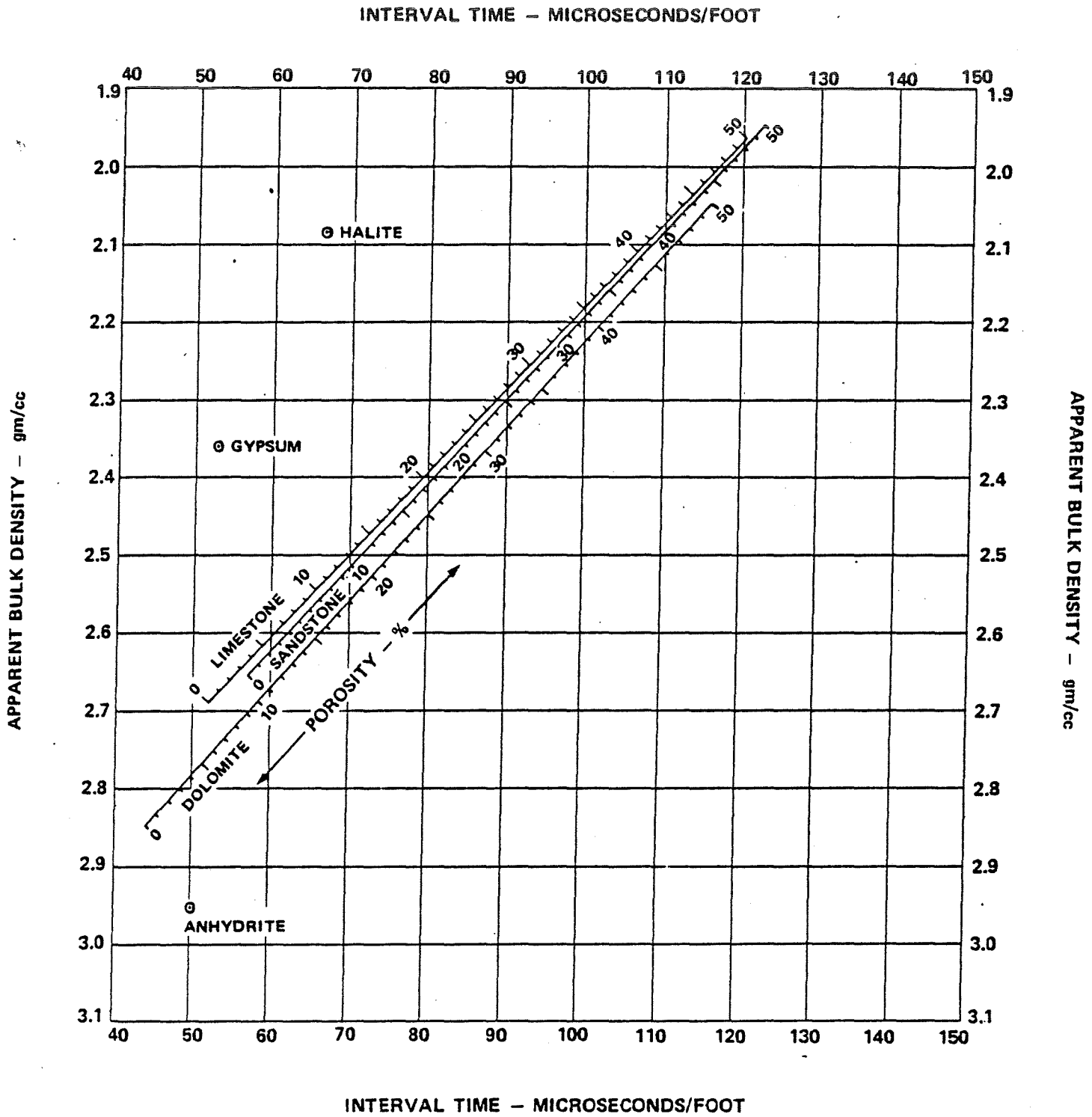


Figure 1

BULK DENSITY - NEUTRON CROSS PLOT

$$\rho_{f_0} = 1.24 \text{ gm/cc}$$

(Density Log Calibration to $Z/A=0.5$)

APPARENT NEUTRON POROSITY - % (ASSUMING LIMESTONE)

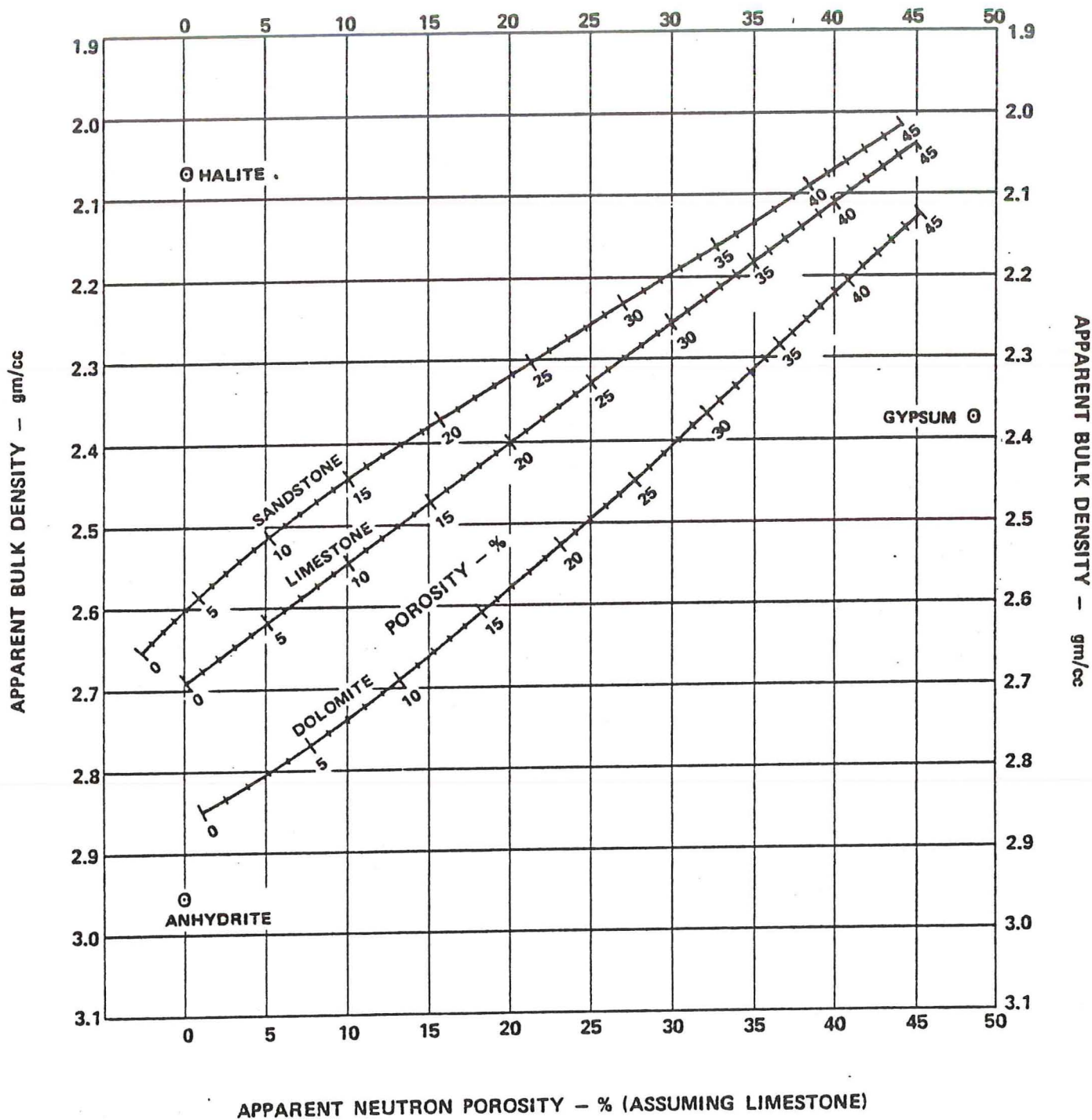


Figure 2

GAS DETECTION AND POROSITY DETERMINATION IN SANDS FROM DENSITY - NEUTRON LOG CROSS PLOTTING

APPARENT BULK DENSITY - gm/cc

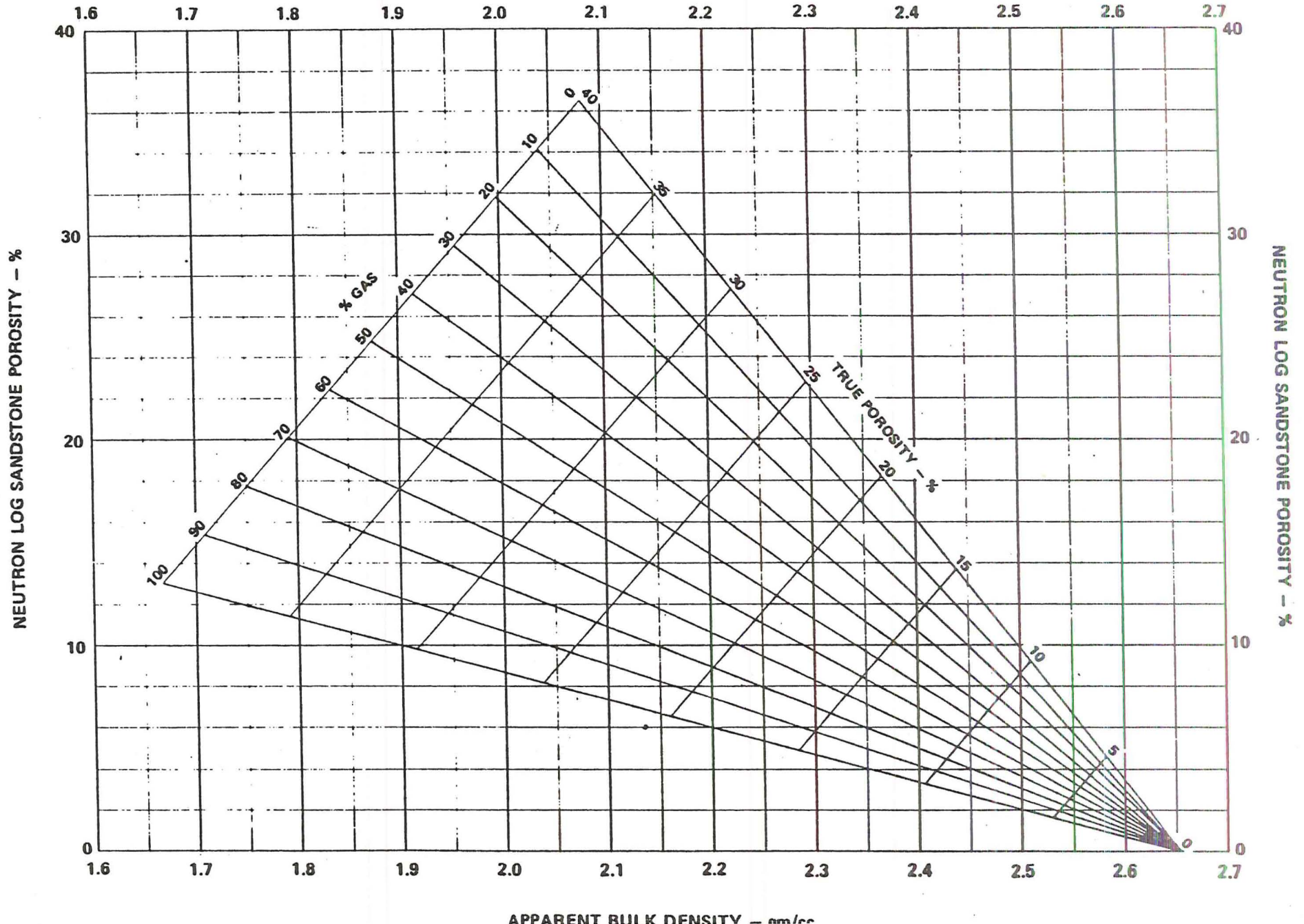


Figure 3

RESISTIVITY VS Δ_t , ρ_b , ϕ_n or ϕ
 POST PALEOZOIC SANDS ($F = 0.62 / \phi^{2.15}$)

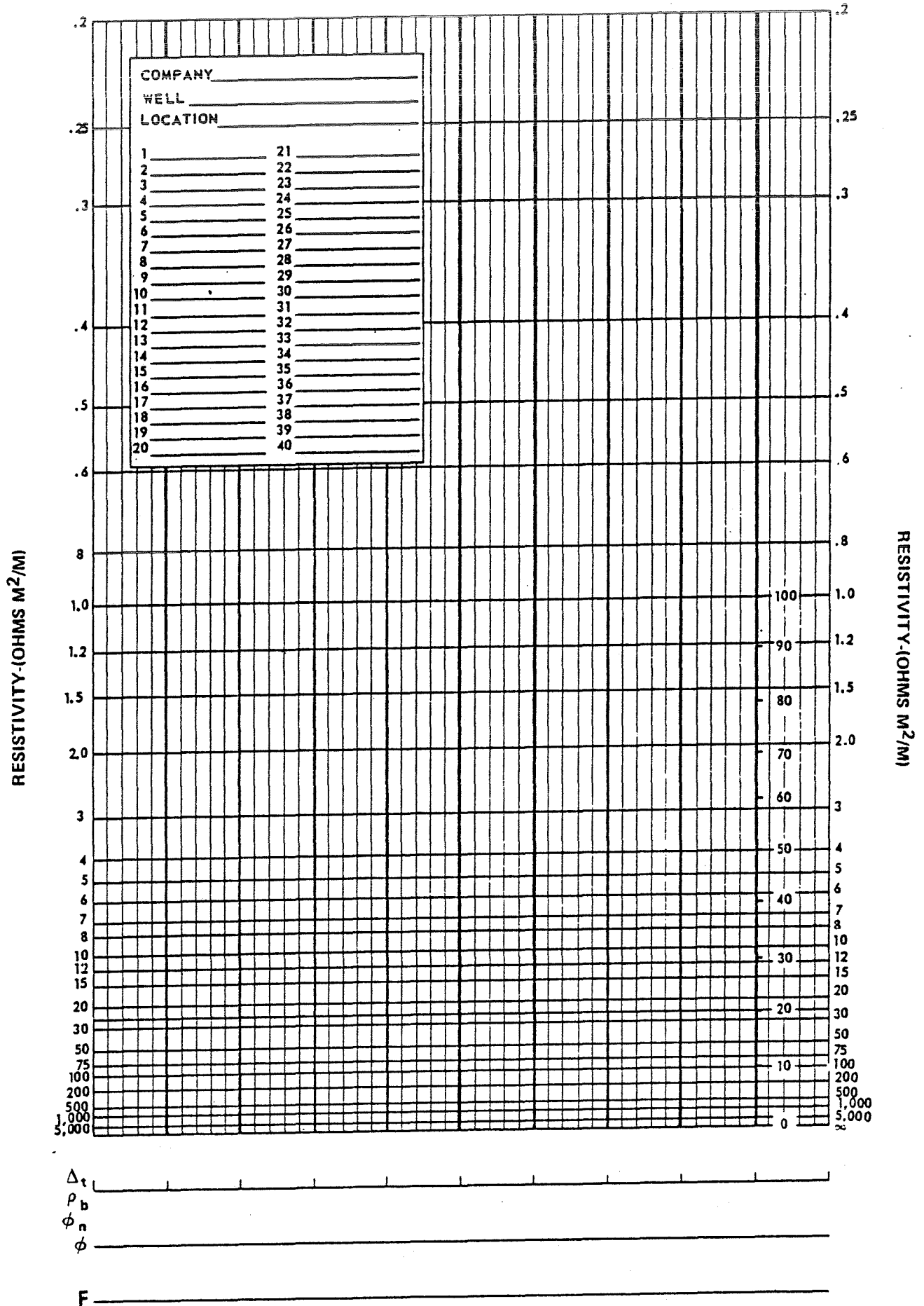


Figure 4
84

SONIC - DENSITY CROSS PLOT (LITHOLOGY)

Density Log Calibration to Z'A=0.5

SONIC TRAVEL TIME - MICROSECONDS/FOOT

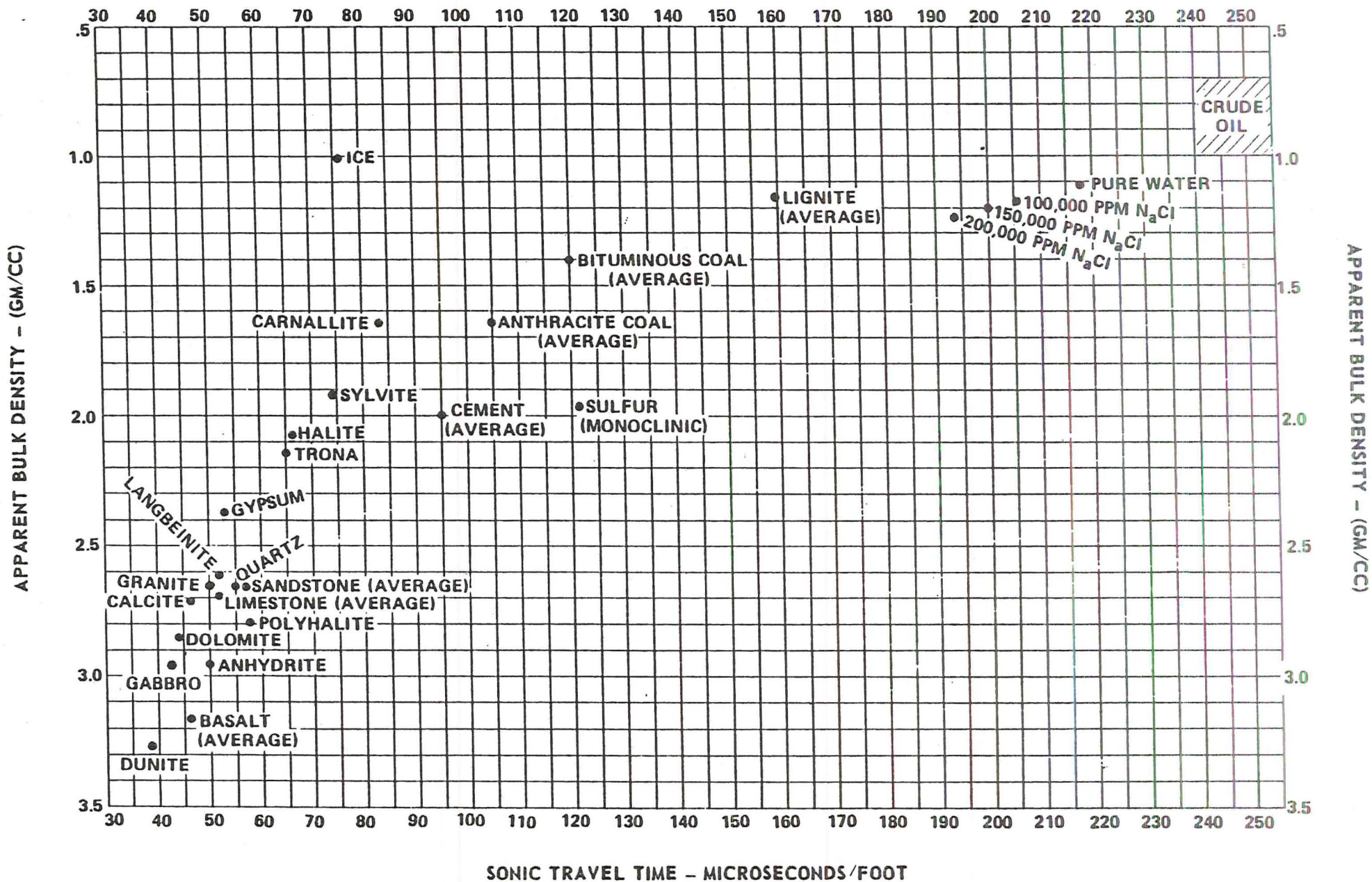


Figure 5 Sec. 8b, p 12 of 12

REFERENCES AND BIBLIOGRAPHY

- American Geological Institute, Dictionary of Geological Terms, Garden City, New York, Double Day & Co., Dolpin Books, 1962.
- Desai, K. P. and E. J. Moore, "Equivalent NaCl Determinations from Ionic Concentrations," Log Analyst, May-June, 1969, Vol. X, No. 3, pp 12-21
- Doll, H. G., "The SP Log in Shaley Sands," AIME T.P. 2912.
- Doll, H. G., "The S.P. Log: "Theoretical Analysis and Principles of Interpretation," AIME T.P. 2463.
- Garrels, Robert M. and George L. Christ, Solutions, Minerals, and Equilibria, New York, Harper & Row, 1965.
- Gondouin, M., M. P. Tixier, and G. L. Simard, "An Experimental Study on the Influence of the Chemical Composition of Electrolytes on the SP Curve," AIME, T. P. 4455.
- Handbook of Chemistry and Physics, 45th Edition.
- Ives, David J. G., and George J. Janz, Reference Electrodes, Theory and Practice, New York & London, Academic Press, 1961.
- Lynch, Edward J., Formation Evaluation, New York, Evanston, and London, Harper & Row, 1962.
- Quarterly Report of the Colorado School of Mines, "Well Logging," April, 1962, Vol. 57, No. 2.
- Schlumberger Document No. 8, "Introduction to Schlumberger Well Logging Formation Evaluation Data Handbook, Gearhart Owens Industries, Inc.
- Schlumberger Log Interpretation Principles.
- Schlumberger Log Interpretation Charts.
- Rubin, Bruce, Uranium Roll Front Zonation W.G.A. Earth Science Bulletin, December 1970.
- Hallenburg, James, Interpretation of Gamma Ray Logs, SPWLA Proceedings 14th Annual Logging Symposium 1973.
- Hallenburg, James, A Resume of Spontaneous Potential Measurements, SPWLA Proceedings 12th Annual Logging Symposium 1971.
- Guyod, Hubert, Interpretation of Electric and Gamma Ray Logs in Water Wells, Well Log Analyst, SPWLA, January-March 1966.
- Crew, M. E. and Berkoff, E. W., Twopit, A Different Approach to Calibration of Gamma Ray Logging Equipment, E.R.D.A. (A.E.C.) Grand Junction, Colorado, 1969.

SYMBOLS

A	Area
A	Atomic Mass Number (The Sum of all Neutrons and Protonin a Nucleus - Integer)
A	Atomic Weight (The average mass number considering all Isotopes)
A	Acres
A	A current electrode used in electric logging (The current electrode nearest the measuring electrode "M" in 16" and 64" normal circuitry)
A	Amplitude
A	Area under the log curve (uranium logging term)
A	Avogadro's Number = 6.035 x 10 ²³ atoms/mole
a	Activity (or contribution to electrode measurements)
a	Constant in formation factor relationship ($F=a/\phi^m$)
AC	Alternating current
AIME	American Institute of Mining and Metaulurgical Engineers
alpha (α)	SP reduction factor indicating the amount of shale (a fraction) ($\alpha = PSP/SSP$) or gamma ray deflection from shale base line \div gamma ray deflection opposite non-sha zone (note: gamma ray method should not be used when non-shaly materials are radioactive.)
ALPHA	Alpha Particle
AM	Normal (two electrode) device electrode spacing
AMP	Amplitude log
AO	Lateral (three electrode) device electrode spacing
API	American Petroleum Institute
API	A specific unit of Radiation Concentrate (a standard)
APIGU	American Petroleum Institute Gamma Ray Unit (a standard)
APINU	American Petroleum Institute Neutron Unit (a standard)
SP _a	Apparent SP as read from the log
SP	Apparent SP as read from the log
atm	Atmospheric or atmosphere
B	A current electrode used inelectrical logging
bbl	Barrel (42 gallons liquid)
bbl/d	Barrels per day
BFR	Borehole fluid resistivity log
BHC	Borehole compensated
BHT	Bottom hole temperature ($^{\circ}$ F in USA)
BIT	Bit diameter in inches
BLI	Bottom of logged interval
BOD	Barrels of oil per day
$^{\circ}$ C	Centigrade
CS	Compressive strength
C	Conductivity at a given temperature, usually formation temperature (in millimhos/m
c	Concentration
CL	Caliper log
cal	Calorie
CBL	Cement bond log (amplitude plus single receiver curves only)
CBL/SL	Cement bond (with wavetrain) log - Signature log
CBL/SS	Cement bond (with variable intensity display) log - Seismic Spectrum long
CCL	Casing Collar log
$c\Delta t_{shale}$	Sonic log compaction correction (unconsolidated formations)
CDL	Density log (compensated)

A P P E N D I X

cm	Centimeter
cm ²	Square centimeters
cm ³	Cubic centimeters
cps	Counts per second
CSVL	Sonic log (compensated)
CDS	Continuous directional survey
cu	Cubic
CVL	Continuous velocity log
CICL	Casing Inspection Caliper log
CWLS	Canadian Well Logging Society
D	Depth
d	Hole diameter (obsolete term)
d	Diameter
d	Day
DC	Direct Current
d _h	Borehole diameter
D _i	Average diameter of invaded zone
DL	Density log
DML	Dipmeter log
DST	Drill stem test
dr	Dram
DTL	Temperature log (differential)
EXP	Exponent (Natural Logarithms)
E	Voltage (potential)
e	Bed thickness (obsolete term)
e	Exponent (Natural Logarithms)
EL	Electrical log derived measurement
EL	Electrical log
E _c	SP electrochemical component
E _h	Reduction or oxidation potential (redox)
E _i	Designation of a particular acoustic wave train event (E ₁ , E ₂ etc.)
E _k	SP electro-filtration component (streaming potential or electrokinetic)
esu	Electrostatic unit of charge
eV	Electron volt(s)
E ₁	Upper "end value" of counting rate (uranium logging term)
E ₂	Lower "end value" of counting rate (uranium logging term)
F	Formation resistivity factor (ratio of resistivity of porous medium 100% saturated with water to resistivity of the saturating water). This value increases with hydrocarbon saturation, i.e., as water geometry becomes more complicated.
°F	Fahrenheit
f _i	Fraction of matrix component in mixed lithology.
FFI	Free Fluid Index (free fluid pore content from nuclear resonance measurements)
FM	Flowmeter log (general terminology for any fluid flow measurement)
FPL	Free Point Log
FR	First reading (lowest reading of log curve for curves that are recorded from the bottom of the hole upward)
FT	Formation temperature (obsolete term)
FT	Formation test or Formation Tester
ft	Foot or feet
FVF	Formation volume factor

A P P E N D I X

G	Geometrical factor
G	Gradient
\bar{G}	Mean concentration by weight of the radioactive element (uranium logging term; Grade)
G	Gravity
g	Acceleration due to gravity
g	Temperature gradient in °F per 100' of depth
gal	Gallon
G_{γ}	Average radiometric grade of uranium ore
GL	Guard log
GLR	Gas-liquid ratio
gm	Gram
GOI	Gearhart-Owen Industries, Inc., publishers of this handbook and the leading manufacturer of well logging tools.
GOR	Gas-oil ratio
GR	Gamma-ray log
GRN	Gamma Ray - Neutron combination log
grain	Grain
GT	Mean true uranium ore grade (established by chemical assay)
H	Hertz (Cycles per second)
h	Thickness
h	Bed thickness (feet in U.S.A.)
$h/2$	Half thickness to penetrating radiation or signal
HI	Hydrogen Index (Equivalent Neutron Porosity)
HVT	Half Value thickness (Radiation absorption value)
hr	Residual hydrocarbons
IEL	Induction - Electrical log
I.D.	Inside Diameter
IP	Initial Potential
IP	Induced Polarization
I	Resistivity index (R_t/R_o)
I	Intensity of any radiation field
I	Intensity of gamma ray field (uranium logging term)
I_o	Initial value of Intensity or current
I_1, I_2, I_n	Intermediate level count level values (uranium logging term)
I	Electrical current magnitude
IL	Induction Log
in	Inch
ITT	Integrated travel time
K	Coefficient in SSP formula $\left[K = -70.7 \left(\frac{460 + ^\circ F}{537} \right) \log \frac{R_{mf}}{R_{we}} \right]$
K	Coefficient in uranium ore grade formula
$^{\circ}K$	$^{\circ}$ Kelvin
k	Modulus of compressibility
k	Permeability
kc	Kilocycles per second
kg	Kilogram
km	Kilometer
lb	Pound
liq	Liquid

A P P E N D I X

L	Liquid
L	Length
ℓ	Length
l	Liter
lm	Limestone
ls	Limestone
ln	Logarithm base e (natural logarithm)
log	Logarithm base 10 (common logarithm)
MMCF	Million cubic feet
MCF	Thousand cubic feet
M	Measuring electrode used in electric logging (measuring electrode nearest current electrode "A" in 16" normal and 64" normal circuitry)
MAX	Maximum value of any parameter
m	Exponent in formation factor-porosity formula (Archie "cementation" factor)
md	Millidarcy (permeability)
Mev	Million electron volts
MGL	Micro-guard log
mi	Mile
Min	Minimum value of any parameter
mm	Millimeter
MN	Distance between two potential measuring electrodes
MPD	Maximum permissible radiation dose.
ML	Micro-electrical log
mr	Milliroentgen (radiation dose)
mr/hr	Milliroentgen per hour (radiation dose rate)
N	Measuring electrode used in electric logging potential (measuring electrode farthest from current electrode "A" in 16" normal and 64" normal circuitry)
N	Intensity or count-rate
N	Neutron log
NL	Neutron log
N	Normal curve (electrical logging term)
Nc	Corrected (for coincidence loss) counting rate
n	Symbol for a neutron
n	Observed counting rate
n	Exponent in Archie water saturation formula
N.A.	Not Applicable
NA	Not available
NLL	Neutron Lifetime log (a trade name for a pulsed neutron system)
NML	Nuclear Magnetism Log (a trade name for a nuclear resonance system)
O.D.	Outside diameter
oz	Ounce
p	Shale fraction of bulk volume (laminated case)
P	Pressure
Pc	Critical pressure
ppm	Parts per million (equals milligrams per liter / specific gravity of solution at STP)
PPr	Pseudo reduced pressure
psi	Pounds per square inch
psia	Absolute pressure in pounds per square inch (meter plus atmospheric pressure)
PSP	Pseudostatic spontaneous potential (the SP found opposite a thick shaly sand)
PTr	Pseudo reduced temperature

A P P E N D I X

PVT	Pressure-volume-temperature
Q (q)	Apparent fraction of the total porosity occupied by dispersed clay or shale
Q	Electrical charge
Q	Quantity
q	Flow rate
qt	Quart
°R	°Rankine (absolute temperature; $F^{\circ} + 460$)
R	Resistivity in ohms meter squared / meter at a given temperature
Re	Reynolds number in fluid flow
R	Receiver
R	Gas constant in PVT relationships
r	Roentgen (Unit of radiation dose)
r	Resistance
r	Radius
Ra	Apparent resistivity as recorded by an resistivity device
rad	Unit of Absorbed Radiation dose
RTL	Radioactive Tracer log
RBE	Relative Biological Effectiveness (of radiation exposure)
rem	Roentgen equivalent man (radiation dose)
RF	Recovery factor
RGS	Residual gas saturation (obsolete term)
RHS	Residual hydrocarbon saturation (obsolete term)
R _i	Resistivity of invaded zone
RILD	Deep (investigating) induction log reading
RILM	Medium (investigating) induction log reading
RFVL	Radioactive fluid velocity log
R _m	Resistivity of mud
R _{max}	Maximum resistivity value (usually lateral curve value opposite beds whose thickness is less than AO)
R _{mc}	Resistivity of mud cake
R _{mf}	Resistivity of mud filtrate
R _{min}	Minimum resistivity value (usually lateral curve value in interval below bed equal to AO spacing)
R _{an}	Resistivity of annular invaded zone
R _o	Resistivity of formation 100% saturated with formation water of resistivity R _w
ROS	Residual oil saturation (obsolete term)
ROS	Radiation orientation survey
RPM	Revolutions per minute
R _s	Resistivity of adjacent formation
R _t	Resistivity of uninvaded zone
R _w	Resistivity of formation water
R _{wa}	Apparent resistivity of formation water
R _{we}	Calculated resistivity of formation water uncorrected for salinity or ion type (apparent formation water resistivity)
R _{xo}	Resistivity of flushed zone
R _z	Resistivity, at a given temperature, of a mixture of fluids or electrolytes such as mud filtrate and formation water (a calculated value)
SFVS	Spinner fluid velocity survey
S	Saturation (general term)
S	Seconds

A P P E N D I X

s	Seconds
S.P.	Specific gravity (obsolete term)
SG	Specific gravity
Sg	Gas saturation as a percent of pore volume
S _h	Hydrocarbon saturation in uninvaded zone as a percent of pore volume
Sd	Sand
sh	Shale
ss	Sandstone
S _{hr}	Residual hydrocarbon saturation as a percent of pore volume
S _i	Saturation in invaded zone
SL	Sonic log (general terminology for acoustic log)
S _{or}	Residual oil saturation as a percent of pore volume
SP	Spontaneous potential
SP	Spontaneous potential log
SPE	Society of Petroleum Engineers (a section of the A.I.M.E.)
SPWLA	Society of Professional Well Log Analysts
SSP	Static SP (the maximum possible SP for a given R _{mf} /R _w)
STP	Standard temperature and pressure (i.e., 60°F at 14.7 psi)
SVL	Sonic velocity log
SU	"Standard Unit" of gamma ray deflection
SL	Liquid saturation as a fraction of pore space
S _w	Water saturation as a percent of pore volume
SWC	Sidewall coring
S _{wi}	Irreducible water saturation as a percent of pore volume
S _{xo}	Water saturation in flushed zone as a percent of pore volume
T	Transmitter
T	Temperature (°F U.S.A.)
T	Thickness (uranium logging term)
T	Thermal decay time in microseconds
t	Time
t	Resolving time of instrument or system
t _{1/2}	Radioactive half life in units of time
T _c	Critical temperature
TC	Time constant
T ₁	Thermal (neutron) relaxation time
TD	Total depth at time of logging
TDI	Thermal Decay Time (a trade name for a pulsed neutron system)
TF	Formation temperature
T _{mc}	Mud cake thickness (obsolete term)
TL	Temperature log
T _s	Surface temperature
To	Near surface temperature where there are no temperature or barometric variations
V	Volume
V	Bulk volume fraction
Δ t	Sonic travel time
V _p	Compressional wave velocity
V _s	Shear wave velocity
VT	Tube wave velocity
v	Velocity
W	Water content expressed as percent moisture by weight (uranium logging term)

A P P E N D I X

- 18' 18' lateral AO spacing electrical log derived measurement
- 1" x 1" 1-1/2" lateral AO spacing micro-electrical log derived measurement
- 2" 2" normal AM spacing micro-electrical log derived measurement
- ∞ Refers to a distant point in the formation
- ½ Half life or half thickness of materials

SYMBOL SUPERSCRIPTS

- m Porosity Exponent
- n Saturation Exponent
- x Exponent (any)
- o Degrees temperature
- o Degrees API gravity
- o Degrees arc
- A Isotope Designation

SYMBOL PREFIXES

- d deci (=10⁻¹)
- c centi (=10⁻²)
- m milli (=10⁻³)
- μ micro (=10⁻⁶)
- n nano (=10⁻⁹)
- p pico (=10⁻¹²)
- f femto (=10⁻¹⁵)
- a atto (=10⁻¹⁸)
- k kilo (=10³)
- M mega (=10⁶)
- G giga (=10⁹)
- T tera (=10¹²)

GREEK ALPHABET

A α	alpha	N ν	nu
B β	beta	Ξ ξ	xi
Γ γ	gamma	Ο ο	omicron
Δ δ	delta	Π π	pi
E ε	epsilon	Ρ ρ	rho
Z ζ	zeta	Σ σ ς	sigma
H η	eta	Τ τ	tau
Θ θ	theta	Υ υ	upsilon
I ι	iota	Φ φ	phi
K κ	kappa	Χ χ	chi
Λ λ	lambda	Ψ ψ	psi
M μ	mu	Ω ω	omega